

CENTRAL RESEARCH LIBRARY  
DOCUMENT COLLECTION

OAK RIDGE NATIONAL LABORATORY LIBRARY



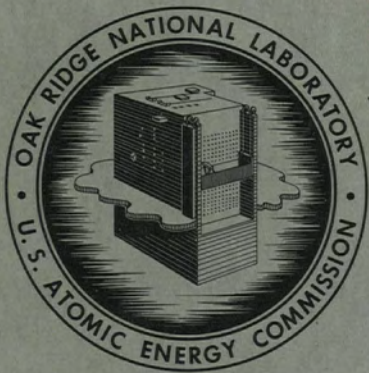
3 4456 0023185 3

ORNL-2773  
UC-37 - Instruments  
TID-4500 (15th ed.)

THERMOCOUPLE RESEARCH TO 1000°C - FINAL REPORT  
NOVEMBER 1, 1957, THROUGH JUNE 30, 1959

J. F. Potts, Jr.  
D. L. McElroy

CENTRAL RESEARCH LIBRARY  
DOCUMENT COLLECTION  
**LIBRARY LOAN COPY**  
DO NOT TRANSFER TO ANOTHER PERSON  
If you wish someone else to see this  
document, send in name with document  
and the library will arrange a loan.



**OAK RIDGE NATIONAL LABORATORY**  
operated by  
UNION CARBIDE CORPORATION  
for the  
U.S. ATOMIC ENERGY COMMISSION

Printed in USA. Price **\$2.75**. Available from the

Office of Technical Services  
Department of Commerce  
Washington 25, D.C.

#### LEGAL NOTICE

This report was prepared as an account of Government sponsored work. Neither the United States, nor the Commission, nor any person acting on behalf of the Commission:

- A. Makes any warranty or representation, expressed or implied, with respect to the accuracy, completeness, or usefulness of the information contained in this report, or that the use of any information, apparatus, method, or process disclosed in this report may not infringe privately owned rights; or
- B. Assumes any liabilities with respect to the use of, or for damages resulting from the use of any information, apparatus, method, or process disclosed in this report.

As used in the above, "person acting on behalf of the Commission" includes any employee or contractor of the Commission, or employee of such contractor, to the extent that such employee or contractor of the Commission, or employee of such contractor prepares, disseminates, or provides access to, any information pursuant to his employment or contract with the Commission, or his employment with such contractor.

ORNL-2773  
UC-37 - Instruments  
TID-4500 (15th ed.)

INSTRUMENTATION AND CONTROLS DIVISION

**THERMOCOUPLE RESEARCH TO 1000°C - FINAL REPORT**

**NOVEMBER 1, 1957, THROUGH JUNE 30, 1959**

J. F. Potts, Jr.  
Instrumentation and Controls Division

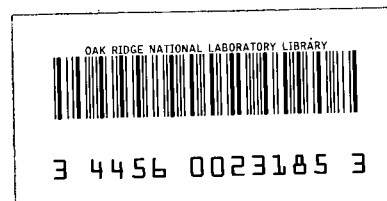
D. L. McElroy  
Metallurgy Division  
(Formerly with Engineering Experiment Station,  
University of Tennessee)

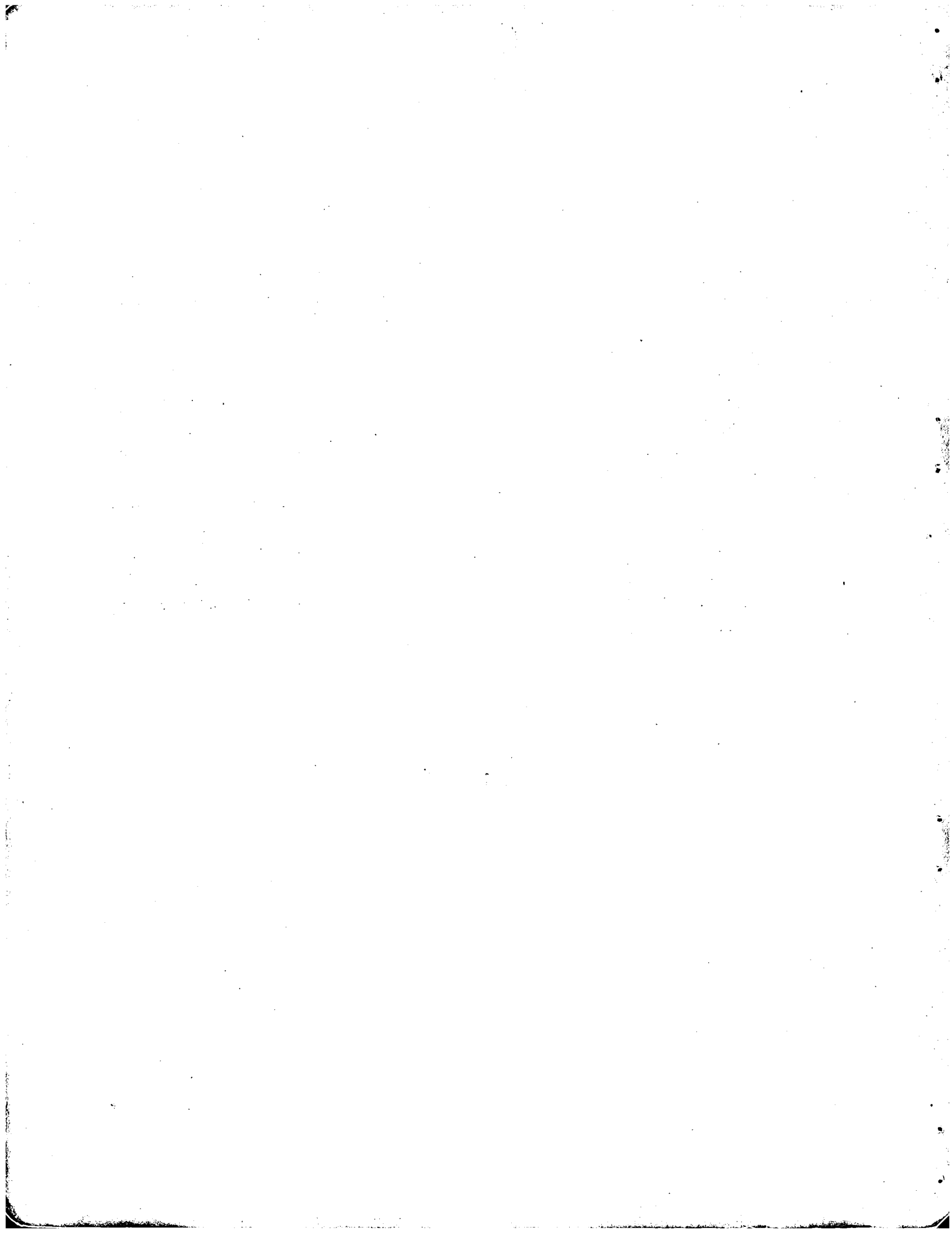
Work Performed Jointly by  
Instrumentation and Controls Division, Oak Ridge National Laboratory,  
and Engineering Experiment Station, University of Tennessee  
Research and Development Contract  
Subcontract Number 1072, Under W-7405-eng-26  
Between Oak Ridge National Laboratory,  
Union Carbide Corporation, and  
University of Tennessee

DATE ISSUED

JAN 16 1961

OAK RIDGE NATIONAL LABORATORY  
Oak Ridge, Tennessee  
operated by  
UNION CARBIDE CORPORATION  
for the  
U. S. ATOMIC ENERGY COMMISSION





#### ACKNOWLEDGMENT

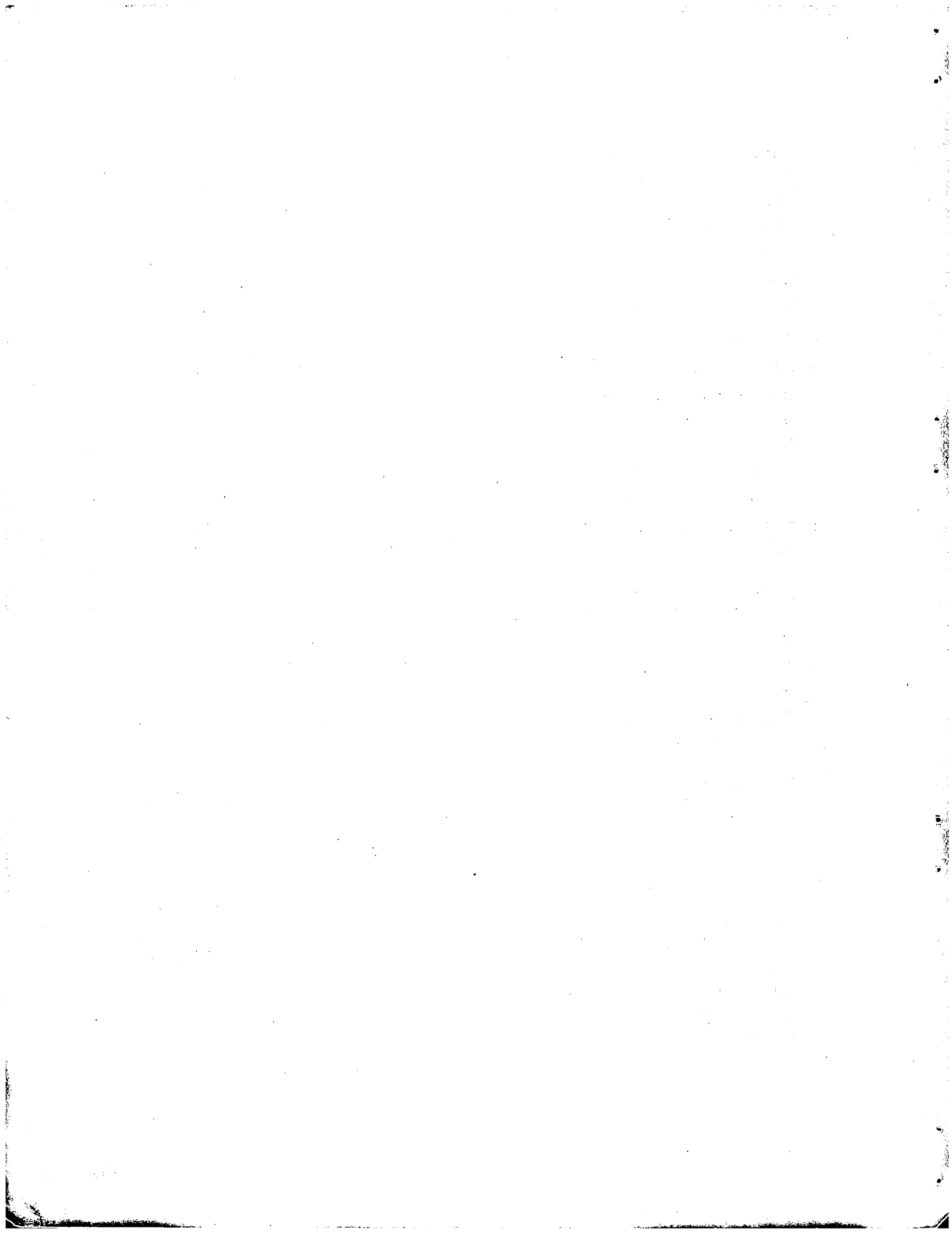
The authors welcome this opportunity to acknowledge the administrative and engineering cooperation of C. A. Mossman, ORNL. His persistent efforts greatly facilitated the completion of this research program.

J. W. Reynolds' work on programming the Oracle for data reduction at the various stages of the research program is greatly appreciated. This data reduction was of immeasurable value in the final analysis. The suggestions of D. A. Gardiner regarding statistical treatment of data were quite helpful.

During the course of the research, the helpful suggestions for experiments and their interpretation supplied by E. E. Stansbury are gratefully acknowledged.

The execution and completion of the many laboratory experiments are due to the capable assistance of the following persons: At ORNL, B. C. Thompson and W. W. Johnston; and at the University of Tennessee, J. P. Nichols, A. E. Lewis, L. A. Hendrix, D. C. Holt, R. Hicks, D. Hewette, R. G. Domer, E. Hina, and Mrs. J. S. Settlemyer.

In addition, the suggestions and encouragement of many interested people at ORNL and at a number of industrial concerns throughout the U.S. are gratefully acknowledged.



## CONTENTS

1. SUMMARY .....	1
Temperature Standards .....	1
Thermocouple Oxidation .....	1
Physical Properties .....	2
Drift Tests .....	2
Summary of Appendices .....	3
General Conclusions .....	3
2. INTRODUCTION .....	5
3. CONSISTENCY OF TEMPERATURE-MEASUREMENT STANDARDS FROM 0 TO 960°C .....	6
Standardization of Equipment .....	6
Standard Melting Points .....	6
Resistance Thermometry .....	6
Thermocouple Thermometry .....	10
Thermocouple Insulator Shunting Effect .....	17
4. OXIDATION STUDIES ON NICKEL-BASE THERMOCOUPLE ALLOYS .....	18
Experimental Procedure .....	20
Weight Gain .....	20
Results of Weight-Gain Measurements .....	21
Photomicrographic Examination .....	29
EMF Correlation Experiment .....	34
5. PHYSICAL PROPERTIES .....	36
Introduction .....	36
Properties and Materials Studied .....	37
Experimental Results and Discussion .....	37
Hardness Results .....	37
Electrical Resistivity Results .....	41
Thermal-EMF Results .....	45
Homogeneity Results .....	49
6. THERMOCOUPLE DRIFT – EMF VS TIME AT TEMPERATURE .....	57
Drift Test Facilities .....	57
Data Processing .....	61
Low-Temperature Drift Test – Part I .....	64
Test Description .....	64
Results .....	65
Low-Temperature Drift Test – Part II .....	78
High-Temperature Drift .....	79
Thermocouple Drift Test at 900°C in Pressurized Oxygen .....	100
Nickel-Silicon Alloys – Thermoelectric Stability in Air at 980°C .....	101

Drift at 1000°C of Nickel-Base Thermoelements in Refractory Protection Tubes Containing	
Special Environments .....	103
Test Configuration .....	104
Environmental Changes .....	104
Discussion of Results .....	110
Supplementary Drift Experiments with Refractory Tubes .....	111
APPENDIX A – SMOOTHED CHROMEL-ALUMEL TABLES .....	114
APPENDIX B – COPPER-CONSTANTAN THERMOCOUPLE TABLE .....	119
APPENDIX C – GEMINOL-P/N TEMPERATURE-EMF CALIBRATION TABLES .....	122
APPENDIX D – CHEMICAL ANALYSIS OF THERMOELEMENTS .....	126
APPENDIX E – CALIBRATION DATA FOR NICKEL-SILICON ALLOY .....	128
APPENDIX F – MISCELLANEOUS CALIBRATIONS .....	131
APPENDIX G – EFFECTS OF ISOTHERMAL HEAT TREATMENTS ON CALIBRATION .....	137
APPENDIX H – EVALUATION OF ACCURACY AND PRECISION OF CHROMEL-P, ALUMEL THERMOCOUPLES FOR A SPECIAL APPLICATION AT 400°C .....	148
APPENDIX I – CARBIDE STUDIES .....	151

# THERMOCOUPLE RESEARCH TO 1000°C – FINAL REPORT

J. F. Potts

D. L. McElroy

## 1. SUMMARY

One of the fundamentals of physical measurement is that any sensing device affects the quantity being measured. A thermocouple is a valuable and powerful tool which tends to minimize temperature errors in nearly inaccessible places. Advantages of a thermocouple as a temperature transducer might be listed as: (1) compactness, (2) ease of fabrication and installation, (3) sensitivity of indication of temperature, and (4) relatively low cost. Disadvantages and error sources exist and might be listed as: alteration of thermoelectric characteristics caused by (1) installation, (2) the environment of the system, (3) nonuniformity of the initial materials, and (4) changes occurring within the system other than those due to environmental changes. Any of the foregoing may tend to decrease the effective life of the device, or alter the balance between life and compactness.

When studying the magnitude of the effects causing changes in thermoelectric characteristics, one finds that a thermocouple assembly may not be totally separable from the environment of the space it occupies. Indeed, a thermocouple assembly (thermoelement wires, insulating refractories, and protection tube) may create its own environment which can be quite different from that of the entire system. This research was generally confined to an environment of air for tests with some consideration of these unique local environments.

In the present research, attempts have been made to isolate and control certain of these variables during investigation of thermocouple behavior. The results of these studies are summarized below.

### TEMPERATURE STANDARDS

As a critical evaluation of standards measurements, a number of fixed-melting-point samples, two platinum resistance thermometers, and a 90% Pt–10% Rh, Pt thermocouple (all certified by the NBS) were intercompared and used to calibrate two other 90% Pt–10% Rh, Pt thermocouples from 0 to 960°C. Care in instrumentation, circuitry, and experimental procedure allowed this work to obtain the accuracy and reproducibility certified by the NBS for these secondary standards.

The melting points determined by the resistance thermometers agreed with the certified values to within 0.05°C. The resistance thermometers agreed with each other to within 0.02°C at these points, with a reproducibility of 0.01°C. The measured thermal emf of the NBS 90% Pt–10% Rh, Pt thermocouple and the certified values at the aluminum and silver points were within 3  $\mu\text{v}$  of each other. A difference of only 0.002°C was found for the distilled-water–ice point for either clear or cloudy distilled-water–ice. Calibrations on a four-wire 90% Pt–10% Rh, Pt thermocouple, using various combinations of the thermocouple legs, gave emf measurements which agreed to within  $\pm 0.2 \mu\text{v}$ , the limit of resolution of the potentiometer. Homogeneity tests of wire used for these thermocouples indicated a fluctuation of  $\pm 2 \mu\text{v}$ , much of which was due to the testing apparatus. The melting-point calibrations were checked by a comparison calibration to within 0.5  $\mu\text{v}$ . Leakage-resistance tests on thermocouple insulation at the silver point suggested a cause of errors but gave no clear correlation of the emf variations found in the thermocouples at that point.

### THERMOCOUPLE OXIDATION

Oxidation of thermoelements is apparently one of the direct causes of the isothermal drift of thermal emf and the ultimate failure of nickel-base thermocouples. Consequently, measurements were made of isothermal weight gain resulting from exposure to air at 700, 800, 900, and 1000°C for times up to 500 hr on a number of commercial and laboratory-prepared nickel-base alloys. The results, though not refined, distinguished the role of alloy composition on reaction rate. Supplementary data on diameter changes, microstructures, and thermal emf were obtained. As expected, minimum oxidation was noted at the lower temperatures.

On alloys of similar composition to that of Chromel-P beneficial effects were noted for niobium additions, refined grain size, reduction of iron content, and removal of manganese. Alloys containing 18 to 20% chromium oxidize less by a factor of 10 than do the 9 to 10% chromium alloys, such as Chromel-P. Alumel oxidizes slightly

faster than pure nickel and reacts about three times faster than does Chromel-P. If the manganese, silicon, and aluminum in Alumel are replaced by silicon only, as in the alloys Special Alumel, Geminol-N, and Kanthal-N, oxidation resistance approaching Chromel-P is obtained.

Alloy diameter changes due to oxidation at 900 to 1000°C for 500 hr classify the tested materials in three groups: (1) highly alloyed materials showing less than a 1% change, (2) Chromel-P-type alloys and binary Ni-Si alloys having 2 to 15% changes, and (3) Alumel and pure nickel showing changes of 15 to 50%. The microstructures of tested materials show the oxidation to be uniform in all cases, except for Alumel, in which an intergranular reaction is operative, and for Chromel-P in certain unique environments.

Chromel-P, Alumel, Geminol-P, and Geminol-N wires were isothermally heated in air at 1000°C for times up to 500 hr and calibrated at the silver point (960.8°C). The calibration changes were correlated with the oxidation results. Alumel showed a positive drift, reflecting an approach to the thermal emf of nickel as its constituents were oxidized. Changes in Geminol-P, Geminol-N, and Chromel-P were as predicted by the composition-emf curves, but slightly more than the expected drift occurred in Geminol-P.

#### PHYSICAL PROPERTIES

Additional changes in the thermal emf of a material may be associated with changes in its physical state caused by cold-working, recovery, and recrystallization. Measurements of hardness, electrical resistance, and thermal emf (by calibration, drift, and homogeneity tests) have been made and correlated with the emf changes of the thermoelements. Most of the emphasis has been on Chromel-P and Alumel, but work was done on other nickel-base alloys as well. There is some published qualitative data regarding the effect of physical properties on the thermal emf of nickel-base alloys. However, we found very little information on the isolated effects of the various properties or states. The work reported here was deemed necessary to approach quantitatively an understanding of cause-effect relations in thermocouples.

Results of the physical-properties studies suggested the following conclusions:

1. As-received thermocouple wire is generally cold-worked less than 5%.

2. Depending on the composition of the alloy, the percentage of cold-working, and the time at temperature, the recrystallization temperature range of the nickel-base thermocouple alloys is between 500 and 750°C. The recovery temperature range is between 250 and 450°C. These values are tabulated for 12 thermoelements.

3. The electrical resistivity of certain of the alloys decreases with increasing cold work, suggesting metallurgical changes such as ordering induced by cold-working.

4. Cold-working causes greater changes in the thermal emf of Chromel-P than in Alumel. For Chromel-P the emf shift increases with increased cold-working. For Alumel the thermal emf first increases and then decreases as cold-working increases.

5. Heat treatment designed to produce the recovered state in originally cold-worked material causes a recovery of nearly 90% of the error induced by cold-working in Chromel-P and somewhat less in Alumel, principally because the initial change in Alumel is less.

6. A unilateral temperature gradient apparatus proved to be a very sensitive and expedient tool in detecting thermal emf changes associated with variations in the physical state of individual wires. Effects due to cold-working, annealing, and oxidation were readily detectable, and the results were shown to be interpretable in terms of thermocouple calibration errors.

Generally, the effects realizable from cold work produce calibration shifts of less than 10°C in nickel-base thermocouples.

#### DRIFT TESTS

A large number of drift tests were performed under both static and time-varying temperatures from 150 to 1000°C on a variety of nickel-base alloys, some commercially available and some prepared by the authors. Unsuccessful attempts were made to quantitatively correlate observed drift rates with the isolated physical and corrosion-resistant properties of the alloys. Qualitative correlation in most cases was possible. It was established that to within  $\pm 1^\circ\text{C}$ , there was no evidenced advantage of any one of the base-metal thermocouples to 390°C. For any of these materials in swaged-sheath construction, one is faced with the tedious problem of careful preparation and nondestructive testing of sheath and

junction integrity prior to use. Tests at temperatures up to 700°C indicated that to within  $\pm 2^\circ\text{C}$  there were no adverse effects of the lack of use of special handling techniques in preparing thermocouple assemblies. In spite of this conclusion from the tests performed, the authors still think it unwise to not exercise all reasonable caution in handling and assembling thermocouples. Above 750°C, the advantages of using meticulous care in preparation and handling were borne out by results here reported. Over the range 750 to 1000°C, the advantage of a nickel-silicon binary alloy such as Special Alumel over Alumel is made obvious. Further, the advantage of thermocouple construction with swaged sheath and dense-packed insulation is established from the point of view of life expectancy for a given wire size. A proved technique for simultaneous sheath closure and junction manufacture was demonstrated for base metal thermocouples. A valuable data-handling technique was developed for use in performance testing of large numbers of thermocouples.

Some preliminary testing at 1000°C of thermocouples in long refractory tubes containing metal powders is reported.

#### SUMMARY OF APPENDICES

The appendices contain results and discussions of revised thermal-emf tables, chemical analysis of alloys, special calibrations, and several short-range studies on thermocouples.

Discontinuities in NBS Circular 561, Table 6, for Chromel-Alumel thermocouples have been removed to within  $\pm 0.5 \mu\text{v}$ , and useful smoothed tables for Chromel-Alumel, Chromel-platinum, and Alumel-platinum are presented from 0 to 1370°C. A similar table smoothed from second-difference calculations is presented for copper-constantan from 0 to 60°C. These tables are not better representations than the NBS tables but are somewhat more regular. A cursory evaluation of the existing Driver-Harris Company table for Geminol-P/N and of a derived table indicates that more data is needed before a standard curve can be established.

Wet chemical analyses obtained on commercially available thermoelements show sufficient variations that manufacturer's differences introduced for "curve matching" cannot be detected for the same nominal compositions. Wet chemical analyses of Special Alumel (Hoskins No. 194 alloy), Chromel-P + Nb, Vacominus, and Vacoplus are presented.

The thermal emf of alloys of nickel with 0 to 5% silicon has been studied at four temperatures. Additions of silicon up to 2% produce the greatest changes in the thermal emf of nickel, and a 3% silicon addition produces the most linear emf-temperature relation of the compositions tested. Miscellaneous thermal emf's of ten nickel-base negative thermoelements and seven nickel-base positive thermoelements are reported. The more oxidation-resistant positive thermoelements produce less thermal emf than Chromel-P, relative to platinum.

A study of the effects of isothermal heat treatments from 500 to 800°C in helium on Chromel-P, Chromel-P + Nb, Kanthal-P, and Geminol-P showed that once recovery and recrystallization are complete, only small random changes occur in the calibration. Significant calibration deviations were noted in wires with thin oxide coatings, which resulted from oxygen leaks into the helium system.

Some of the methods and understanding developed in the course of this research were used to define the precision attainable from Chromel-Alumel at 400°C. Agreement of homogeneity and calibration results on wire from a given heat-treating schedule, which was primarily designed to accomplish recovery, revealed 30 gage wire unsatisfactory, but 24 gage wire sufficiently stable to allow absolute measurements to no worse than  $\pm 0.5^\circ\text{C}$  at 400°C. Thermocouple drift data indicates that this tolerance could be achieved for at least 5000 hr at 400°C.

A study was made of the change in thermal emf of Chromel-P if all the carbon normally found in Chromel-P (<0.03%) were to precipitate as chromium carbide. Metallographic and calibration data obtained refute this as a potential internal cause of thermocouple drift. An external source of carbon can lead to extensive precipitation of chromium carbide in Chromel-P and a 20% drift in thermal emf at 750°C.

#### GENERAL CONCLUSIONS

In addition to the above conclusions the authors would like to present the following as their answers to certain recurring questions regarding thermocouples and their applications.

It is possible to purchase Chromel-P and Alumel thermocouple wire which is quoted as being within  $\frac{3}{8}\%$  of the accepted Chromel-Alumel table, whereas normal Chromel-Alumel is within  $\frac{3}{4}\%$  of this table. It is important that the user realize that the  $\frac{3}{8}\%$

material has less initial calibration error on heating and that this does not in any way imply that the drift performance will be superior to normal  $\frac{3}{4}\%$  material. Drift tests conducted on both types of material have borne out these statements.

If certain compromises are allowed, this research indicates that a beneficial choice of available thermoelements exists to obtain drift performance superior to that of the conventional Chromel-Alumel thermocouple. As a substitute for the Alumel, it has been shown that the binary Ni-Si alloys show superior oxidation resistance without a sacrifice in thermal emf. As a substitute for Chromel-P, several choices exist: (1) the highly alloyed Hoskins alloys 875 or 825, or alloys of a higher chromium content, as in Geminal-P, show better oxidation resistance but have less thermal emf; and (2) the oxidation resistance is somewhat improved without a sacrifice in thermal emf if the Chromel-P + Nb is chosen. Certain of these alloys demand further study to ensure the reproducibility available in Chromel-P and Alumel. The ultimate limit available in Chromel-P and Alumel is probably  $\pm 1^\circ\text{F}$ . Whether this is attainable in these alloys is contingent also upon a study of the short-range-order effects known to exist in the 80% nickel-20% chromium alloys and suspected in Chromel-P.

Future drift tests should be so planned as to investigate fewer variables per test. By increasing the family size, decreasing the type differences, shortening the particular test time, and including more auxiliary diagnostics to isolate the cause of observed changes, the value of a given test series is tremendously increased over that of the one to two year tests described herein. The

tools for accomplishing these objectives have been developed by the present research but were not completely available until the very last low-temperature tests were being planned and executed.

Exemplification of this need exists in the lack of correlation found between the basic studies and the observed thermocouple drift performance, especially in the early stages of a drift test, where recovery and recrystallization are operational. Future tests should be designed to more closely follow these stages and to incorporate a means of deciding the source of observed changes or of compensating effects. Lack of correlation has also been found in tests where mass transfer was thought to be the cause of observed changes.

In spite of the fact that tests were done in air, evidence has been found on tube tests and on swaged assemblies which indicates the presence of a gradient in potential oxidizing power in the confines of the thermocouple. Loosely packed and tightly packed swaged assemblies have shown oxide growths in local areas which were sufficient to cause the Chromel thermoelement (wire surrounded by the oxide) to be magnetic. This looms as a potentially serious problem for a thermocouple functioning in a system subject to large temperature changes and should be studied in more detail.

The whole area of the relative advantage of the various refractory oxides as thermocouple insulators was not seriously considered and should be the subject of further investigations along with, of course, development of stable thermocouple materials for higher-temperature use.

## 2. INTRODUCTION

High-temperature-research programs have increased the need for meaningful temperature measurements. To meet this need the Oak Ridge National Laboratory and its subcontractor, the University of Tennessee, jointly established a thermocouple research program. The program was to provide a means for improving the art of thermoelectric measurement through a better understanding of the basic behavior of thermocouples. This is opposed to the limiting approach of establishing confidence in a given measurement situation by closely duplicating service conditions.

Basic studies have been directed toward the solution of two problems: (1) How reliable are Chromel-P, Alumel thermocouples for measuring temperatures up to 1000°C? (2) Why is this combination good or bad? Does a better combination exist and, if so, why? Toward this end, a report<sup>1</sup> on the progress of the first year's effort was published. This report included a general discussion of thermocouple history, and that of

<sup>1</sup>D. L. McElroy, *Progress Report I, Thermocouple Research, Report for the Period Nov. 1, 1956 to Oct. 31, 1957*, ORNL-2467.

Chromel-P, Alumel in particular, details of experimental equipment constructed for the thermocouple test program, and results and conclusions from the initial tests on various thermocouples.

Generally the initial approaches have been extended, and, in addition, new ones have been undertaken in seeking the basic cause-effect relations for thermocouple behavior. The present report contains the results of detailed studies on (1) the consistency of temperature measurement standards from 0 to 960°C; (2) the oxidation of commercial and special thermoelements and the accompanying calibration changes; (3) the physical properties, such as cold-working, recovery, and recrystallization, and their effects on calibration; and (4) the specific performance of commercial thermocouples as influenced by time and temperature of operation. In addition, a number of diagnostic short-range tests are reported. It had been hoped that the results of these studies would lead to a thermocouple handbook; however, it has been found that this was not possible, but the results do provide guidance to the solution of certain types of applications.

### 3. CONSISTENCY OF TEMPERATURE-MEASUREMENT STANDARDS FROM 0 TO 960°C

#### STANDARDIZATION OF EQUIPMENT

A critical evaluation of standards measurements was made in order to establish the validity of the presently used and of some contemplated methods of temperature-measurement calibration employed at the Oak Ridge National Laboratory Instrument Standards Facility. A number of fixed-melting-point samples, two platinum resistance thermometers, and a 90% Pt-10% Rh, Pt thermocouple (all certified by the National Bureau of Standards) were intercompared by the use of precision electrical instruments which had been carefully calibrated against NBS-certified resistors and unsaturated standard cells. The ice, tin, lead, and zinc melting points (0, 231.9, 327.4, and 419.5°C, respectively) determined by the resistance thermometers agreed with the NBS-certified values to within 0.05°C. The two platinum resistance thermometers agreed with each other to within 0.02°C at these points, with reproducibility of 0.01°C. Observed values of the melting point (630.4°C, not certified) of the antimony sample were reproducible within 0.02°C. The resistance thermometer indication of the aluminum freezing point (660.0°C) agreed with the NBS-certified value within 0.1°C. The maximum discrepancy was 3  $\mu$ v (approx. 0.3°C) between the measured thermal emf of the 90% Pt-10% Rh, Pt thermocouple and the certified values at the aluminum and silver freezing points.

Constant attention was paid to every aspect of the instrumentation. The accuracy of the Mueller bridge used for resistance thermometer determinations, after calibration, was within two parts in  $10^5$ . The potentiometer and the standard cell used with it were stable to within five parts in  $10^5$ , with an over-all absolute accuracy of one part in  $10^4$  (approximately 0.1°C with the thermocouples used.) There was a maximum discrepancy in the thermocouple calibrations of 0.2°C caused by insulator leakage resistance at the silver freezing point.

Ice-point checks with the standard resistance thermometers indicated that there was less than 0.002°C variation in the ice point in an air-saturated slurry of distilled water and ice made from distilled water, irrespective of whether the ice was "cloudy" or clear. There was, as expected, as much as 0.01°C variation in the ice-point temperature in

tap-water ice slurries. The former was used throughout these tests.

From experience gained in this standards work, circuitry should be employed for routine checks of stray thermal emfs in order to realize the utmost accuracy of thermocouple calibrations. In addition, more than one thermocouple of common hot junction should be calibrated each time to provide a verification of results by using all possible algebraic combinations of emf (see Fig. 3.2).

#### STANDARD MELTING POINTS

In view of the apparent reproducibility (according to preliminary tests) of the melting points of the pure metal samples, they were used in conjunction with NBS-certified platinum resistance thermometers and 90% Pt-10% Rh, Pt thermocouples to resolve a long-standing question at ORNL as to the absolute accuracy and reproducibility realizable from these secondary standards.

The furnaces and crucibles in which the metal samples were melted have been previously described.<sup>1</sup> The samples and their assigned melting and/or freezing temperatures are shown in Table 3.1. Included for later reference are the microvolt readings corresponding to these temperatures for a 90% Pt-10% Rh, Pt thermocouple, as taken from NBS Circular 561, Table 2. The measured melting points were determined by use of the resistance thermometers, to be discussed in the next section. The lead melting point temperature showed the greatest deviation from NBS value and proved to be the least reproducible. This was primarily because there was no distinct arrest at the freezing point of the lead used.

#### RESISTANCE THERMOMETRY

The two platinum resistance thermometers used in the tests shown in Table 3.1 had been certified by the NBS at the ice, steam, and sulfur points. One of the thermometers, Leeds and Northrup Company type 8163 Special, serial No. 1052547 (hereafter designated No. 1) was usable to 630°C. At the conclusion of this series of lower-temperature tests, No. 1 thermometer was used to verify the

<sup>1</sup>D. L. McElroy, *Progress Report 1, Thermocouple Research, Report for Period Nov. 1, 1956 to Oct. 31, 1957*, ORNL-2467, p 15.

Table 3.1. Assigned and Measured Values of Fixed Points

Sample	Fixed Point (°C)		90% Pt - 10% Rh, Pt EMF(μv) <sup>a</sup>
	Assigned	Measured	
Tin, NBS 42e			
Melting		231.91	1709.3
Freezing	231.91 <sup>b</sup>	231.86	1708.9
Lead, NBS 49d	327.40 <sup>b</sup>	327.35	2567.2
Zinc, NBS 43g			
Melting		419.50	3437.5
Freezing	419.5 <sup>b</sup>	419.49	3436.1
Antimony <sup>c</sup>			
Melting		630.41	5536.1
Freezing		630.37	5535.7
Aluminum, NBS 44e			
Freezing	660.0 <sup>b</sup>	659.92 <sup>d</sup>	5842.0
Silver <sup>e</sup>			
Freezing	960.8 <sup>f</sup>		9119.8

<sup>a</sup> Taken from NBS circular 561, Table 2.

<sup>b</sup> NBS-assigned value.

<sup>c</sup> Associated Lead Manufacturers, Ltd., 99.999% pure.

<sup>d</sup> Resistance thermometer reproducibility questioned.

<sup>e</sup> Handy & Harman, 99.999% pure.

<sup>f</sup> Internationally accepted value.

aluminum freezing point. The second resistance thermometer, Leeds and Northrup Company type 8163 Standard, serial No. 1191768 (hereafter designated No. 2) was usable to 500°C. A Leeds and Northrup type G-2 Mueller bridge was used to measure the resistance of the thermometers. Before use, the resistance bridge was carefully calibrated against a standard 10-ohm resistor, the value of which had been certified by the NBS to one part in 10<sup>5</sup>. Corrections, so determined, were applied to the observed resistance values.

The Callendar equation was used to calculate the temperature corresponding to the measured resistance. The Callendar equation,

$$t = \frac{R_t - R_0}{C} + \delta \left( \frac{t_0}{100} - 1 \right) \frac{t}{100},$$

where  $C \equiv (R_{100} - R_0)/100$ , was used in calculating these values. The coefficients used in the Callendar equation were those specified in the respective NBS certificates, with the exception of the  $R_0$  term (the resistance of the thermometer at the ice point,

0°C). This value could have changed due to aging of the thermometers or a discrepancy in the absolute calibration of the Mueller bridge. Since the resistance-temperature relation for these thermometers involves the ratio of the resistance at an unknown temperature to that at the ice point, the  $R_0$  value determined during these tests was used. The discrepancy between the  $R_0$  (NBS) and the  $R_0$  (here measured) was approximately 0.001 ohm, depending upon whether distilled water and distilled-water ice or tap water and ice were used. The difference noted due to the distilled-water ice being clear or cloudy was less than 0.0005 ohm.

The results of the melting point determinations are tabulated in Tables 3.2 and 3.3 for the two thermometers in the order in which the measurements were made. Distilled water and ice were used for  $R_0$  determination.

Figure 3.1 illustrates the variation observed in the respective thermometers at the assigned melting points. This plot serves to summarize the results presented in Tables 2.2 and 2.3.

Table 3.2. Fixed-Point Determinations by No. 1 Resistance Thermometer, Arranged Chronologically

Fixed Point	Resistance (ohms)	Temperature* (°C)
Ice	25.5021	
Tin (melt)	48.2631	231.926
Tin (melt)	48.2626	231.921
Tin (melt)	48.2632	231.927
Tin (melt)	48.2626	231.921
Tin (freeze)	48.2578	231.870
Tin (freeze)	48.2570	231.862
Tin (freeze)	48.2581	231.873
Lead (melt)	57.1614	327.351
Lead (melt)	57.1606	327.342
Lead (melt)	57.1610	327.347
Zinc (freeze)	65.4949	419.487
Zinc (melt)	65.4962	419.501
Zinc (melt)	65.4969	419.508
Zinc (freeze)	65.4950	419.488
Zinc (melt)	65.4969	419.508
Antimony (melt)	83.6189	630.423
Antimony (melt)	83.6182	630.415
Antimony (melt)	83.6169	630.399
Antimony (freeze)	83.6162	630.391
Antimony (freeze)	83.6130	630.352
Antimony (freeze)	83.6126	630.348
Zinc (melt)	65.4969	419.508
Zinc (melt)	65.4967	419.506
Zinc (freeze)	65.4947	419.485
Zinc (freeze)	65.4948	419.486
Lead (melt)	57.1654	327.394
Lead (melt)	57.1614	327.351
Lead (melt)	57.1622	327.359
Tin (melt)	48.2632	231.927
Tin (melt)	48.2630	231.925
Tin (freeze)	48.2559	231.850
Tin (freeze)	48.2558	231.849
Aluminum (freeze)	86.0445	659.919

\*Calculated by means of the Callendar equation, with

$$R_0 = 25.5021 \text{ (UT),}$$

$$C = 0.00392554 \text{ (NBS),}$$

$$\delta = 1.49_2 \text{ (NBS).}$$

Table 3.3. Fixed-Point Determinations by No. 2 Resistance Thermometer, Arranged Chronologically

Fixed Point	Resistance (ohms)	Temperature* (°C)
Ice	25.4997	
Tin (melt)	48.2601	231.905
Tin (freeze)	48.2530	231.830
Tin (melt)	48.2605	231.909
Tin (freeze)	48.2531	231.831
Tin (melt)	48.2606	231.910
Lead (melt)	57.1589?	327.327
Lead (melt)	57.1582?	327.319
Lead (melt)	57.1598?	327.336
Zinc (melt)	65.4966	419.499
Zinc (freeze)	65.4955	419.487
Zinc (melt)	65.4968	419.501
Zinc (freeze)	65.4956	419.488
Lead (melt)	57.1603	327.341
Lead (melt)	57.1630	327.371
Tin (melt)	48.2600	231.904
Tin (freeze)	48.2588	231.891
Tin (melt)	48.2595	231.899
Tin (freeze)	48.2574	231.877
Ice	25.4997	
Ice	25.4997	
Zinc (melt)	65.4961	419.494
Zinc (freeze)	65.4943	419.473
Zinc (melt)	65.4959	419.492
Zinc (freeze)	65.4944	419.474
Ice	25.4996	

\* Calculated by means of the Callendar equation, with

$$R_0 = 25.499_7 \text{ (UT),}$$

$$C = 0.0039261_2 \text{ (NBS),}$$

$$\delta = 1.491_4 \text{ (NBS).}$$

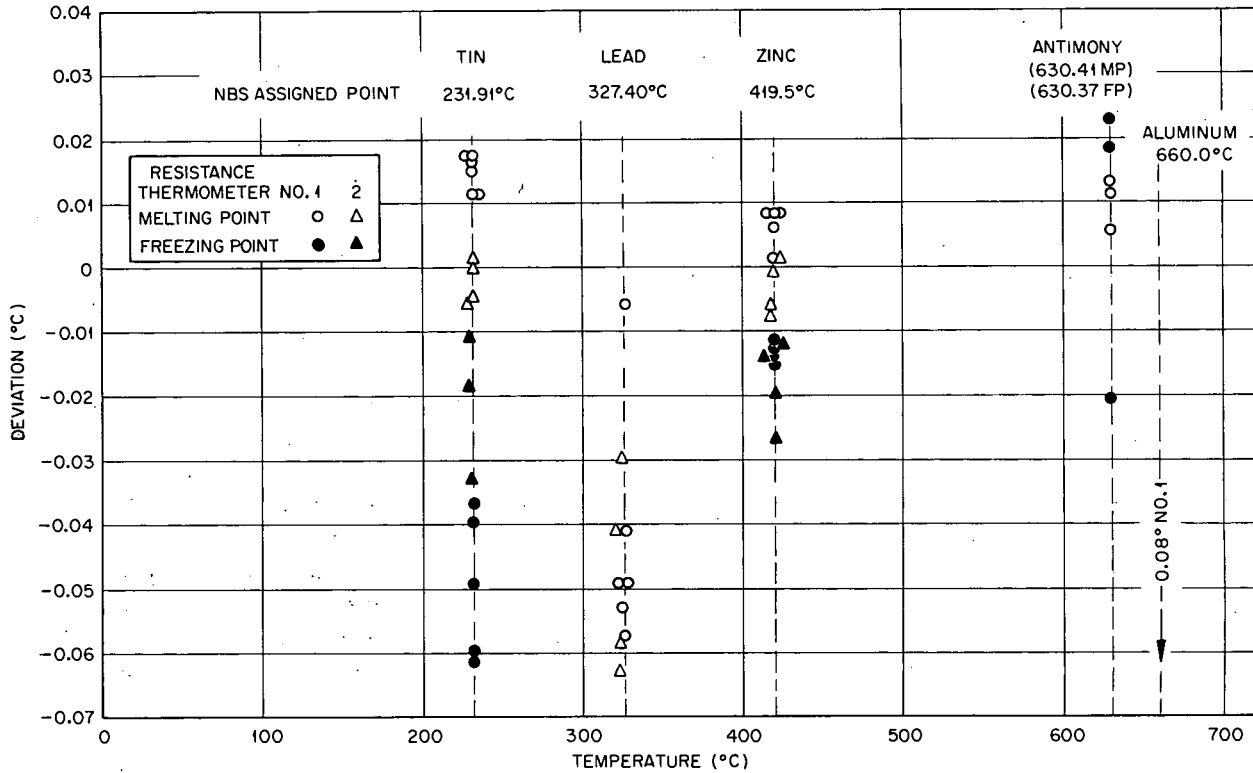
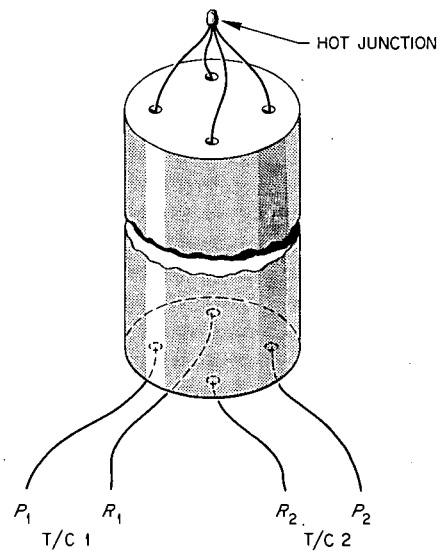


Fig. 3.1. Variation Observed in Resistance Thermometers Nos. 1 and 2 at Fixed Points.

**THERMOCOUPLE THERMOMETRY**

Four 90% Pt-10% Rh, Pt thermocouples were calibrated in a series of tests at the tin, lead, zinc, antimony, aluminum, and silver points. Thermocouples 1 and 2 were simultaneously calibrated, using a common junction (see Fig. 3.2). Thermocouples 3 and 5A were fabricated from the same spools of wire, but thermocouple 5A was previously calibrated at NBS. With the exception of the NBS-certified thermocouple (No. 5A), which was calibrated without disturbing its junction or insulator, the thermocouple wires were washed with ether and then annealed at 1200°C in air for 1 hr before being inserted into insulating tubes of vitrified alumina. The junctions were welded in a reducing oxy-acetylene flame. The thermocouple emf was measured by use of a Leeds and Northrup Company type K-3 potentiometer and a galvanometer with a long optical lever arm providing a deflection sensitivity of 0.1  $\mu$ V/cm.

In all the measurements, the residual thermal emf of switches and connections was accounted for by removing the thermocouple leads from the mercury



$$E_{P_1 R_1} = E_{P_2 R_2} + E_{P_1 P_2} + E_{R_1 R_2}$$

Fig. 3.2. Common Junction for Thermocouple Calibration.

tubes in the reference temperature bath and shorting between the two sides of the circuit with a copper wire. The residual emf thus measured was subtracted algebraically from the total thermocouple emf, and it is this corrected emf which is presented in tabular form.

The first series of calibrations was made on a B&S 20-gage 90% Pt-10% Rh, Pt thermocouple at the tin, zinc, lead, and antimony points to establish the validity of the method. The results of this calibration appear in Table 3.4 (thermocouple No. 3) and are summarized graphically in Fig. 3.3.

Next, the dual thermocouple system was checked. In this series of tests advantage was taken of the possibility of obtaining emf measurements on the various combinations of thermocouple legs, since the four wires terminated in a common junction. In general these intercomparisons produced a tally to within  $\pm 0.2 \mu\text{v}$ , which is the limit of resolution of the K-3 potentiometer. Samples of wire adjacent to those from which thermocouple No. 2 was fabricated were checked for inhomogeneity in the unilateral

gradient furnace after an anneal similar to the one described above. This test indicated emf fluctuations of about  $\pm 2 \mu\text{v}$  in both the 90% Pt-10% Rh alloy and the platinum. Since the test was done at  $300^\circ\text{C}$  and the wires were fully annealed, it is felt that a considerable amount of this  $\pm 2 \mu\text{v}$  fluctuation could have been induced by the furnace traversing mechanism. This possibility was evidenced by the distortion in the wire after the gradient test.

The results of the calibrations of the dual thermocouples appear in Table 3.5, which presents the data in chronological order. This data is summarized graphically in Fig. 3.4. The rather poor emf reproducibility of  $\pm 2 \mu\text{v}$  improved to  $\pm 0.5 \mu\text{v}$  in the series at the end of the test wherein the thermocouples were cycled five times between the aluminum and silver freezing points. There is no explanation for the improved reproducibility.

The NBS-certified thermocouple No. 5A was next calibrated at the same points. The results of this work appear in Table 3.6 and are summarized

Table 3.4. Fixed-Point EMF Values for Thermocouple No. 3, Arranged Chronologically

Fixed Point	Measured EMF ( $\mu\text{v}$ )	Deviation from Values in NBS Circular 561* ( $\mu\text{v}$ )
Tin (freeze)	1713.3	+4.4
Tin (melt)	1713.8	+4.5
Zinc (freeze)	3441.0	+3.6
Lead (freeze)	2571.8	+4.6
Lead (melt)	2571.8	+4.6
Tin (freeze)	1712.7	+3.8
Lead (freeze)	2571.0	+3.8
Zinc (melt)	3441.3	+3.8
Antimony (melt)	5539.3	+3.2
Zinc (freeze)	3441.3	+3.9
Antimony (freeze)	5540.5	+4.8
Zinc (freeze)	3441.5	+4.1
Antimony (melt)	5539.2	+3.1
Lead (freeze)	2571.1	+3.9
Tin (freeze)	1713.5	+4.6
Antimony (freeze)	5540.5	+4.8
Zinc (freeze)	3441.3	+3.9
Zinc (freeze)	3441.4	+4.0
Tin (melt)	1713.5	+4.2
Lead (melt)	2572.1	+4.9
Zinc (melt)	3441.4	+3.9
Lead (melt)	2572.0	+4.8

\*See standard values, last column, Table 3.1.

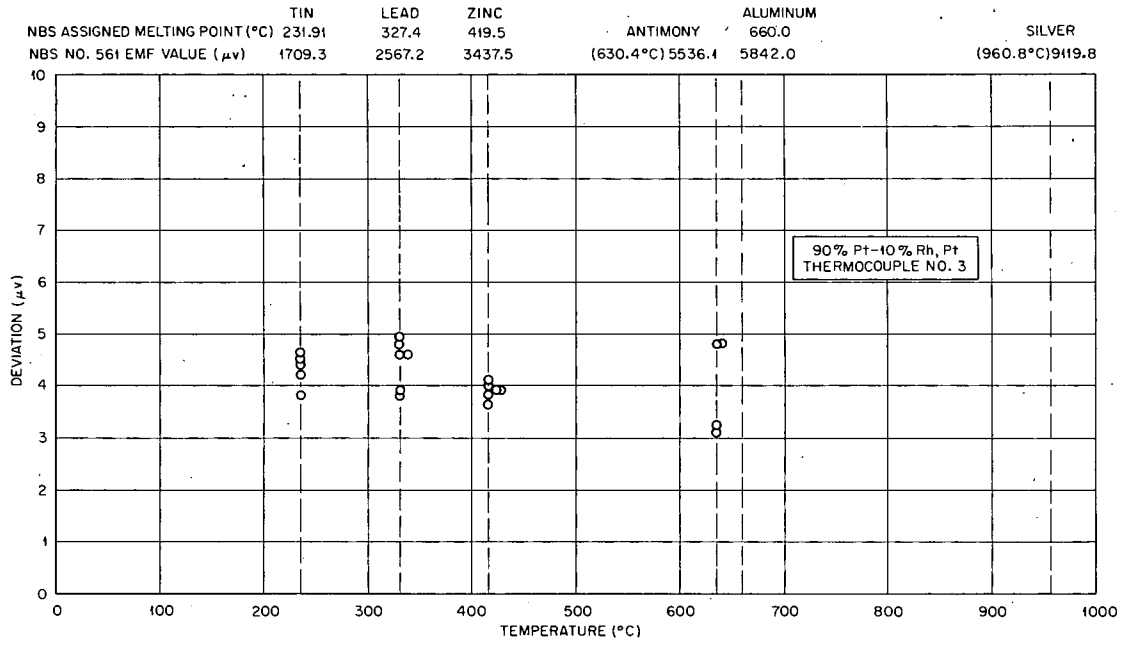


Fig. 3.3. Calibration of Thermocouple No. 3 at Fixed Points.

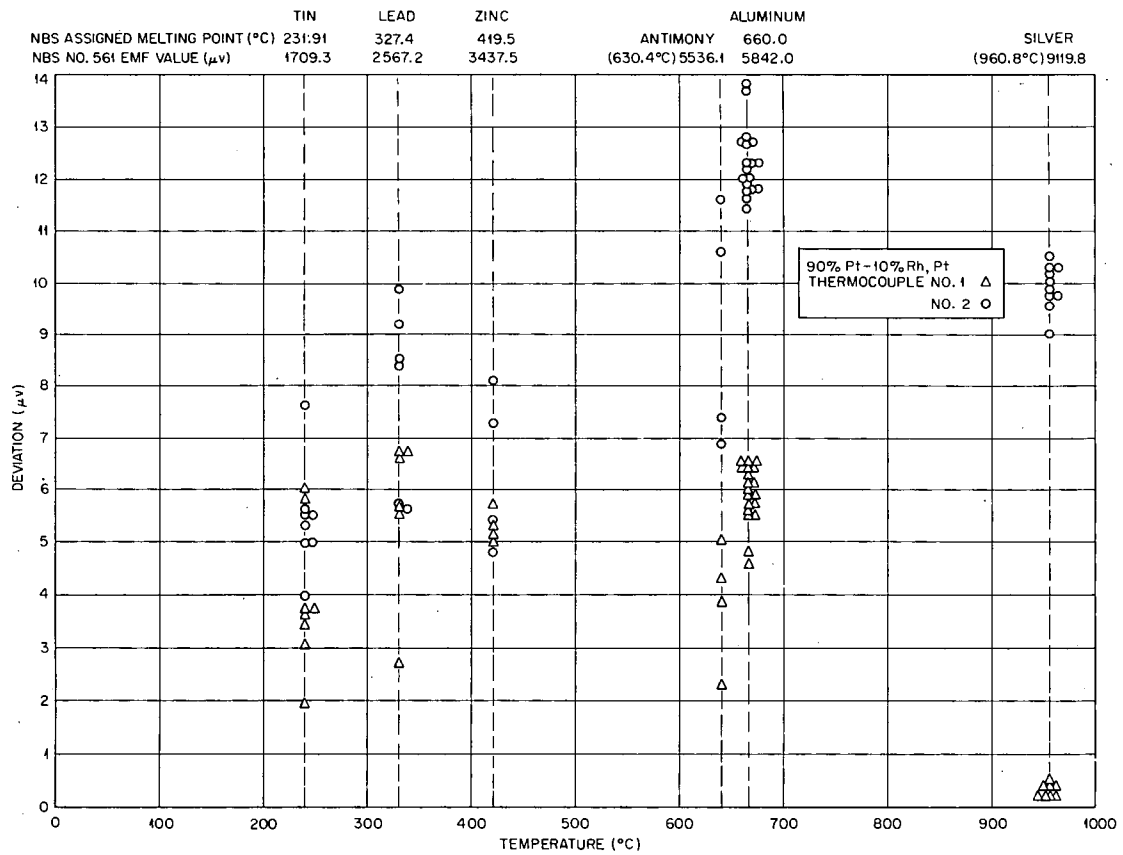


Fig. 3.4. Calibration of Thermocouples Nos. 1 and 2 at Fixed Points.

Table 3.5. Fixed-Point EMF Values for Thermocouples 1 and 2, Arranged Chronologically

Fixed Point	Thermocouple No. 1		Thermocouple No. 2	
	Measured EMF ( $\mu\text{V}$ )	Deviation* ( $\mu\text{V}$ )	Measured EMF ( $\mu\text{V}$ )	Deviation* ( $\mu\text{V}$ )
Ice point	- 0.6		- 0.2	
Tin (melt)	1711.2	+1.9	1713.3	+4.0
Tin (freeze)	1712.6	+3.7	1714.5	+5.6
Tin (melt)	1712.4	+3.4	1714.3	+5.0
Tin (freeze)	1712.6	+3.7	1714.4	+5.5
Tin (melt)	1712.3	+3.0	1714.3	+5.0
Tin (freeze)	1712.5	+3.6	1714.4	+5.5
Lead (melt)	2569.9	+2.7	2572.8	+5.6
Lead (melt)	2572.7	+5.5	2575.7	+8.5
Lead (melt)	2573.9	+6.7	2577.1	+9.9
Zinc (melt)	3442.8	+5.3	3445.6	+8.1
Zinc (freeze)	3442.4	+5.0	3444.7	+7.3
Antimony (melt)	5538.4	+2.3	5543.0	+6.9
Antimony (freeze)	5540.0	+4.3	5543.1	+7.4
Zinc (melt)	3443.2	+5.7	3442.9	+5.4
Zinc (freeze)	3442.5	+5.1	3442.2	+4.8
Lead (melt)	2573.8	+6.6	2572.9	+5.7
Tin (melt)	1715.1	+5.8	1714.7	+5.4
Tin (freeze)	1714.8	+6.0	1716.6	+7.7
Ice point	- 0.8		- 0.8	
Ice point	- 0.5		- 0.7	
Lead (melt)	2573.9	+6.7	2576.4	+9.2
Antimony (melt)	5539.9	+3.8	5546.7	+10.6
Antimony (freeze)	5540.7	+5.0	5547.3	+11.6
Lead (melt)	2572.8	+5.6	2575.6	+8.4
Ice point	- 0.6		- 0.9	
Aluminum (freeze)	5848.4	+6.4	5855.7	+13.7
Aluminum (melt)	5848.5	+6.5	5855.8	+13.8
Aluminum (freeze)	5848.5	+6.5	5855.8	+13.8
Silver (melt)	9119.0	-0.8	9130.3	+10.5
Silver (freeze)	9119.1	-0.7	9130.1	+10.3
Aluminum (melt)	5846.6	+4.6	5853.9	+11.9
Aluminum (freeze)	5846.8	+4.8	5853.8	+11.8

Table 3.5. (continued)

Fixed Point	Thermocouple No. 1		Thermocouple No. 2	
	Measured EMF ( $\mu\text{V}$ )	Deviation* ( $\mu\text{V}$ )	Measured EMF ( $\mu\text{V}$ )	Deviation* ( $\mu\text{V}$ )
Aluminum (melt)	5847.9	+5.9	5854.3	+12.3
Aluminum (freeze)	5848.1	+6.1	5854.2	+12.2
Aluminum (melt)	5848.4	+6.4	5854.8	+12.8
Aluminum (freeze)	5848.1	+6.1	5854.3	+12.3
Aluminum (melt)	5848.4	+6.4	5854.7	+12.7
Silver (freeze)	9120.3	+0.5	9128.8	+9.0
Silver (freeze)	9120.0	+0.2	9129.4	+9.6
Silver (freeze)	9120.2	+0.4	9130.1	+10.3
Aluminum (freeze)	5847.7	+5.7	5853.8	+11.8
Aluminum (freeze)	5847.5	+5.5	5853.4	+11.4
Aluminum (melt)	5848.3	+6.3	5854.7	+12.7
Aluminum (freeze)	5847.7	+5.7	5854.0	+12.0
Aluminum (melt)	5848.0	+6.0	5854.3	+12.3
Silver (freeze)	9120.2	+0.4	9129.8	+10.0
Silver (freeze)	9120.2	+0.4	9130.0	+10.2
Silver (freeze)	9120.0	+0.2	9129.5	+9.7
Aluminum (melt)	5848.5	+6.5	5854.7	+12.7
Aluminum (freeze)	5847.9	+5.9	5853.6	+11.6
Aluminum (melt)	5847.6	+5.6	5854.0	+12.0
Aluminum (freeze)	5847.5	+5.5	5853.8	+11.8
Silver (freeze)	9120.0	+0.2	9129.7	+9.9
Silver (freeze)	9120.0	+0.2	9129.6	+9.8

\*See standard values, last column, Table 3.1.

Table 3.6. Fixed-Point EMF Values for Oak Ridge Standard No. 5-A Thermocouple, Arranged Chronologically

Fixed Point	Measured EMF ( $\mu\text{V}$ )	Deviation from Values in NBS Circular 561* ( $\mu\text{V}$ )
Ice point	+ 0.0	
Tin (melt)	1715.3	+6.0
Tin (freeze)	1714.3	+5.4
Zinc (melt)	3444.5	+7.0
Zinc (freeze)	3444.2	+6.8
Antimony (melt)	5545.1	+9.0
Antimony (freeze)	5545.7	+10.0
Zinc (melt)	3444.9	+7.4
Zinc (freeze)	3444.7	+7.3
Lead (melt)	2574.8	+7.6
Tin (melt)	1716.0	+6.7
Tin (freeze)	1714.7	+5.8
Ice point	- 0.2	
Zinc (melt)	3445.2	+7.7
Zinc (freeze)	3444.8	+7.4
Antimony (melt)	5545.1	+9.0
Antimony (freeze)	5545.6	+9.9
Zinc (melt)	3444.8	+7.3
Zinc (freeze)	3444.7	+7.3
Ice point	- 0.1	
Aluminum (melt)	5852.4	+8.4
Aluminum (freeze)	5852.5	+8.5
Silver (melt)	9130.0	+10.2
Silver (freeze)	9129.9	+10.1
Aluminum (melt)	5852.8	+8.8
Aluminum (freeze)	5852.9	+8.9

\*See standard values, last column, Table 3.1.

graphically in Fig. 3.5, which also includes the NBS-certified values at the standard melting points. In addition, there was a certificate available covering an NBS comparison calibration on a thermocouple from the same spools from which No. 5A was fabricated. This data is also plotted in Fig. 3.5. The results obtained here were repeatable to  $\pm 0.5 \mu\text{v}$  and agreed with the NBS results to within  $\pm 3 \mu\text{v}$ . It is noteworthy that the NBS comparison calibration was also in agreement

with the NBS melting point calibration within approximately the same tolerance.

After the melting point determination, thermocouples Nos. 1 and 2 were intercompared in the rapid-heating furnace<sup>2</sup> and their difference agreed to within  $0.5 \mu\text{v}$  with the difference determined by the melting point calibrations.

<sup>2</sup>D. L. McElroy, *Progress Report I, Thermocouple Research, Report for Period Nov. 1, 1956 to Oct. 31, 1957, ORNL-2467, p 18-20.*

UNCLASSIFIED  
ORNL-LR-DWG 48560

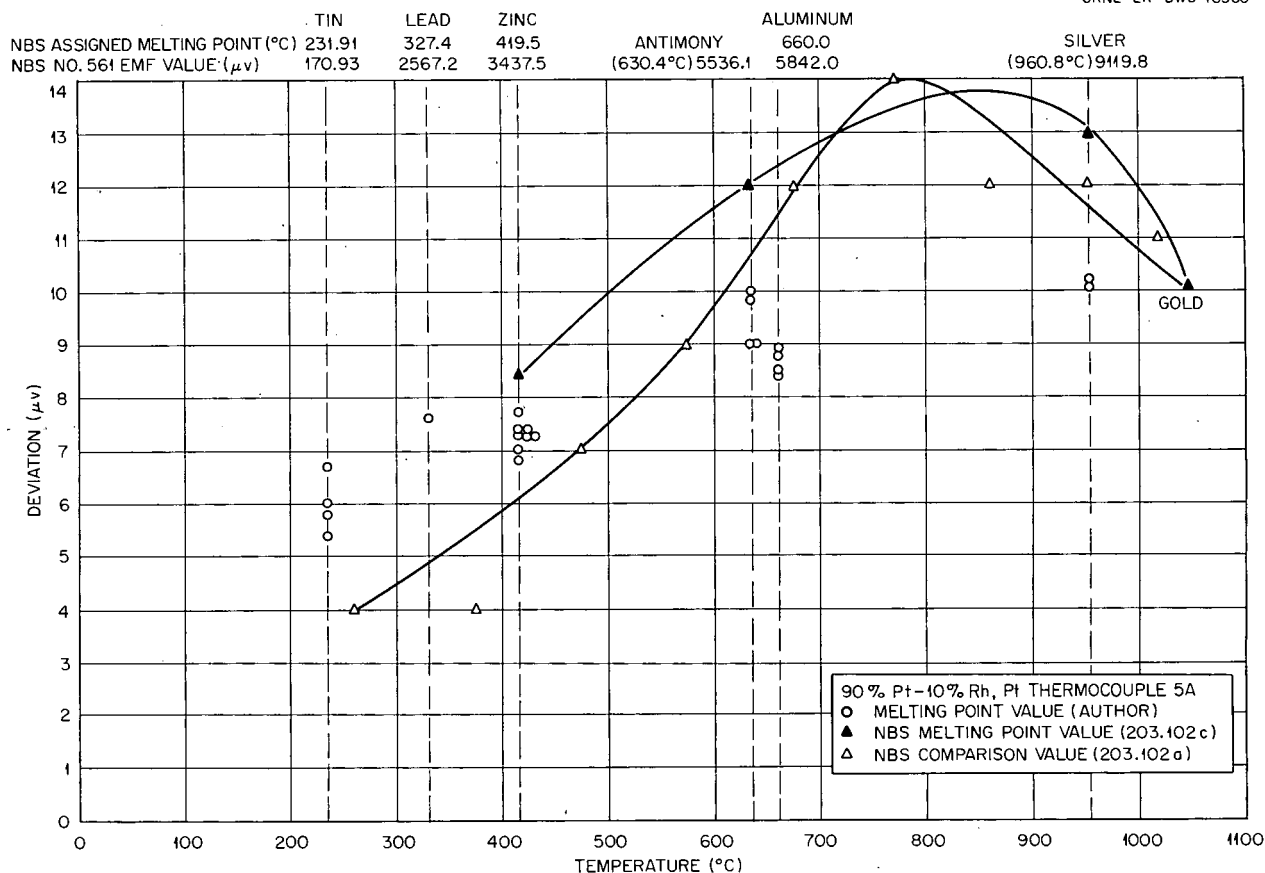


Fig. 3.5. Calibration of Thermocouple No. 5A at Fixed Points, with NBS Calibrations Also Shown.

### THERMOCOUPLE INSULATOR SHUNTING EFFECT

To disclose possible thermocouple calibration errors brought about by the shunting effect of insulators used in the work reported in the previous section, a series of tests were performed at the silver melting point (960.8°C).

First, the electrical resistance of a number of refractory tubes was measured by inserting a platinum wire and a 90% Pt-10% Rh wire (both B&S 24 gage) to within  $\frac{1}{4}$  in. of the end of a refractory insulator. The assembly was inserted in the melting point apparatus re-entry well. This simulated the conditions of contact between wires and insulator during thermocouple calibration. The measured electrical resistance was influenced by the magnitude and polarity of the applied potential. In addition, there was about 30  $\mu\text{V}$  output from the open-circuited "thermocouple." Leakage current was measured with direct and reverse polarity of applied voltages of 1.3, 4.0, 8.0, and 90 v. Results were more erratic with higher applied potentials.

The resistance values obtained at 1.3 v were reasonably consistent and are reported. The insulators tested are described in Table 3.7. All the above materials came from McDanel Refractory Porcelain Company, Beaver Falls, Pennsylvania.

After measuring the leakage resistance of the samples, a thermocouple junction was formed and the emf determined at the melting and freezing points of silver ( $960.8^\circ \pm 0.05^\circ\text{C}$ ) with the successive use of the four insulator types. The results of both the insulation resistance and the thermal emf measurements appear in Table 3.7.

There is no proportional correlation between calibration change and leakage resistance, although the trend suggests some effect. The possible variations in intimacy of contact between wire and insulator would have a bearing on the results. The difference of 1.8  $\mu\text{V}$  between samples IV and II indicates that the effect of insulators should be considered at the silver melting point and higher. Checks made at 980°C indicated a factor of 2 decrease in shunt leakage resistance from the value at 960°C.

Table 3.7. Insulator Leakage Resistance Effects on Thermocouple Calibration

Insulator Sample No.	Description*	Leakage Resistance at 960°C (megohms)	Silver Point (960.8°C) EMF ( $\mu\text{V}$ )
IV	Type 4T046316, 4-hole round, $\frac{3}{16}$ -in. OD $\times$ 0.046-in. holes, high-temperature porcelain	0.72	9119.4
I	Type AV2T040316, 2-hole round, $\frac{3}{16}$ -in. OD $\times$ 0.04-in. holes, alumina	0.57	9119.1
III	Type 2T078732, 2-hole round, $\frac{7}{32}$ -in. OD $\times$ 0.078-in. holes, high-temperature porcelain	0.38	9119.0
II	Type AV2T040316, 2-hole oval, 0.156 $\times$ 0.094 $\times$ 0.040-in. holes, alumina	0.37	9117.6

\*McDanel Co. catalog data.

#### 4. OXIDATION STUDIES ON NICKEL-BASE THERMOCOUPLE ALLOYS

The drift of thermal emf and the rate of failure of thermocouples seem to be directly related to the reaction rate of the thermocouple wire with its environment. This chapter reports measurements of isothermal weight gain due to oxidation in air at temperatures of 700, 800, 900, and 1000°C for times up to 500 hr on a number of commercial and laboratory-prepared nickel-base alloys. Two methods were used: (1) direct wire exposure in a furnace and (2) wires contained in refractory insulators exposed in the furnace. The methods were not highly refined but did effectively distinguish the alloys of minimum oxidation rates. The weight-gain, microstructure, and diameter changes of the oxidized wires were noted and compared with chemical analyses of the alloys. Changes in calibration at the silver point (960.8°C) after various times of exposure at 1000°C were measured on four alloys.

The oxidation of metals and alloys is a complex and much-investigated subject; theory, mechanisms, reaction rates, and control are all of interest in the development of more useful high-temperature components, and some results of previous studies will be noted in interpreting the results of the work reported here.

The *ASM Metals Handbook*<sup>1</sup> has a section devoted to oxidation of metals at high temperatures. Some of the comments in this section are quoted below, with slight changes:

1. The nature and extent of attack on metals and alloys, when heated in oxidizing environments, are determined largely by the properties of the scale that is formed – its structure, chemical composition, melting point, and boiling point. The base metal and gas environment are usually important only as they affect the scale. At high temperatures, the oxidation of many metals proceeds according to a parabolic relation:

$$x^2 = kt \quad (1)$$

where  $x$  is weight or thickness of metal consumed or formed into scale,  $t$  is time and  $k$  the rate constant.

The essential condition for the validity of the above equation was shown by Pilling and Bedworth to be the

formation of a dense and adherent scale, a condition that obtains when the specific volume of the oxide is equal to or greater than the specific volume of the metal; that is, when

$$\frac{Md}{mD} \geq 1 \quad (2)$$

where  $M$  and  $D$  are the molecular weight and density of the oxide and  $m$  and  $d$  those of the metal. The value for nickel is 1.52; hence it should form a protective oxide.

2. In general, those metals forming oxides of high melting point are most useful as alloying additions to confer resistance to oxidation. Scales generally consist of a layerlike structure, each layer comprising an oxide phase which is stable at the reaction temperature.

In alloys, the added element may occur in the scale in several forms, depending on its relative oxidizability with respect to the base metal. Thus, when small amounts of the additions form refractory oxides, the added element may occur in the inner scale layer adjacent to the base either as its own oxide or as a double oxide with the base metal. The concentration of such elements in the inner layer of the scale may be as high as four times the concentration of the element in the alloy. In the outer layers of scale, the added element may decrease to 10% of its concentration in the base metal.

When metals are added that are less reactive with oxygen than the base metal, the added metal is also enriched in the layer of scale adjacent to the metal surface; however, in this instance the added metal occurs as fine metallic particles embedded in the scale. Thus, on an iron-nickel alloy containing 5% Ni, metallic particles containing 30% Ni or more are found in the scale.

3. A number of methods are available for measuring the resistance of metals to attack by oxidizing atmospheres; the choice of method will depend on the particular application of the metal and on its physical form. Methods that have been used are:

- (a) Determination of the increase in weight of specimens after a given duration of exposure.
- (b) Determination of the decrease in weight after removing the external scale.
- (c) Measurement of the amount of gas consumed in the oxidation reaction.
- (d) Determination of the time necessary for the destruction of a given size of material (ASTM heat-cool cycle wire test is similar to this).

<sup>1</sup>B. Lustman (ed.), "The Resistance of Metals to Oxidation at Elevated Temperatures," p 223-27, *ASM Metals Handbook*, 1948 ed., American Society for Metals.

(e) Metallographic examination of the oxidized material.

(Methods *a* and *e* were used in the UT-ORNL experiments.)

4. The principal criterion for an oxidation-resistant alloy is the ability of the alloy to form an oxide scale of low electrical conductivity, which indicates a low rate of diffusion of metal ions, and equally important a high melting point. In general the higher the melting point of an oxide, the lower its conductivity. Presence of alloying elements that form low-melting eutectics or compounds with other constituents of the scale must be avoided, since molten scales give no protection.

5. The most important component of heat-resistant alloys is chromium, both because it forms a highly refractory oxide and because its alloys with nickel and iron, or both, are workable even when the percentage of chromium is high. [Figure 4.1] shows the effect of chromium content on the scaling of a steel. The chromium content at which a low rate of scaling is obtained denotes the composition at which the scale consists entirely of refractory  $\text{Cr}_2\text{O}_3$ ; it may be noted that the proportion of chromium required increases with increasing temperature.

6. The oxidation of nickel-chromium alloys relatively high in chromium cannot be described by Eq. (1) for long duration of exposure to oxidation, because such

alloys oxidize much more slowly than would be expected. For comparison, it has been found that 20% Cr alloys withstand 1200 intermittent heatings to  $1050^\circ\text{C}$ , while 6% Cr alloys stand only 150. It is to be noted that small additions of chromium decrease the resistance of nickel to oxidation. An addition of about 0.25% Cr induces free spalling of the oxide.

[Figure 4.2] shows the structures formed on iron-chromium-nickel alloys at  $1000^\circ\text{C}$ . Up to about 10% Cr, the oxide formed is NiO. With higher chromium contents the resulting oxide has the crystal structure of  $\text{Cr}_2\text{O}_3$ , which is more refractory than NiO and affords greater protection. The good resistance to oxidation of nickel-chromium alloys has been attributed to the presence of the spinel  $\text{NiO}\cdot\text{Cr}_2\text{O}_3$ , which has been reported in alloys containing 15 to 20% Cr. Additions of carbon or manganese increase the rate of scaling of these alloys, while silicon and aluminum improve the resistance to oxidation.

7. It has been found that the purity of the initial materials has an appreciable effect on the life of nickel-chromium alloys. Alloys made of electrolytic chromium failed much more quickly than did those made of chromium reduced by the Thermit reaction. Additions of calcium, thorium and cerium in amounts less than 0.5% improve resistance to scaling to a degree out of proportion to the amounts of added element. Such improvement was found to be general with additions

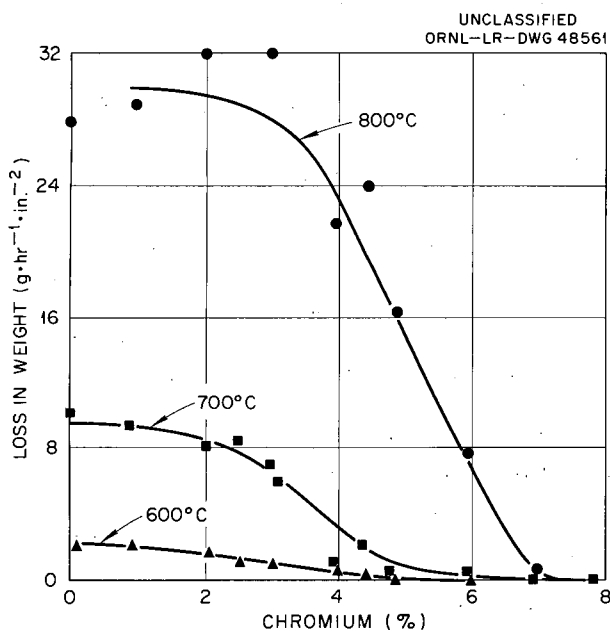


Fig. 4.1. Effect of Chromium Content on the Scaling of a Steel Containing 0.15% C and 0.7 to 0.9% Si. (From ASM Metals Handbook - Houdremont's data.)

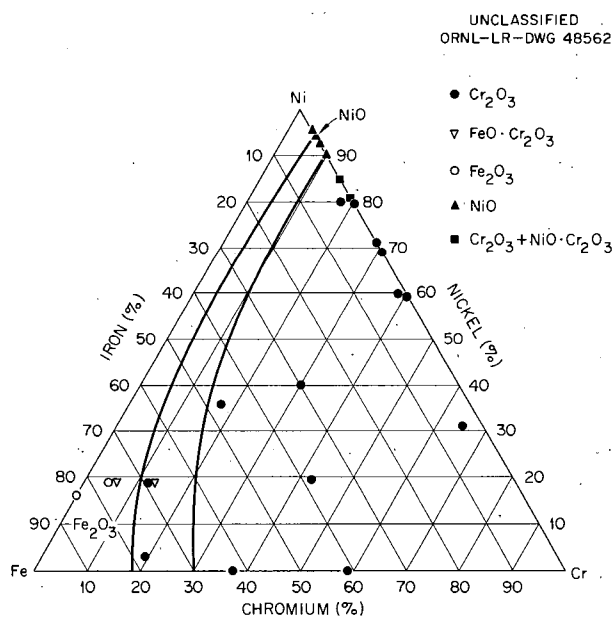


Fig. 4.2. Constituents of Scale Layers on Fe-Ni-Cr Alloys. (From ASM Metals Handbook - Houdremont's data.)

of the alkaline earths and rare earth elements. The service life of nickel-chromium alloys in American practice is greatly extended by the addition of 0.01 to 0.2% Cu, 0.01 to 0.5% Zr, and 0.01 to 1.0% Al. This has been tentatively explained on the observation that those elements which have smaller atomic volumes have no effect. Presumably such minor impurities are to be considered as obstacles to the passage of nickel ions through the scale.

8. Any listing of alloys in their order of merit with respect to scaling must be considered as comparative only for given atmospheres, heating and cooling cycles, and other test conditions.

Recently, Zima<sup>2</sup> has studied the oxidation of a series of Ni-Cr alloys of interest to this study. Zima's conclusion, that small chromium additions are detrimental, is mentioned in point 6 above. Figure 4.3 is a plot of the rate constant Zima determined for the Ni-Cr alloys. At 9.5% Cr, the approximate composition of Chromel-P and Kanthal-P, more oxidation may take place on these alloys than on pure nickel.

#### EXPERIMENTAL PROCEDURE

Several different approaches were employed in order to determine the relative oxidation characteristics of positive and negative thermoelements. These were:

1. weight-gain determinations of bare wires freely supported in the furnace and wires in refractory tubes;
2. metallographic examinations of bulk diameter changes and oxide-metal microstructures.

#### Weight Gain

The metal wire specimens were bent in a hairpin shape, weighed to  $\pm 0.0002$  g, and placed in a specified position on the morganite rods of an oxidation cell. This assembly was placed in the furnace, brought to operating temperature for a set time, and the samples were then removed for weighing. This method was later altered so that the test specimens could be placed on the rods with the assembly at temperature. The increase in specimen weight was noted after exposure, care was taken to catch any oxide which spalled off on cooling, and the weight gain per unit area was

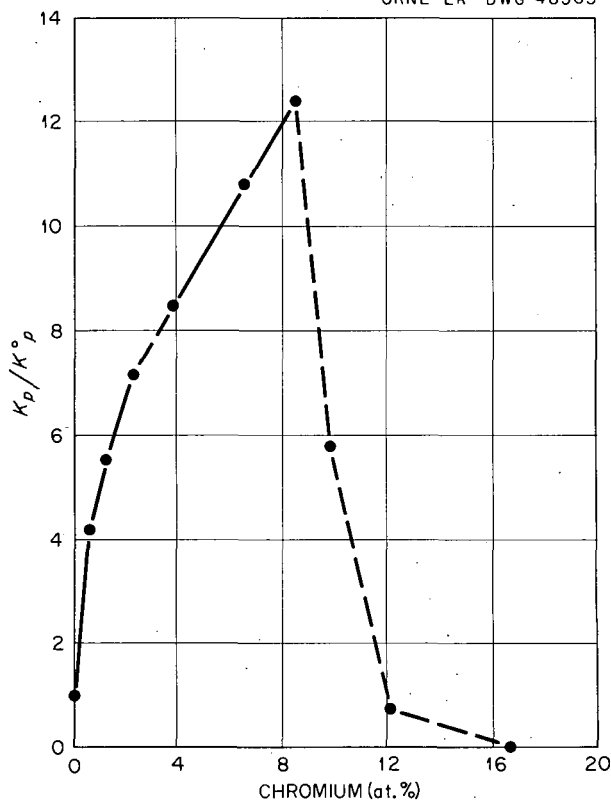


Fig. 4.3. Rate Constant for Ni-Cr Alloys;  $K_p/K_p^0$  vs at. % Cr, 1096°C, O<sub>2</sub> at 76 cm Hg. [From *Trans. ASM* 49, 933 (1957) - Zima's data.]

calculated and plotted. Generally, weight increases were about 0.003 g for 100 hr at 1000°C for specimens of 150-mm<sup>2</sup> surface area. Thus the average weight gain per unit area was about 20  $\mu\text{g}/\text{mm}^2$ . Specimens were exposed for times up to 500 hr at 700, 800, 900, and 1000°C. The alloys studied and the results obtained are given in the next section.

A weight-gain experiment is an isolated experiment which under a given set of conditions gives certain useful information about the oxidation of specimens being tested. The following limitations should be considered in analyzing the results:

*Uniform Nonspalling Oxide.* - There is an assumption, particularly affecting the testing of bare wires, that a uniform nonspalling oxide is being produced on the specimen. If spalling of the oxide does occur, misleadingly low data will be obtained which might lead to a false conclusion in favor of a spalling specimen.

<sup>2</sup>G. E. Zima, *Trans. ASM* 49, 933 (1957).

*Type of Oxide.* – There is no indication of the type or composition of the oxide being formed. In specimens where the alloy content strongly influences the thermal emf, this is of special consideration. The relative rates of oxidation of the components are of extreme importance because they can influence the over-all composition of the specimen and hence its thermal emf.

*Thermoelectric Properties of the Oxide.* – Such an experiment gives no information concerning the thermoelectric properties of the oxide. These properties may alter the emf of the thermocouple either directly or by changing the composition of the base metal.

*Method of Oxide Attack.* – This type of experiment does not indicate the method of attack of the oxidation. This is a serious defect in those cases where intergranular oxidation occurs, since this could rapidly lead to a complete surrounding of the individual grains of a metal by oxide, without appreciable weight gain. Furthermore, if the oxide is not uniform, certain local regions may be more strongly attacked than others and ultimately lead to failure of the wire. If a series of oxides is formed, then the rate of oxidation may vary during exposure. Protective and non-protective oxides may form, and reactions may occur within and between the oxides which have formed. The latter has been suggested for Ni-Cr alloys in which NiO is reduced to nickel by the oxidation of chromium.

These limitations indicated the weakness of conducting only one type of weight-gain experiment. A second, and more simply performed, test was chosen in which the specimens were inserted into a 3-in.-long, four-hole refractory of known weight and this assembly exposed to oxidation at a constant temperature. The surface area of the specimen was calculated, and the net increase in weight of the specimens was determined by subtracting the weight of the refractory. An empty refractory was given identical exposures and weighed to determine any weight change due to reactions which might be occurring in the refractory. This test closely approaches the true environment of a thermocouple wire in a refractory tube and has the advantage of trapping any spalled oxide for weighing. Because the specimens were cooled before weighing, there is the possibility that cooling caused differential stresses leading to spalling or cracking of the oxide. In such a case

the weight gain might be higher on reheating than if the specimen had not been cooled. Weight gain is probably also affected by the position of the wire in the refractory, since the bottom side of the wire, touching the refractory, is somewhat protected from the atmosphere. One additional source of error inherent in such a test, but which is also typical of a thermocouple wire in actual use, is the possibility of an oxygen gradient existing in the hole of the tube. This would possibly lead to lower weight gains for the sample.

Cross sections of exposed wire specimens have been examined by using a metallurgical microscope to determine (1) the diameter of the remaining metal wire and (2) the appearance of the remaining metal and oxide layer. The diameter measurements were compared with the original diameter to check the weight-gain measurements. The microstructures of the specimens have revealed some characteristics of the oxidation.

#### Results of Weight-Gain Measurements

Most of the commercial high-temperature thermoelements and heating elements are nickel-base alloys. Sixteen of these alloys were tested, and some of the results enable correlation of alloying-element effects. In addition, a series of specially fabricated Ni-Si alloys has been studied. Table 4.1 summarizes some of the important facts and results. Table III in Progress Report I<sup>3</sup> and Appendix D of this report contain the chemical analyses of the alloys tested.

Figure 4.4 is a plot of weight gain vs time at temperature for the positive thermoelements tested by the hairpin method. The weight-gain scale of the various materials is different in various cases. The results are not totally consistent with respect to time or temperature; however, reasonable interpretations may be made. The shape of the curves of weight gain vs time for the positive thermoelements indicates that the oxide is generally protective. Fortunately, for thermocouple uses, the observed weight gains are small at 700 and 800°C. It is difficult to make firm comparative statements about these data. Statements

---

<sup>3</sup>D. L. McElroy, *Progress Report I, Thermocouple Research, Report for Period Nov. 1, 1956, to Oct. 31, 1957*, ORNL-2467, Table III.

Table 4.1. Thermocouple Materials Tested and Summary of Results

Material	Source*	B&S Gage	Wires Exposed in Refractory Tubes								Figure References to Microstructures		
			Hairpin Weight Gain After 400 hr ( $\mu\text{g}/\text{mm}^2$ )				Weight Gain After 400 hr ( $\mu\text{g}/\text{mm}^2$ )			Diameter Change After 500 hr [ $(D_0 - D_f)/D_0 \times 100\%$ ]			
			700°C	800°C	900°C	1000°C	800°C	900°C	1000°C	900°C	1000°C	900°C	1000°C
Hoskins alloy 875	H	20					3.7	7.5	5.5	0	0.5	4.15a	3.13a
Hoskins alloy 827	H	20					1.7	6.5	24	0	0.7		
Hoskins alloy 717	H	20					4.8	8.0	19	0	0.6		
Chromel-A	H	20					2	8.0	25	0	0.4		
Geminol-P	DH	20	3.5	2.0	1.5	-2.0	1.9	6.5	21			4.15b	4.13b
Chrom-Nickel B	V	20				+2.5							
Chromel-P	H	22	16	39		70	24	34	108	0	2.2	4.15d	4.13d
Chromel-P + Nb	H	20	15	31	63	18	3.2	13	72	1	3.5	4.15c	4.13c
Kanthal-P	K	22	10	15	16	22	3.8	7	42	1	5.2	4.15e	4.13e
Vacuumschmelzer-P (100 hr)	V	22	8.5	13	15	180							
Alumel	H	22	19	49	160	320	49	133	269	15	48	4.15f	4.13f
Scott NiAl	S	22				100							
Vacuumschmelzer-N (100 hr)	V	22	6	15	45	116							
Kanthal-N	K	20	20	38	54	76	40	55	134	8	9	4.15b	4.13b
Geminol-N	D-H	20	15	26	26	44	24	51	90	5.4	13.5	4.15i	4.13i
Special Alumel	H	20					39	73	77	4.5	9	4.15g	4.13g
Nickel (exp)	UT	20					37	81	184	11.5	24		4.14a
Nickel-1% silicon	UT	20					27	85	142	8	12		4.14b
Nickel-2% silicon	UT	20					36	75	98				4.14c
Nickel-3% silicon	UT	20					26	59	114	5.5	6		4.14d
Nickel-4% silicon	UT	20					19	70	106				4.14e
Nickel-5% silicon	UT	20					17	45	75	2.5	3		4.14f
Iron (approx. SAE 1010)	L&N	20					630					4.14i (800°C)	
Constantan	L&N	20					390					4.14b (800°C)	
Copper	L&N	20					350					4.14g (800°C)	

\*H = Hoskins Manufacturing Co.; D-H = Driver-Harris Co.; V = Vacuumschmelzer Co.; K = A. B. Kanthal Co.; S = A. C. Scott Co.; UT = University of Tennessee; L&N = Leeds & Northrup Co.

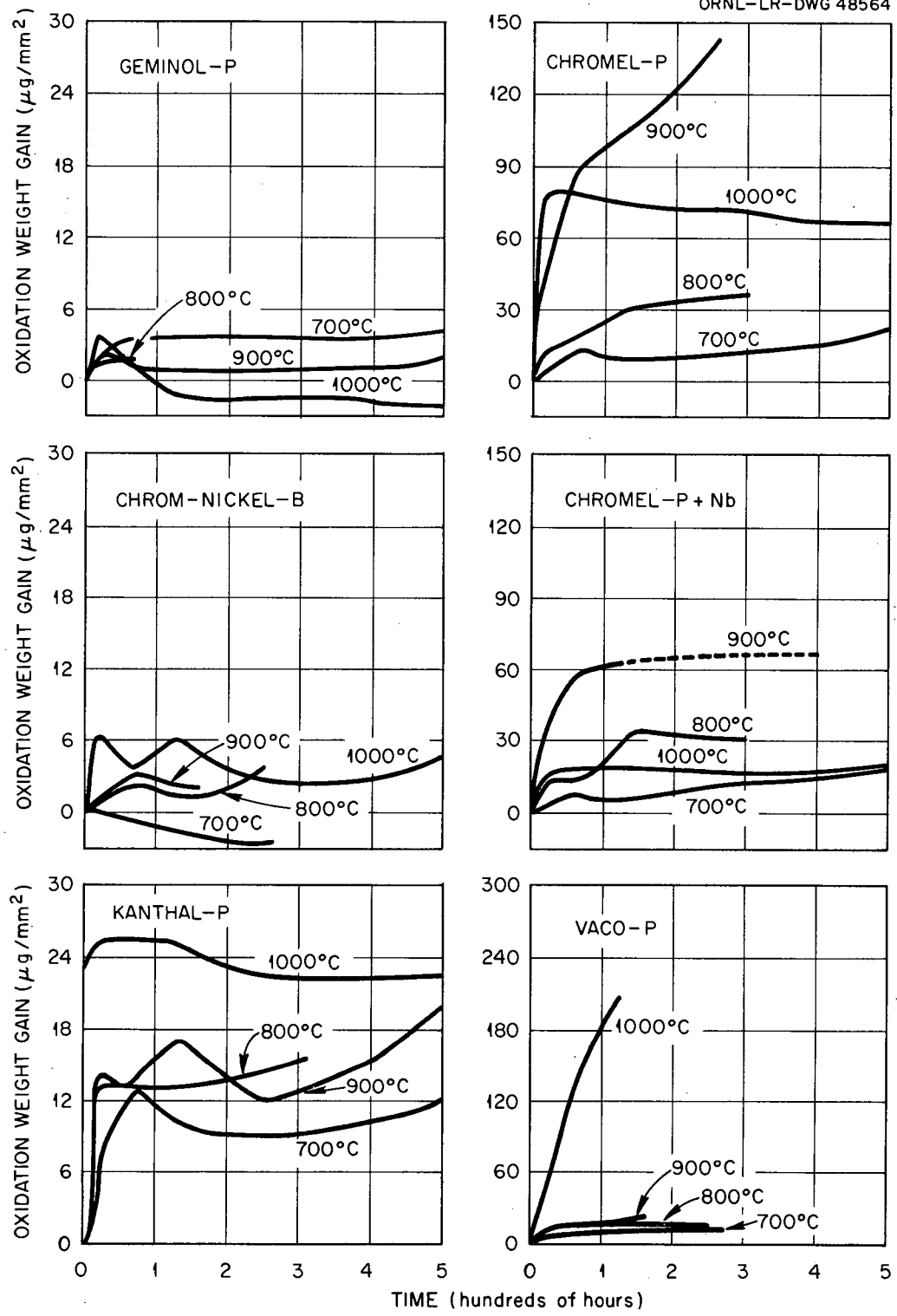


Fig. 4.4. Oxidation Weight Gain vs Time at Temperature for Positive Thermoelements (Hairpin Method).

can be made about the data at 900 and 1000°C, although exceptions exist here also, as follows:

1. Increasing the chromium content of Chromel-P, as in the case of Geminol-P and Chrom-Nickel B, results in less oxidation at all temperatures. It should be noted that in the oxidation-resistant materials, some spalling of the oxide is observed, which is indicated by the loss of weight. The formation of this powdery, spalling, and, hence, nonprotective oxide is not serious in these two alloys, since the inherent oxidation rates are low.

2. Alloys of composition similar to that of Chromel-P behave quite differently from Chromel-P:

- a. Vacuumschmelzer P gave a higher weight gain. The cause for this may be associated with its 2% Mn content, not present in Chromel-P.
- b. The addition of niobium to Chromel-P (see Chromel-P + Nb) and the removal of iron from Chromel-P (see Kanthal-P) result in lower weight gains. The exact causes of these improvements or detriments can only be hypothesized from these apparent composition differences in the alloys. Kanthal-P does have an appreciably finer initial grain size than other alloys of the Chromel-P type, and this might contribute to the formation of a more protective and adherent oxide and hence the lower weight gains.

If one is concerned primarily with thermoelectric power (sensitivity), the more sensitive Kanthal-P seems, from the above data, to be the best positive thermoelement. However, if the thermoelectric potential is of secondary importance, then Geminol-P and Chrom-Nickel B, having better oxidation resistance, appear to be better choices.

Figure 4.5 is a plot of weight gain vs time at temperature for the negative thermoelements tested by the hairpin method. There appears to be more general consistency in these results than in those for the positive thermoelements. Generally, the oxides formed do not appear to be quite as protective as those of the positive thermoelements; that is, the weight gain continues to increase at a reasonably fast rate with time rather than taper off as for the positive materials. Decreasing the temperature results in less oxide weight gain, as is expected. Alumel and Vacuumschmelzer N appear to be the least suitable alloys, and both appear to oxidize faster than the positive elements.

Geminol-N and Kanthal-N have appreciably lower weight gains than does Alumel. The Geminol-N is somewhat superior to the Kanthal-N, and this is probably due to the slightly higher silicon content in the former, 2.75 as compared with 2.40%. Thus the beneficial effects of silicon alone, as opposed to silicon, manganese, and aluminum combined, are apparent in the oxidation results on these negative elements. The A. C. Scott NiAl material oxidizes at a rate intermediate between those of Alumel and Kanthal-N and this illustrates the effect of a lower silicon content, 1.50% as opposed to the higher silicon content, 2.40%, of the Kanthal-N. In general, the best negative thermoelements oxidize at nearly twice the rate of the positive thermoelements, principally because the oxide formed is not as protective.

Finally, some hairpin oxidation tests were followed by measurements on the diameter of the remaining metal. The results for 1000°C are plotted in Fig. 4.6. Because certain of these measurements were made as an afterthought, values for some of the materials are missing. In general, these results show the extremely rapid attack on Alumel, as opposed to the relatively protective nature of the oxide on the Geminol-N. The results on Geminol-P, Kanthal-P, Chromel-P + Nb, and Chromel-P indicate the superior performance of the positive thermoelements and the beneficial roles of chromium and silicon.

Oxidation results obtained in refractory tubes are more self-consistent than those of the hairpin method. However, the general conclusions for the hairpin-test alloy apply also to the refractory tube tests. Figure 4.7 shows the beneficial effects of the alloying constituents on the high-alloy elements. Generally, the observed weight gains are  $\frac{1}{4}$  to  $\frac{1}{20}$  as high as those for Chromel-P, which shows why these materials are used for heating elements and why they are potentially excellent thermoelements. All these materials apparently form protective oxides.

Figures 4.7 and 4.8 show the results for Chromel-P, Chromel-P + Nb, and Kanthal-P at 800, 900, and 1000°C. The beneficial effects of niobium and of removal of iron are readily seen in the results for Chromel-P + Nb and Kanthal-P respectively. The form of the plots indicates that these latter alloys form a more protective oxide than does Chromel-P. Increasing the temperature is seen

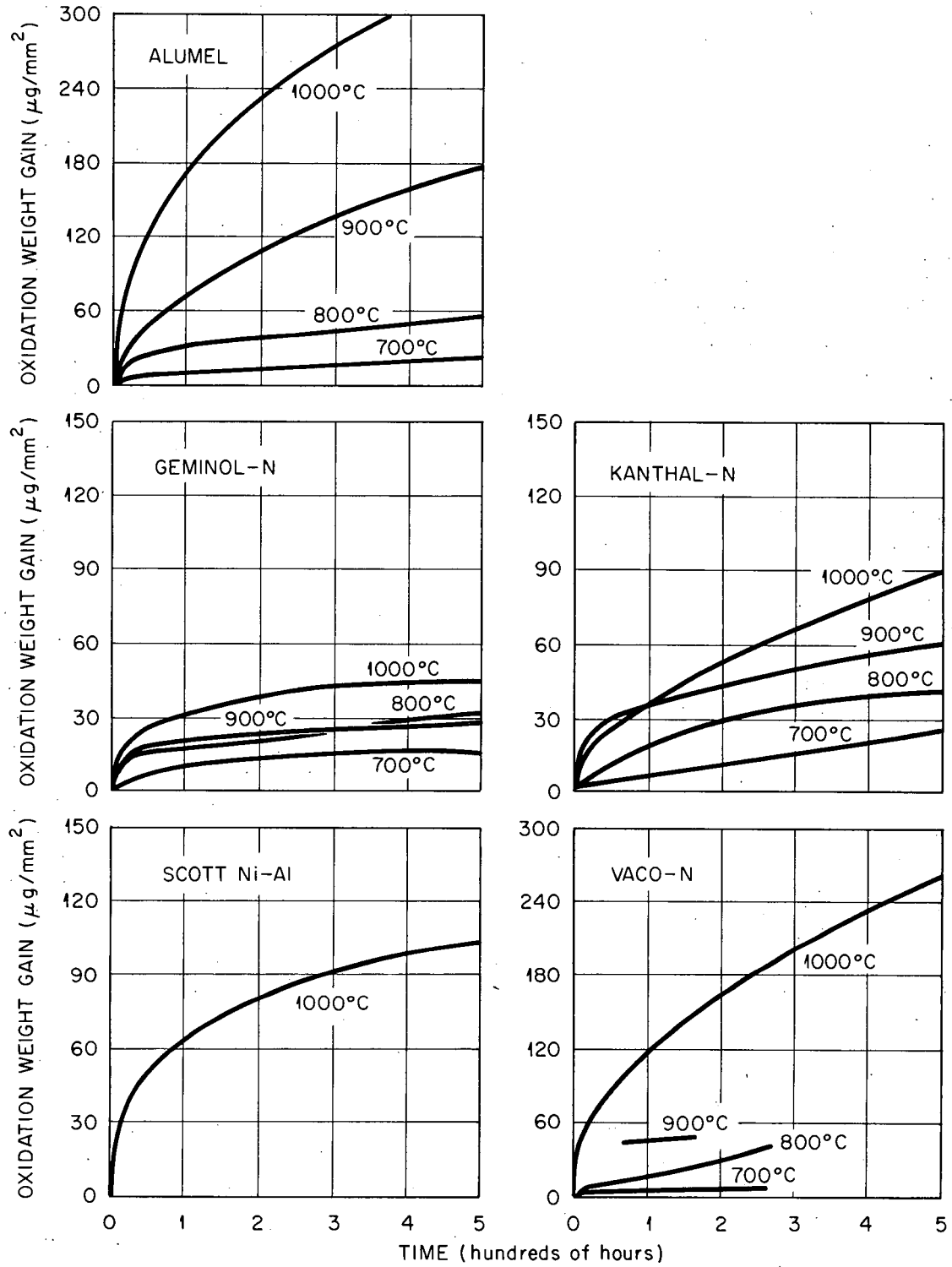


Fig. 4.5. Oxidation Weight Gain vs Time at Temperature for Negative Thermoelements (Hairpin Method).

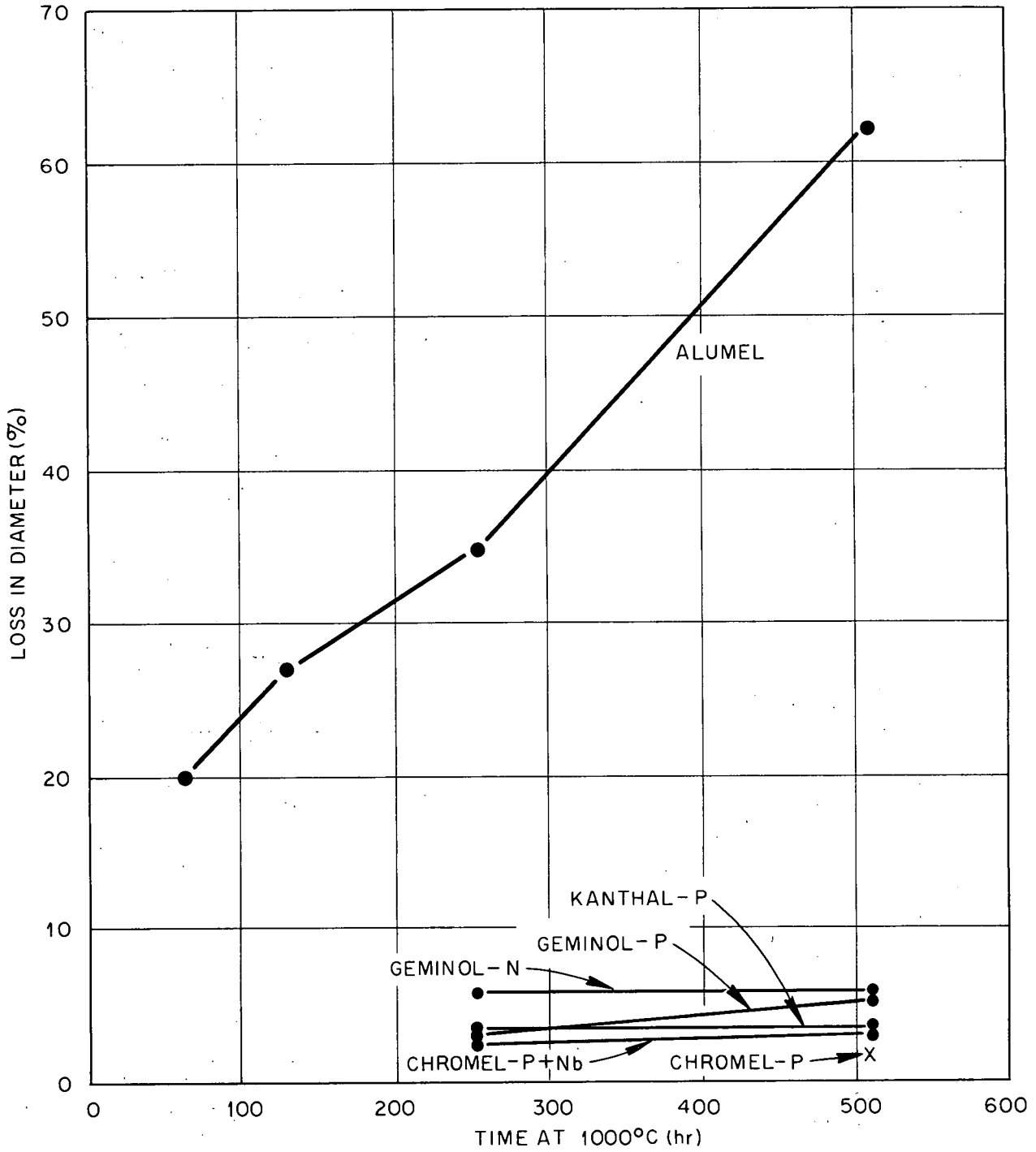


Fig. 4.6. Change in Diameter vs Time for Thermoelements Tested at 1000°C (Hairpin Method).

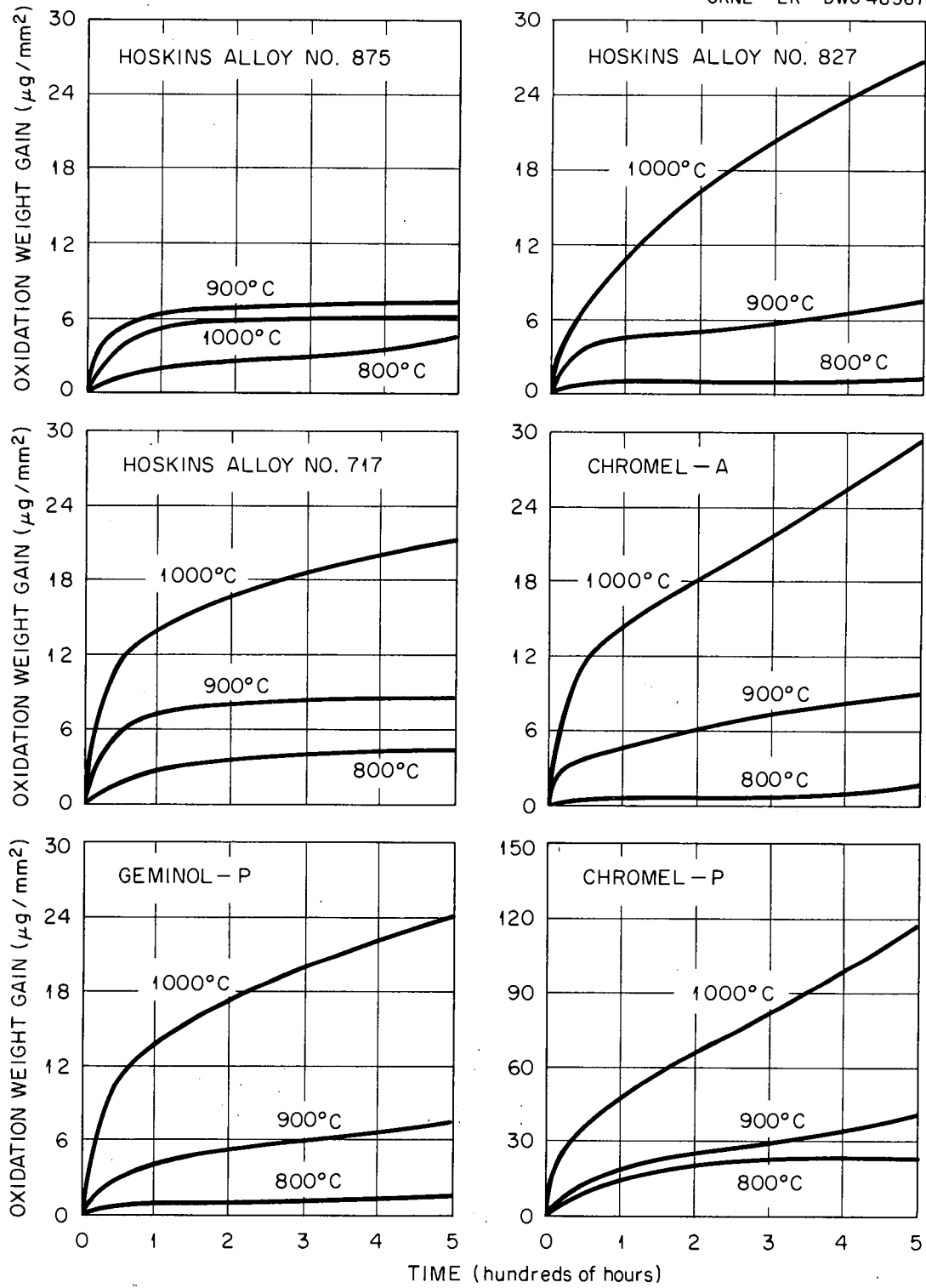


Fig. 4.7. Oxidation Weight Gain of High-Alloy Wires vs Time at 800, 900, and 1000°C (Refractory-Tube Method).

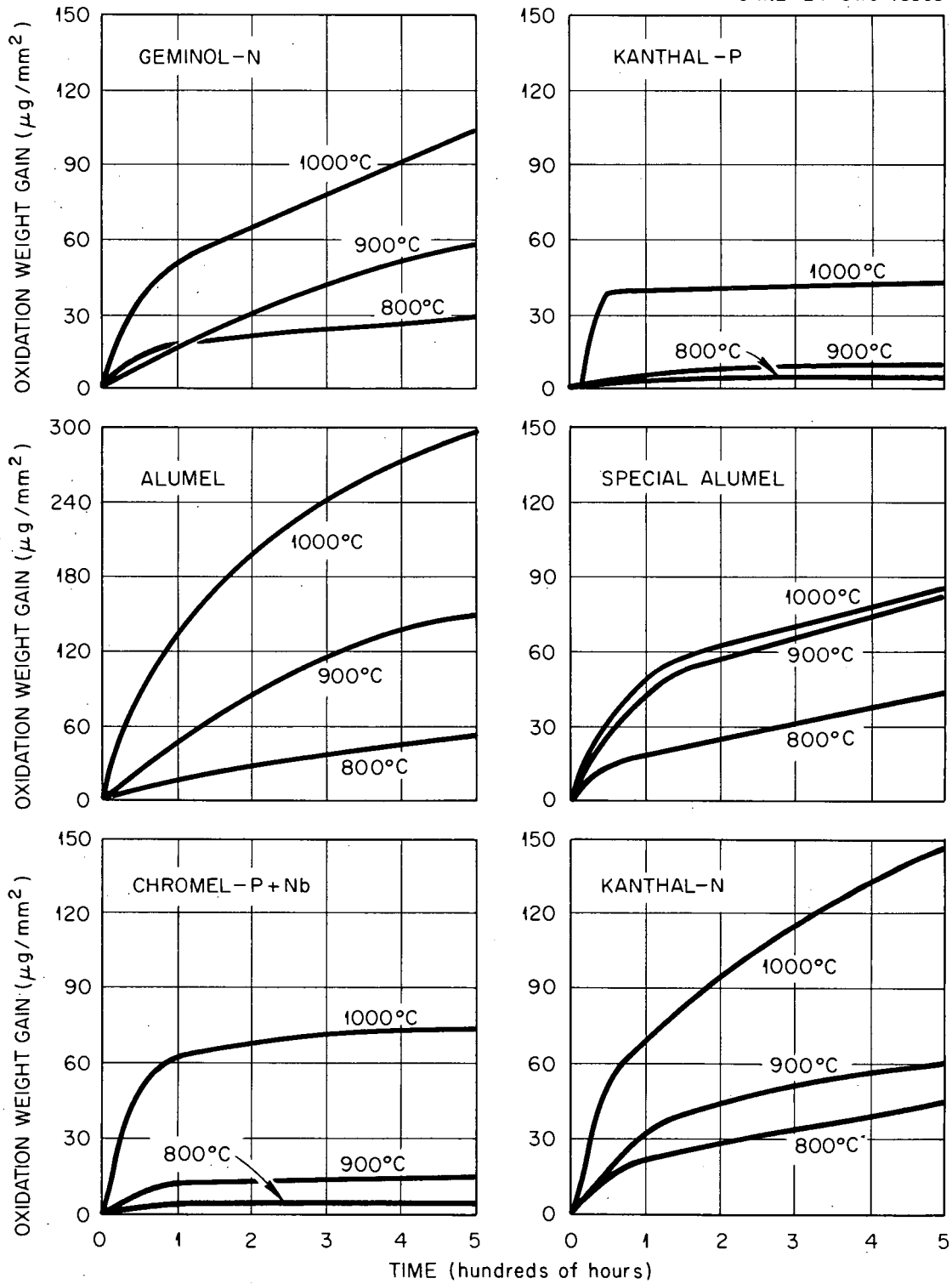


Fig. 4.8. Oxidation Weight Gain of Wires vs Time at 800, 900, and 1000°C (Refractory-Tube Method).

to increase the reaction rate in all these materials. The large weight-gain increase obtained by increasing the temperature from 900 to 1000°C may indicate that the 900°C oxide is different from the 1000°C oxide.

Figure 4.8 also shows the results for the negative thermoelements at 900 and 1000°C. The poor performance of Alumel at 900 and 1000°C is apparently caused by the formation of a nonprotective oxide. The oxidation resistance of the negative element is considerably improved if silicon is used as the only alloying element with nickel, and this is graphically shown for the three alloys Geminol-N, Kanthal-N, and Special Alumel. All the latter are nominally binary alloys of nickel and silicon, and there are only slight differences in oxidation reaction rates, with perhaps the Kanthal-N being the poorest material of the three.

**Experimental Alloys.** — Because of the apparent superior performance of nickel-silicon alloys, a series of solid-solution experimental alloys were prepared, and the oxidation characteristics of these alloys were investigated. These results are shown in Fig. 4.9. The beneficial effects of increasing the percentage of silicon are seen in a cross plot of this data vs silicon percentage, which is shown in Fig. 4.10. It is interesting to note that increasing the silicon content causes the amount of oxidation to be continually decreased at 1000°C, while at 900°C the weight-gain measurements show a slight increase before decreasing. At 1000°C little difference exists between the 2 and 3% silicon alloys, and both of these are better than the 1% silicon alloy or pure nickel. These results are in agreement with the previously mentioned results found for Geminol-N, Kanthal-N, A. C. Scott NiAl, and Special Alumel. Finally it is noted that Alumel oxidizes faster than pure nickel at 900 and 1000°C.

The possibility of treating the nickel-silicon data theoretically has been considered, but it has been felt that since the design of the present experiment was primarily to distinguish between the alloys, it is questionable whether sufficient data is available for a complete theoretical extension.

From the above data it is apparent that Alumel is the weaker leg of the Chromel-Alumel thermocouple in an oxidizing atmosphere. Improved performance could be attained by using a binary nickel-silicon alloy, and the resulting error in

calibration differences from the Alumel-platinum emf table apparently can be minimized by proper alloy choice, at least in the high-temperature region. Alumel was developed primarily for sulfurous atmospheres, and it may be that in this type of atmosphere Alumel would perform better than the Ni-Si alloys.

The oxidation resistance of iron, constantan, and copper was determined at 800°C, and the results are shown in Fig. 4.11. Constantan used with either iron or copper oxidizes at a slower rate than iron or copper. It appears that copper oxidizes faster than iron, and that copper is completely consumed in 300 hr, whereas iron lasts for about 400 hr. The photomicrographs also show this effect. In any case, the behavior of these materials at 800°C is poorer than that of Alumel at 1000°C.

Diameter measurements on the remaining wire after 500 hr at 900 and 1000°C are shown in Figs. 4.12a and 4.12b. These are drawn as straight lines because of the lack of data at intermediate temperatures. The results bear out the previous conclusions based on weight-gain data at 900 and 1000°C:

1. The high-alloy materials show diameter changes of less than 1%.
2. The alloys having compositions near that of Chromel-P and the binary Ni-Si alloys show diameter changes between 2 and 15%.
3. Alumel and pure nickel show diameter changes from 15 to 50%.

#### Photomicrographic Examination

The cross-section photomicrographs of these unetched alloys after 500 hr at 1000 and 900°C are shown in Figs. 4.13–4.15 respectively.

Figures 4.13a and 4.13b are typical for the alloys 875, 827, 717, Chromel-A, and Geminol-P, where a small amount of oxide formed. Figure 4.13c shows that a decrease in chromium content, as in Chromel-P + Nb, increases the amount of oxide formed. The beneficial effect of niobium in reducing this somewhat is seen in comparing Fig. 4.13c with 4.13d. Figures 4.13d and 4.13e show the similarity between Chromel-P and Kanthal-P. Figure 4.13f shows the gross oxide formed on Alumel and the penetration of oxide into the wire. Figures 4.13g–4.13i show the similar behavior of the Special Alumel, Kanthal-N, and Geminol-N. Their superiority to Alumel is readily seen. Figures 4.14a–4.14f show the effect of increasing

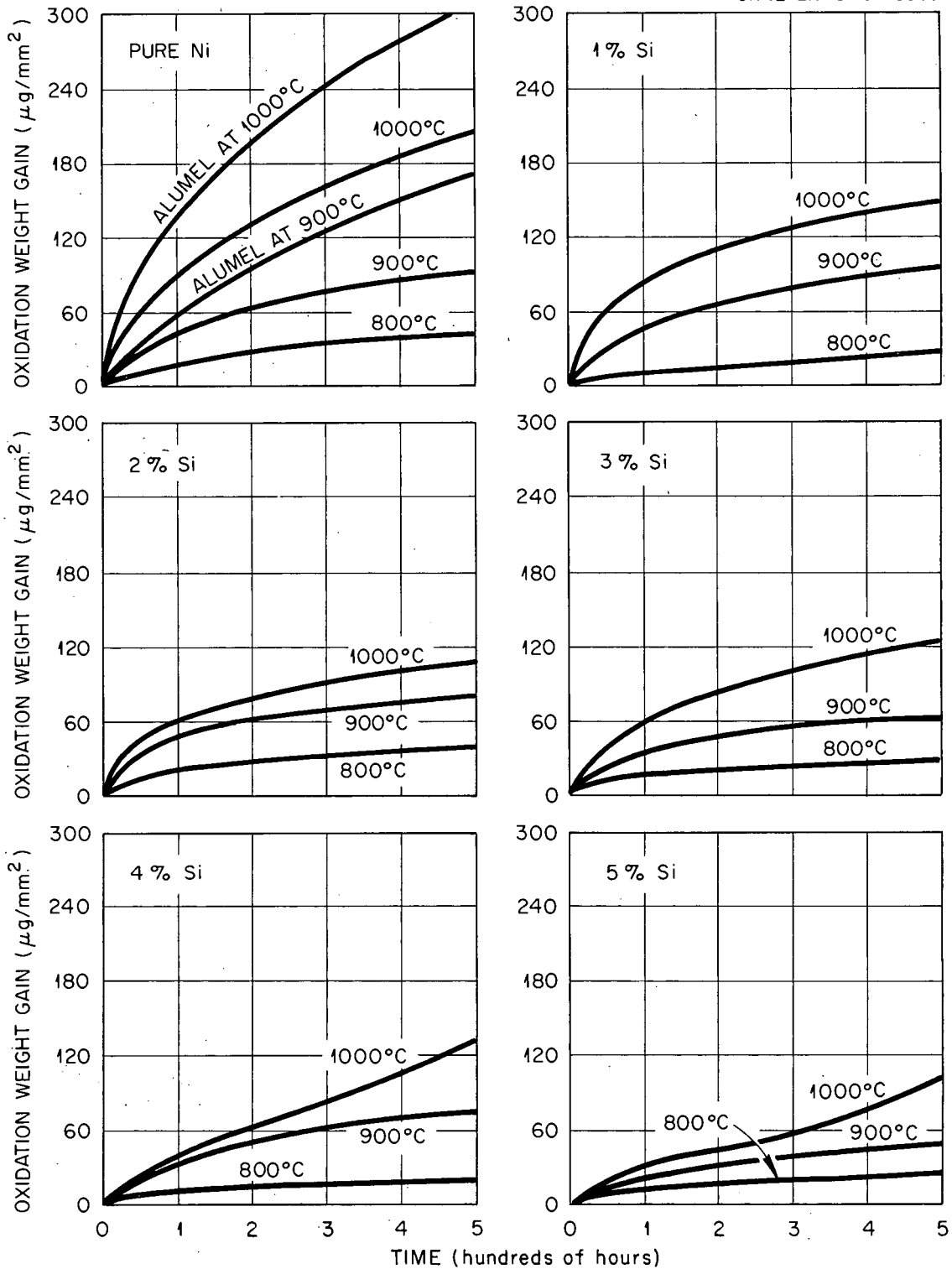


Fig. 4.9. Oxidation Weight Gain of Wires (0 to 5 wt % Silicon in Nickel) vs Time at 800, 900, and 1000°C (Refractory-Tube Method).

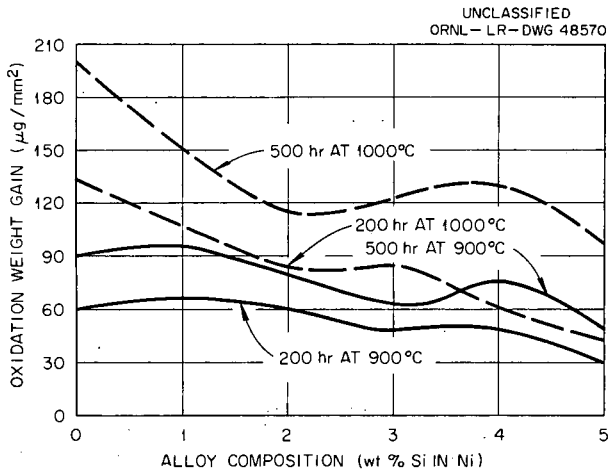


Fig. 4.10. Oxidation Weight Gain of Ni-Si Wires vs wt % Si (Refractory-Tube Method).

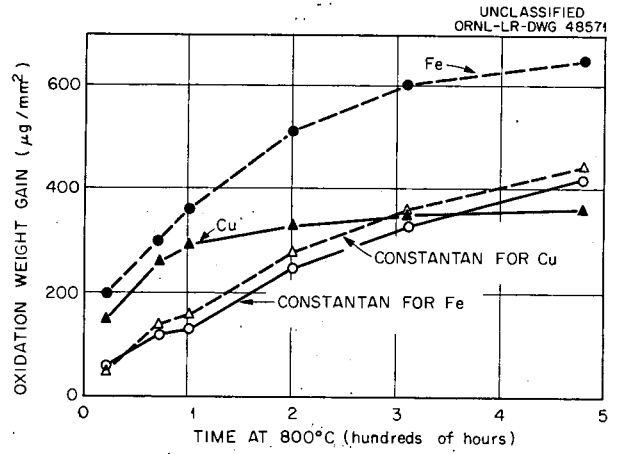


Fig. 4.11. Oxidation Weight Gain vs Time at 800°C for Iron, Copper, Constantan for Use with Iron, and Constantan for Use with Copper (Refractory-Tube Method).

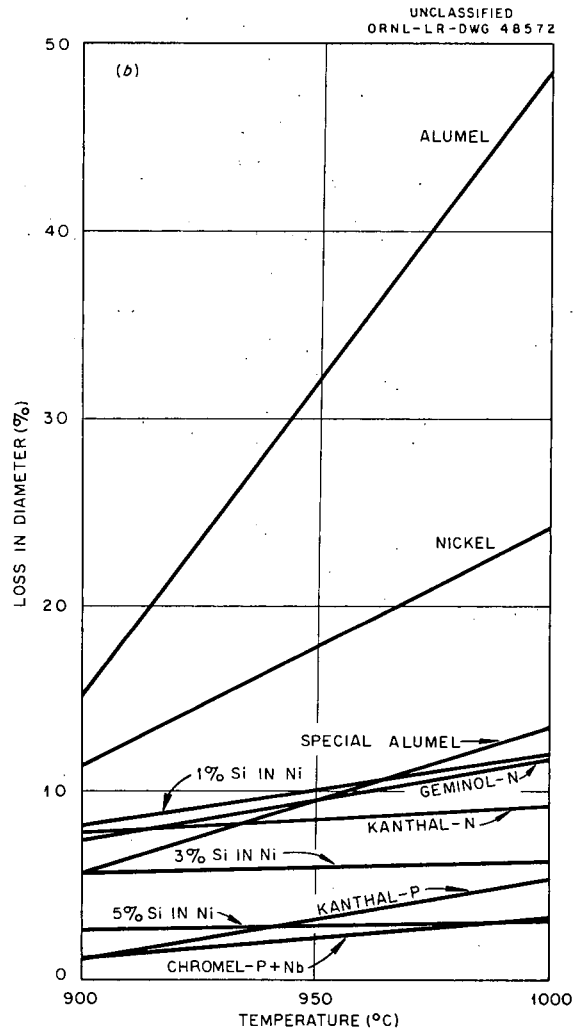
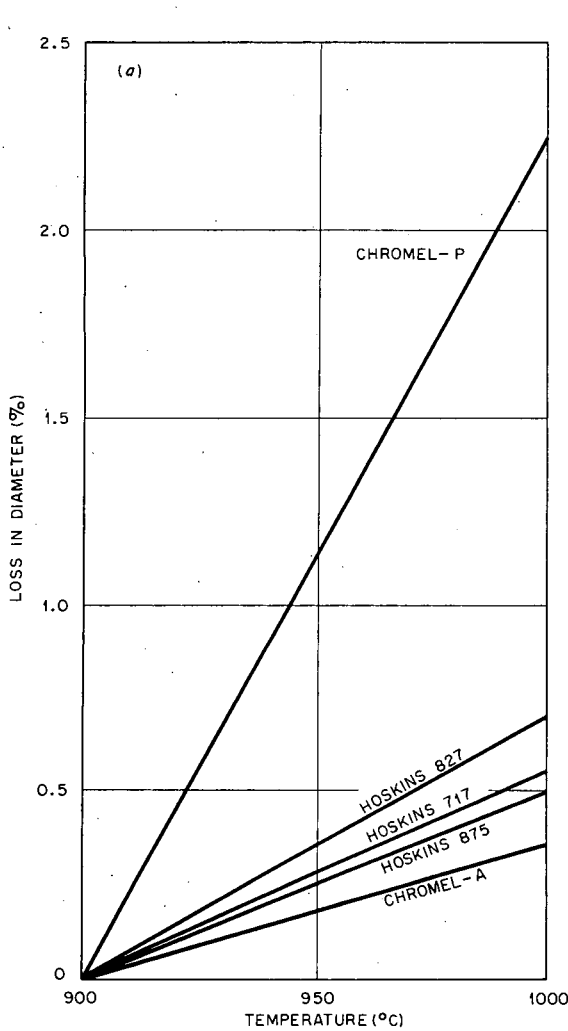


Fig. 4.12. Diameter Loss of Wires Exposed 500 hr at 900 and 1000°C (Refractory-Tube Method). (a) Positive alloys; (b) negative alloys.

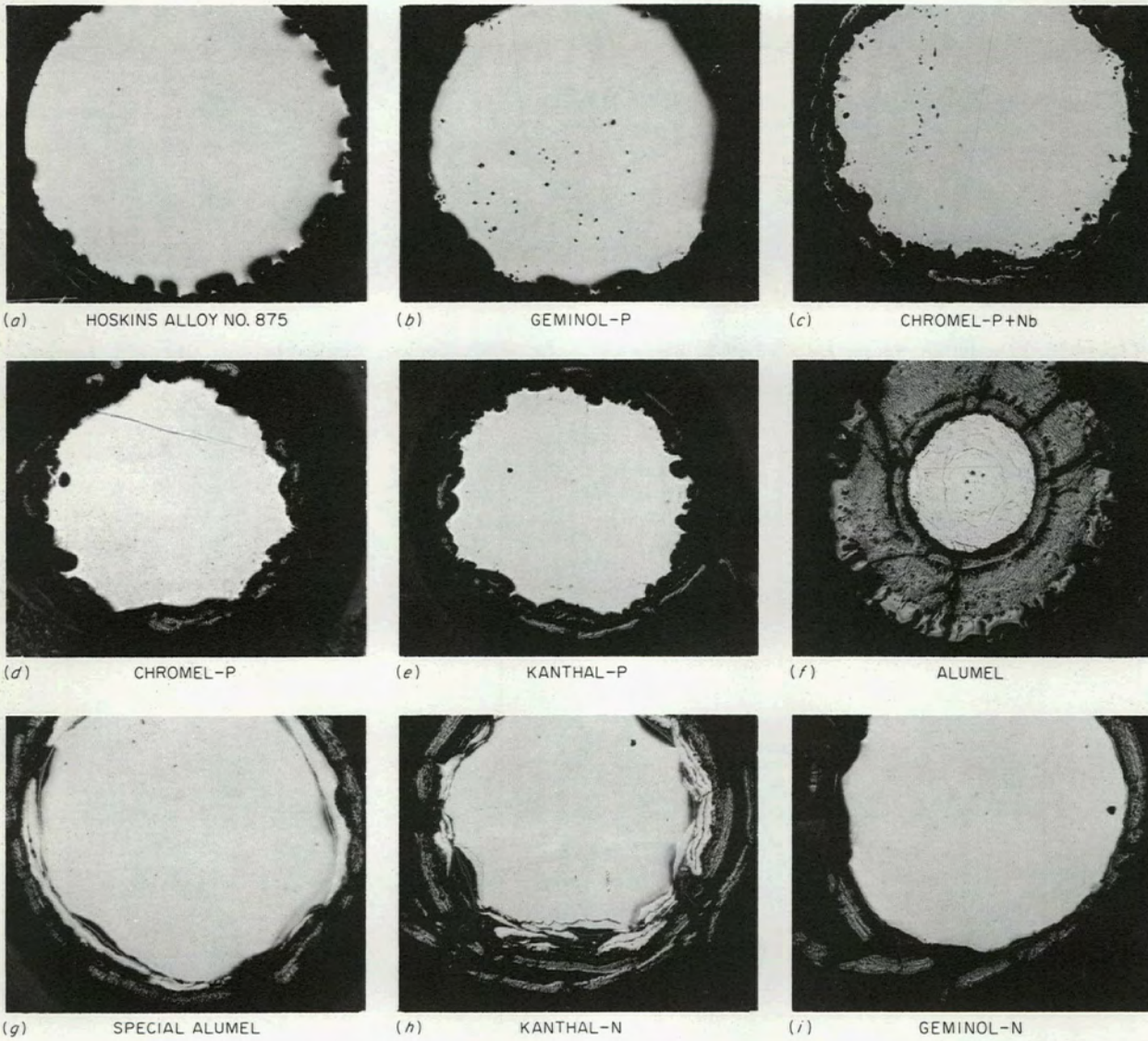


Fig. 4.13. Cross-Section Photomicrographs of Unetched Alloys Exposed 500 hr at 1000°C (Refractory-Tube Method). ~100X. Reduced 41%.

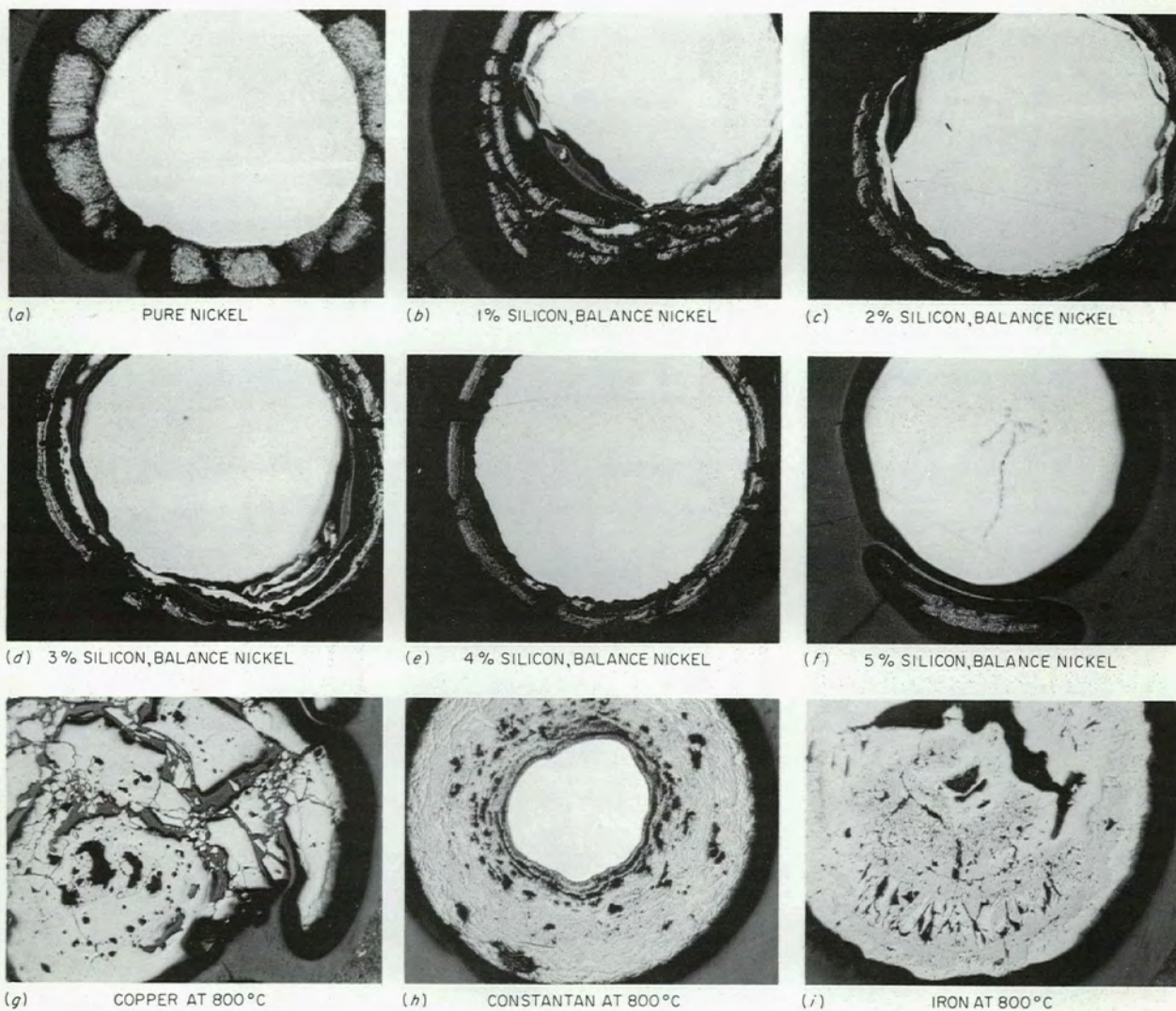


Fig. 4.14. Cross-Section Photomicrographs of Unetched Experimental Ni-Si Alloys Exposed 500 hr at 1000°C, and of Copper, Constantan, and Iron Exposed 500 hr at 800°C (Refractory-Tube Method). ~100X. Reduced 44%.

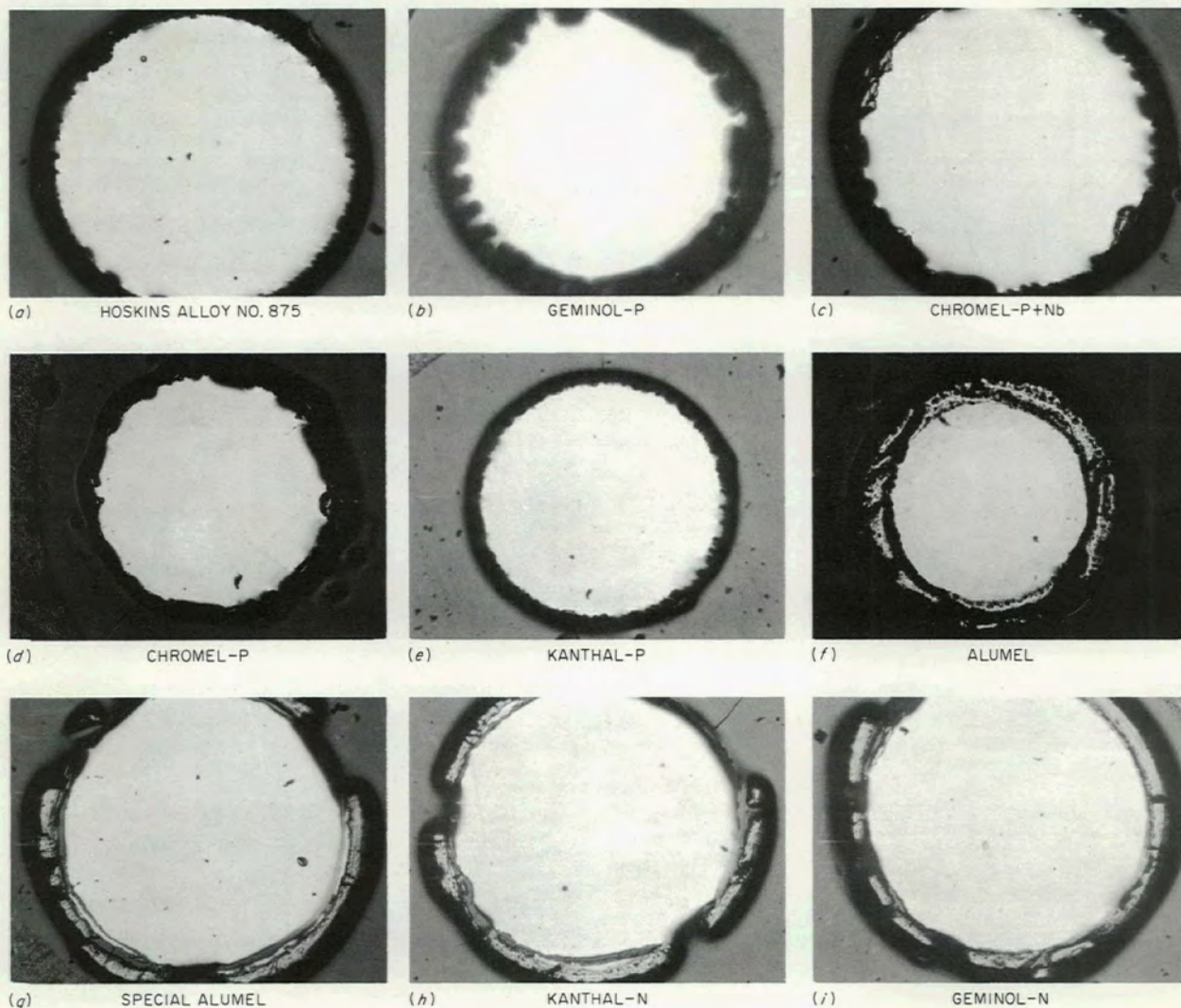


Fig. 4.15. Cross-Section Photomicrographs of Unetched Alloys Exposed 500 hr at 900°C (Refractory-Tube Method).  $\sim 100\times$ . Reduced 44%.

silicon on oxidation resistance, and only minor differences are seen from 2 through 5% silicon. The results for Hoskins No. 194, Kanthal-N, and Geminol-N are similar to those of the 2 to 3% binary Ni-Si alloys. In Figs. 4.14g-4.14i the behavior of copper, constantan, and iron, respectively, is seen after 400 hr at 800°C. Both copper and iron are completely oxidized, and constantan has suffered a severe attack.

The results in Fig. 4.15 at 900°C show similar but less attack than those at 1000°C. The oxide

penetration in Almel (Fig. 4.15f) is particularly interesting and shows that the attack is occurring both at the surface of the almel wire and probably intergranularly.

#### EMF CORRELATION EXPERIMENT

In a further effort toward the understanding of high-temperature effects upon thermocouple materials, as-received 22-gage Geminol-P, Geminol-N, Almel, and Chromel-P were strung into four-hole, 1-in.-long ceramic refractories and placed in a

1000°C furnace with a normal air atmosphere. The assemblies were isothermally exposed for times up to 500 hr and calibrated against platinum at the freezing point of silver (960.8°C).

Figure 4.16 shows the percentage change in silver-point calibrations vs time at 1000°C. Alumel showed a nearly 17% positive drift in 65 hr. This is in good agreement with the oxidation results. Furthermore, data could not be obtained for Alumel for longer than 65 hr because of brittleness of the wires, and even with the best care in attaching the platinum to the assembly, the Alumel wire broke into small pieces. The positive drift for Alumel is in the direction of the pure nickel calibration, possibly indicating

that silicon, manganese, and aluminum are being lost by oxidation.

Geminol-N changes only -1.5% in calibration in 500 hr. Again this is in agreement with the oxidation results, and furthermore this negative change is in the direction of slightly less silicon content. The thermal emf of 1 and 2% Si-Ni alloys is less than that for 2.5% silicon, so that if silicon is lost by oxidation this is the direction of change to be expected.

The drift of Chromel-P is surprisingly low, but indicates that chromium is being lost, with the drift going slightly positive then sharply negative. This would be expected from the thermal emf vs composition curves reported previously<sup>4</sup> if the composition of Chromel was slightly over the emf peak of the composition curve.

The drift of Geminol-P was positive and much larger than expected. If the oxidation results are true, only a small positive change in calibration would have occurred. The positive change is observed, but it is confusing that the isothermal drift results show such a large drift, compared with previous "nonisothermal" or conventional drift tests. This points up one more important factor in thermocouple research: the lack of correlation which may exist at times between the conditions designed to isolate a particular phenomenon and the operating conditions of a thermocouple. Thus in the isothermal exposure, the region of the thermocouple located in the temperature gradient is oxidized Geminol-P; however, in a conventional drift test, the temperature gradient region might not have seen such severe exposure. The former condition serves to amplify the effects of the high-temperature exposure, whereas the latter condition, because of the law of intermediate materials, tends to minimize this effect.

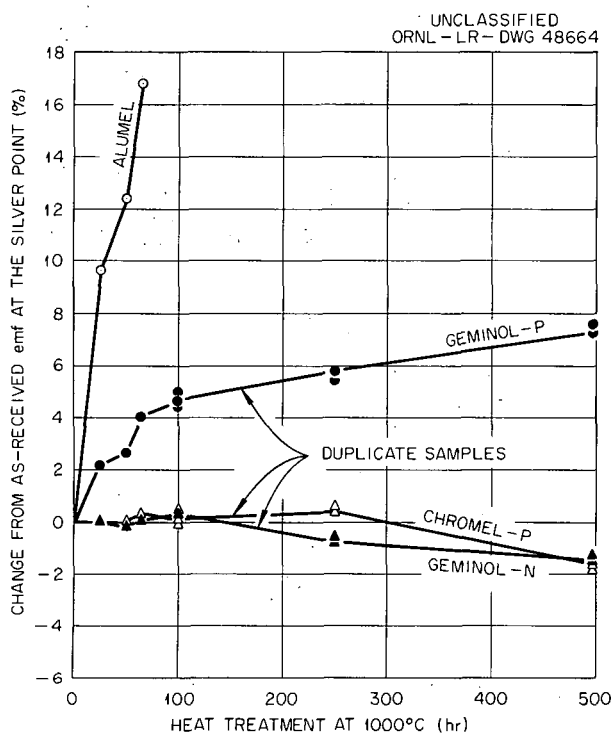


Fig. 4.16. Per Cent Change in Calibration at the Silver Point (960.8°C) vs Time of Exposure at 1000°C for Geminol-P, Geminol-N, Chromel-P, and Alumel.

<sup>4</sup>Ibid., Fig. 7.

## 5. PHYSICAL PROPERTIES

### INTRODUCTION

The thermoelectric effects discovered by Seebeck, Peltier, and Thomson plus accurate experimental measurements led to the three laws which encompass thermoelectric phenomena.<sup>1</sup> The term "homogeneous" is found in all three laws; and this underscores the observable fact that a spurious emf will be developed in a thermoelectric circuit if an inhomogeneous portion of a wire is in a temperature gradient. Thus, the thermal emf properties of a metal or an alloy may be altered by the existence of inhomogeneities.

There has been some uncertainty associated with the magnitude and sign of the inhomogeneity emf of the wire in a temperature gradient. It has been frequently stated that, because of this uncertainty, little could be predicted about the net influence of inhomogeneity on the emf of a thermocouple. Experiments have shown that an inhomogeneity should be defined as being due to a variation of the mechanical state or the chemical composition of a wire along its length. This definition is based on the fact that a variation of either of these will cause a spurious emf to be generated in a temperature gradient.

A homogeneous mechanical state of a wire can be defined as that state which exists when no change in physical properties occurs after subjecting a chemically homogeneous wire to any temperature in the range over which it is used. This definition excludes reactions which would change the chemical composition. Thus a wire which is, and remains, perfectly annealed and therefore contains no cold-worked regions represents the ideal homogeneous mechanical state. Two notable metallurgical processes involved in producing a homogeneous mechanical state in a metal in the temperature range of interest are the recovery and the recrystallization of the cold-worked metal. Recovery is characterized by a restoration of the electrical and magnetic properties of the cold-worked metal to those of an annealed metal, with no observed change in the

metal microstructure or other mechanical properties. In the metals studied in this experiment, recovery is the predominant metallurgical process taking place below 500°C. The rate of recovery in a metal is of first order with respect to the amount of unrecovered material present and increases exponentially with the absolute temperature.

The recrystallization of a cold-worked metal begins at a higher temperature than recovery does. It is characterized by the growth of new strain-free grains in partially recovered metal with a restoration of the mechanical properties characteristic of the annealed metal. The recrystallization temperatures of the metals used in these experiments are in the range from 400 to 700°C. Recrystallization rate theory states that it is a second-order process, depending on the amount of unrecovered material present and on the degree of recrystallization. The rate of recrystallization therefore increases exponentially with the absolute temperature. Since both recovery and recrystallization are nucleation and growth processes, their completion is dependent on time, temperature, and the original amount of cold work.

A homogeneous chemical composition is best defined as that state of the wire which exists when all portions of the wire are chemically identical. Thermal emf is very sensitive to composition gradients, much more so than chemical analysis; so a most stringent test for a homogeneous chemical composition would be to expose a *mechanically* homogeneous wire to a temperature gradient. Zero emf would be indicative of composition homogeneity.

Changes in thermal emf of a material may be due to:

1. oxidation,
2. cold-working and annealing,
3. precipitation of a new phase,
4. grain growth,
5. Soret effect, or
6. composition conversion caused by thermal-neutron irradiation.

Oxidation has been previously discussed (Chap. 4). Precipitation of chromium carbide is discussed in Appendix I. The effects on thermal emf of grain

---

<sup>1</sup>D. L. McElroy, *Progress Report 1, Thermocouple Research, Report for Period Nov. 1, 1956 to Oct. 31, 1957*, ORNL-2467, p 4.

growth and the Soret effect are thought to be negligibly small.<sup>2</sup> Irradiation damage is covered in a separate report.<sup>3</sup> This chapter is concerned with the changes in physical properties of thermocouple wire caused by cold-working and annealing and how these changes influence thermal emf.

#### PROPERTIES AND MATERIALS STUDIED

Tukon hardness measurements have been made in order to determine:

1. the hardness in the homogeneous physical state,
2. the change in hardness with increased cold-working,
3. the recrystallization temperature range for the materials, and
4. the effect of additions of silicon to nickel on these properties.

Electrical resistivity measurements have been made in order to determine:

1. the recovery temperature range for the materials,
2. the effect of cold-working on electrical resistivity, and
3. the effect of additions of silicon to nickel on these properties.

Thermal-emf measurements, including calibrations, drift tests, and homogeneity tests, have been made in order to determine thermal-emf changes:

1. in as-received materials,
2. due to cold-working,
3. due to annealings of cold-worked materials,
4. due to time-at-temperature of a cold-worked material, and
5. due to oxidation of materials.

The details of the experimental procedures used and the materials tested are reported by Nichols<sup>4</sup> and Lewis,<sup>5</sup> however, for the sake of completeness they are reviewed here. All Tukon hardness measurements were made using a Vickers penetrator on specimens mounted in Lucite. The diamond

<sup>2</sup>J. H. Crawford, Jr., ORNL, private communication, April 1959.

<sup>3</sup>M. J. Kelly, ORNL, private communication, Nov. 11, 1958.

<sup>4</sup>J. Nichols, *Spurious Thermal EMF's in Thermocouple Wire Subjected to Temperature Gradients*, ORNL CF-59-6-60 (June 15, 1959).

<sup>5</sup>A. E. Lewis, *The Effect of Cold Working and Annealing on the Thermal EMF of Thermocouple Materials*, ORNL CF-59-6-61 (June 15, 1959).

pyramid hardness was calculated in the normal manner. All heat treatments were done in air or helium. Cold-working was done by drawing wire through Carboloy dies at room temperature, with a subsequently removed lubricant. The amount of cold-working was determined by wire diameter measurements and calculated from

$$\frac{A_0 - A_f}{A_0} \times 100,$$

where  $A_0$  is the original area and  $A_f$  is the final area. Recrystallization specimens were produced by heat-treating them in air in an Inconel block with holes drilled for the individual wire specimens and with a hole for a thermocouple for temperature measurement. The nickel-silicon alloys were prepared in a molybdenum-wound, hydrogen-atmosphere resistance furnace. Melting was done in hydrogen, and after outgassing the melt in a vacuum it was chill-cast into a copper mold. The cast ingots were homogenized in a hydrogen atmosphere for 72 hr at 1000°C. Fabrication to 18- and 20-gage wire from the ingots was done by the Hoskins Manufacturing Company. The wire was bright-annealed after drawing. Electrical resistance measurements were made at 0°C, using four leads and a Mueller bridge. Thermal-emf calibrations were made by the comparison and melting point methods. The thermal-emf homogeneity tests were made using the unilateral gradient furnace previously described.<sup>1</sup> Nichols<sup>4</sup> has extensively investigated the errors of this experiment and the optimum operating conditions.

Virtually all the alloys listed in Table 4.1 were tested, with emphasis on Chromel-P and Alumel.

## EXPERIMENTAL RESULTS AND DISCUSSION

### Hardness Results

The mechanical state of the as-received wire was determined by measuring the diamond pyramid hardness of the wire specimens in the as-received condition and after the specimens had been annealed at 900°C in air for times of 0.25, 0.50, 1, 2, 4, 8, 20, and 70 hr. Figure 5.1 shows that at 900°C the hardness, in general, decreases with time. Geminol-N, Kanthal-N, and Alumel all showed rapid decreases in hardness for the first 30 min, then a more gradual change until a minimum hardness was reached after approximately 2 hr

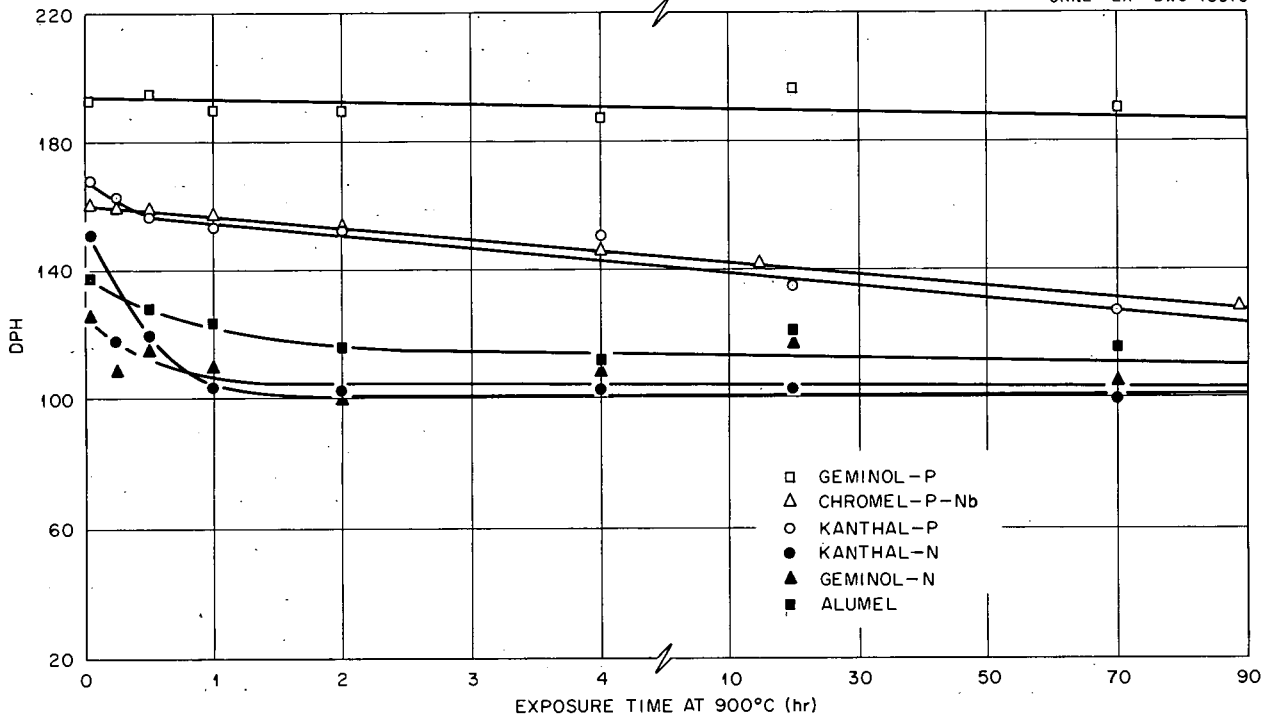


Fig. 5.1. Effect of Time vs Hardness at 900°C for the As-Received Materials.

of heat treatment. Kanthal-P and Chromel-P + Nb showed some hardness changes with time, with most of the change in hardness occurring after 8 hr of annealing, although a small change in hardness was observed for the Kanthal-P during the first 30 min. Essentially no change in hardness had occurred in Geminol-P. These results indicate that the as-received Geminol-N, Kanthal-N, and Alumel were initially in a cold-worked state, with recrystallization having occurred rapidly at 900°C. It appears that Kanthal-P, Chromel-P + Nb, and Geminol-P were respectively in states of progressively less initial cold-working.

The hardness (DPH) as a function of percentage of cold work has been plotted in Fig. 5.2 for the alloys discussed above. The initial value of hardness was determined after the wires had been annealed at 900°C for 4 hr. From Fig. 5.2 it is possible to determine approximately the degree of work-hardening of the as-received wires. This was done by correlating the hardness of the as-received wires shown in Fig. 5.1 with the hardness vs cold-working shown in Fig. 5.2. This showed that

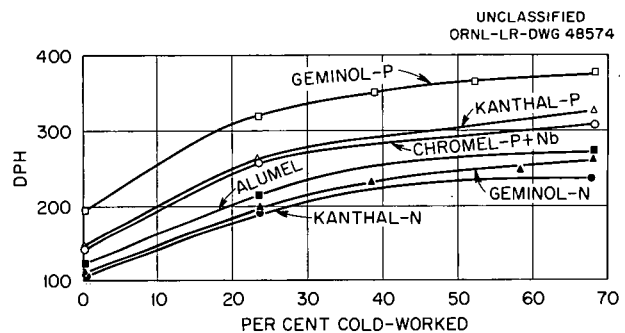


Fig. 5.2. Effect of Cold-Working on Hardness.

the as-received wires were cold-worked to the extent shown below:

Chromel-P + Nb	2.5%
Alumel	3.5%
Kanthal-P	4.5%
Kanthal-N	12%
Geminol-P	0.5%
Geminol-N	5%

The recrystallization of Geminol-P, Geminol-N, Chromel-P + Nb, Alamel, Kanthal-P, and Kanthal-N was studied after they were cold-worked 20 and 70%. Figures 5.3 and 5.4 show the results. The recrystallization temperature was defined as the temperature at which the DPH was 50% less than the initial cold-worked hardness. The results of these assignments for the recrystallization temperature are given in Table 5.1. The results were

consistent in that they showed higher recrystallization temperatures for shortened annealing times, less cold-working, and higher alloying content. In some instances the data for 1 and 4 hr of annealing indicated deviations from the expected behavior.

Results of similar studies on a series of nickel-silicon alloys are shown in Fig. 5.5. Figure 5.5a shows that the as-received hardness increased

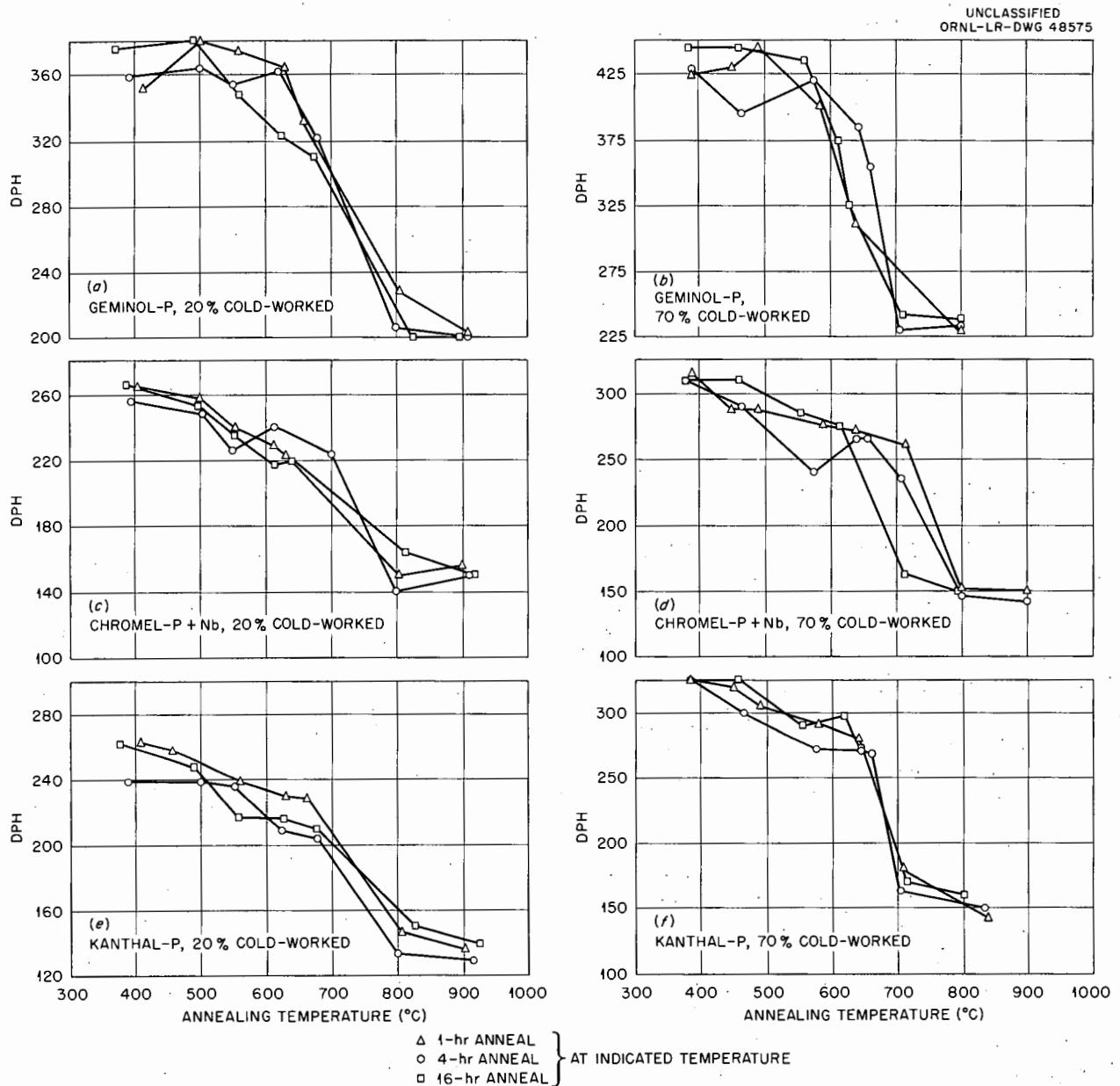


Fig. 5.3. Recrystallization Curves for Geminol-P, Chromel-P + Nb, and Kanthal-P After 20 and 70% Cold-Working.

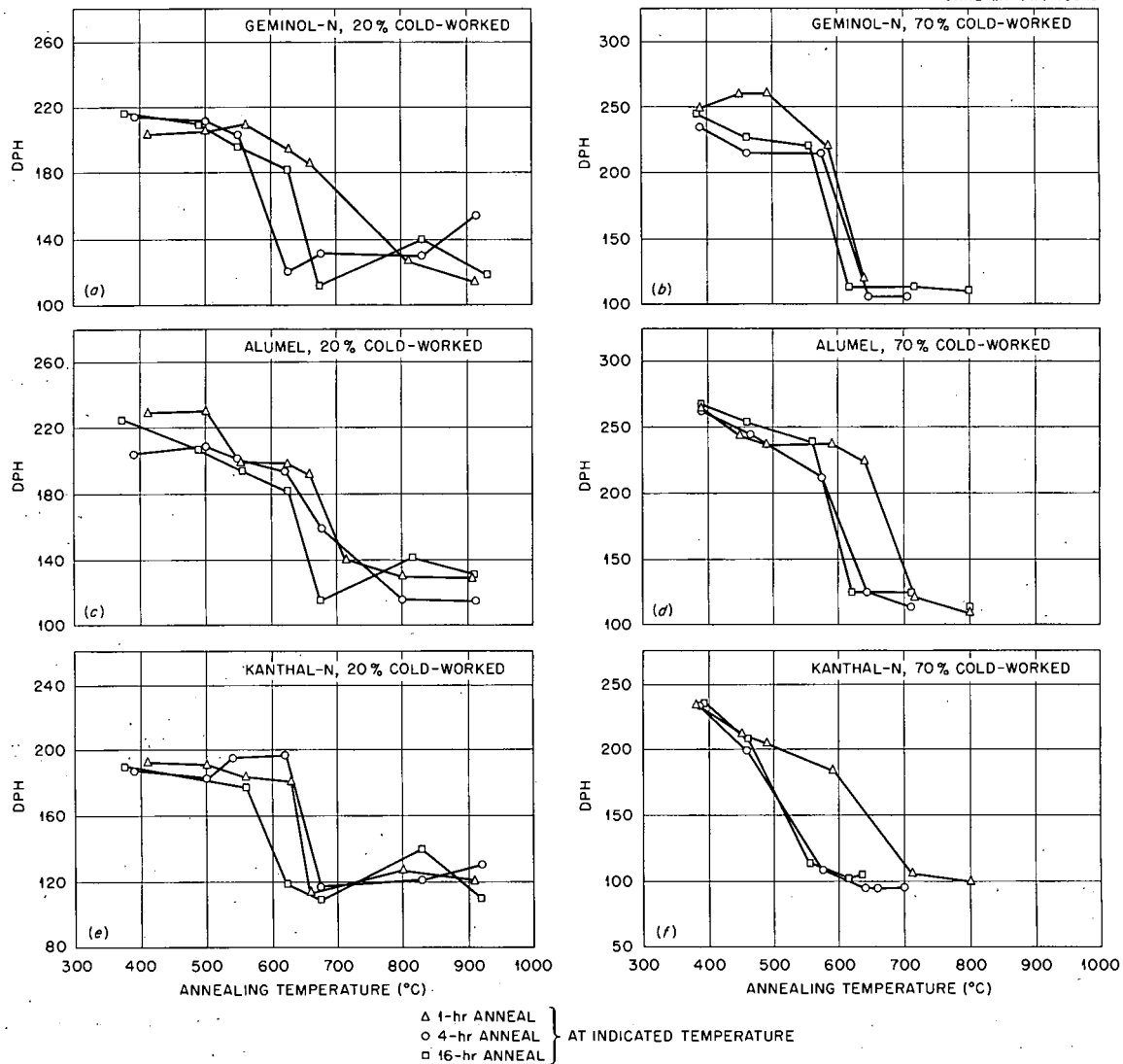


Fig. 5.4. Recrystallization Curves for Geminol-N, AlumeI, and Kanthal-N After 20 and 70% Cold-Working.

Table 5.1. Recrystallization Temperatures for Commercial Alloys Studied

Alloy	Recrystallization Temperature (°C)					
	20% Cold Work			70% Cold Work		
	1-hr Anneal	4-hr Anneal	16-hr Anneal	1-hr Anneal	4-hr Anneal	16-hr Anneal
Geminol-P	725	715	705	640*	665*	640
Chromel-P + Nb	695*	720*	705	735	710	655
Kanthal-P	755	755	725	670*	670*	655
Geminal-N	700	635	580	610	590	530
AlumeI	685	660	635	650	590	575
Kanthal-N	640*	650*	590	590	520*	520*

\*Possible discrepancy in data.

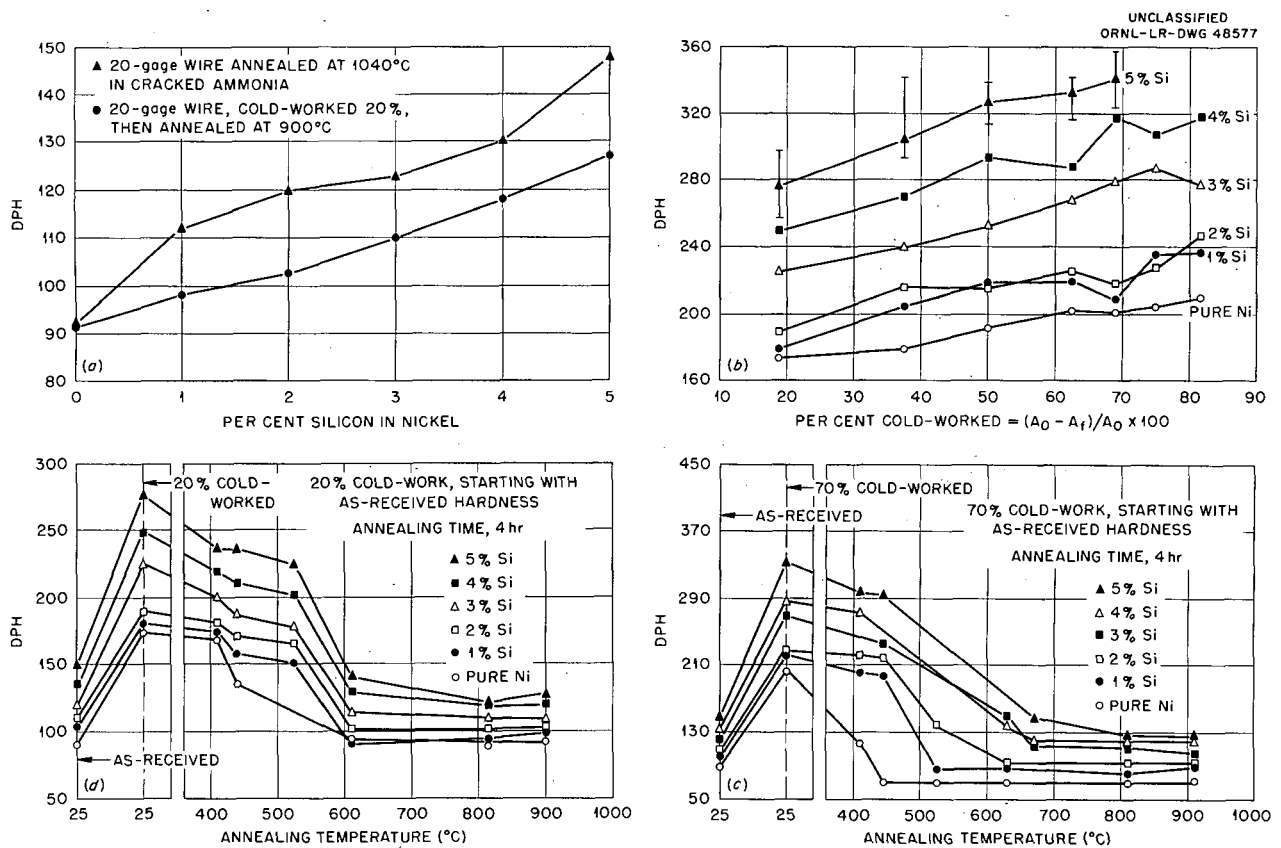


Fig. 5.5. Effect of Cold-Working and Annealing on the Hardness of Ni-Si Alloys. (a) Annealed hardness vs % Si in Ni; (b) hardness vs % cold-working for Ni-Si alloys; (c) hardness vs annealing temperature ( $^{\circ}\text{C}$ ) for 20% cold-working for Ni-Si alloys; (d) hardness vs annealing temperature for 70% cold-working for Ni-Si alloys.

with increasing silicon concentrations as expected, but also shows that the hardness after a 4-hr anneal at  $900^{\circ}\text{C}$  was somewhat lower than the as-received hardness. This indicates that the as-received alloys of 3, 4, and 5 wt % Si were cold-worked. Figure 5.5b shows the increase in hardness with increased cold-working. Severe hardening occurred in the first 20% area reduction. Figures 5.5c and 5.5d show the recrystallization data for 4-hr anneals at the indicated temperatures. The recrystallization temperatures (50% DPH) for the two percentages of cold-working are summarized in Table 5.2.

#### Electrical Resistivity Results

The measured electrical resistance at  $0^{\circ}\text{C}$  ( $R_0$ ) of the thermocouple wire specimens with four measuring leads was assigned as the reference for all successive treatments given the respective specimens. The specimens were treated for times varying from 0.5 to 18 hr at temperatures of 100,

225, 350, 470, and  $600^{\circ}\text{C}$ , in air. Changes due to oxidation at the higher temperatures were noted. All resistance measurements were made at  $0^{\circ}\text{C}$  after the various heat treatments.

Barrett<sup>6</sup> reports an electrical resistance decrease,  $\Delta R/R$ , for 70% cold-worked nickel after annealing in the range 200 to  $400^{\circ}\text{C}$ . This indicates that the electrical resistivity of nickel is increased by cold-working, which is attributed to locally distributed internal strains that cause scatter of electrons. Figure 5.6a shows the results after 4 hr at temperature for Geminol-P, Kanthal-P, and Chromel-P + Nb. Figure 5.6b shows corresponding results for Geminol-N, Alumel, and Kanthal-N. The assignment of recovery temperatures from these data is difficult. One can only assign ranges over which this phenomenon occurs,

<sup>6</sup>C. S. Barrett, *Structure of Metals*, p 375; McGraw-Hill, New York, 1943.

Table 5.2. Recrystallization Temperatures for Ni-Si Alloys

Material	Recrystallization Temperature (°C)	
	20% Cold Work	70% Cold Work
Nickel	315	245
1% silicon, bal. nickel	320	290
2% silicon, bal. nickel	350	340
3% silicon, bal. nickel	430	360
4% silicon, bal. nickel	475	435
5% silicon, bal. nickel	495	440

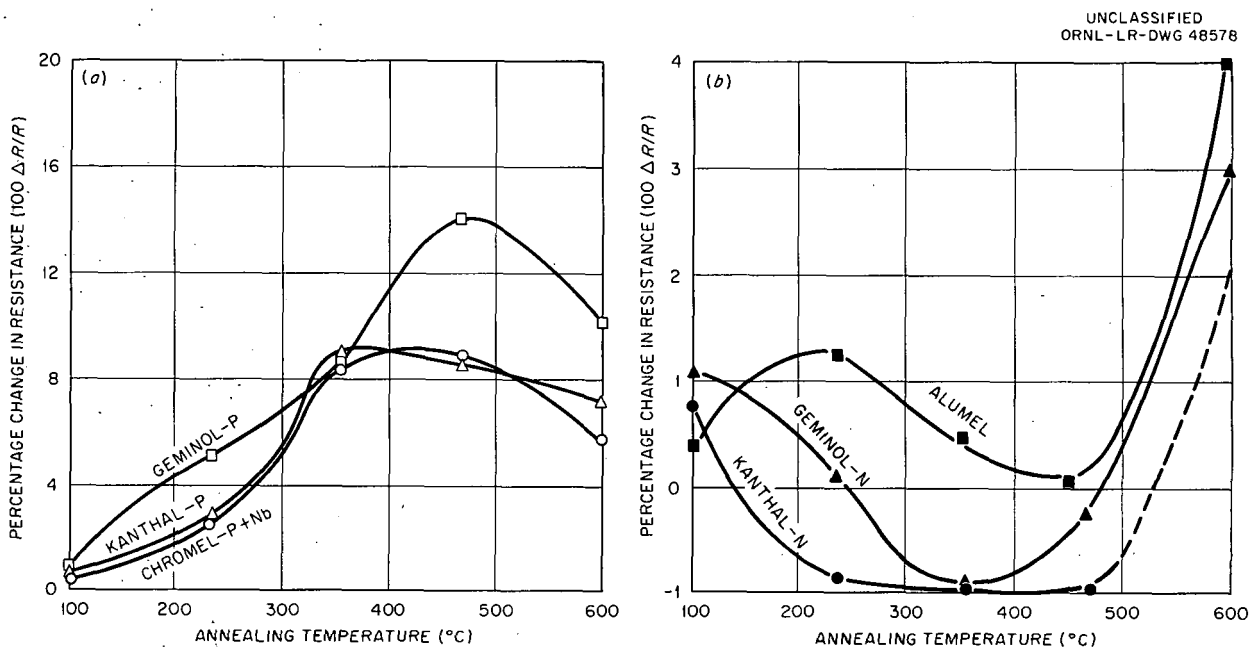


Fig. 5.6. Change in Electrical Resistance at 0°C after 4-hr Exposure at Temperature. All wires had been initially cold-worked 70%.

and a temperature for complete recovery. These values are tabulated in Table 5.3. If the data interpretation is correct, the recovery temperature increases with increased alloying content in a manner similar to that for the recrystallization temperature. These assigned recovery temperatures are well below the recrystallization temperatures, as would be expected.

The above statements regarding recovery are as theory would predict, except it should be noted that the data for Geminol-P, Chromel-P + Nb, and Kanthal-P indicate that the resistivity of these cold-worked wires is less than that of as-received

or annealed wire. This is contrary to accepted theory. Measurements on Chromel-P + Nb, as-received and 70% cold-worked, gave resistivity values of 69.2 and 63.6 microhm-cm, respectively, at 0°C. This corresponds to a decrease in electrical resistivity of 8%, in agreement with the annealing data. A possible explanation of this may exist in a hypothesized ordering reaction for the Ni-Cr system, which occurs at 25 at. % Cr-75 at. % Ni (20-80 wt %). Douglas and Dever<sup>7</sup> report

<sup>7</sup>T. B. Douglas and J. L. Dever, *J. Research Natl. Bur. Standards* 54, 15 (1955).

**Table 5.3. Recovery Temperature for the Alloys Tested at 70% Cold Work**

Alloys	Temperature Range (°C)	Temperature for Maximum $\Delta R/R$ (°C)
Geminol-P	500 > T > 100	450
Chromel-P + Nb	450 > T > 100	370
Kanthal-P	400 > T > 100	330
Geminol-N	350 > T > 50	290
Alumel	400 > T > 100	300*
Kanthal-N	300 > T > 50	225

\*Value may be in error.

values for the specific heat of the alloy 80% Ni-20% Cr from 0 to 900°C which show a discontinuity in the vicinity of 600°C. Although this discontinuity was not explained, ordering could cause such an effect.

Thus the causes for the observed decrease in resistivity with cold-working could be twofold: (1) cold-working, per se, could cause it, but this is highly improbable, according to the electron theory of metals; (2) a more probable cause is that cold-working induces short-range order, which in turn leads to the observed decrease. This is to say that cold-working enhances local diffusion and results in nickel and chromium atoms finding preferred lattice sites.

The electrical resistivity at 0°C of the as-received nickel-silicon alloy wires was measured and is shown in Fig. 5.7a. For pure nickel the

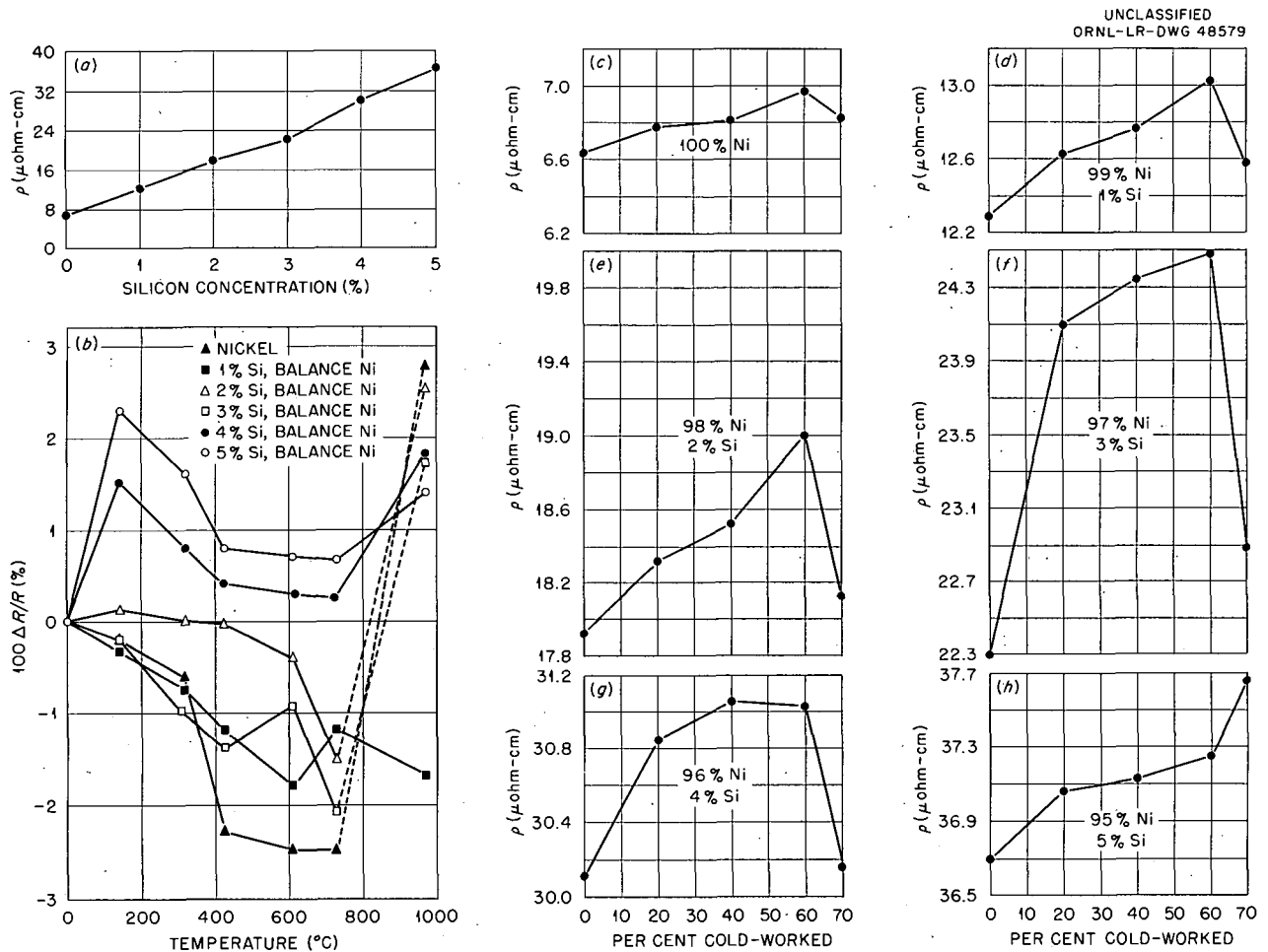


**Fig. 5.7. Electrical Resistivity Studies on Ni-Si Alloys. (a) Effect of silicon content, 0°C; (b) effect of annealing temperature on alloys cold-worked 70%; (c-h) effect of cold-working, 0°C.**

measured  $\rho_0 = 6.63$  microhm-cm is in good agreement with the previously published 6.84 microhm-cm at 20°C. The results show that silicon additions to nickel produce a nearly linear increase in resistivity at 0°C. As previously described, attempts were made to determine the recovery temperature range for these Ni-Si alloys. The results shown in Fig. 5.7b were small positive and negative changes, difficult to interpret. In an attempt to understand this erratic behavior, measurements of  $\rho_0$  for each of the alloys as a function of percentage of cold work were made. These results are shown in Figs. 5.7c-5.7b. Generally the resistivity increased with increasing cold work; however, it was noted that for 70% cold-working there was a sudden drop in resistivity in all alloys except the 5% silicon. This placed the 70% cold-worked resistivity very near to the as-received resistivity. Thus, one would expect

only small changes on annealing. A choice of 60% reduction might have led to results more easily correlated with recovery. Again, it is very difficult to explain these relations except possibly that the wires were heated by friction during die-drawing, which caused some recovery to occur prior to the measurement of  $\rho_0$ ; or an ordering similar to that proposed for the Ni-Cr alloys is occurring. Since the recrystallization temperatures for these alloys were determined, the temperature range for recovery could be approximated as about half the temperature for recrystallization.

Resistance measurements were made on cold-worked iron, copper, and constantan for use with iron and copper, respectively. The  $\Delta R/R$  vs temperature for 4 hr of exposure are shown in Fig. 5.8. These results are somewhat more interpretable than those for the nickel-silicon series. However, the data on 20% cold-worked

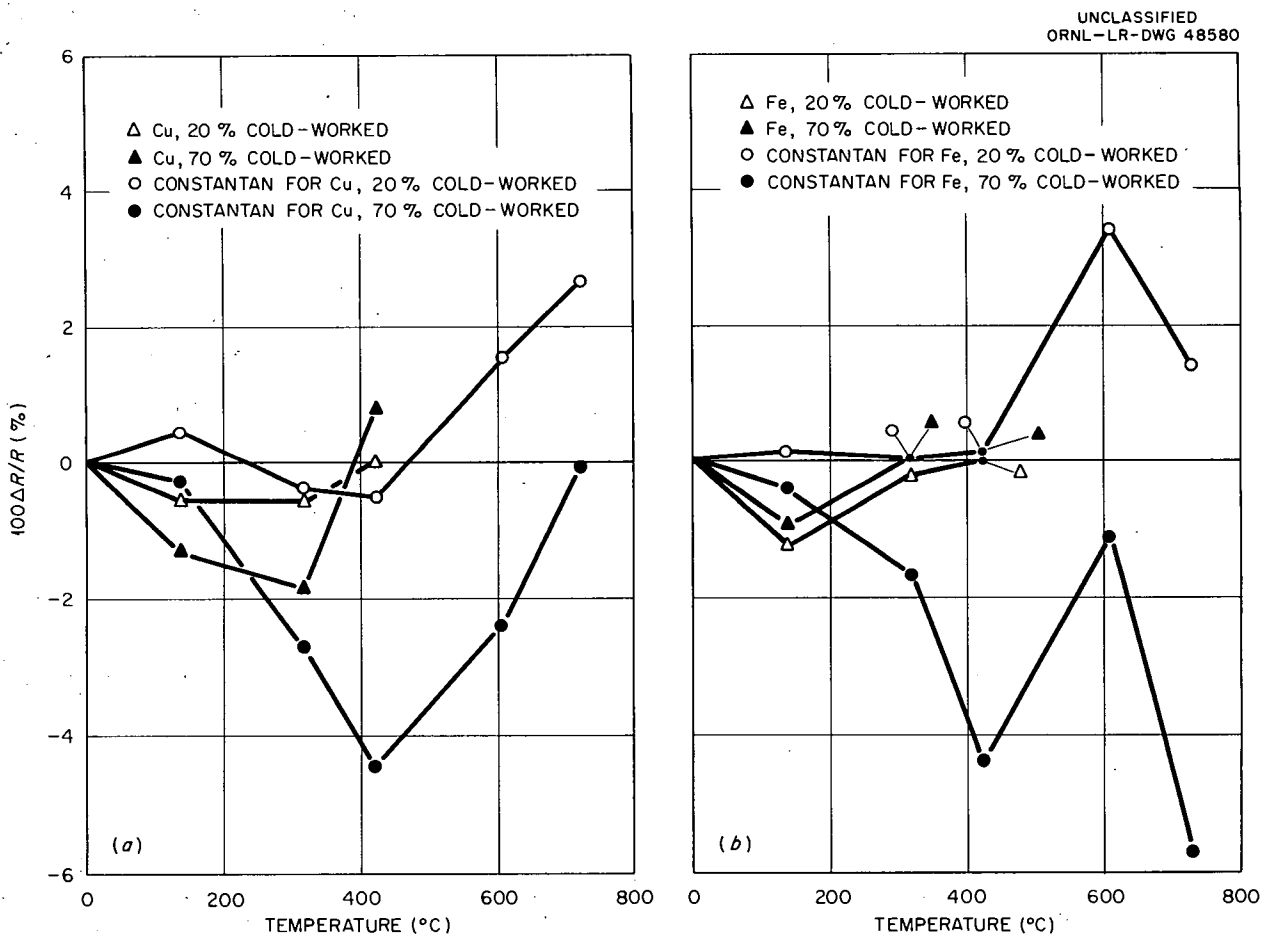


Fig. 5.8. Electrical Resistance Changes for Thermoelements Cold-Worked and Annealed. (a) Copper, constantan for use with copper; (b) iron, constantan for use with iron.

constantan illustrates the confusion encountered in the previous cases. For copper, recovery is complete by 150°C for 20% cold-worked but not until 300°C for 70% cold-worked material. The sudden rise in resistance above 300°C was due to oxidation. The data for iron are masked by oxidation, but indicate recovery was occurring at 150°C. Little can be said about constantan cold-worked 20%, but data for the 70% cold-working indicate that recovery was still in progress at 400°C.

In conclusion, it appears that electrical resistance recovery is an important factor to consider in studies on cold-worked thermoelements. At least in Geminol-P, recovery may not be complete until a temperature of 450°C is reached. Generally, for the other alloys, a 400°C anneal for 4 hr results in complete metallurgical recovery.

### Thermal-EMF Results

The first of these tests was a short-time drift test at 700°C, in which the thermal emf's of cold-

worked and annealed wires of Chromel-P + Nb and Almel were measured relative to platinum. The deviations of the cold-worked wires were obtained from the differences of their emf's relative to platinum and from the average reading of two annealed wires relative to platinum. The error for 20, 40, and 70% cold-worked wires at 700°C is plotted for Almel in Fig. 5.9 and for Chromel-P + Nb in Fig. 5.10. Figure 5.11 is a cross plot of these data showing the effect of cold-working on the initial error, the steady-state error, and the difference of these at 700°C. Cold-worked Almel showed a rapid change for the first 100 min of test and then a steady error was established. The initial change was most likely due to establishment of the position of the "interfaces" between unrecovered, recovered, and recrystallized material in the originally uniform cold-worked wire in the calibrating furnace temperature gradient. The changes observed as the amount of cold-working increased were particularly interesting in Almel. Less than 40% cold-working caused the thermal

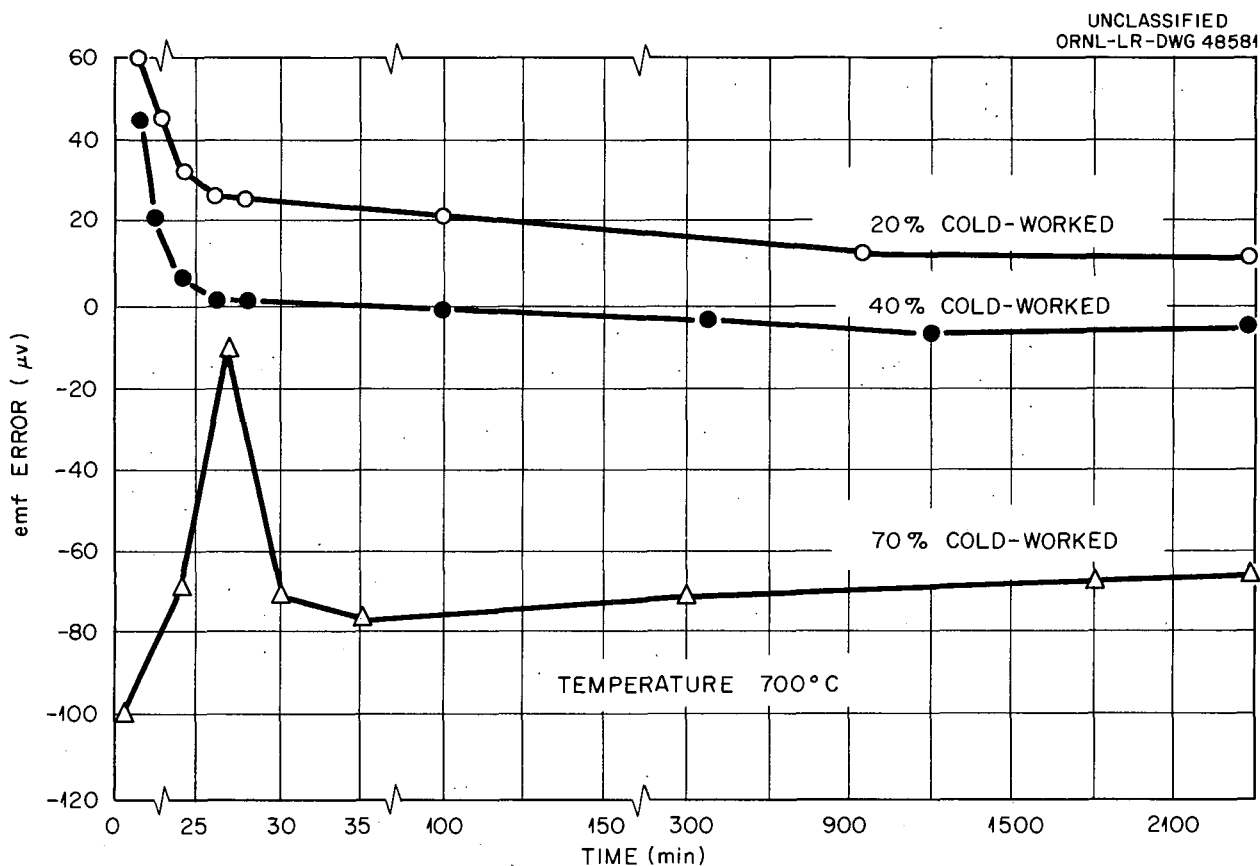


Fig. 5.9. Time-Dependent Error in EMF at 700°C for 20, 40, and 70% Cold-Worked Almel vs Platinum.

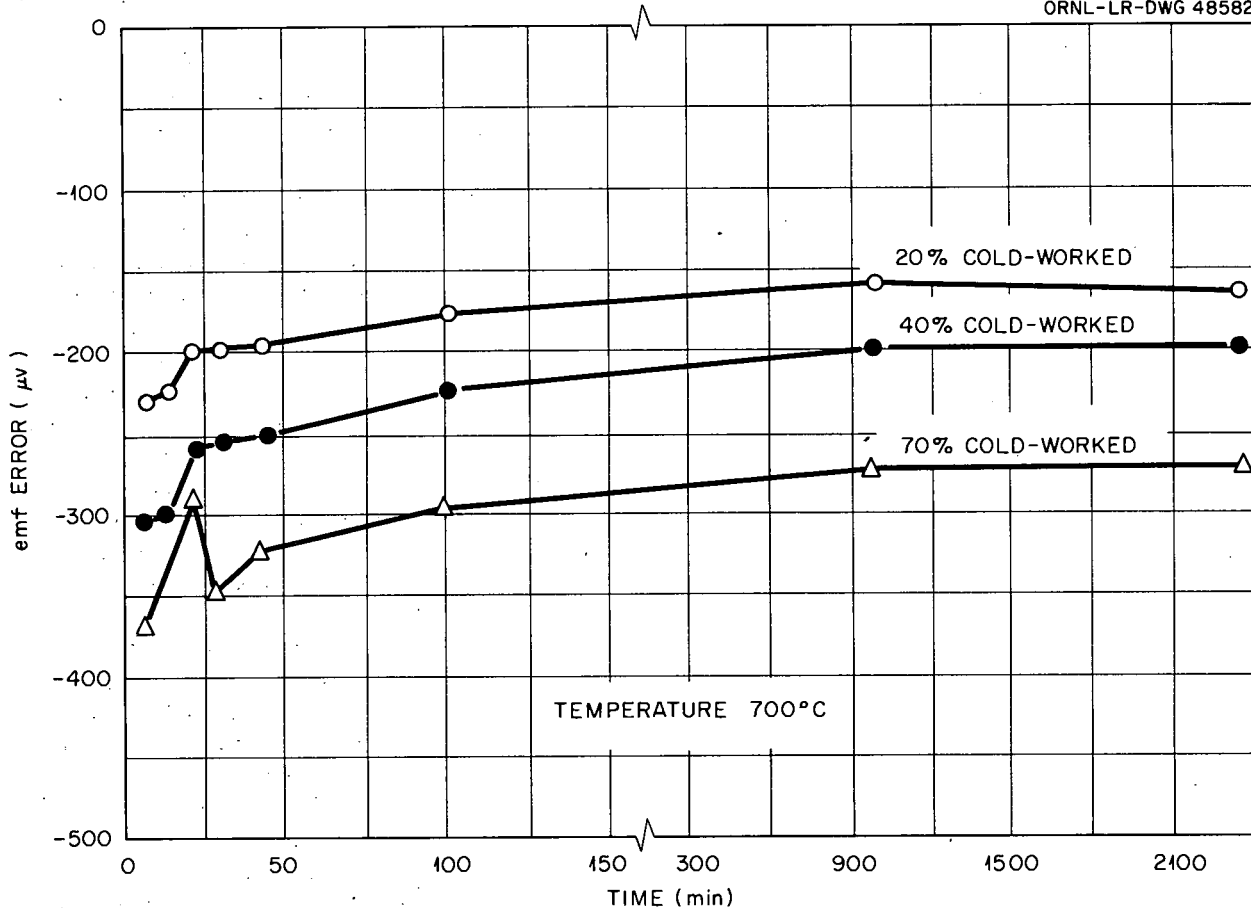


Fig. 5.10. Time-Dependent Error in EMF at 700°C for 20, 40, and 70% Cold-Worked Chromel-P + Nb vs Platinum.

emf to become greater than the thermal emf of the annealed Alumel, platinum. Cold-working more than 40% caused the thermal emf to become less than the thermal emf of the annealed Alumel, platinum. Unlike predictions from the theory of metals for the effects of cold-working on electrical resistivity, the effects of cold-working on the thermal emf of metals were not found in the open literature. Therefore, the above data is presented without interpretation. The novelty of the observed change in emf of cold-worked Alumel is certainly deserving of further study to seek the proper interpretations.

The interpretation of the thermal-emf data is further clouded when one considers the effects of cold work on the emf of Chromel-P + Nb. The deviation increased with increased cold work, as is seen in Fig. 5.10. Thus, if one is to explain the results on Chromel-P + Nb from the electron theory of metals, then he may be hard pressed to similarly explain the results on Alumel, since the

two are in opposite directions for less than 40% cold work.

Chromel-P + Nb is nearly five times as sensitive to cold-working as Alumel. The two are compensating to a certain extent for higher percentages of cold-working. At 70% cold work and at 700°C, the expected deviation in a thermocouple of these materials is approximately 8°C, or nearly 1% low.

A more extensive study of possible errors in Chromel-P + Nb and Alumel was made in which they were cold-worked 10, 20, 40, 50, 60, and 70%; then the emf of each of these wires relative to a stable wire was measured as a function of temperature. The stable wire was of Alumel or Chromel-P + Nb which had been annealed at 1000°C for 6 hr in helium. Typical examples of the results obtained in this test are given in Fig. 5.12. Figure 5.13 is a cross plot for Chromel-P + Nb of the emf deviation at 760°C vs cold-working from the various calibration treatments listed below. In

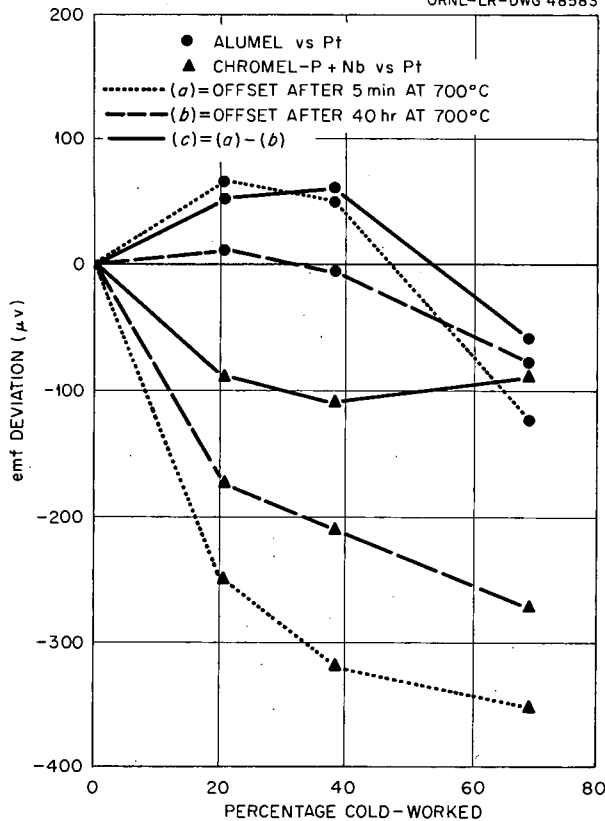


Fig. 5.11. Effects of Cold-Working on Initial Error and Steady-State Error, with Their Difference at 700°C. Represents summary of effects shown in Figs. 5.9 and 5.10.

this plot there are four parts to consider: (1) the first heating and cooling of the cold-worked Chromel-P + Nb wires, (2) the second heating and cooling of the Chromel-P + Nb wires without disturbing the system, (3) the heating and cooling of the Chromel-P + Nb wires after the entire thermocouple assembly had been annealed at 450°C for 6 hr, and (4) the heating and cooling after a 780°C anneal. The curve for the first heating of the cold-worked Chromel-P + Nb wires shown in Fig. 5.13 indicates that the deviation in emf increased with increase in cold-working. At 760°C this deviation is as much as  $-475 \mu\text{v}$  at 70% cold work. However, this emf deviation was not stable and drifted to a "stable" point when held at 760°C for 12 hr. This "stable" emf deviation was reflected in the second heating, as shown on the plot in Fig. 5.13. The drift of the emf between the first and second heating is caused

by establishment of the position of the "interfaces" in the temperature gradient between unrecovered, recovered, and recrystallized material in the wire originally of uniform cold work. This emf drift became gradually larger as the cold-working percentage increased.

It was postulated above that along the cold-worked wire in a temperature gradient there was a gradual change (or possibly an abrupt change, depending on the slope of the temperature gradient) in the physical state of the wire. The portion of the wire in the temperature gradient that is at a temperature less than the recovery temperature remained fully cold-worked. Moving into the furnace, the wire becomes more completely recovered. The net result is a distribution of "thermocouples" producing an emf. It was further postulated that no emf was produced from the fully recovered portion of the formerly cold-worked wire relative to the reference wire.

On the strength of these postulates it was predicted that the emf deviation could be greatly decreased if the entire thermocouple assembly were annealed at a temperature above the recovery temperature, but below the recrystallization temperature, that is, 450°C. This postulate was substantiated by the results shown in Fig. 5.13 for heating and cooling calibration of the thermocouple assembly after annealing at 450°C in an inert helium atmosphere. It is noted that the emf deviation was then reduced to an almost constant value of about 25% of the original deviation caused by 70% cold-working.

The results of the calibration runs on Alumel are shown in Fig. 5.14. Here, as in the short-time drift experiment, the results for Alumel did not follow a simple trend. For increasing amounts of cold-working up to approximately 55%, the emf deviation was positive at 760°C; that is, a cold-worked wire produced a greater emf relative to platinum than did an annealed or as-received wire. At values of cold-working greater than 55% the cold-worked wire produced less emf relative to platinum than did an annealed wire. It was also observed that these deviations on first heating were very much smaller than was observed for the Chromel-P + Nb. Furthermore, these deviations were changed very little by recovery. It will be shown later, however, that recovery tends to bring the calibration of the cold-worked wire closer to the calibration of an annealed wire.

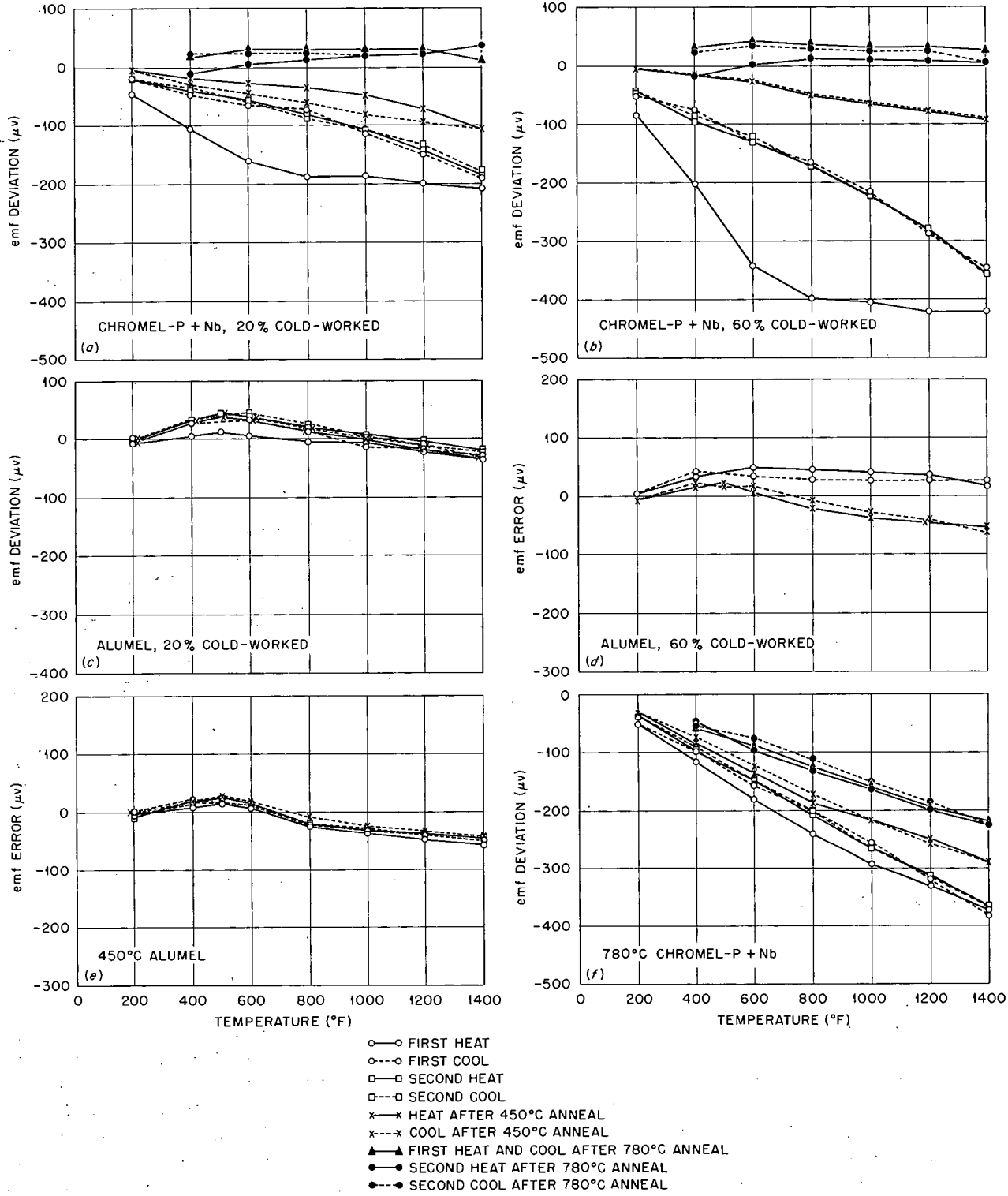


Fig. 5.12. Thermal EMF of Specific Wires Relative to Wires Annealed at 1000°C. (a) Chromel-P + Nb, 20% cold-worked; (b) Chromel-P + Nb, 60% cold-worked; (c) AluMel, 20% cold-worked; (d) AluMel, 60% cold-worked; (e) AluMel, annealed at 450°C; (f) Chromel-P + Nb, annealed at 780°C.

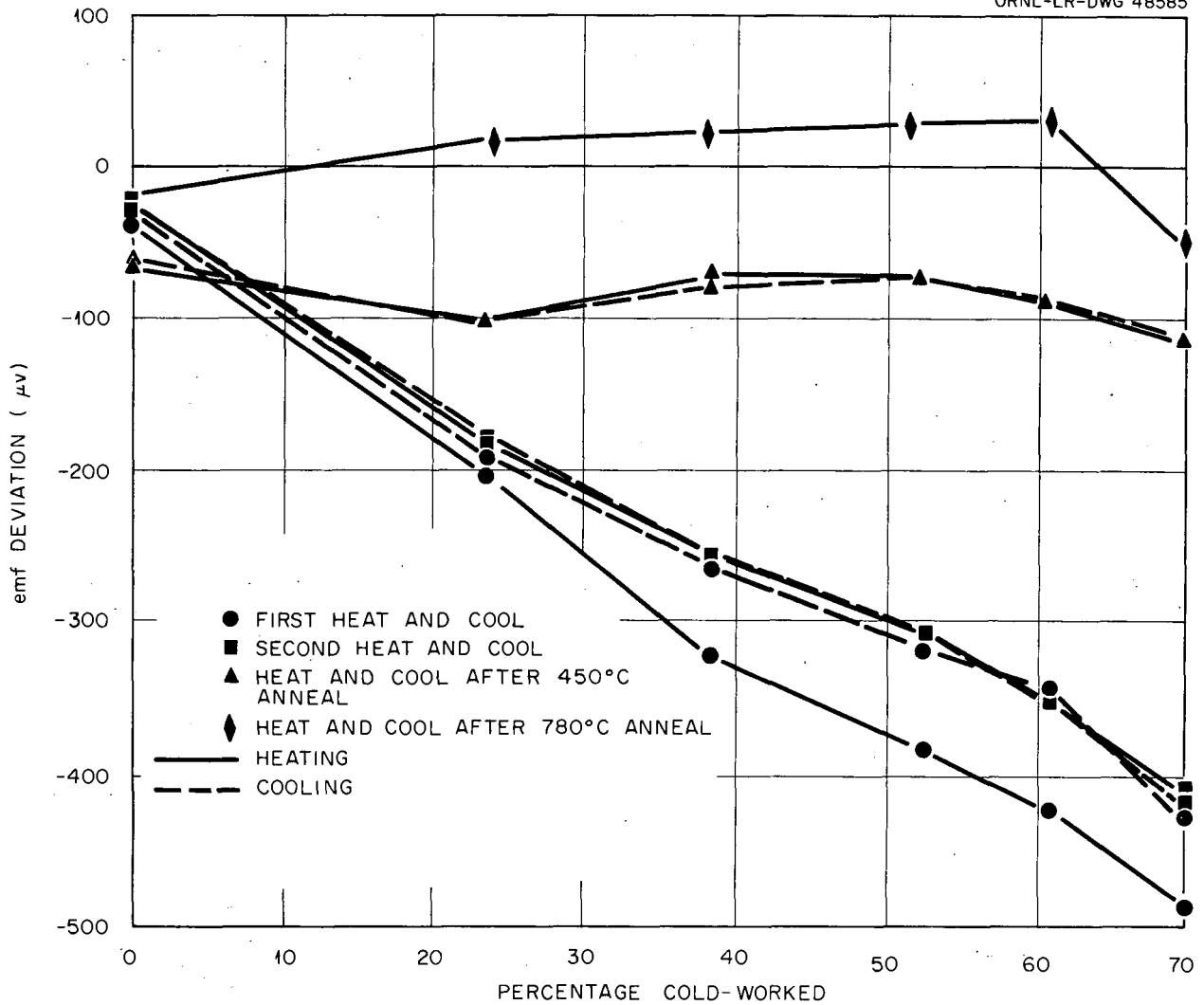


Fig. 5.13. EMF at 760°C vs Percentage of Cold-Working for Chromel-P + Nb, Compared with EMF for Chromel-P + Nb Annealed at 1000°C.

Included in these calibration tests was the emf of a 1000°C-annealed vs an as-received wire from room temperature to 760°C. A maximum deviation of  $-40 \mu\text{v}$  was observed at 760°C. Therefore, the calibrations of cold-worked materials were accurate to  $\pm 20 \mu\text{v}$ . A maximum deviation of  $-90 \mu\text{v}$  was observed for a 1000°C-annealed wire relative to a 480°C-annealed wire. The emf deviation of a 1000°C-annealed wire relative to a 780°C-annealed wire was unexpectedly  $-350 \mu\text{v}$  at 760°C. This will be discussed later.

### Homogeneity Results

The optimum operating conditions and the magnitude of errors associated with the unilateral temperature gradient furnace have been reported by Nichols<sup>4</sup> and Lewis<sup>5</sup> in developing and using this nondestructive test of thermocouple wires. This has included measurement of: (1) inlet and outlet temperature gradients, (2) the emf generated by the test wire cutting the earth's magnetic field and by tension in the test wire, (3) the emf

generated by cycling of the furnace controller, and (4) the possible emf due to the Benedicks effect.<sup>8</sup> Results of these measurements have shown that the apparatus is capable of detecting wire inhomogeneity to  $\pm 1 \mu\text{v}$ . Thus, the emf developed by a wire being drawn through the furnace inlet temperature gradient may be measured relative to

the constant emf developed in the wire which is fixed in position through the side of the furnace.

The initial tests were run on platinum and 90% platinum-10% rhodium thermocouple wires at a furnace temperature of 300°C. Examples of the results are shown in Fig. 5.15a. The emf's due to inhomogeneities in platinum are of the order of the experimental error ( $\pm 1 \mu\text{v}$ ) and thus the wire appears to be very homogeneous.

<sup>8</sup>C. Benedicks, "Thermocouple Effects in Homogeneous Metals," *Compt. rend.* 163, 751 (1916).

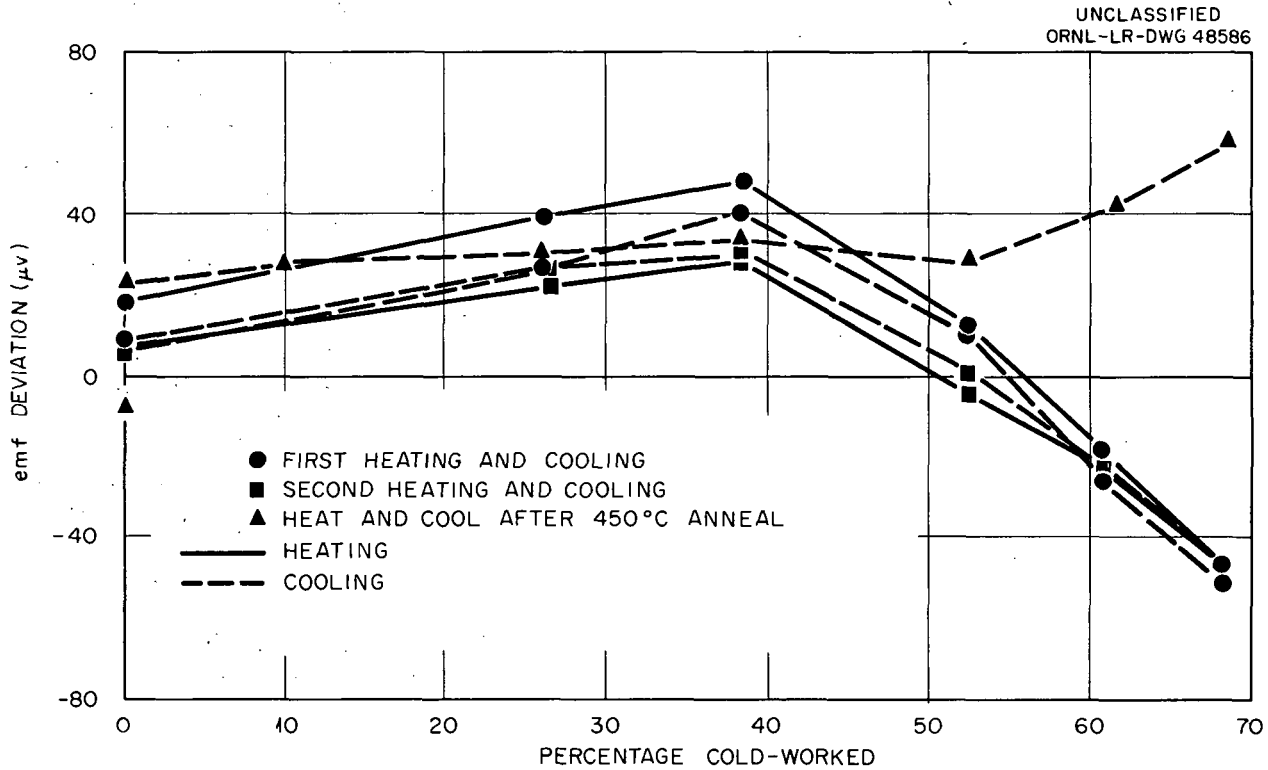


Fig. 5.14. EMF at 760°C vs Percentage of Cold-Working for Almel, Compared with EMF for Almel Annealed at 1000°C.

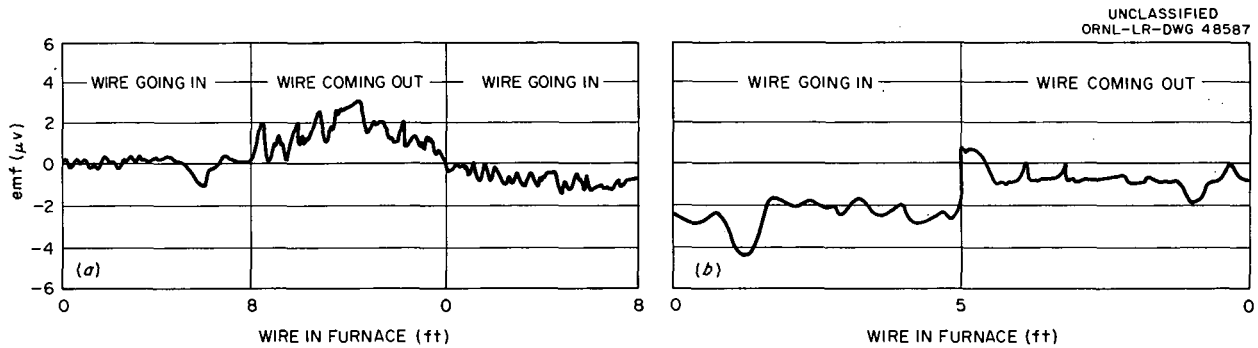


Fig. 5.15. EMF Trace Generated by (a) 100% Pt Wires and (b) 90% Pt-10% Rh as Wound into, out of, and Back into the Furnace at 300°C.

Figure 5.15b shows the results on a 90% Pt-10% Rh alloy which had been cut and rewelded. The emf associated with the weld is about  $3 \mu\text{v}$ . A portion of this emf is removed by the short-time low-temperature anneal received in the  $300^\circ\text{C}$  furnace, as can be seen from the emf trace on running the wire out of the furnace. Similar, but of less magnitude, was the emf associated with a cut and rewelded platinum wire.

Figure 5.16 shows a typical trace for an as-received Chromel-P wire at  $300^\circ\text{C}$ , which showed an offset of approximately  $10 \mu\text{v}$  as the wire was run

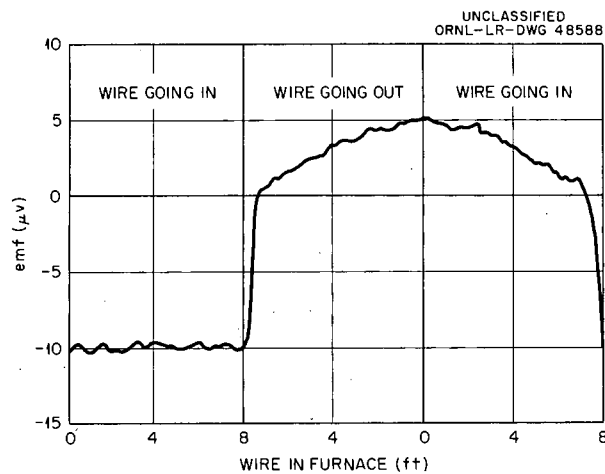


Fig. 5.16. EMF Trace Generated by 8 ft of As-Received Chromel Wire as Wound Alternately Into, Out of, and Back into the Furnace at  $300^\circ\text{C}$ .

into the furnace. On running the wire out of the furnace this emf had changed approximately  $15 \mu\text{v}$  because of the treatment received in the furnace. On rerunning the wire into the furnace the record was virtually a mirror image of that for wire coming out, with the exception of a slight difference at the end of the trace which was due to this segment of wire having received the longest anneal at  $300^\circ\text{C}$ . It is believed that this large change is associated with the metallurgical recovery phenomenon. Thus it is believed that the as-received Chromel-P wire was slightly cold-worked and that this was removed by a recovery anneal at  $300^\circ\text{C}$ .

A trace for as-received Alumel wire is shown in Fig. 5.17a. As the wire entered the furnace an average offset of approximately  $25 \mu\text{v}$  was observed. A distinct cycle in the thermal emf was observed for the entering wire. On leaving the furnace the average offset was observed to have shifted as in the case of the Chromel-P. However, the cyclic behavior was still apparent.

As previously stated, the proper interpretation of the emf's associated with inhomogeneities has thus far been lacking. Therefore it seemed that this cyclic behavior might well lend itself to a more interpretative experiment. A 10-ft length of Alumel from the same spool was doubled at the center and a platinum wire attached at the bend. This double thermocouple was then calibrated at the lead melting point,  $327.4^\circ\text{C}$ . Three-inch sections of the Alumel wires were removed, and each new junction was calibrated. This process

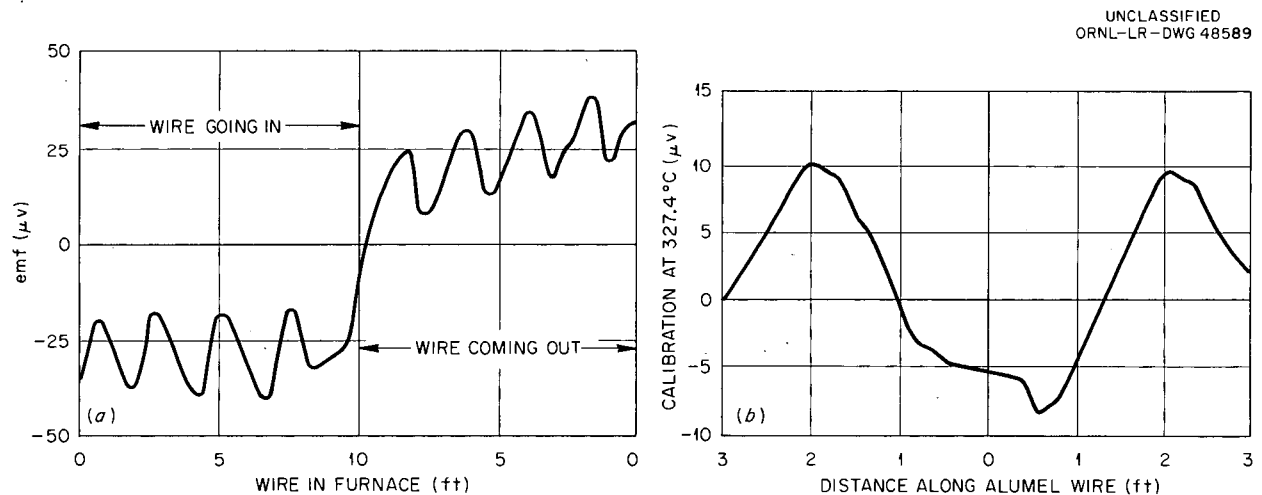


Fig. 5.17. EMF Generated Along an Alumel Wire as Measured by Two Methods. (a) Unilateral-gradient-furnace trace generated by 10 ft of as-received wire, wound into and out of furnace; (b) calibration along an as-received Alumel wire at melting point of Pb (Alumel-Pt).

was continued until nearly 7 ft of the original wire had been calibrated at 3-in. increments. The plot of deviation in microvolts at the lead point vs distance along the wire is shown in Fig. 5.17*b*. The cyclic behavior is readily seen, and the observed amplitude agrees quite well with the results of the homogeneity test. Any observed differences could be explained by the difference in the temperature gradients in the two tests.

Gradient furnace experiments were run on individual wires which were doubled in the center and partially immersed in an oxidizing atmosphere in a furnace at 1000°C for times up to 100 hr. The results after 28 hr of exposure are shown in Fig. 5.18. This test simulates operating conditions for a thermocouple wire and clearly illustrates the errors which would be associated with changing the depth of the thermocouple in a furnace.

The initial small offset is associated with wire which was at room temperature during the test. The exact form of the total trace was somewhat unexpected until it was found that the individual wires had been immersed past the maximum temperature of the furnace. The results do indicate that oxidation at 1000°C generated inhomogeneities which cause emf change nearly ten times that observed in as-received wire. Four types of wire were tested in this experiment, and the cumulative data were tabulated in Table 5.4 by selecting the maximum emf observed for each time of exposure. These data are plotted as a function of time at temperature in Fig. 5.19. The selected maximum

thus represents the greatest possible error which would be observed in thermocouples receiving this type of exposure.

An auxiliary experiment involving thermocouples of these two types has been run at 1000°C. The thermocouples were removed from the furnace after various times at temperature and were calibrated at 300°C. These results are shown in Fig. 5.20. For comparative purposes the data from the previous experiment are included, and it can be seen that the observed error is not as large as the maximum possible error indicated by the homogeneity tests. However, the two tests do show that the same trend is followed as a function of time at temperature and that the error at 300°C after 100 hr of exposure at 1000°C is quite large.

The unilateral gradient apparatus was also used to investigate the thermal-emf changes of cold-worked wire at various temperatures. The temperatures used in this investigation were 100, 300, 400, 500, and 700°C. Chromel-P + Nb and Almel cold-worked 50, 60, and 70% were studied. Moving the wire in and out of the furnace provided a rapid and convenient method of uniformly heat-treating the wire that was exposed to the temperature gradient. This uniform heat treatment eliminated to a large extent the effect of spurious emf caused by interfaces between wire in various stages of recovery. The change in thermal emf due to recovery at a particular temperature was thus easily obtained. The emf measured by the recording potentiometer is the difference between the emf of the wire in the fixed gradient and the emf of the

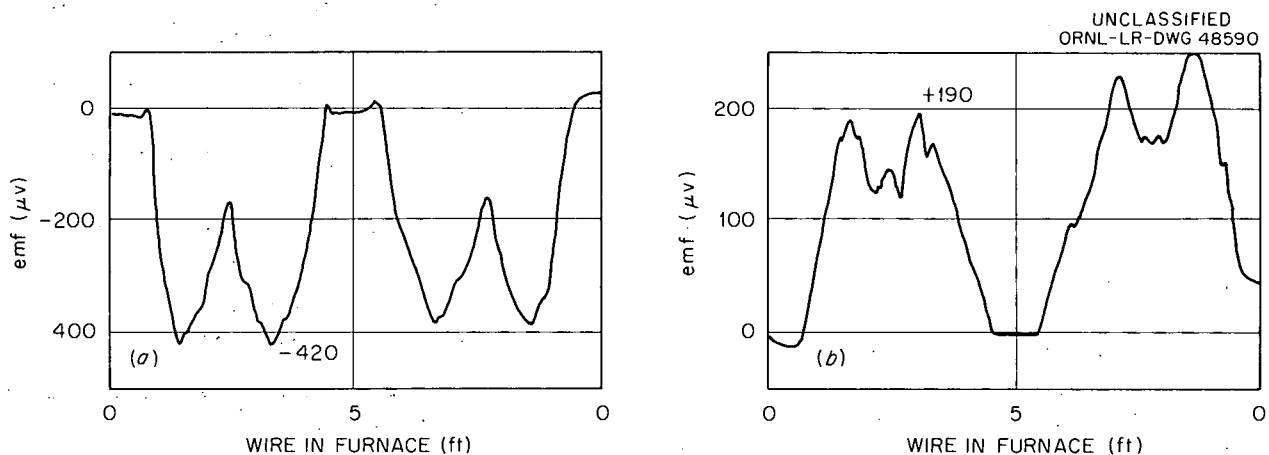


Fig. 5.18. EMF Trace at 300°C Generated by 5 ft of As-Received Almel Wire and by 5 ft of Kanthal-P Wire. Both wires had been doubled in the center and immersed 2 ft into a furnace at 1000°C for 28 hr prior to testing.

Table 5.4. Maximum EMF Generated by Thermocouple Wire in a Temperature Gradient as a Function of Time Immersed in a 1000°C Furnace

Wire	Duration of Immersion (hr)	Maximum EMF Generated ( $\mu\text{V}$ )	EMF Converted to Degrees C for a Chromel-Alumel Thermocouple
Alumel	5	-125	-3
Alumel	28	-420	-10
Alumel	96	-780	-19
Chromel-P	5	185	4.5
Chromel-P	28	390	9.5
Chromel-P	96	460	11
Kanthal-N	5	-46	-1.1
Kanthal-N	28	-115	-2.8
Kanthal-N	96	-320	-7.8
Kanthal-P	5	102	2.5
Kanthal-P	28	190	4.6
Kanthal-P	96	350	8.5

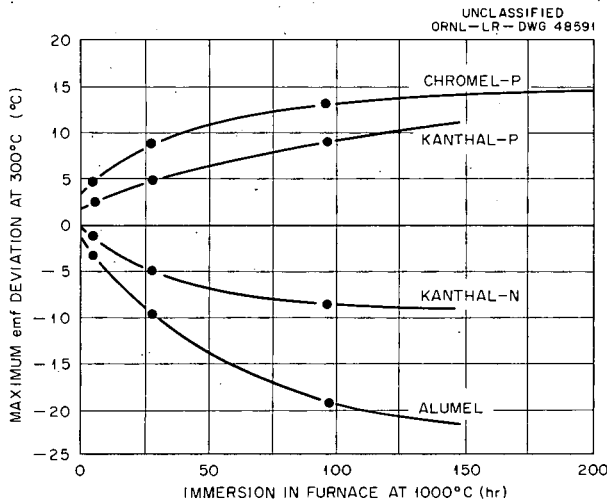


Fig. 5.19. Maximum EMF Deviation of Thermoelements as Measured at 300°C After Furnace-Immersion Time at 1000°C (Unilateral-Gradient Test).

entrance wire. It will be necessary to state the exact method used for ascribing the sign to an offset, which will be done with the aid of Fig. 5.21.

The solid line in Fig. 5.21 schematically represent the published emf of Chromel-P relative to platinum as a function of temperature. If we let the dashed line in Fig. 5.21 represent the emf of a

cold-worked wire relative to platinum as the wire is driven in and out of the furnace, the emf recorded by the recording potentiometer can be expressed as:

$$\Delta E_{in} = E_k - E_{in}^{cw} \quad (1)$$

$$\Delta E_{out} = E_k - E_{out}^{cw} \quad (2)$$

where

$\Delta E_{in}$  = the difference in emf when wire is moving into the furnace,

$\Delta E_{out}$  = the difference in emf when wire is moving out of the furnace,

$E_k$  = the emf of the as-received wire in a fixed gradient,

$E_{in}^{cw}$  = the emf of the cold-worked wire while moving into the furnace,

$E_{out}^{cw}$  = the emf of the cold-worked wire while moving out of the furnace.

The emf change due to recovery may be expressed by subtracting Eq. (2) from Eq. (1):

$$\begin{aligned} \Delta(\Delta E) &= E_k - E_{in}^{cw} - (E_k - E_{out}^{cw}) \\ &= E_{out}^{cw} - E_{in}^{cw} \quad (3) \end{aligned}$$

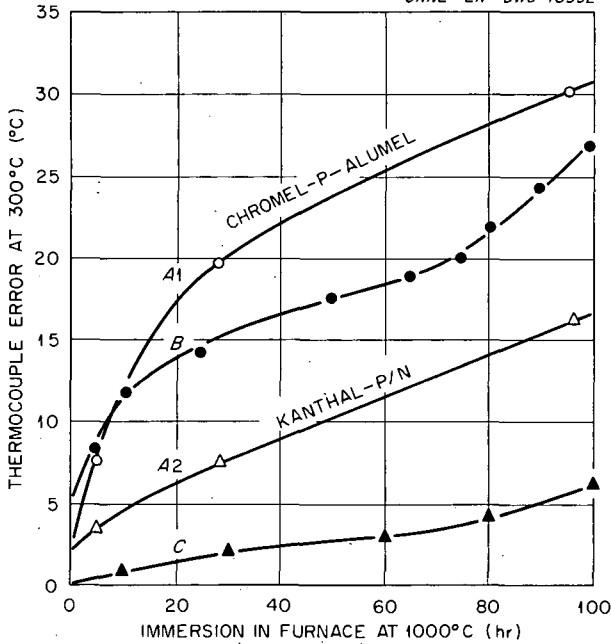


Fig. 5.20. Comparison of Thermocouple Errors as Determined by the Unilateral-Gradient-Furnace Method and a Platinum Resistance Thermometer. Curves A1 and A2 represent error in °C for Hoskins and Kanthal thermocouples according to unilateral-gradient-furnace results (see Fig. 5.19). Curve B represents resistance-thermometer calibration for Chromel-P, Alumel, and curve C was obtained in the same way as curve B, but for Kanthal-P/N.

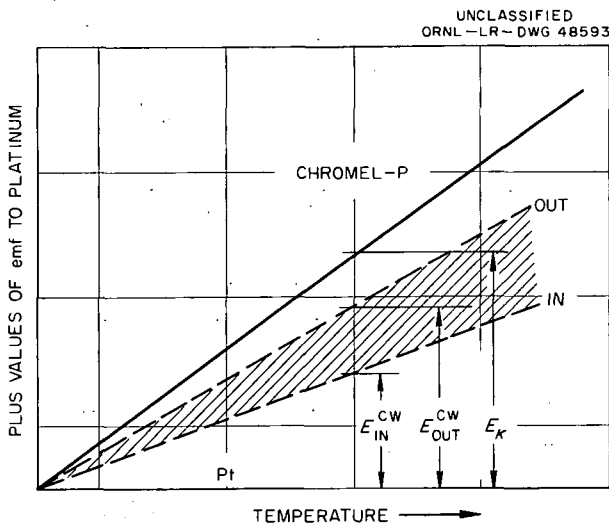


Fig. 5.21. Schematic Plot of EMF vs Temperature for Chromel-P, Relative to Platinum.

where  $\Delta(\Delta E)$  = the emf deviation in calibration due to recovery. The shaded area between the  $E_{in}^{CW}$  curve and the  $E_{out}^{CW}$  curve represents the change in the calibration of the cold-worked wire. Movement of the calibration toward the solid line will be positive, since  $E_{out}^{CW} - E_{in}^{CW}$  is greater than zero. If the direction of movement is opposite, the value of  $E_{out}^{CW} - E_{in}^{CW}$  will be negative. The above comments are also true for Alumel if the emf of cold-worked Alumel relative to platinum is considered negative.

From the above development it is possible to determine the amount of change heat treatment causes in the cold-worked wire. It is necessary to know the sign of the emf relative to platinum, and the sign of  $\Delta(\Delta E)$  must be known.

A schematic plot of the emf vs distance is shown in Figs. 5.22 and 5.23. Figure 5.22 shows a continuous trace at 100, 300, 400, and 500°C which is qualitatively representative of Chromel-P + Nb. Figure 5.23 shows a continuous trace at 100, 300, 400, 500, and 700°C which is a qualitative representation of the traces for Alumel. Line *ab* for each temperature does not fall on the zero line because there is an emf generated by the cold-worked wire relative to the fixed wire. After the

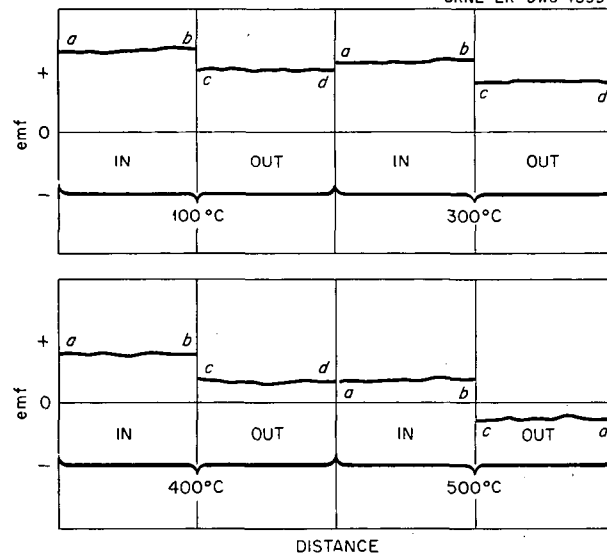


Fig. 5.22. Schematic Plot of EMF Trace vs Distance for Chromel-P + Nb Derived from Unilateral-Gradient Test at Various Temperatures. Note that the change in thermoelectric properties of the wire can be measured by the vertical shift in the *a-b* and *c-d* lines.

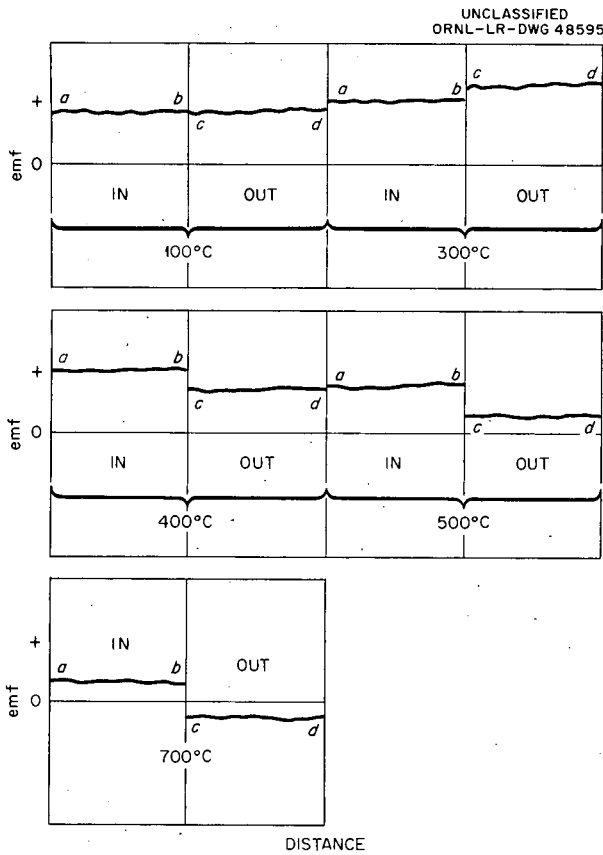


Fig. 5.23. Schematic Plot of EMF Trace vs Distance for Alumel Derived from Unilateral-Gradient Test at Temperature. Note vertical shift in *a-b* and *c-d* lines as they reflect changes in thermoelectric properties.

wire is driven into the furnace, the motor drive is reversed, and the wire comes out of the furnace. The change in the physical properties of the wire can be measured by the shift in the emf reading from line *ab* to line *cd*. This is  $\Delta(\Delta E)$  of Eq. (3), which for Chromel-P + Nb is  $\Delta(\Delta E) = E_{ab} - E_{cd}$ . For Alumel  $\Delta(\Delta E)$  is defined as the emf at the line *cd* minus the emf at the line *ab*.

The original plan was to use a new sample of cold-worked wire for each run. However, it was found experimentally that the total emf offset at a specific temperature for a piece of cold-worked wire was equal to the algebraic sum of the offset at that temperature and the offset from the previous temperatures to which the wire had been exposed.

Treatment of the emf-vs-distance traces in the above manner has yielded the results shown in Figs. 5.24 and 5.25. The relationship of emf offset to temperature for Chromel-P + Nb is shown in

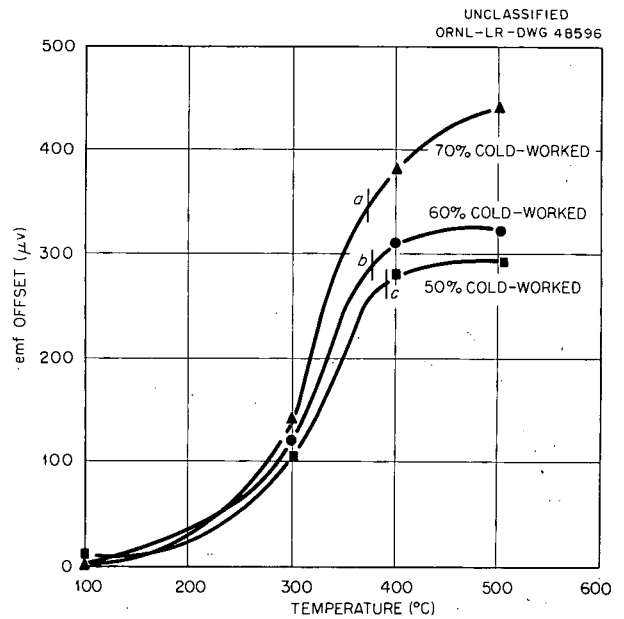


Fig. 5.24. EMF Effects of Cold-Working and Annealing for Chromel-P + Nb. Summary of unilateral-gradient-furnace results.

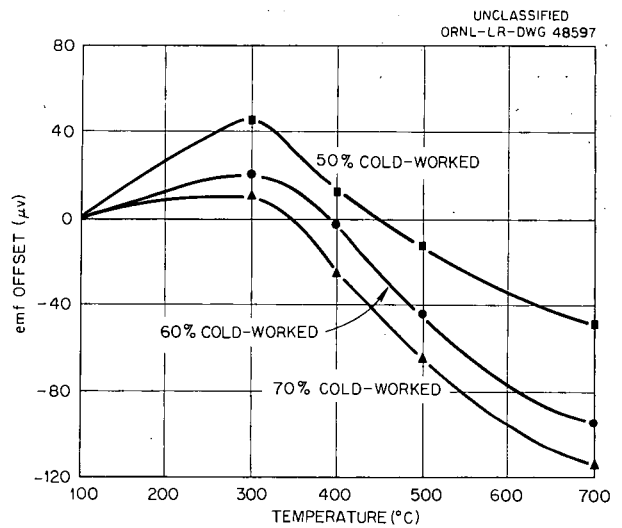


Fig. 5.25. EMF Effects of Cold-Working and Annealing for Alumel. Summary of unilateral-gradient-furnace results.

Fig. 5.24. The value of the emf offset  $\Delta(\Delta E)$  is positive and increases with increase in cold-working. From the calibration studies, it was determined that the emf of a cold-worked Chromel-P + Nb wire relative to platinum was less than the emf of an annealed wire relative to platinum. The phenomenon of recovery caused the calibration

of the originally cold-worked wire to approach annealed calibration.

From the results of the experiment on recovery, the recovery temperature was assigned to be 370°C for 70% cold work. It may be observed from Fig. 5.24 that at this temperature (point *a*) the slope of the emf offset with temperature begins to decrease. At points *b* and *c* on the curves for 60 and 50% cold-worked wire in Fig. 5.24 this slope decrease begins at 380 and 390°C respectively. Therefore the recovery temperature for Chromel-P + Nb increases with decrease in cold-working.

The emf offset for Alumel vs temperature at 50, 60, and 70% cold-working is shown in Fig. 5.25. This plot shows that  $\Delta(\Delta E)$  for Alumel is positive up to a certain maximum value and then becomes negative. From the calibration tests it is seen that the emf of a cold-worked wire relative to platinum is greater than that for an annealed Alumel wire up to a certain temperature, and then it becomes less. The positive offset is for the Alumel wire showing a greater emf than the annealed wire. Therefore, it is observed that the deviations are in the direction of the annealed wire calibration and are opposite in sign for different temperatures simply because of the original position of the emf of the cold-worked wire relative to the annealed wire. From Fig. 5.25 it is also seen that for temperatures of 335, 393, and 440°C for Alumel wires cold-worked 70, 60, and 50%, respectively, no change in emf was observed as a result of recovery. We are at a loss to explain this latter behavior.

The unilateral temperature gradient furnace was used to interpret the effects of small amounts of cold-working on the thermal emf of various commercial thermoelements. The furnace was run at 400°C and the wire to be tested was driven in and out of the furnace prior to cold-working. A 2-ft section of this wire was then stretched 2%, and the emf trace was obtained on driving in and out of the furnace. From this trace the change due to cold-working was determined as previously described. For the 5 and 10% cold-working, a new section of the original wire was stretched and tested.

The translated results in terms of errors to be expected are shown in Fig. 5.26. Chromel-P, Chromel-P + Nb, Kanthal-P, and constantan shift to less emf to platinum with small percentages of cold-working, and Kanthal-P is the most susceptible to cold-working. Alumel shifts to a higher emf to platinum with increased cold-working. The emf to platinum of copper, iron, Geminol-P, Geminol-N, and Kanthal-N are not changed appreciably up to 10% cold-working. Generally these results are in agreement with the previous calibration experiments.

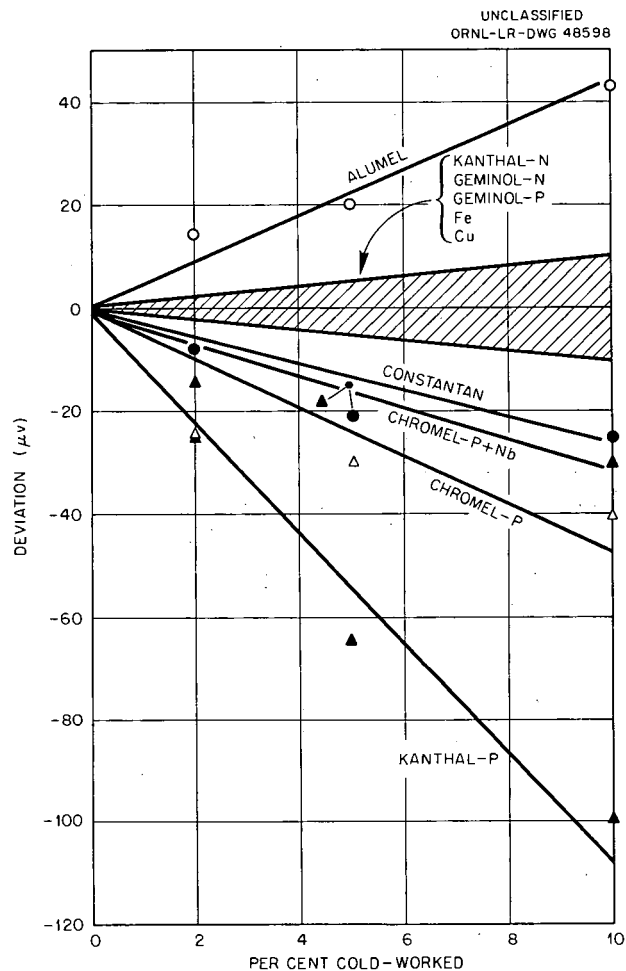


Fig. 5.26. Effects of Small Amounts of Cold-Working on EMF of Various Thermoelements, as Obtained with the Unilateral-Gradient Furnace at 400°C.

## 6. THERMOCOUPLE DRIFT - EMF VS TIME AT TEMPERATURE

The ORNL Thermocouple Research Program had its origin in the evaluation of the static performance of thermocouples to be used in the ORNL Aircraft Reactor Test (ART) and in the evaluation of heat exchangers and other components of the ART. Space and materials limitations dictated the use of thermocouples. It was expected that Chromel-P, Alumel might not live up to the necessary accuracy and stability requirements over the 1200 to 1800°F range to be encountered. Thus a series of thermocouple drift tests was begun as a part of the ART thermocouple design program. A more complete coverage of that program was reported by DeLorenzo.<sup>1</sup> Although some of the thermocouple configurations tested and here reported were dictated by Aircraft Reactor Project needs, that distinction is not made.

The need for better correlation between cause and effect in studying actual thermocouple performance led to a broader objective in this program, as has already been discussed. Nevertheless, a continued accumulation of actual thermocouple performance data was considered valuable. The environments used were chosen as representing many of the conditions encountered at ORNL, outside nuclear reactors as well as in in-pile environments excluding radiation, and excluding protection tube corrosion problems. The temperature range of 1000 to 1900°F was chosen according to the above consideration and prior knowledge of the limitations of the materials to be tested. Both cyclic and static temperatures were used. The majority of the tests were done in air, but some supplementary work was done in hydrogen, helium, and *in vacuo*.

### DRIFT TEST FACILITIES

The prime requisite of a drift test facility is that a prolonged isothermal space be obtained of such size that a variety of materials, the performances of which are to be compared, may be tested in the same environment. In addition, sufficient samples should be tested to establish reliable statistics for each type. Consequently,

---

<sup>1</sup>J. T. DeLorenzo, *Thermocouple Design and Test Program for Reactor Projects*, ORNL-2686 (Apr. 20, 1958).

broad comparative tests necessitate a large number of thermocouples.

To fulfill these criteria, Marshall Products Company standard tube furnaces were used. Figure 6.1 is a schematic cross section of the furnace, including the solid copper inertia block into which were inserted test thermocouples. The copper block was completely enclosed by an all-welded Inconel casing. As a further precaution against oxidation of the copper block, a positive pressure of helium was continuously maintained between the copper and the Inconel casing. Stainless steel radiation shields, match-drilled to the re-entry wells, were used to minimize end losses and to reduce the amount of radiant heat incident upon thermocouple connectors. The wiring harness from the test thermocouples through the thermocouple connectors was divided into three groups of 20, terminating in 20-point thermocouple connector switches. From the switches, jacks provided connections to ice-bath reference junctions and finally to a precision potentiometer (Rubicon type B or L & N type K-3). The connections from the test thermocouples to the harnesses are shown in Fig. 6.2, which is a rear view of a thermocouple drift-test assembly. The front view of a section of the drift test apparatus is shown in Fig. 6.3. As may also be seen in Fig. 6.3, the drift furnaces were controlled by pulse-time modulation controllers. The multipoint potentiometer recorders were used to continuously monitor a representation from each group of thermocouples under test. Precision data were taken at intervals of from one day to one week, depending on the type and duration of a particular test. Elapsed-time meters served as test chronometers. Figure 6.4 schematically illustrates the connections between test thermocouples and the monitoring instruments.

The measurement error induced by the thermocouple connectors and jacks during steady-state operation was a maximum of  $\pm 0.5^\circ\text{F}$ . During transient ambient conditions, the connector-induced error was as much as  $\pm 4^\circ\text{F}$ .

The maximum radial deviation of actual test thermocouple junction temperature relative to the centrally located standard thermocouple was  $\pm 2^\circ$  at 1800°F. Under steady-state conditions, this relation did not vary by more than  $\pm 0.25^\circ\text{F}$ . The difference in temperature in a test hole before and

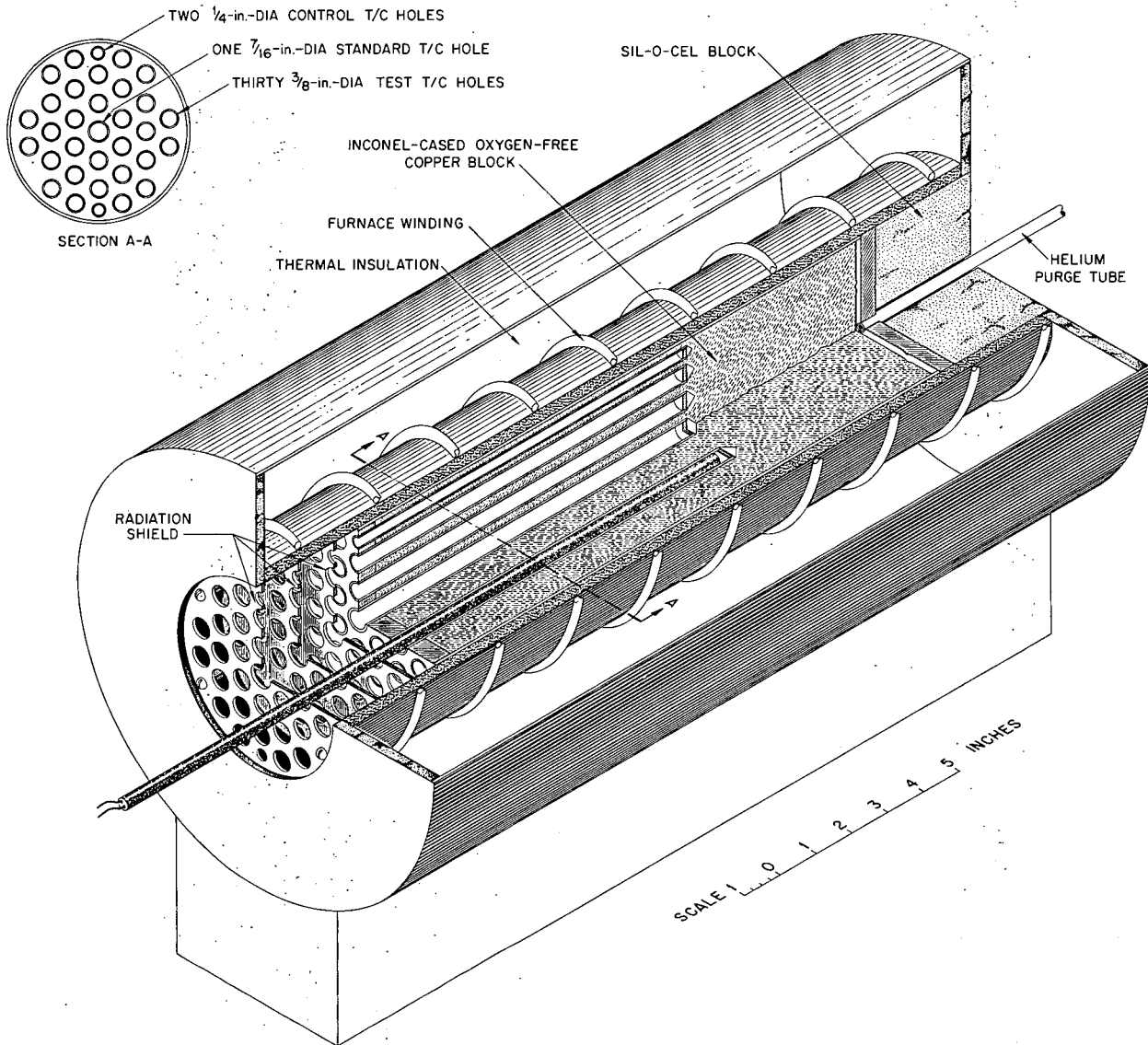


Fig. 6.1. Cutaway Drawing of Tube Furnace Used in Drift Tests.

after thermocouple loading in the surrounding holes was  $0.5^{\circ}\text{F}$  in the steady state at  $1800^{\circ}\text{F}$ . At  $1800^{\circ}\text{F}$  the axial variation in temperature within 2 in. of the hot junction of the test thermocouple was  $2^{\circ}\text{F}$ , and  $6^{\circ}\text{F}$  in the next 6 in. from the hot junction. This axial variation was minimized by adjusting shunts between the ten winding taps on the furnace. The deviations mentioned above were less at lower operating temperatures.

During determinations of the precise test-thermocouple emf, the furnace temperature was monitored

with a standard 90% Pt-10% Rh, Pt thermocouple, inserted sufficiently prior to these determinations in order for thermal equilibrium to be established. The equilibration time was minimized by preheating the standard thermocouple before insertion. The standard was protected by an alumina re-entry well and was left in a furnace only long enough to make measurements, except in the case of tests at  $300^{\circ}\text{C}$  ( $572^{\circ}\text{F}$ ) and  $390^{\circ}\text{C}$  ( $734^{\circ}\text{F}$ ). The maximum error of absolute temperature determination was  $\pm 0.5^{\circ}\text{C}$  ( $\pm 1^{\circ}\text{F}$ ).

UNCLASSIFIED  
PHOTO 40665

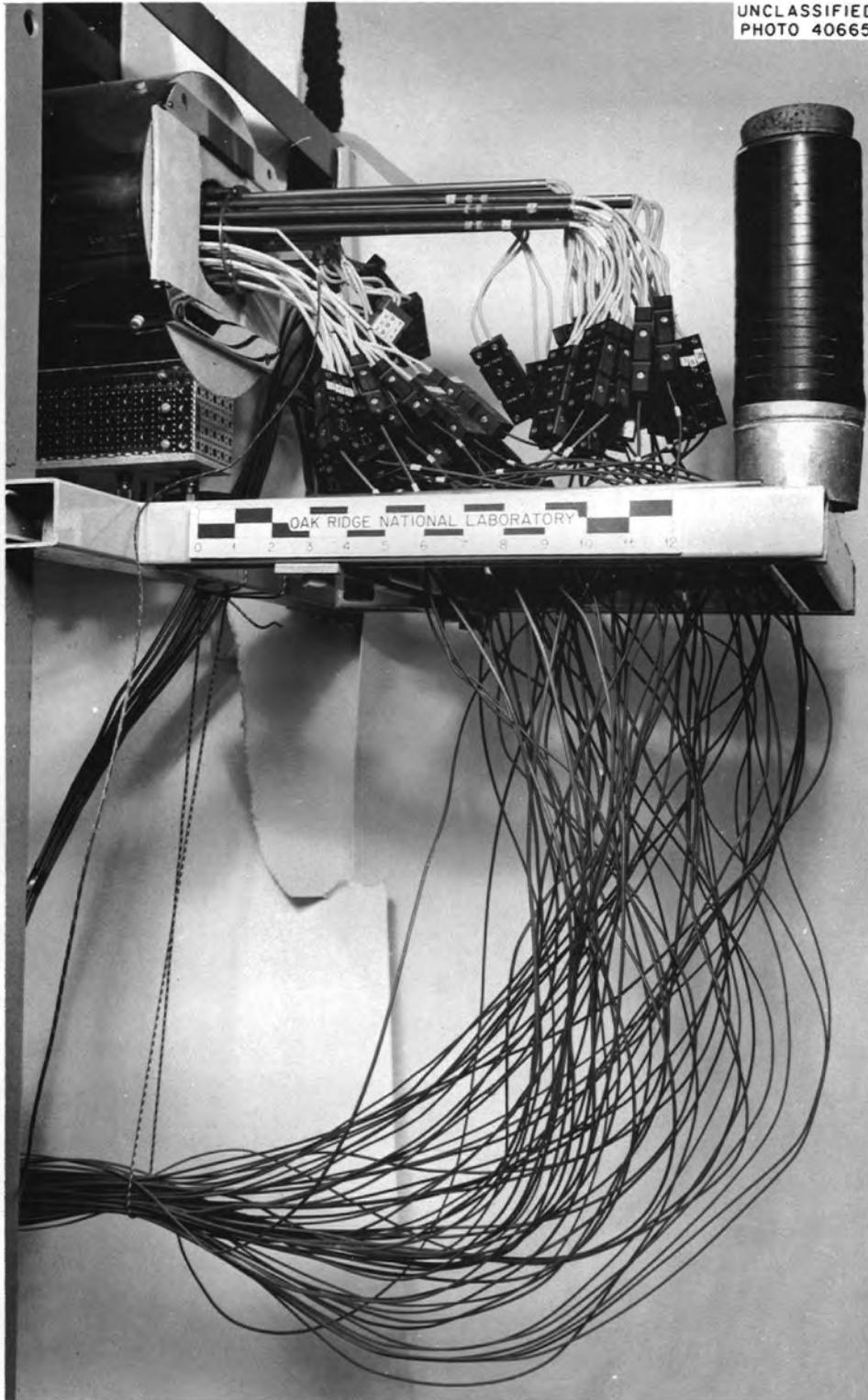


Fig. 6.2. Rear View of a Thermocouple Drift-Test Assembly.

UNCLASSIFIED  
PHOTO 40667

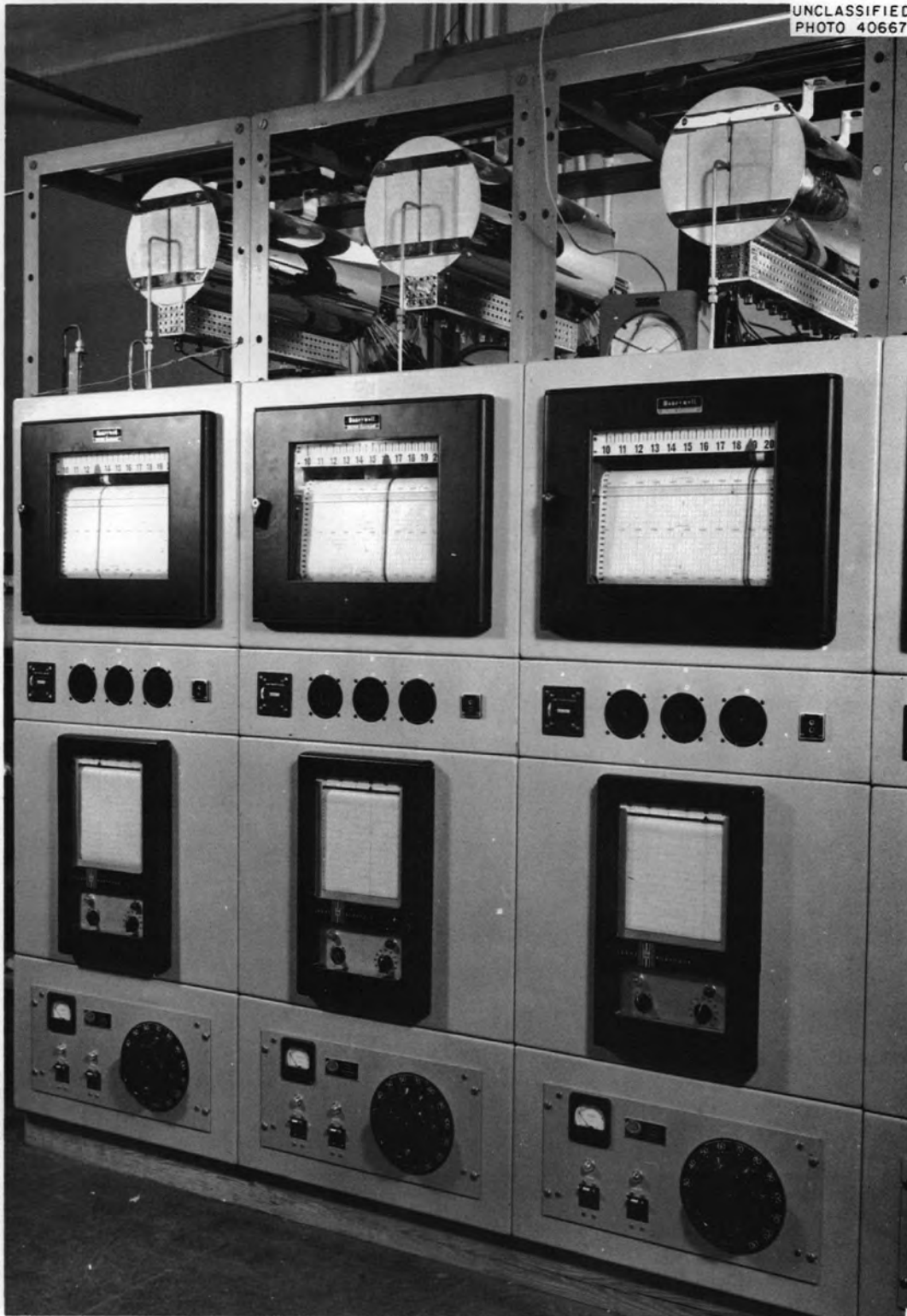


Fig. 6.3. Front View of Thermocouple Drift-Test Apparatus.

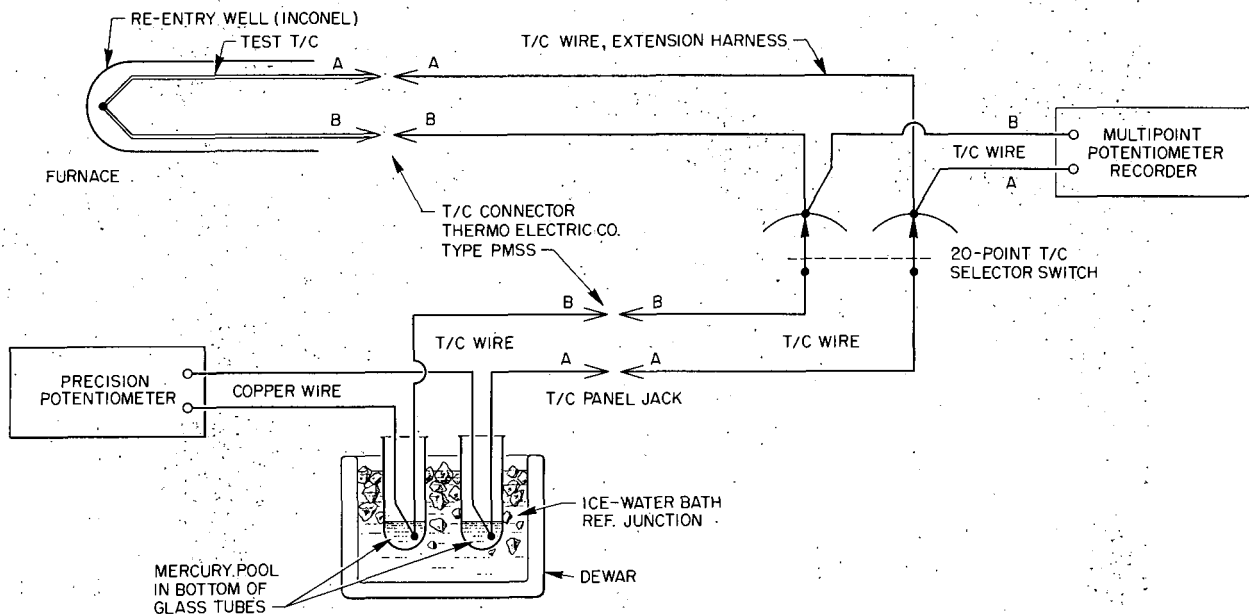


Fig. 6.4. Schematic Drawing of Drift-Test Thermocouple Connections.

#### DATA PROCESSING

The processing of data obtained during the drift-testing of thermocouples was a most formidable task. Initial attempts to manually process the data resulted in appreciable time delay before the results were in an understandable form. It was found that some tests could have been concluded earlier, or that new tests were suggested which should have been started much sooner than was possible after manual processing. In addition, even though the data reduction was a simple arithmetic problem, many human errors crept into the result because of the precision required and the redundancy of these arithmetic operations. As many as 500 datum points per week were obtained, representing a variety of materials and a plurality of samples of each variety.

To remove the impediment of manual data processing, a semiautomatic data processing system was evolved, as the result of the efforts of J. W. Reynolds, ORNL Instrumentation and Controls Division. The functions of the data processing system will be presented in some detail because it is strongly recommended that any additional effort in this type of research will be enhanced by a similar approach to data processing.

The digital computer at ORNL (Oracle) was used in the following general way. Original test and standard thermocouple millivolt data were manually recorded on a prepared form (Fig. 6.5a), designed to functionally fit the furnace-and-selector-switch arrangements as well as to fit the designed Oracle input routine. Paper tape (Fig. 6.5b) was then manually punched to prepare the data for input to the Oracle. The Oracle reduced the millivolt readings of both standard and test thermocouple to temperature, obtained the difference between these two temperatures, which is the error ( $E_i$  in degrees) of each thermocouple, averaged the errors  $\bar{E}$  of that type of thermocouple, computed its standard deviation  $S$ , and tabulated the results on the Oracle curve-plotter output. This output was presented on an oscilloscope tube. A 35-mm picture was automatically taken of this output and subsequently printed, as shown in Fig. 6.5c. Data are stored by the Oracle magnetic tape, and each time new data are processed, a current analog plot of the average error vs time for each type of thermocouple was also presented by the Oracle curve plotter for 1000-hr increments, as shown in Fig. 6.5d. With each analog plot are included the average of the standard deviation  $\overline{SER}$  and the degrees of freedom  $DF$  of all the data represented

(a)

O. R. N. L. INSTRUMENT DEPT.  
THERMOCOUPLE TEST DATA

DATE 06-17-59 TIME 02126.6

STANDARD TABLE 1 NO. 83 CORR. F0000.50000 FURN. NO. 007

---

TEST TABLE 7 NO. PTS. 4 ID. 10101B0100 STD. RDG. 04.24600

1-1 22.91000 1-2 22.91000 1-3 22.89000 1-4 22.92000

---

TEST TABLE 7 NO. PTS. 4 ID. 10101B0200 STD. RDG. 04.24600

1-5 22.90000 1-6 22.90000 1-7 22.89000 1-8 22.89000

---

TEST TABLE 7 NO. PTS. 4 ID. 10101B0300 STD. RDG. 04.24600

1-9 22.86000 1-10 22.86000 1-11 22.86000 1-12 00.00000

---

TEST TABLE 7 NO. PTS. 4 ID. 10101B0400 STD. RDG. 04.24600

1-13 22.95000 1-14 22.94000 1-15 22.95000 1-16 22.94000

---

TEST TABLE 7 NO. PTS. 4 ID. 10101B0500 STD. RDG. 04.24600

1-17 22.70000 1-18 22.70000 1-19 22.69000 1-20 22.70000

---

TEST TABLE 7 NO. PTS. 4 ID. 10101D0100 STD. RDG. 04.24600

2-1 22.80000 2-2 22.78000 2-3 22.82000 2-4 22.80000

---

TEST TABLE 7 NO. PTS. 8 ID. 10101D0400 STD. RDG. 04.24600

2-5 22.14000 2-6 22.85000 2-7 00.00000 2-8 22.95000

2-9 22.80000 2-10 22.78000 2-11 22.75000 2-12 00.00000

---

TEST TABLE 7 NO. PTS. 4 ID. 10101D0700 STD. RDG. 04.24600

2-13 23.01000 2-14 22.86000 2-15 23.06000 2-16 22.84000

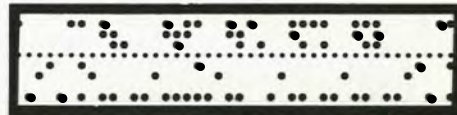
---

TEST TABLE 7 NO. PTS. 4 ID. 10101D0A00 STD. RDG. 04.24600

2-17 22.90000 2-18 22.85000 2-19 22.95000 2-20 22.85000

COMMENTS:

(b)



(c)

```

601 REYNOLDS 06-17-59 MRS.02126.6 02685
STD. TABLE 1 NO. 83 CORR. -0.50 FM 007
T POINT ERROR TEST
C
7 040 001.18 22.93000
001.18 22.93000
001.18 22.93000
001.18 22.93000
001.18 22.93000
STD. RDG. = 04.24600 TEMP. = 0552.30°C
R = 001.306 R-SS = 001.712 R-SS = 000.900
ΣE = 0006.22 ΣE = 000006.8 S = 00.13521

7 050 -004.19 22.70000
-004.19 22.70000
-004.19 22.70000
-004.19 22.70000
-004.19 22.70000
STD. RDG. = 04.24600 TEMP. = 0552.30°C
R = -004.256 R-SS = -003.903 R-SS = -004.607
ΣE = -0017.02 ΣE = 0000072.4 S = 00.11718

7 010 -001.85 22.80000
-001.85 22.80000
-001.85 22.80000
-001.85 22.80000
-001.85 22.80000
STD. RDG. = 04.24600 TEMP. = 0552.30°C
R = -001.855 R-SS = -000.707 R-SS = -003.002
ΣE = -0007.42 ΣE = 000014.2 S = 00.38245
    
```

(d)

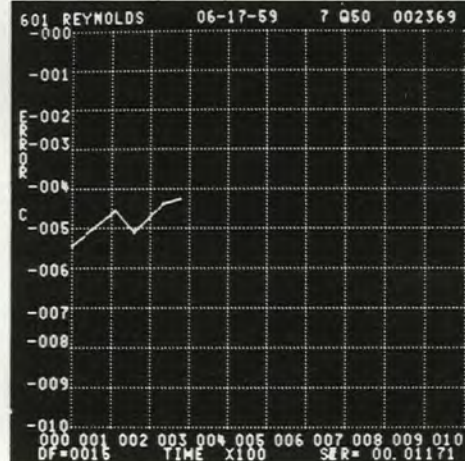


Fig. 6.5. Example of the Steps in the Reduction of Drift Data. (a) Raw-data sheet; (b) data-input tape for the Oracle; (c) tabulated data - Oracle output; (d) analog plot - Oracle output.

by that plot. There is normally a five- to ten-day delay before the results are available, largely because of difficulty in scheduling Oracle time. Nevertheless, this represented an appreciable improvement over the six-month delay encountered when the data were manually processed. The time for the computer to process data represented in Fig. 6.5a, including nine curve-plotter outputs for the nine groups of data, is 3 min. It takes 10 min to punch and verify the paper tape representing the amount of data in Fig. 6.5a.

The original program used, Thermo I code, calculated only the error for each thermocouple. Then the averages and their plots were done

manually. These latter manual steps rendered the original program of questionable net value, so they were automated in the Thermo II code.

Either the standard- or the test-thermocouple data can be referred to any one of 16 possible reference tables, specified by one bi-hex digit. The ten reference tables currently used are listed in Table 6.1. Thermocouple (T/C) tables may be replaced without disturbing other parts of the memory. It is possible to use resistance-thermometer tables or any other tables or curves, to be referred to as temperature-reference tables, in a manner similar to that for the thermocouple data. The tables can be introduced either as a function

**Table 6.1. Reference Tables for Millivolt-Temperature Equivalents Currently in Oracle Memory**

Number	Table
1	NBS 90% Pt-10% Rh, Pt
2	NBS Chromel-P, Alumel
3	Hoskins Chromel-P, Alumel
4	NBS iron-constantan
5	NBS copper-constantan
6	Geminol-P/N (see Appendix C)
7	Chromel-P, Alumel (see Appendix A)
8	Chromel-P, platinum (see Appendix A)
9	Alumel-platinum (see Appendix A)
A	NBS Chromel-P, constantan

of temperature or as a function of millivolts. Either binary or decimal inputs may be accommodated. Provision has been made to calculate or store a table as a fourth-order-or-less power series. It is also possible to feed a table into the computer as a function of temperature and to retrieve it as a function of millivolts, or vice versa. The final storages of all tables represented in Table 6.1 are with millivolts as an argument [ $T = f(\text{mv})$ ] in 0.1-mv increments, when  $T$  is in °C.

The calculations performed by the Thermo II code are as follows:

$$T_{(\text{std T/C})} = \frac{m_s - m_a}{0.1} (T_b - T_a) + T_a,$$

$$T_{(\text{test T/C})} = \frac{m_t - m_a}{0.1} (T_b - T_a) + T_a,$$

$$E = T_{\text{test}} - (T_{\text{std}} + T_c).$$

The terms are defined as follows:  $m_s$  and  $m_t$  are standard- and test-millivolt readings respectively;  $T_a$  is a temperature corresponding to  $m_a$ , the table entry next lower than  $m_s$  or  $m_t$ ;  $T_b$  is a temperature corresponding to  $m_b$ , a table entry  $m_b = m_a + 0.1$  mv;  $T_{\text{std}}$  and  $T_{\text{test}}$  are calculated temperatures corresponding to  $m_s$  and  $m_t$  respectively; and  $T_c$  is the calibration of correction temperature for the standard thermocouple,  $T_{\text{std}}$ . In other words, the computer linearly interpolates between 0.1-mv increments in the referenced table.

The average error  $\bar{E}$  is computed as follows:

$$\bar{E} = \frac{\sum_{i=1}^K E_i}{K},$$

where  $K$  is the number of thermocouples in a test. For thermocouple Q5, Fig. 6.5 (I.D. 10101B0500, Fig. 6.5a),  $K = 4$  and  $\bar{E} = -4.25^\circ\text{C}$ .

The standard deviation is

$$S = \sqrt{\frac{\sum_{i=1}^K E_i^2 - K(\bar{E})^2}{K - 1}}$$

The degrees of freedom of all data represented in the plot of the variations of average error for a particular type of thermocouple as a function of time (Fig. 6.5d) are given by

$$DF = \sum_{j=1}^R (K_j - 1),$$

where  $R$  is the total number of times data has been taken as represented on the analog plot, and  $K_j$  is the number of test thermocouples in the  $j$ th group of input data.

The mean of the standard deviation of  $R$  groups of data is

$$S\bar{E}R = \sqrt{\frac{\sum_{j=1}^R S_j^2}{R}},$$

where  $S_j$  is the standard deviation of the  $j$ th group of input data.

A group of test thermocouples (representing a number of samples of a particular type and environment) is identified by a number consisting of the test-thermocouple table number and an alphanumeric identification. That is, 07101B0500 represents test number 7 Q50, where the 7 is reference to a Chromel-Alumel table. Alphabetic information is contained in a bi-hex representation.<sup>2</sup>

It is possible to obtain answers in either centigrade or Fahrenheit degrees, with error curves in the same system. All data is stored in °C. Curves were plotted in 1000-hr increments (0-1000 hr,

<sup>2</sup>S. E. Atta, *ORACLE Manual for Programmers*, ORNL CF-57-6-68, p 20 (June 20, 1957); and ORACLE Subroutine 00 OBD.

1000–2000 hr, etc.) until a test was completed, at which time a separate entry allowed plotting of the error curve for the total test time on any assigned nominal time scale. The vertical, or error axis, is automatically adjusted by the computer to accommodate the range of errors in the test.

The Thermo II program is contained on two magnetic tapes – one for storage of data and the other for the code and tables. The data storage is divided into a working storage of 512 blocks and a permanent storage of 4500 blocks. Each test group is allowed three blocks of storage. (There are 128 words per block and five alphanumeric or ten decimal characters per word.) The program consists of ten sections with a total of 24 entries so designed that any particular section of the code may be revised, leaving the remainder of the code undisturbed.

#### LOW-TEMPERATURE DRIFT TEST – PART I

A number of questions arose concerning the comparative performance of a variety of thermocouple materials at temperatures at which serious corrosion of the thermocouples was not expected. Three motivating questions were: (1) How do Chromel-P, Alumel and other nickel-base thermocouple alloys, iron-constantan (ISA type J), and copper-constantan (ISA type T) compare at low temperatures? If it is necessary to use an oxidation-resistant combination such as Chromel-Alumel at 1000°C, is iron-constantan sufficiently superior at 500°C and is copper-constantan sufficiently superior at 300°C that we make the conventional type differentiation over these ranges? If we could settle for one material type over the entire range 0 to 1000°C, the service and supply problems would be much simplified. (2) Are the cold-working and oxidation effects reported in Chap. 5 really a serious factor at low temperatures? (3) Are thermocouples of swaged-sheath construction equally applicable at low temperature in the face of their desirability for high-temperature use?

Although the previously described drift-test facilities were conceived for the purpose of "life-testing" thermocouples over the range 1000°F (538°C) to 1900°F (1038°C), the ease with which this apparatus could be used to obtain results from a spectrum of materials at lower temperatures led to its use. The precision of the apparatus was quite sufficient for higher-temperature tests in

which significant changes were expected, but precision was in question at lower temperature, at which small changes would be expected. Consequently, it was necessary to scrutinize the statistical significance of low-temperature data much more closely before drawing conclusions.

#### Test Description

Considerable care was used in the preparation and handling of wire, insulators, and re-entry wells. All thermocouple wells were of uniform size: Inconel, 14 in. long,  $\frac{1}{4}$  in. OD, 0.025 in. wall. After Heliarc-welding one end of each well closed, the wells were degreased first in  $\text{CCl}_4$ , then in acetone, followed by a 1000°C heating in a hydrogen atmosphere. The thermocouple insulators (except for swaged thermocouples) were Conax Corporation I-20-4 ceramics [95% magnesium silicate, 2% aluminum oxide, sodium and potassium 0.5% (ref 3)], four-hole, 0.150 in. OD, 0.125 in. long, and of 0.040 in. hole diameter. The insulators were washed in acetone, and then in ether. They were then baked at 1000°C for 1 hr in air, then stored in sealed glass bottles until used. Bare thermocouple wire in the as-received condition was cut to length from the vendors' spools, subjected to a slight straightening stress to facilitate the stringing of insulators, then wiped with a clean, lint-free acetone-soaked cloth. During all subsequent assembly and handling of wire and insulators, technicians wore clean, white cotton gloves. All thermocouple junctions were arc-welded in a mercury-pool argon-atmosphere device. Except in the case of some swaged-sheath thermocouples, two thermocouples were fabricated in the four-hole insulators with one common four-wire junction. In some cases the two common-junction thermocouples were the same size, in other cases a 20- and a 30-gage thermocouple comprised the dual sample. In every case both thermocouples of common junction were of the same type.

The low-temperature drift tests were completed in three stages. First, employing one furnace, a 300°C constant-temperature test lasting 5000 hr was performed on 20- and 30-gage materials of Chromel-P, Alumel; Kanthal-P/N; iron-constantan; and copper-constantan. Second, employing two furnaces, a 390°C constant-temperature test and a

<sup>3</sup>R. G. Minges, Conax Corp., Buffalo, N.Y., private communication, Nov. 13, 1957.

test at 390°C except during a periodic drop to 300°C for taking data (data taken at both 390 and 300°C), were simultaneously run for 2000 hr testing the same types of materials run in the first stage to which had been added Chromel-P, constantan; a special Chromel-Alumel; swaged-sheath 90% Pt-10% Rh, Pt; Geminol-P/N; and  $\frac{1}{8}$ -,  $\frac{1}{16}$ -, and  $\frac{1}{25}$ -in.-OD swaged-sheath MgO-insulated Chromel-P, Alumel. The third stage was begun by elevating the temperature of the two furnaces of stage 2 to 550°C without disturbing the thermocouples. The furnace which had been operating at 390°C constant was operated at 550°C constant, and the furnace which had cycled between 390 and 300°C in stage 2 was cycled between 550 and 390°C in stage 3. The stage 3 test lasted for approximately 600 hr. Table 6.2 reviews the thermocouple types and history of all the low-temperature tests and includes the codes used for the respective tests.

A stage 4 test was started with the materials of stage 3 by boosting the temperature of both furnaces to 980°C, but one of the furnaces failed within the first day. The test was continued for approximately 400 hr with only the swaged-sheath Chromel-P, Alumel and the Chromel-P + Nb, special Alumel.

An atmosphere of air was experienced by all the thermocouples of this low-temperature test series, as suggested by Figs. 6.1 and 6.2 of this chapter. No attempts were made to control ambient air temperatures or relative humidity.

## Results

**300°C Constant Temperature.** — The results of the first stage of the low-temperature drift tests on three familiar types of base-metal thermocouples (ISA types J, T, and K) appear in Fig. 6.6. In this first test, as in the other low-temperature results which follow, many aspects of the test conditions were carefully perused in search for explanation of consistent statistical significance. Except for some traceable human and Oracle errors which were removed from the final presentation where feasible, no conclusive correlations were established which lend more to the interpretation of these results than is obvious from a glance at the summarizing curves. Studied were such things as furnace temperature fluctuations, relative position of thermocouples in the furnace, performance of individual thermocouples of a test relative to each other and their averages, calibrations of the

respective types, and whether the apparent drift of a particular type of thermocouple was the same as for other types in the same test.

The apparent roughness of the drift curves for types J and T relative to type K in Fig. 6.6 was attributed to: (1) the interpolation jumps of the NBS Circular 561 tables for types J and T relative to the Chromel-Alumel tables used (see Appendix A for a discussion of smoothed Chromel-Alumel tables); (2) difficulty of wetting iron with mercury and the rapidity of amalgamation of copper in a mercury pool-ice bath reference junction. (Note similarity of shape of curves of 20- and 30-gage thermocouples of each type.)

The "calibration" values from the drift tests of Fig. 6.6 were approximately the same relative to each other but about 1°C lower than separate conventional calibrations performed on samples from the same spools. This was not explainable on the basis of temperature gradients existing in the furnace temperature equalizing block, since there was random distribution of the samples of each type throughout the block. The standards used in the two instances were known absolutely to  $\pm 0.5^\circ\text{C}$ , which probably accounted for the discrepancy. The apparent drift of all the thermocouples of Fig. 6.6 during the first few hours (note similarity of curves for all thermocouples in first 100 hr) was not explainable on the basis of metallurgical recovery.

Finally, it was hoped that the mean of the standard deviations ( $\overline{SER}$ ) of all the data represented in the respective curves might point up an advantage of one type over another. No such conclusion is warranted. On the basis of all considerations made concerning the 4700-hr drift test at 300°C on types J, T, and K thermocouples, there is no advantage of one type over the other, to within a precision of  $\pm 1^\circ\text{C}$  ( $2^\circ\text{F}$ ), assuming prior calibration of samples from the spools used. Furthermore, and to within the same precision, none of the types exhibited a drift trend with time. These conclusions do not negate the possible advantages of one type for exacting laboratory experiments. Comparison of homogeneity, relative susceptibility to cold work, and more careful test results on a number of samples greater than 4 would be required to establish such an advantage.

**390°C Constant Temperature and 390 to 300°C Cyclic.** — Results of the second stage of the low-temperature tests appear in Fig. 6.7. All the

Table 6.2. Low-Temperature Drift Tests - Part I

Description of Thermocouple		Wire Gage	Number Tested	Thermocouple Code and Thermal History						
Thermocouple Materials	Insulation			Stage 1	Stage 2			Stage 3		
				I <sup>a</sup>	II	III	IV	V	VI	VII
Iron-constantan	Conax I-20-4L four-hole beads, $\frac{1}{8}$ in. long	20	4	F2 <sup>b</sup>	QK	Q6 <sup>b</sup>	KQ	Q6 <sup>b</sup>	KQ	QK
Iron-constantan	Same	30	4	F3 <sup>b</sup>	QL	Q7 <sup>b</sup>	LQ	Q7 <sup>b</sup>	LQ	QL
Copper-constantan	Same	20	4	C2 <sup>b</sup>	QM	Q8 <sup>b</sup>	MQ	Q8 <sup>b</sup>	MQ	QM
Copper-constantan	Same	30	4	C3 <sup>b</sup>	QN	Q9 <sup>b</sup>	NQ	Q9 <sup>b</sup> (3) <sup>c</sup>	NQ (4)	QN (4)
Chromel-P, constantan	Same	20	4		QO	QA	OQ	QA	OQ	QO
Chromel-P, constantan	Same	30	4		QP	QC	PQ	QC	PQ	QP
Chromel-P, Alumel	Same	20	4	H2 <sup>b</sup>	QI	Q4 <sup>b</sup>	IQ	Q4 <sup>b</sup>	IQ	QI
Chromel-P, Alumel	Same	30	4	H3 <sup>b</sup>	QJ	Q5 <sup>b</sup>	JQ	Q5 <sup>b</sup>	JQ	QJ
Chromel-P +Nb, special Alumel	Same	20	4		QH	Q3	HQ	Q3	HQ	QH
90% Pt-10% Rh, Pt	$\frac{1}{4}$ -in. swaged-sheath Inconel, MgO insulation, duplex	20	4		SF (2)	SE (1)	SG (2)	SE	SG	SF
Kanthal-P/N	Conax I-20-4L four-hole beads, $\frac{1}{8}$ in. long	20	4	K2 <sup>b</sup>	QF	Q1 <sup>b</sup>	FQ	Q1 <sup>b</sup>	FQ	QF
Kanthal-P/N	Same	30	4	K3 <sup>b</sup>	QG	Q2 <sup>b</sup>	GQ	Q2 <sup>b</sup>	GQ	QG
Geminol-P/N	Same	20	4		QQ	QD	QU	QD	QU	QQ
Geminol-P/N	Same	30	4		QR	QE	RQ	QE	RQ	QR
Chromel-P, Alumel	$\frac{1}{8}$ -in. swaged-sheath Inconel, MgO insulation	22	4		S2 (1)	S1	S3 (1)	S1	S3	S2
Chromel-P, Alumel	$\frac{1}{16}$ -in. swaged-sheath Inconel, MgO insulation	30	8		S5	S4 (3)	S6	S4	S6	S5
Chromel-P, Alumel	$\frac{1}{25}$ -in. swaged-sheath Inconel, MgO insulation	36	4		S8	S7	S9	S7	S9	S8
Chromel-P, Alumel	Same	36	4		SC	SA	SD	SA	SD	SC

<sup>a</sup>Test I. 300°C constant temperature for 5000 hr.

Test II. Data at 300°C; test at 390°C for 2000 hr, except for time to periodically lower furnace temperature to 300°C and take data.

Test III. Constant temperature of 390°C for 2000 hr.

Test IV. Data taken at 390°C during test II. Same thermocouples.

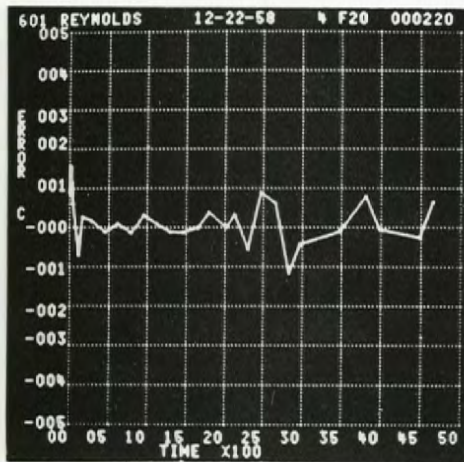
Test V. Constant temperature of 550°C for 600 hr.

Test VI. Data at 550°C; test at 550°C for 600 hr, except for time to periodically lower furnace temperature to 390°C and take data.

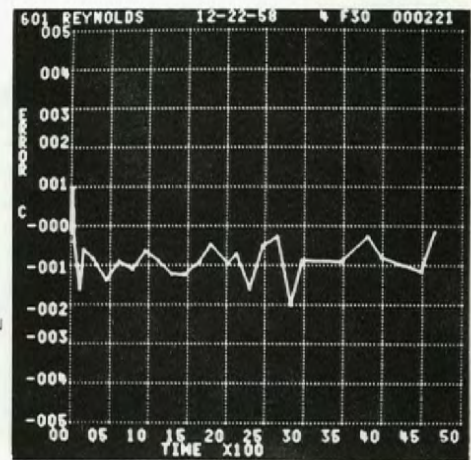
Test VII. Data taken at 390°C during test VI. Same thermocouples.

<sup>b</sup>Common-junction thermocouples same size. In all other applicable cases, a 20-gage and 30-gage thermocouple of same type had common junctions.

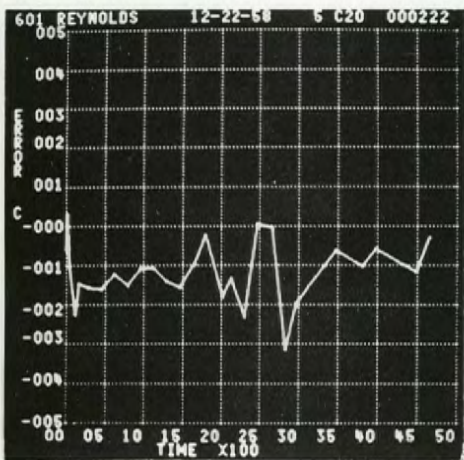
<sup>c</sup>Numbers in parentheses alongside the code number represents the number of thermocouples that failed during test.



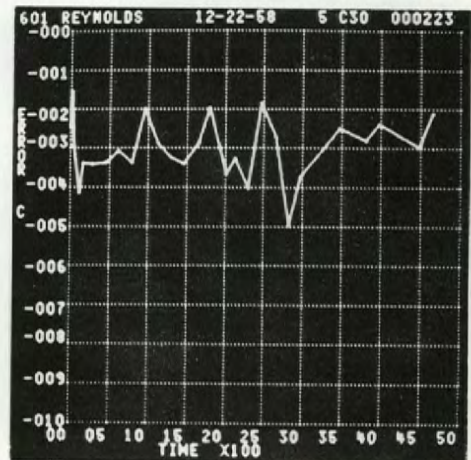
ISA TYPE J  
IRON-CONSTANTAN  
20 GAGE  
DF 0081  
 $\overline{SER}$  0.32



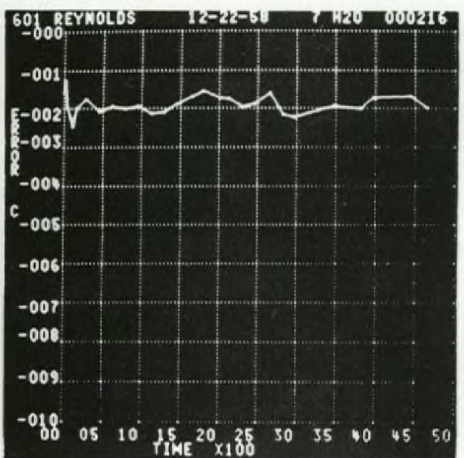
IRON-CONSTANTAN  
30 GAGE  
DF 0081  
 $\overline{SER}$  0.22



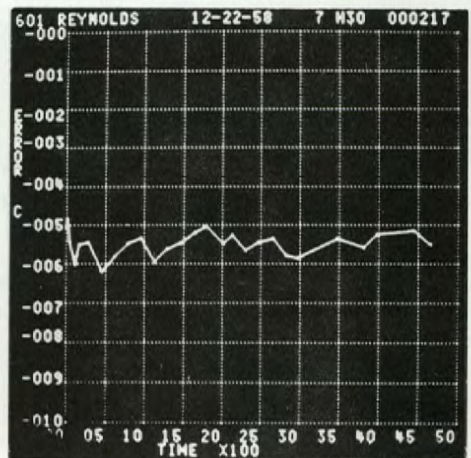
ISA TYPE T  
COPPER-CONSTANTAN  
20 GAGE  
DF 0081  
 $\overline{SER}$  0.39



COPPER-CONSTANTAN  
30 GAGE  
DF 0081  
 $\overline{SER}$  0.17



ISA TYPE K  
CHROMEL-P--ALUMEL  
20 GAGE  
DF 0081  
 $\overline{SER}$  0.23



CHROMEL-P--ALUMEL  
30 GAGE  
DF 0081  
 $\overline{SER}$  0.30

Fig. 6.6. Results of 300°C Isothermal Drift Test for 4700 hr in Air: Three Common Types of Thermocouples.

Fig. 6.7. Data from Isothermal and Cyclic Drift Tests at 300 and at 390°C for Several Types of Thermocouples. Thermal histories (I, II, III, IV) and notations within the blocks are explained in Table 6.2. Numbers in parentheses within the blocks represent standard deviations. Figures 6.7a and b are for drift tests at 300°C, constant and cyclic; Figs. 6.7c and d are for drift tests at 390°C, constant and cyclic.

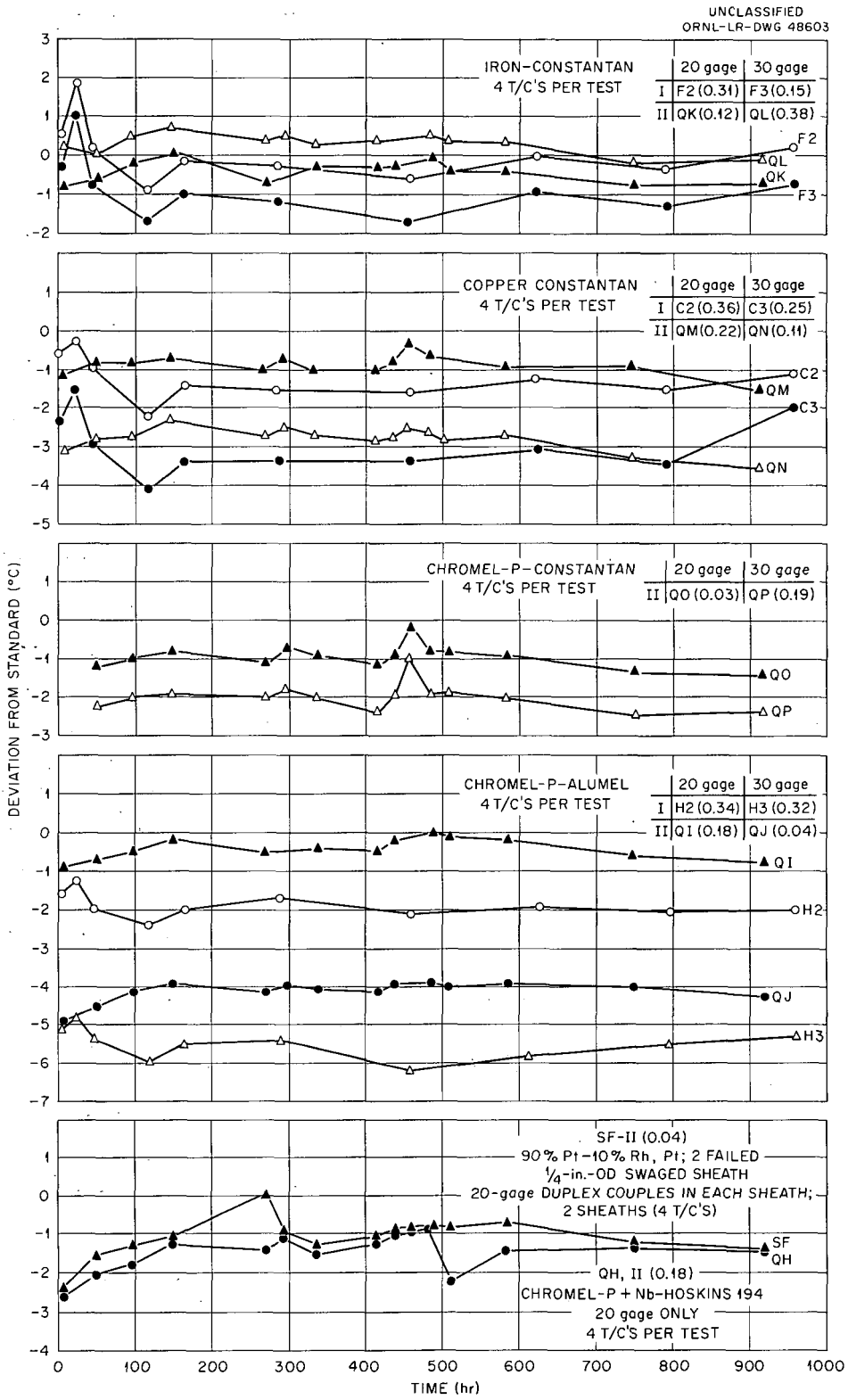


Fig. 6.7a.

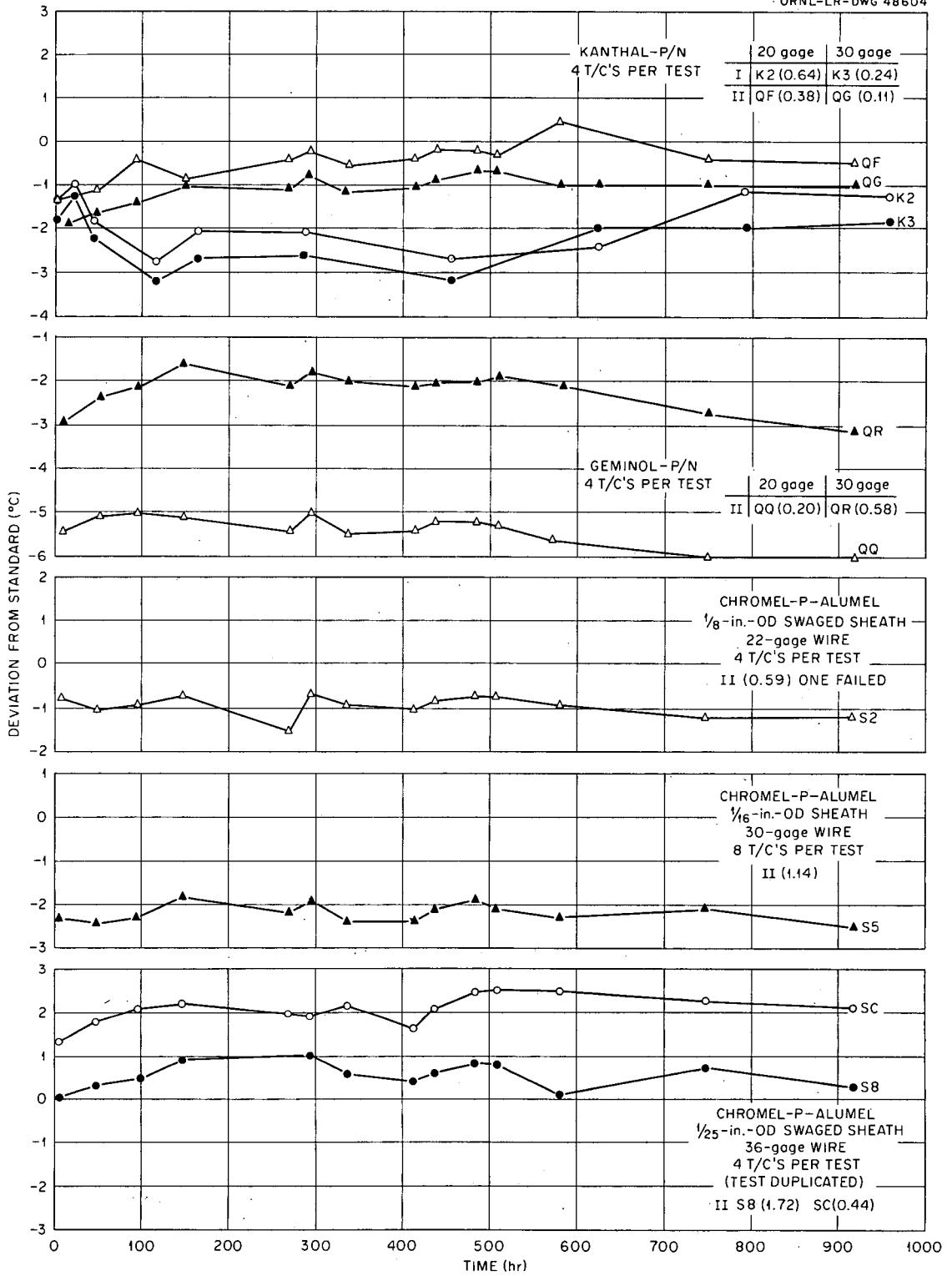


Fig. 6.7b.

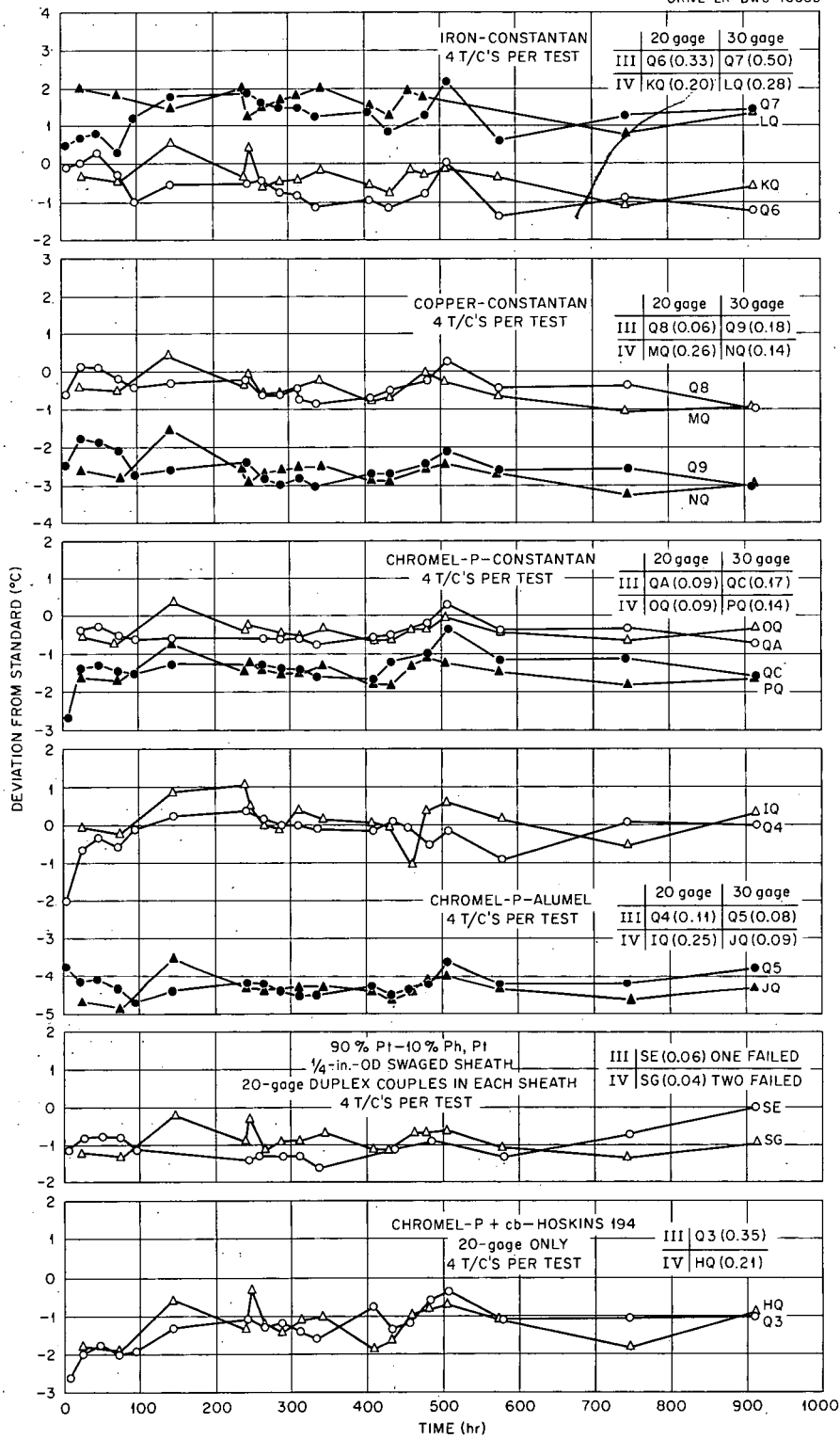


Fig. 6.7c.

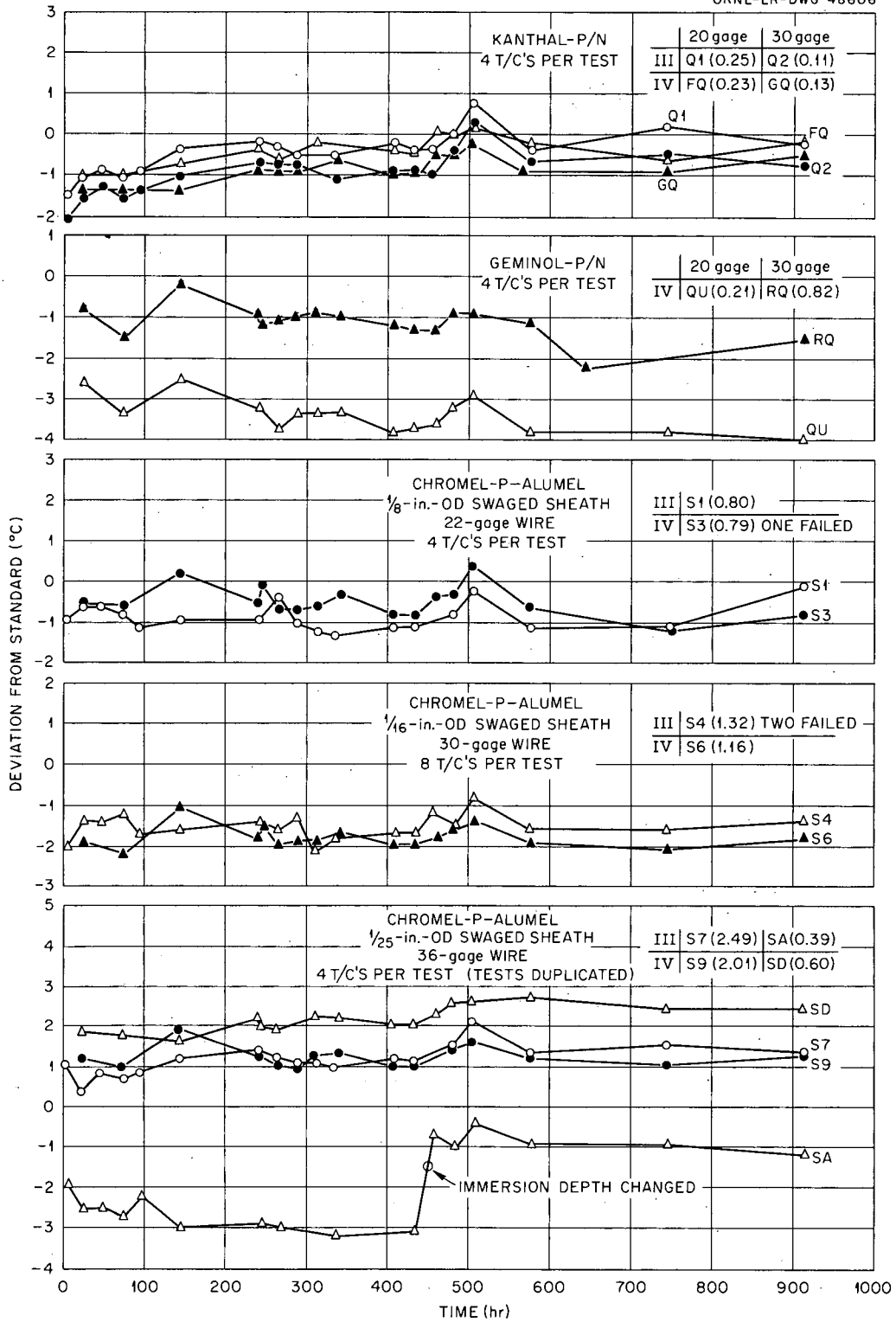


Fig. 6.7d.

thermocouple materials listed in Table 6.2 were tested in this series. Although this test lasted for 2000 hr, results are shown for the first 1000 hr. There was no significant change in the thermocouples' performance during the second 1000 hr. The standard deviations shown are for 0 to 1000 hr.

The previous general remarks regarding a lack of correlation between environmental factors and individual type performance hold here. At 300 and 390°C there is no difference between thermocouples subjected to static temperature and those subjected to cyclic variation of temperature. There is no marked advantage of one base-metal type over another to within  $\pm 1^\circ\text{C}$ , assuming prior calibration. There was no drift trend for the 2000-hr testing period. On the basis of a consistently low deviation ( $\overline{SER}$ ), the 90% Pt-10% Rh, Pt thermocouples showed better performance. However, this observation must be tempered by the small number of samples. Junction failure in the 90% Pt-10% Rh, Pt thermocouples was high. As was borne out by later work, the technique (see Fig. 6.8) of fusing the noble-metal wires into the sheath during sheath closure should be avoided. The combination of wire embrittlement and thermal stress suggests junction preparation prior to sheath end closure.

Failures also occurred in the swaged-sheath Chromel-P, Alumel thermocouples. This emphasizes the necessity of subjecting swaged-sheath thermocouples to thermal cycles after fabrication, in addition to dye penetration tests and x-ray examination, to ensure strong junctions and good sheath closure. It is interesting to note that the failure rate of the  $\frac{1}{25}$ -in.-OD material was lower than for the  $\frac{1}{8}$ - and  $\frac{1}{16}$ -in.-OD material. Incidentally, continuity checks were good on these thermocouples after the tests. The same techniques of fabrication and inspection were used on all the swaged-sheath thermocouples. Figure 6.8 illustrates the method employed for hot-junction closure.

The explanation offered for the significantly higher standard deviation among the sheathed Chromel-P, Alumel thermocouples is that there were several sheathed thermocouples in the same re-entry well, contributing to a greater and more variable heat loss along the thermocouple assemblies. Finally, the 30-gage Chromel-P, Alumel possessed the greatest calibration deviation.

#### 550°C Constant Temperature and 550 to 390°C Cyclic.

These tests were begun by elevating the temperature of the two furnaces in the previous test (stage 2) without otherwise disturbing the setup, and lasted for over 500 hr. The results of these tests appear in Fig. 6.9. With the below-stated qualifications, the results and observations were the same as discussed in the two sections above. As was expected, there was a high failure rate of 30-gage copper-constantan. None of the 20-gage type T thermocouples failed. It was noted with interest that there was no noticed drift in emf to signal the onset of failure in the 30-gage type T thermocouples as had been experienced with other types at higher temperature. Referring to Fig. 6.9a, test QK (20-gage ISA type J), one notes two isolated spikes in the data. The first, at 95 hr, was traced to an interpolation error in recording the standard thermocouple reading. The second, at 330 hr, was traced to an Oracle memory error. This second data point was accurately computed by the Oracle but the wrong value of  $\overline{E}$  was stored for analog plot. It may be noticed that these same errors appear at other points in this series. The time correlation may not be precise because of the way the program was set up: the timer reading at the first data entry was considered zero time. The actual testing time at the first data collection may have varied from test to test. A number of traceable

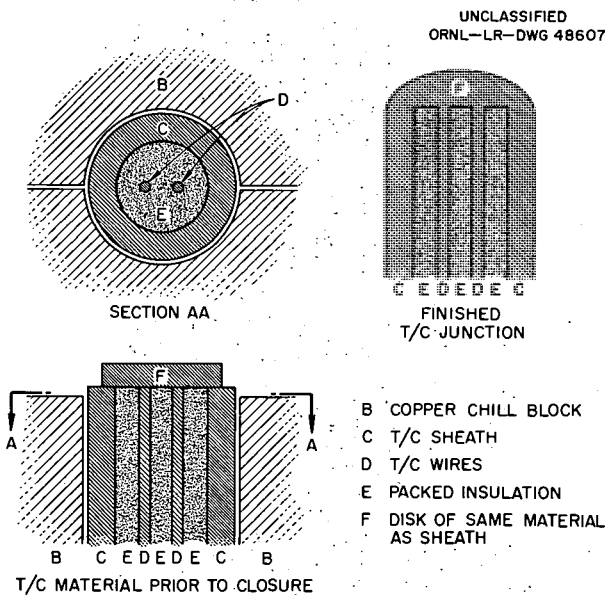


Fig. 6.8. Method of Hot-Junction Closure for Swaged-Sheath Thermocouple. An arc is struck between the tungsten electrode and B; the Heliarc is then moved to F in order to produce the finished thermocouple junction.

Fig. 6.9. Thermocouple Drift at Constant Temperature (550°C) and at Cycling Temperature (550 and 390°C). See Table 6.2 for thermal histories (V, VI, VII), thermocouple code identification (Q6, etc.), and details of thermocouple construction.

UNCLASSIFIED  
ORNL-LR-DWG 48608

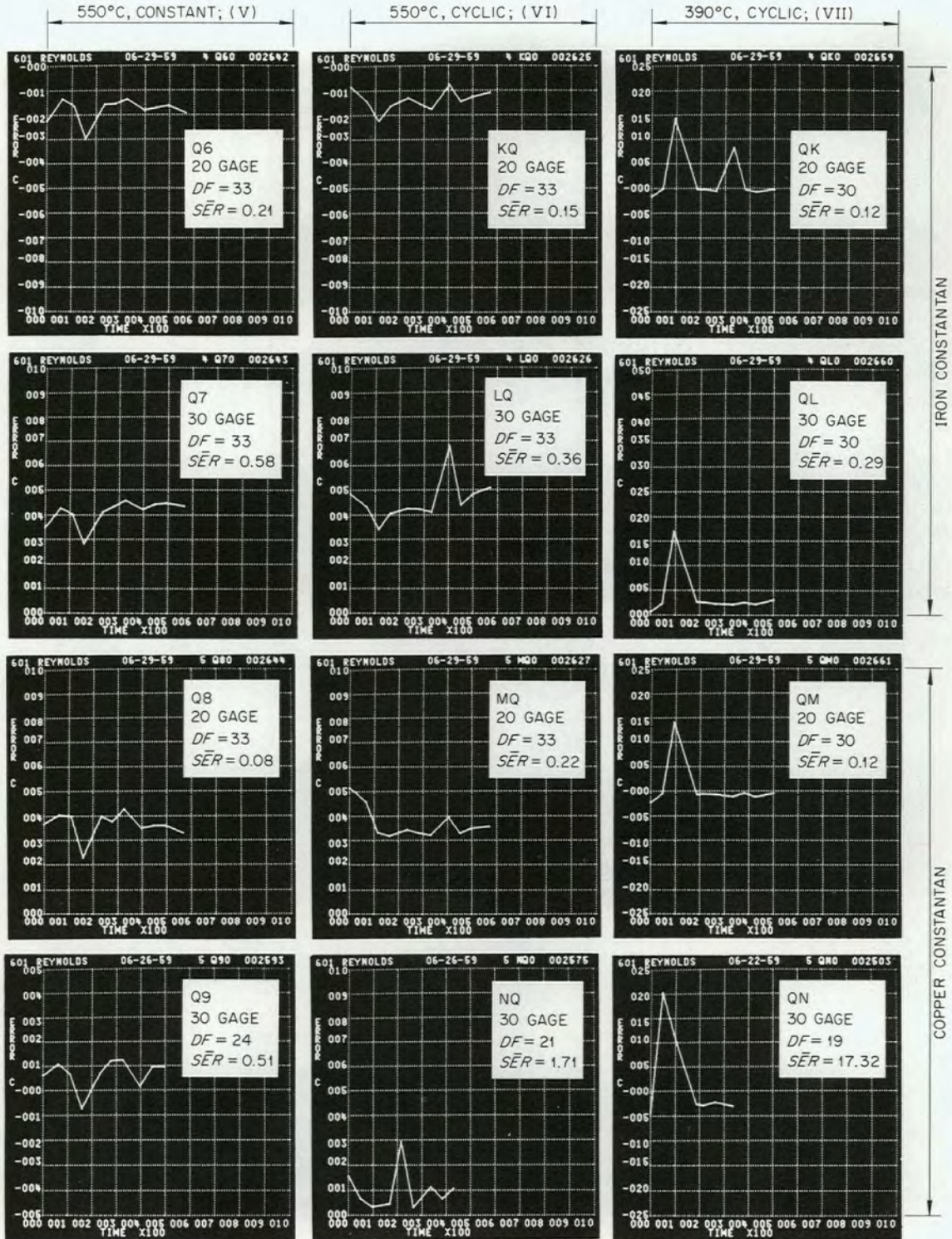


Fig. 6.9a.

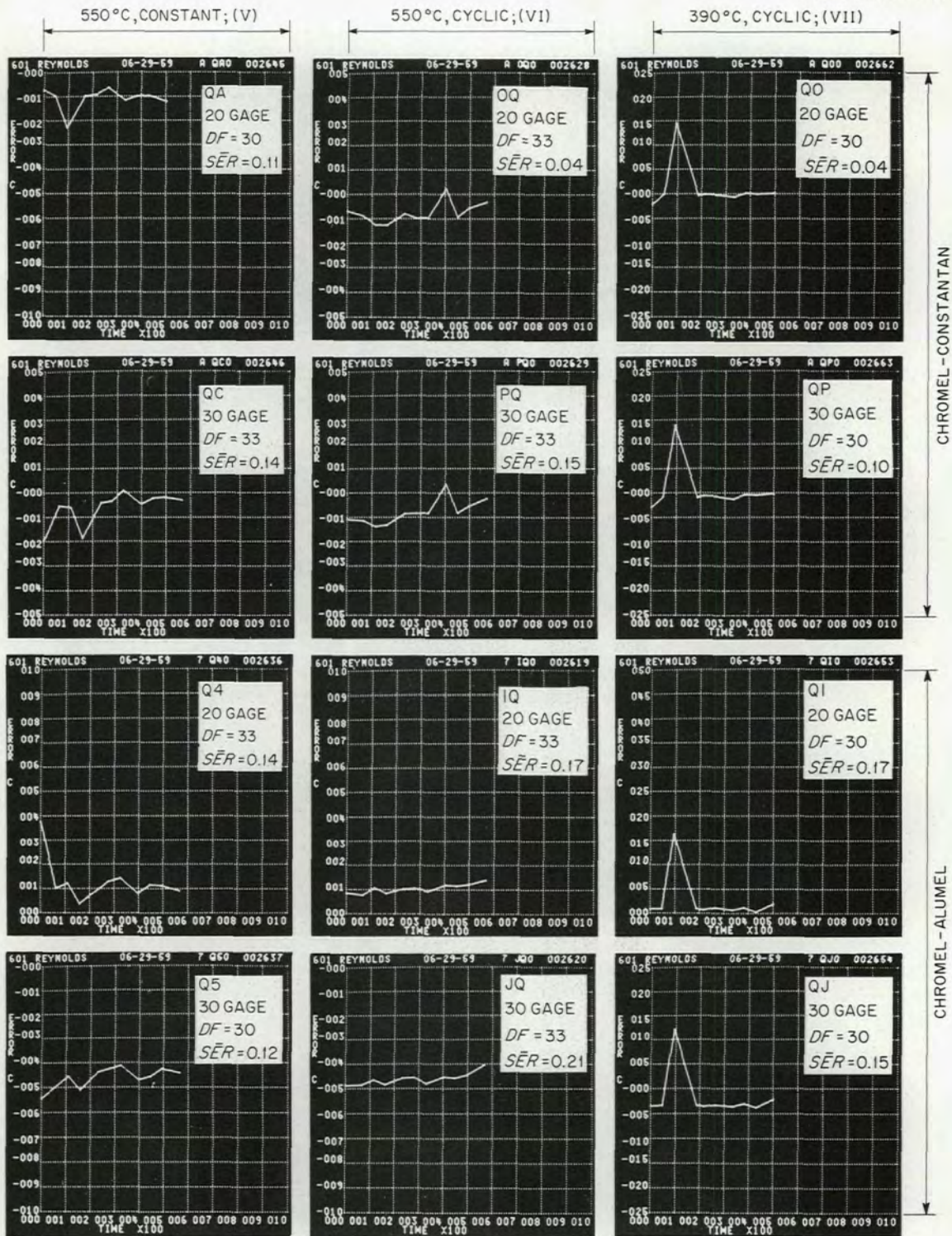


Fig. 6.9b.

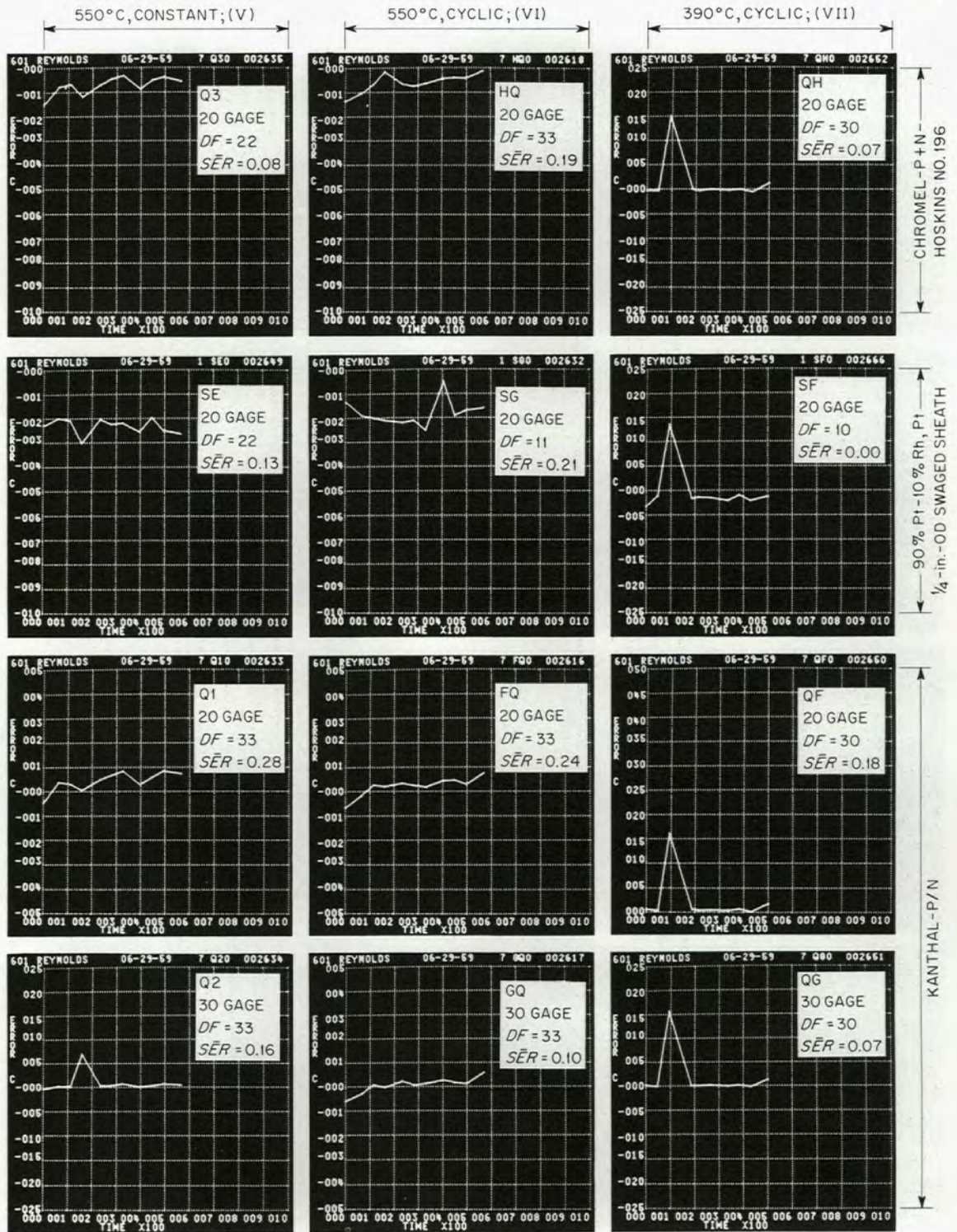


Fig. 6.9c.

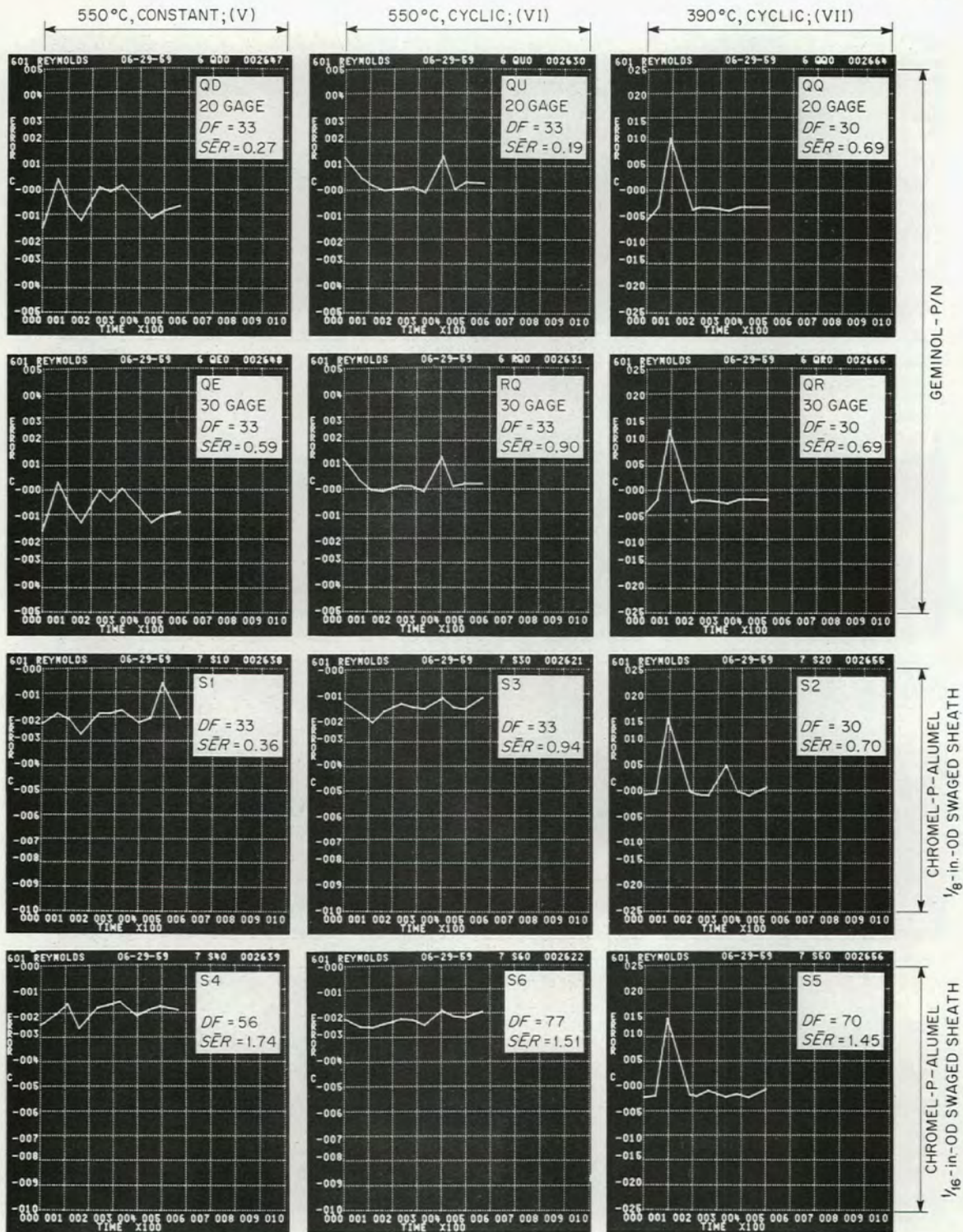


Fig. 6.9d.

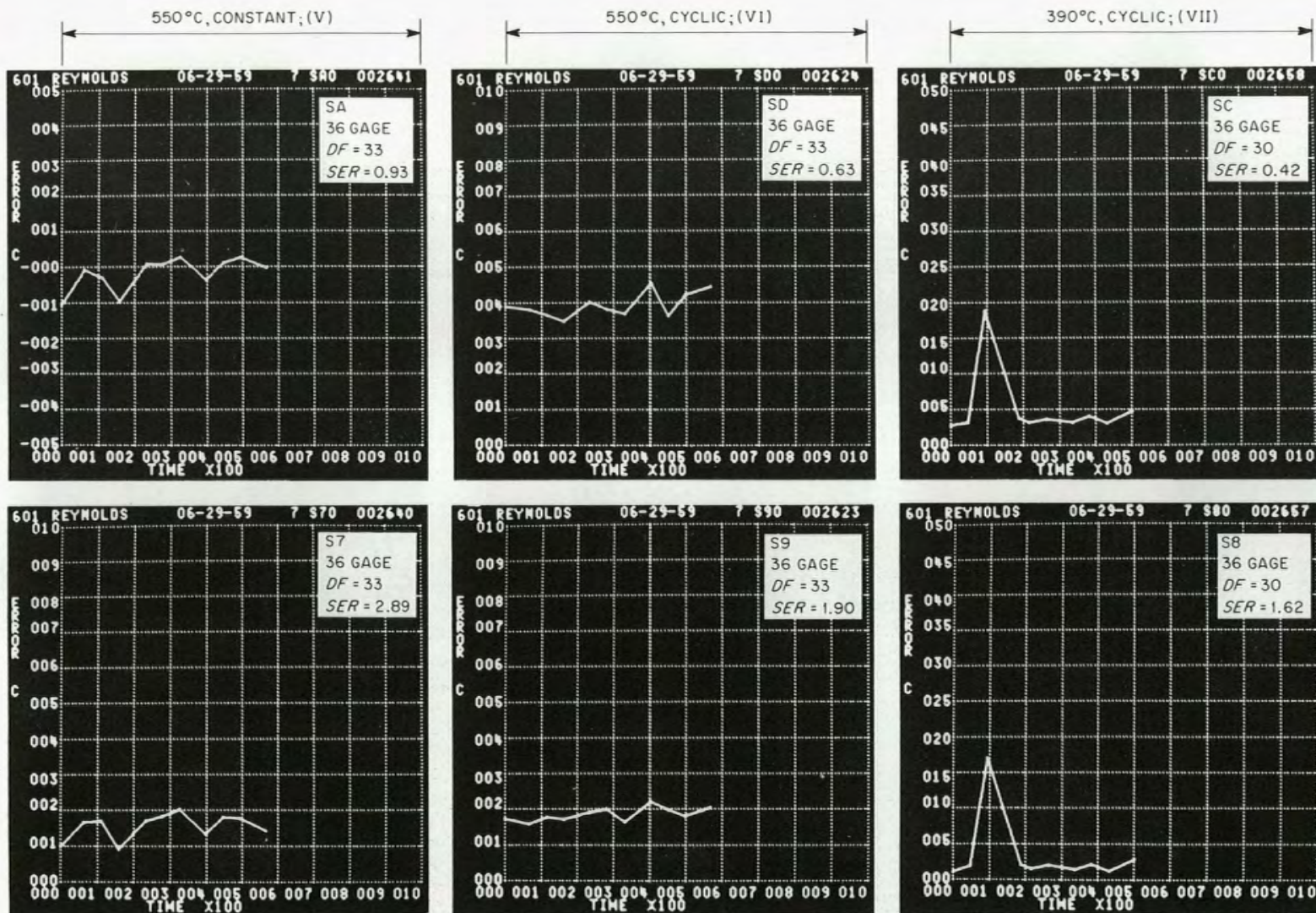


Fig. 6.9e.

extraneous errors were removed from the data of Figs. 6.6 and 6.7.

**Extension of Tests of Some Thermocouples to 980°C.** – All samples of 20-gage Chromel-P + Nb, special Alumel, and of  $\frac{1}{8}$ -,  $\frac{1}{16}$ -, and  $\frac{1}{25}$ -in.-OD swaged Inconel sheath Chromel-P, Alumel from the above tests were grouped in one furnace and drift-tested for approximately 400 hr at 980°C. The data was irregular for unexplainable reasons but the following conclusions were drawn with reasonable assurance.

The eight samples of 20-gage Chromel-P + Nb, special Alumel performed without failure and drifted +2°C in the 400-hr test at 980°C. This is a considerable improvement over the performance experienced with regular Chromel-P, Alumel. Careful visual examination of these thermocouples after the test revealed that the hot junctions were sound. The special Alumel had a brittle oxide, part of which was slightly magnetic, estimated to be about 2 mils thick, whereas the Chromel-P + Nb was oxidized to a depth of less than 1 mil. The degree of oxidation monotonically increased with temperature (position along wire). There was no indication of a higher oxidation rate at some intermediate temperature, as had been observed on occasion with regular Alumel.

Table 6.3 summarizes the findings from the swaged-sheath Chromel-P, Alumel thermocouples.

Some hot-junction samples of these materials were ground down for microscopic examination after the test. In one case the thermocouple failure was observed as a cleavage between the Alumel wire and sheath closure. Not all samples were inspected. Otherwise, the samples observed indicated sound, void- and crack-free weldments

Table 6.3. Performance of Swaged-Sheath Chromel-P, Alumel Thermocouples

Sheath OD (in.)	Number of Samples in Test	Number of Samples Failed	Approximate Drift (°C)
$\frac{1}{8}$	8	2	+6
$\frac{1}{16}$	13	4	+6
$\frac{1}{25}$	16	1	+4

with only slight indication of surface oxidation not markedly greater than in the material near the cold junction. The only distinguishing feature between sheath sizes was that the closure "puddle" height was approximately one sheath diameter for the  $\frac{1}{25}$ -in.-OD material and approximately half a sheath diameter for the  $\frac{1}{16}$ - and  $\frac{1}{8}$ -in.-OD material.

#### LOW-TEMPERATURE DRIFT TEST – PART II

An independent low-temperature drift test was performed with personnel and facilities different from those in Part I on 20-gage materials of the following: (1) Chromel-P, Alumel, both as-received dull oxide finish and bright-finished-and-annealed materials; (2) Geminol-P/N; (3) Kanthal-P/N; (4) samples of Chromel-P, Alumel from two vendors, with double-wrapped glass insulation (individual wires and over-all) with silicone resin impregnation; (5) materials of type 4 with all insulation stripped.

These tests were run using three furnaces at constant temperatures of 150, 325, and 500°C for 6000 hr. Samples were placed in temperature-equalizing copper blocks measuring 10 × 2 × 2 in., with  $\frac{1}{32}$ -in.-dia drilled holes, 8 in. deep. The test thermocouples were compared with a 90% Pt-10% Rh, Pt thermocouple. The test assemblies consisted of approximately 3 ft of wire strung into six-hole alumina refractories, 1 in. in length (three thermocouples per hole) with thermocouple hot junctions individually welded, using a nitrogen-atmosphere carbon-arc welder. The ambient-temperature reference junctions were monitored with a mercury-glass thermometer. The results of these tests are reviewed in Table 6.4.

The results at 150 and 325°C suggest no appreciable effect on any of the materials. At 500°C the results for both bright and oxidized Chromel-P, Alumel and Kanthal-P/N show a positive drift in 6000 hr of +2 to +3°C. Removal of the glass fiber insulation from the two vendors' samples caused a slight ( $\approx -0.5^\circ\text{C}$ ) lowering of the calibration, or initial value, which was probably due to the cold work imparted to the samples during stripping of the insulation. Comparison of the stripped and unstripped wire from the two vendors at 500°C indicates that the stripped wire drifted positive by about 4°C. This suggested that the silicone-impregnated glass fiber afforded some protection of the wire from oxidation at 500°C.

Table 6.4. Results of Part II Low-Temperature Drift Tests

Thermocouple Type (all but one 20 gage)	Number Tested	Test Temperature (°C)	Deviation (°C)			Spread (°C)	
			Initial	After 6000 hr	Change	Initial	After 6000 hr
Chromel-Alumel, as received, oxidized	2	150	+1.9	+1.5	-0.4	0	0
		325	+0.7	-0.1	-0.8	0	0.2
		500	+0.6	+3.0	+2.4	0	0.2
Chromel-Alumel, bright-annealed	1	150	+1.6	+1.3	-0.3		
		325	+0.5	0	-0.5		
		500	+1.3	+3.1	+1.8		
Geminol-P/N*	3	150	+19.7	+8.0	-11.7**	0.1	
		325	+13.4	+10.2	-3.2	0.3	0.1
		500	+14.6	+12.3	-2.3	0	0.2
Kanthal-P/N, 22 gage	3	150	+1.5	+1.0	-0.5	0	0
		325	+2.2	+2.8	+0.6	0.7	0.3
		500	+4.2	+7.3	+3.1	0.2	0.3
Chromel-Alumel, glass-insulated, silicone- impregnated, vendor A	3	150	+1.2	+0.5	-0.7	0.2	0.1
		325	+0.7	+0.4	-0.3	0	0.5
		500	+1.0	+1.5	+0.5	0.3	0.5
Same as above, but with insulation removed	3	150	+0.7	+0.2	-0.5	0.3	0.3
		325	-0.2	-0.6	+0.4	0.5	0.2
		500	-0.5	+3.3	+3.8	0.7	0.2
Chromel-Alumel, glass-insulated, silicone- impregnated, vendor B	3	150	+1.9	+1.1	-0.8	0	0.1
		325	+0.7	+0.6	-0.1	0.7	0.5
		500	+2.7	+3.8	+1.1	0.2	0.5
Same as above, but with insulation removed	3	150	+1.3	+0.8	-0.5	0.3	0.3
		325	+1.0	+0.9	-0.1	0	0
		500	+0.5	+4.9	+4.4	1.4	0

\*Reflects uncertainty of calibration curve (see Appendix C) and difficulty with switching circuitry. These results viewed with some uncertainty.

\*\*Data questionable.

#### HIGH-TEMPERATURE DRIFT

As was discussed at the beginning of this chapter, many of the high-temperature drift tests were motivated by specific temperature measurement problems.<sup>4</sup> Consequently the presentation and intercomparison of these tests do not possess the uniformity of purpose and result that would be most desired. The results of many tests were omitted from this report because they only constituted confirmation of results presented here. A few test results were omitted because they were ambiguous without sufficient information to explain the ambiguity.

High-temperature drift tests were run at 1300°F (704°C), 1600°F (871°C), and 1800°F (982°C) with the furnace temperature maintained constant throughout the test. In addition, a cyclic drift test was run wherein the furnace was held at 1800°F except that once per week the furnace temperature was dropped to 1600°F for about half a day and then to 1300°F for about one day for the purpose of obtaining calibration data at these temperatures, after which the furnace temperature was reset at 1800°F. Data were taken at 1800°F before and

<sup>4</sup>J. T. DeLorenzo, *Thermocouple Design and Test Program for Reactor Projects*, ORNL-2686 (Apr. 20, 1959).

after each thermal cycle. As it turned out, even though all the data from the cyclic test was processed, only the data taken at 1800°F before each thermal cycle is here presented because the data at the lower temperatures reflected the same trend as the 1800°F data. No drift data was collected at temperatures above 1800°F in order to stay safely below the melting point of the copper used in the temperature-equalizing blocks. A summary of the tests performed is contained in Table 6.5, which also gives the code designation for each test. Figures 6.10–6.13 contain the Oracle curve-plotter outputs for these tests. The order in which the data is presented appears in Table 6.5. Photomicrographs were made of samples from some of these tests and are presented in the same order in Figs. 6.14–6.20.

The results at 1300°F are shown for Chromel-P, Alumel, using hand-assembled four-hole insulating beads with two common-junction thermocouples per assembly. The "normal" handling of these assemblies consisted in using no particular care to avoid contamination of wire or insulators. Bare hands were used, and no solvents or pre-firing of components were employed. The "special" or meticulous handling and the detailed description of materials used are as described for the assembly of all thermocouples in the low-temperature tests. Also shown in Fig. 6.10 are the results from tests on swaged-sheath MgO-insulated Chromel-P, Alumel and 90% Pt–10% Rh, Pt. The initial offset for the 90% Pt–10% Rh, Pt thermocouple (Fig. 6.10*d*) was caused by improper connections of reference junction leads. The results shown in Fig. 6.10 indicate no advantage in using meticulous care in assembling thermocouples used at 1300°F. The reader is cautioned, however, that neglectful handling was not used here. There was no visible amount of grease or dirt stains on insulators or wire. It is just that the extreme precautions were not employed. The performance of the swaged-sheath thermocouples was better than the beaded ones. To within the accuracy of these tests, there was no marked advantage of 90% Pt–10% Rh, Pt at 1300°F.

A distinction exists between normally handled and specially handled thermocouples at 1600 and 1800°F. A cursory glance at Figs. 6.11*a* and 6.11*b* indicates that at 1600°F the performance of normally handled thermocouples is better. A comparison of the mean of the standard deviations indicates that

the spread of data of normally handled thermocouples is eight times worse ( $\overline{SER} = 6.1$  for normally handled;  $\overline{SER} = 0.77$  for specially handled.) This indicates that all of the specially handled thermocouples performed in the same way, drifting only because of oxidation, whereas the variable amount of dirt, grease, and acid on the normally handled ones caused some to drift positive because of oxidation, some to drift negative because of a reducing atmosphere, and some to not drift because of a balance between the two competing processes. A similar comparison may be made between normal and special handling of materials tested at 1800°F (see Figs. 6.12*a* and 6.12*b*). The drift rate is obviously higher at 1800°F constant than at 1600°F, and the reducing effect of contaminants is overshadowed by effects of oxidation, but there is a distinctly greater spread (a factor of 2.3) in the test of normally handled materials than for the meticulously handled materials. The effect of 1800°F cyclic temperature is to accelerate the drift, as seen in Fig. 6.13*a*. The tests shown in Figs. 6.12*c* and 6.12*d* were intended to provide a comparison between Chromel-P, Alumel of  $\frac{3}{4}\%$  accuracy,  $\frac{3}{8}\%$  accuracy, and bright finish with the results above. These tests were performed at a different time and in Inconel re-entry wells which had been used previously and were heavily oxidized on the interior surface. It is thus concluded that these tests reflect some of the phenomena suggested in the section to follow on "Special Tube Thermocouple Drift," rather than a comparison of the various as-received Chromel-P, Alumel.

The above tests were done with Inconel tubes,  $\frac{1}{4}$ -in.-OD  $\times$  0.025-in.-wall thermocouple wells, 12 in. long. To test the effect of length-to-diameter ratio of re-entry wells, and the possible advantage of titanium getter<sup>5</sup> in long wells, a series of experiments were run, using 3-ft long,  $\frac{1}{4}$ -in.-OD Inconel wells. The results of tests in long wells without titanium appear in Figs. 6.11*c*, 6.12*e*, and 6.13*b*, whose respective temperatures are 1600 and 1800°F constant and 1800°F cyclic. It is observed that Chromel-P, Alumel drifts negative under this condition, the initial drift rate being higher at 1800°F than at 1600°F and higher under cyclic conditions than under static conditions. Two possible explanations for this marked

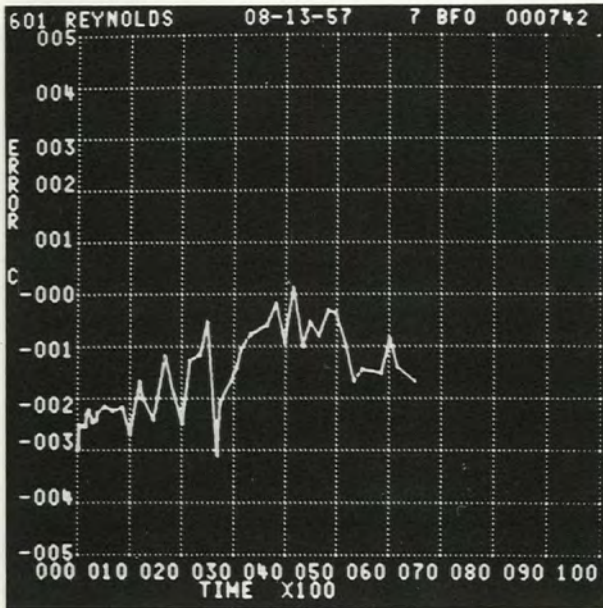
<sup>5</sup>N. F. Spooner and J. M. Thomas, *Metal Progr.* 68, 81 (1955).

Table 6.5. High-Temperature Drift Tests

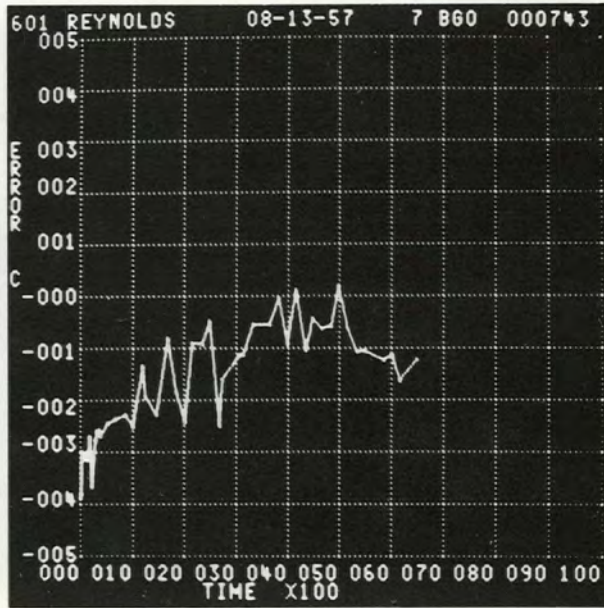
Description of Thermocouple		Thermocouple Code and Thermal History				
Thermocouple Materials	Insulation	Wire Gage	704°C Constant (see Fig. 6.10)	871°C Constant (see Fig. 6.11)	982°C Constant (see Fig. 6.12)	982° Cyclic (see Fig. 6.13)
Chromel-P, Alumel, normal handling	1-ft well, 1/4 in. OD; Conax 1-20-4L four-hole beads, 1/8 in. long	20	BF (a)*	VB (a)	BH (a)	
Chromel-P, Alumel, special handling	Same	20	BG (b)	WB (b)	BI (b), B8 (c), B9 (d)	8B (a)
Chromel-P, Alumel, special handling	Same, 3-ft well, 1/4 in. OD	20		5B (c)	BA (e)	DB (b)
Chromel-P, Alumel, special handling	Same, but titanium wire added	20		2T (d)	8T (f)	3T (c)
Kanthal-P/N, special handling	1-ft well, 1/4 in. OD; Conax 1-20-4L four-hole beads, 1/8 in. long	22		7B** (e)	BE (g)	FB (d)
Geminol-P/N, special handling	Same	20				EB (e)
Geminol-P/N, special handling	Same, 3-ft well, 1/4 in. OD	20		XB (f)	BC (b)	
90% Pt-10% Rh, Pt 1/4 in. OD	Swaged Inconel sheath, MgO insulation, duplex	20	QS (c)		SS (i)	
Chromel-P, Alumel, 1/4 in. OD, 24 hr aged	Same	20	PS (d)	HS (g), 3S (b)	OS (j)	8S (f)
Chromel-P, Alumel, 1/4 in OD, 200 hr aged	Same	20		IS (i)	NS (k)	7S (g)
Chromel-P, Alumel, 3/16 in. OD, loose pack	Same	22		JS (j)	MS (l)	
Chromel-P, Alumel, 3/16 in. OD, loose pack	Same, but one thermocouple replaced by titanium	22		6T (k)	7T (m)	
Chromel-P, Alumel, 1/8 in. OD, loose pack	Swaged Inconel sheath, MgO insulation	22		KS (l), 1S (m)	LS (n)	5S (h), 6S (i)
Chromel-P, Alumel, 1/16 in. OD, dense pack	Same	30		4S (n)		

\*Letters in parentheses indicate part of figure referred to.

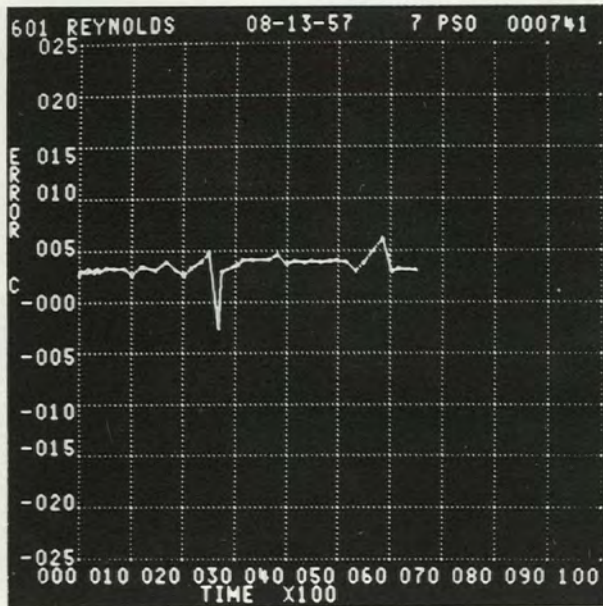
\*\*Italics signify that photomicrographs appear in Figs. 6.14 to 6.20.



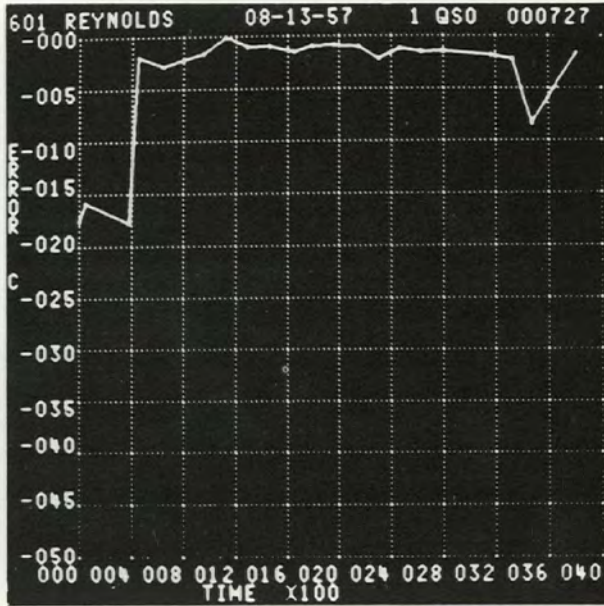
(a) CHROMEL-ALUMEL, 20 GAGE; NORMAL HANDLING;  
CONAX BEADS; INCONEL WELL, 1ft LONG. BF;  $DF=0495$ ,  
 $S\bar{E}R=0.80$



(b) CHROMEL-ALUMEL, 20 GAGE; SPECIAL HANDLING;  
CONAX BEADS; INCONEL WELL, 1ft LONG. BG;  $DF=0479$ ,  
 $S\bar{E}R=0.79$



(c) CHROMEL-ALUMEL, 20 GAGE; SWAGED SHEATH,  $\frac{1}{4}$  in. OD  
AGED 24 hr. PS;  $DF=0468$ ,  $S\bar{E}R=0.57$

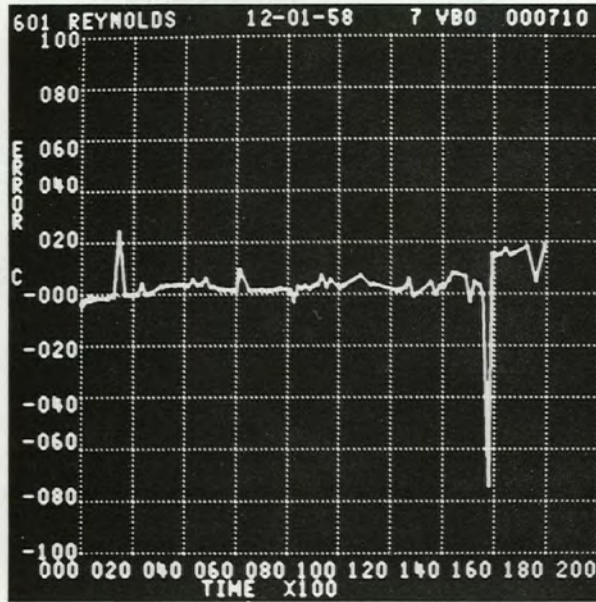


(d) 90% Pt-10% Rh, Pt, 20 GAGE; SWAGED INCONEL SHEATH,  
 $\frac{1}{4}$  in. OD. QS;  $DF=0105$ ,  $S\bar{E}R=0.64$

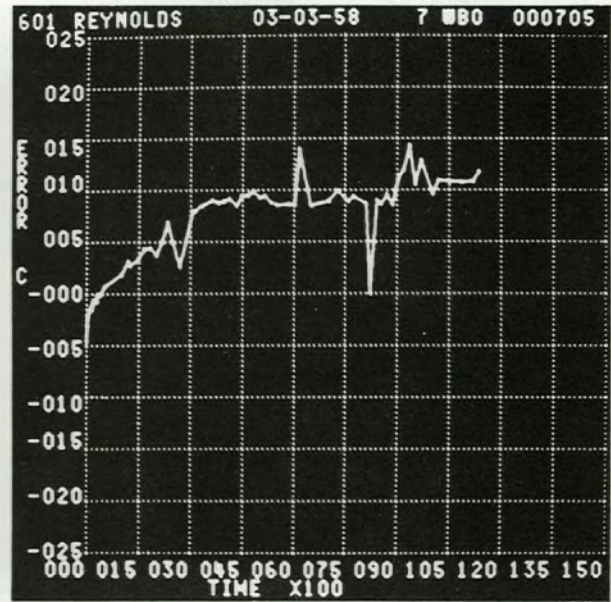
Fig. 6.10. Results of Constant-Temperature ( $704^{\circ}\text{C}$ ) Drift Tests. See Table 6.5 for identification of thermocouple (BF, etc.).

Fig. 6.11. Results of Constant-Temperature (871°C) Drift Tests. See Table 6.5 for identification of thermocouple (VB, etc.).

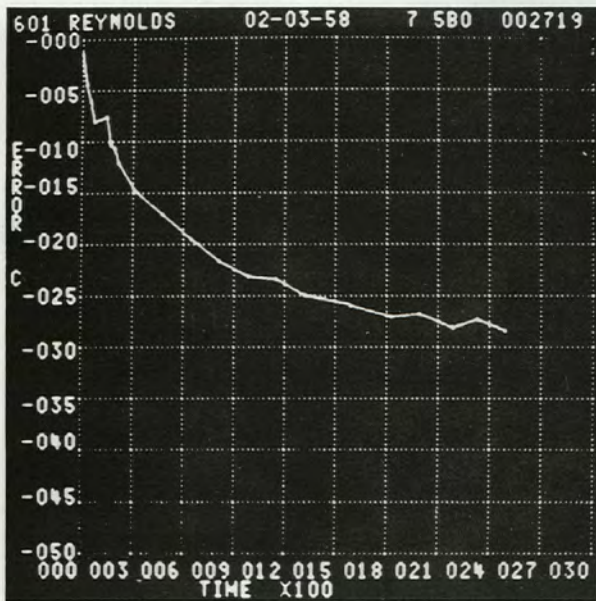
UNCLASSIFIED  
ORNL-LR-DWG 48614



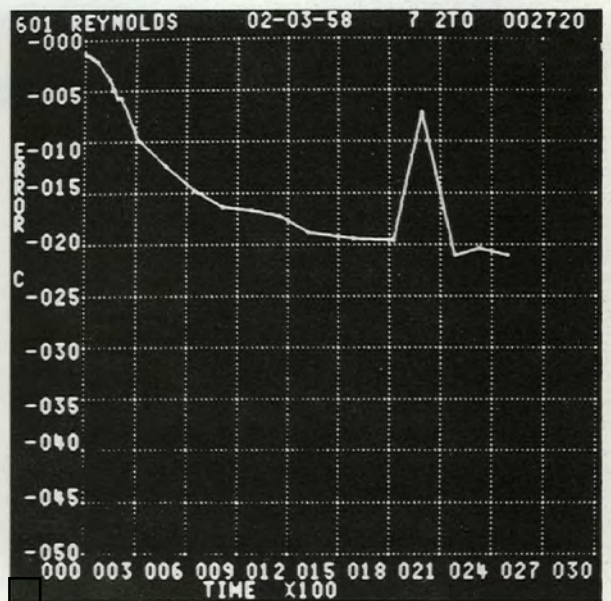
(a) CHROMEL-ALUMEL, 20 GAGE; NORMAL HANDLING; CONAX BEADS; 1-ft INCONEL WELLS. VB;  $DF=0813$ ,  $S\bar{E}R=6.15$



(b) CHROMEL-ALUMEL, 20 GAGE; SPECIAL HANDLING; CONAX BEADS; 1-ft INCONEL WELLS. WB;  $DF=0628$ ,  $S\bar{E}R=0.77$

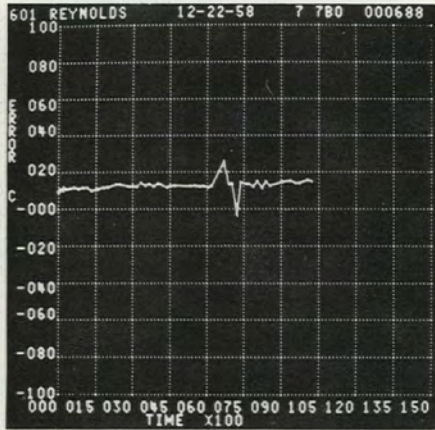


(c) CHROMEL-ALUMEL, 20 GAGE; SPECIAL HANDLING; CONAX BEADS; 3-ft INCONEL WELLS. 5B;  $DF=0147$ ,  $S\bar{E}R=8.53$

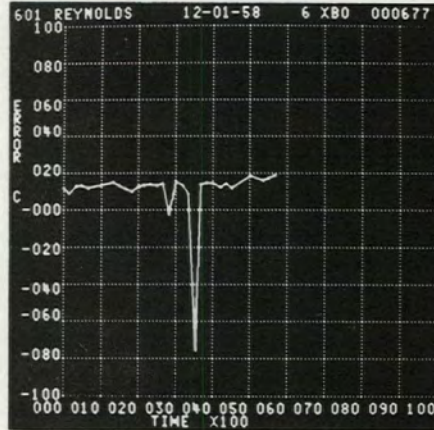


(d) CHROMEL-ALUMEL, 20 GAGE; SPECIAL HANDLING; CONAX BEADS; 3-ft INCONEL WELLS; TITANIUM WIRE ADDED. 2T;  $DF=0063$ ,  $S\bar{E}R=7.6927$

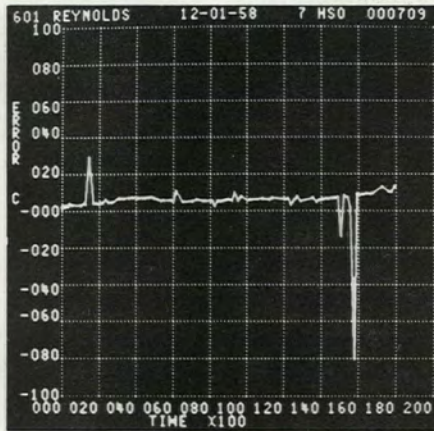
Fig. 6.11a-d.



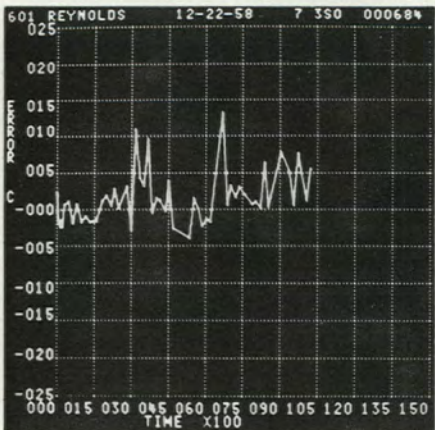
(e) KANTHAL-P/N, 22 GAGE; SPECIAL HANDLING; CONAX BEADS, 1-ft INCONEL WELLS. XB;  $DF = 0.278$ ,  $SER = 0.53680$



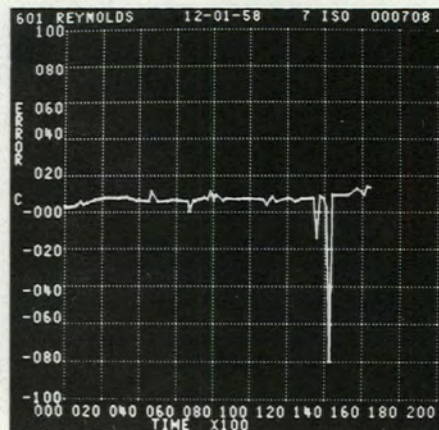
(f) GEMINOL-P/N, 20 GAGE; SPECIAL HANDLING; CONAX BEADS, 3-ft INCONEL WELLS. XB;  $DF = 0.145$ ,  $SER = 0.2310$



(g) CHROMEL-ALUMEL, 20 GAGE; AGED 24 hr; SWAGED INCONEL SHEATHS, 1/4 in. OD; MgO INSULATION. HS;  $DF = 0.895$ ,  $SER = 0.9817$ .

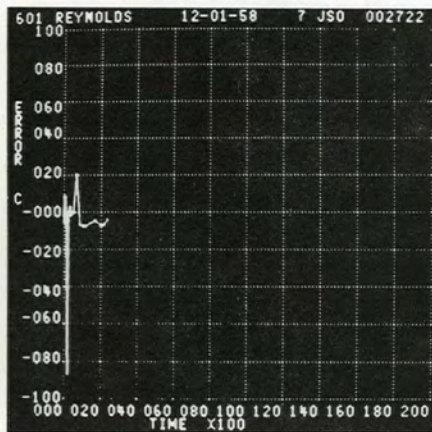


(h) CHROMEL-ALUMEL, 20 GAGE; REPEATED TEST; SAME SPECIFICATIONS AS FOR (g). 3S;  $DF = 0.167$ ,  $SER = 7.7346$ .

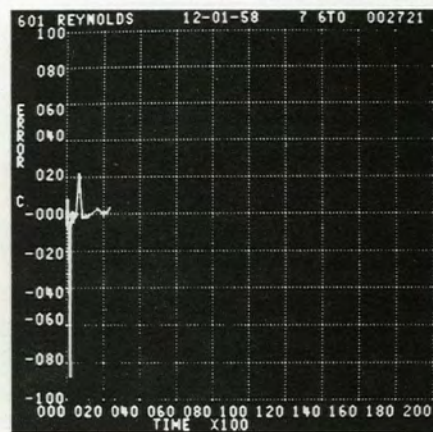


(i) SAME SPECIFICATIONS AS FOR (g), EXCEPT THAT AGING TIME WAS 200 hr. IS;  $DF = 0.551$ ,  $SER = 1.6412$ .

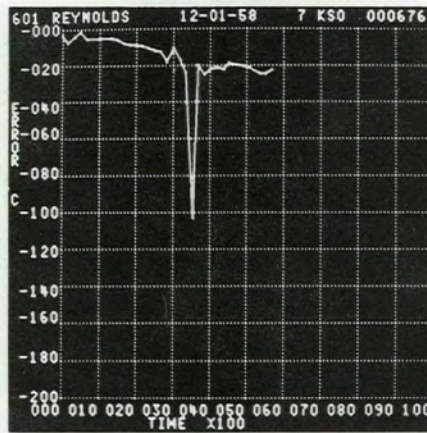
Fig. 6.11e-i.



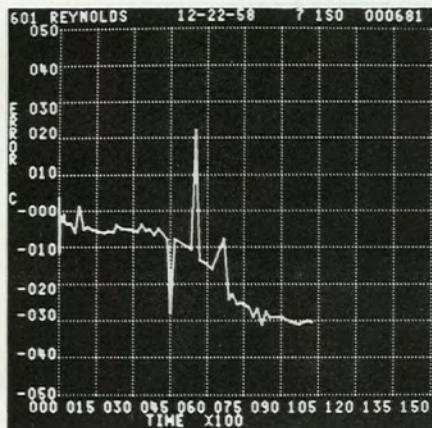
(j) CHROMEL-ALUMEL, 22 GAGE; SWAGED SHEATH;  
INCONEL,  $\frac{3}{16}$  in. OD; LOOSELY PACKED MgO; DUPLEX.  
JS; DF=0038, SER=3.7804.



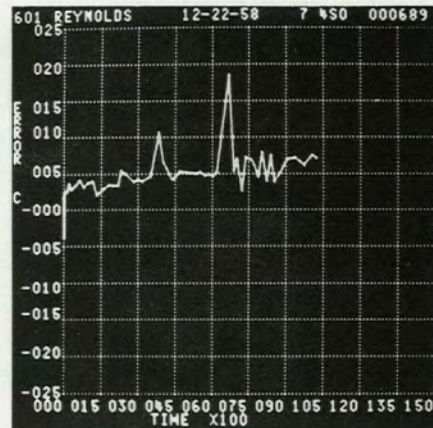
(k) CONDITIONS SAME AS FOR (j), EXCEPT THAT ONE  
THERMOCOUPLE WAS REPLACED BY T<sub>1</sub> WIRES.  
6T; DF=0081, SER=1.9172.



(l) CHROMEL-ALUMEL, 22 GAGE; SWAGED SHEATH;  
INCONEL,  $\frac{1}{8}$  in. OD; LOOSELY PACKED MgO. KS;  
DF=0145, SER=9.4251.



(m) REPEATED TEST; SAME SPECIFICATIONS AS FOR (l)  
1S; DF=0114, SER=0.4634.

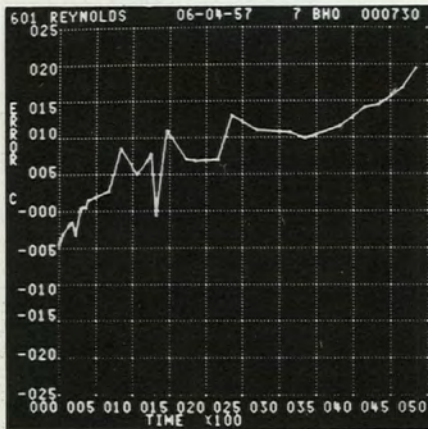


(n) CHROMEL-ALUMEL, 30 GAGE; SWAGED SHEATH;  
INCONEL,  $\frac{1}{16}$  in. OD; DENSELY PACKED MgO. 4S;  
DF=0164, SER=6.1197.

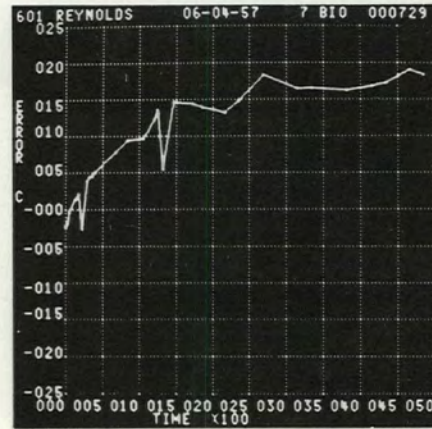
Fig. 6.11j-n.

Fig. 6.12. Results of Constant-Temperature (982°C) Drift Tests. See Table 6.5 for identification of thermocouple (BH, etc.).

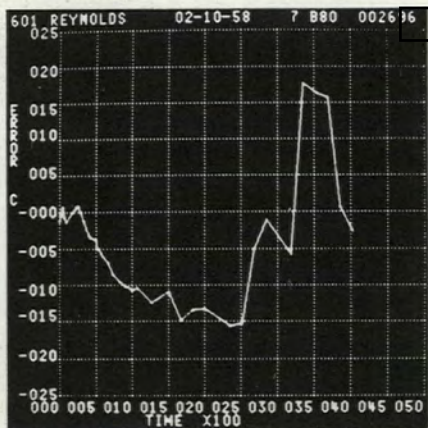
UNCLASSIFIED  
ORNL-LR-DWG 48617



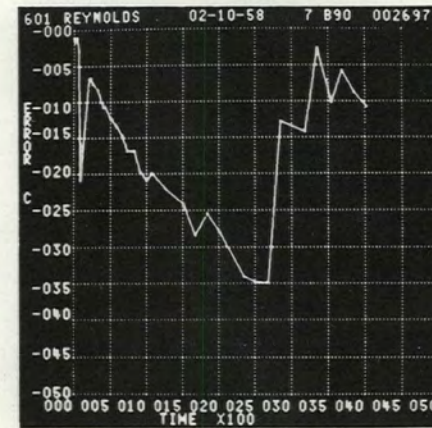
(a) CHROMEL-ALUMEL, 20 GAGE; NORMAL HANDLING; CONAX BEADS; 1-ft INCONEL WELLS. BH;  $DF=0341$ ,  $SER=6.0950$ .



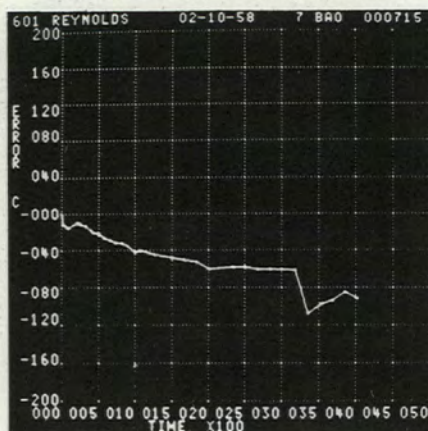
(b) CHROMEL-ALUMEL, 20 GAGE; SPECIAL HANDLING; CONAX BEADS; 1-ft INCONEL WELLS. BI;  $DF=0352$ ,  $SER=2.6344$ .



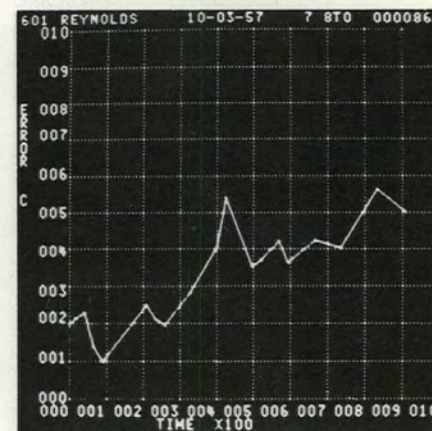
(c) CHROMEL-ALUMEL, 20 GAGE; SPECIAL HANDLING;  $\frac{3}{4}\%$  WIRE; BRIGHT FINISH CONAX BEADS; 1-ft INCONEL WELLS. BB;  $DF=0180$ ,  $SER=31.9758$ .



(d) CHROMEL-ALUMEL, 20 GAGE; SPECIAL HANDLING;  $\frac{3}{8}\%$  WIRE; CONAX BEADS; 1-ft INCONEL WELLS. B9;  $DF=0180$ ,  $SER=44.3265$ .

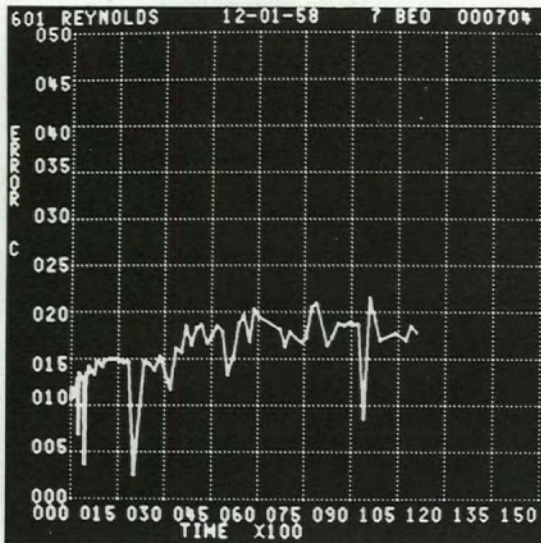


(e) CHROMEL-ALUMEL, 20 GAGE; SPECIAL HANDLING; CONAX BEADS; 3-ft INCONEL WELLS. BA;  $DF=0252$ ,  $SER=19.2116$ .

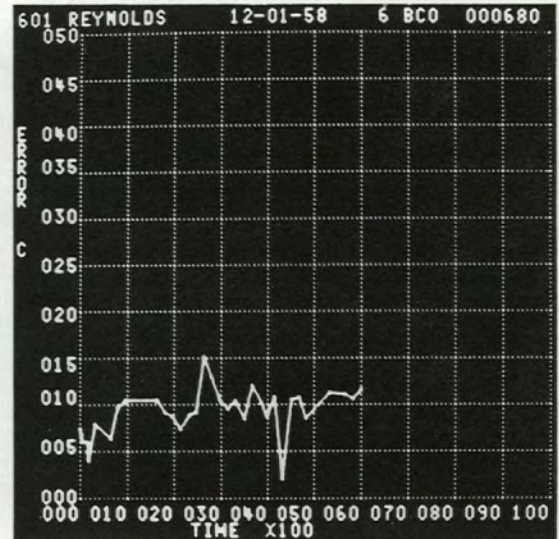


(f) SAME CONDITIONS AS FOR (e), EXCEPT THAT Ti WIRE WAS ADDED. 8T;  $DF=0057$ ,  $SER=3.4939$ .

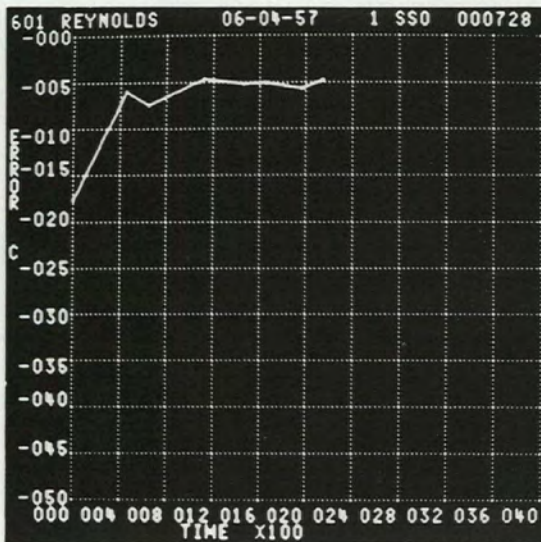
Fig. 6.12a-f.



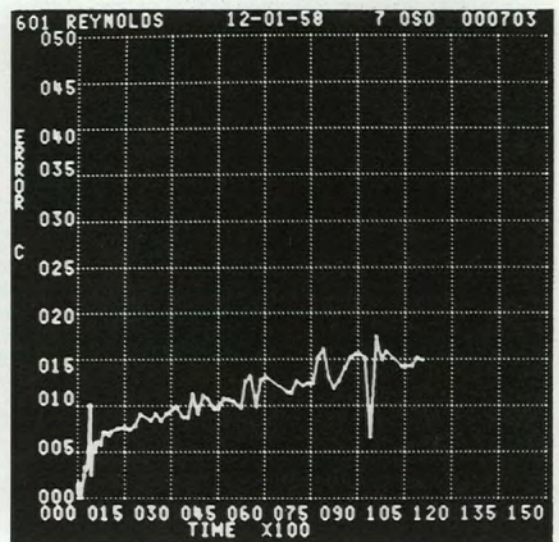
(g) KANTHAL-P/N, 20 GAGE; SPECIAL HANDLING; CONAX BEADS; 1-ft INCONEL WELLS. BE;  $DF=0355$ ,  $SE\bar{R}=2.4304$ .



(h) GEMINOL-P/N, 20 GAGE; SPECIAL HANDLING; CONAX BEADS; 3-ft INCONEL WELLS. BC;  $DF=0363$ ,  $SE\bar{R}=2.7224$ .

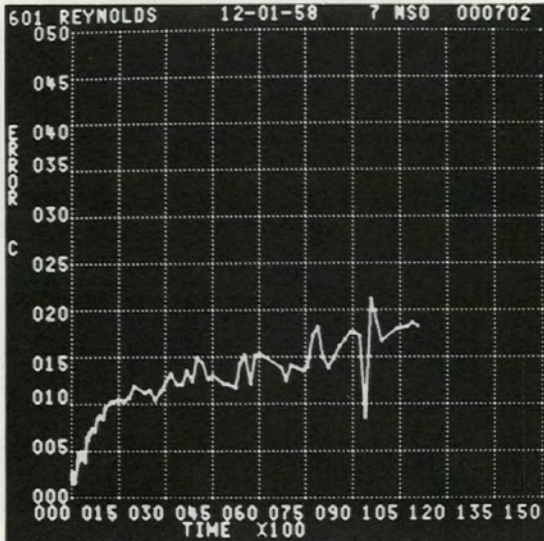


(i) 90% Pt--10% Rh, Pt; 20 GAGE WIRE; SWAGED 1/4-in.-OD INCONEL SHEATH; MgO INSULATED. SS;  $DF=0051$ ,  $SE\bar{R}=1.3807$ .

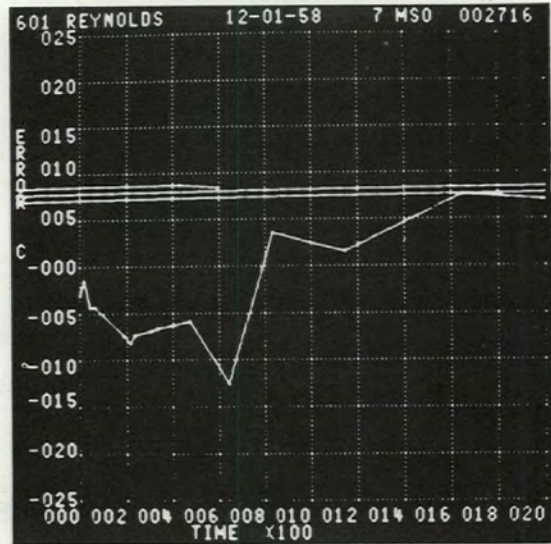


(j) CHROMEL-ALUMEL, 20 GAGE, 24-hr AGED; SWAGED 1/4-in.-OD INCONEL SHEATH; MgO INSULATED. OS;  $DF=0051$ ,  $SE\bar{R}=1.3807$ .

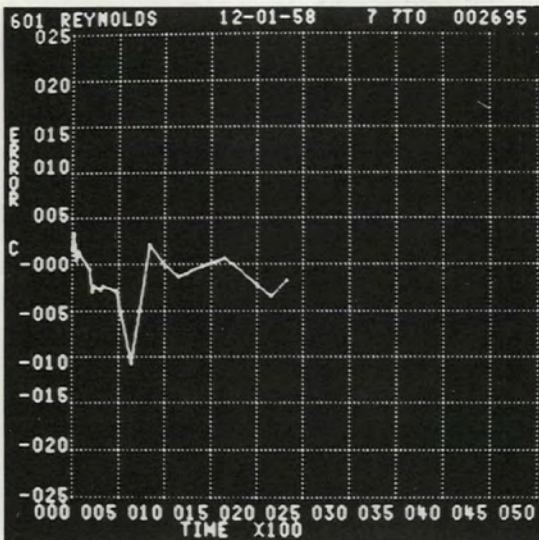
Fig. 6.12.g-j.



(k) SAME CONDITIONS AS FOR (j), BUT WAS AGED 200 hr.  
NS;  $DF=0.219$ ,  $SER=2.5341$ .



(l) CHROMEL-ALUMEL, 22 GAGE; SWAGED SHEATH,  $\frac{3}{16}$ -in.  
-OD INCONEL; LOOSELY PACKED MgO; DUPLEX. MS;  
 $DF=0.123$ ,  $SER=9.5667$ .



(m) SAME AS (l), EXCEPT THAT ONE THERMOCOUPLE WAS  
REPLACED BY Ti WIRES. 7T;  $DF=0.054$ ,  $SER=6.3927$ .

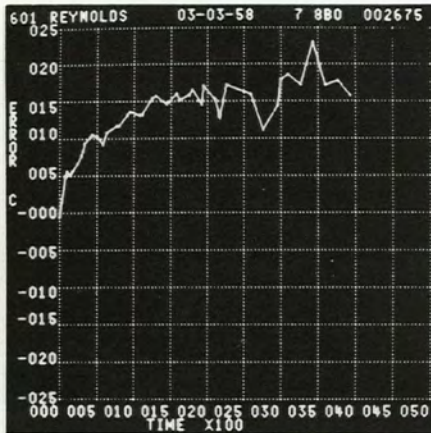


(n) CHROMEL-ALUMEL, 22 GAGE; SWAGED SHEATH,  $\frac{1}{8}$ -in.  
OD INCONEL; LOOSELY PACKED MgO. LS;  $DF=0.061$ ,  
 $SER=27.4152$ .

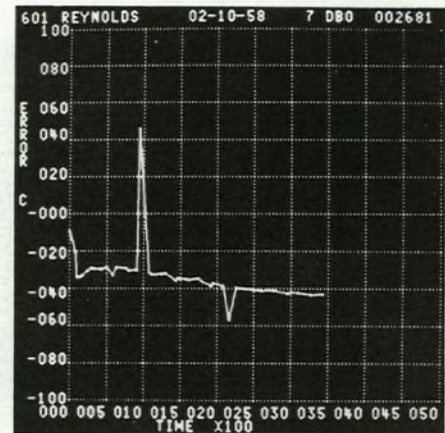
Fig. 6.12k-n.

Fig. 6.13. Results of Cyclic (982°C) Drift Tests. See Table 6.5 for identification of thermocouple (8B, etc.).

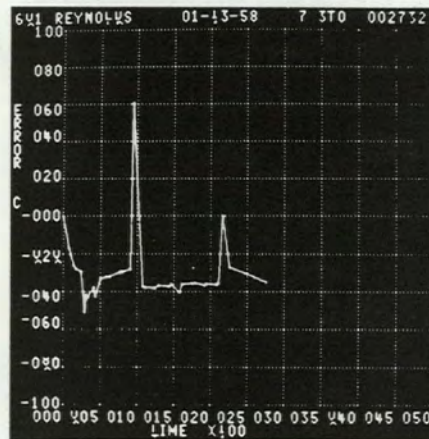
UNCLASSIFIED  
ORNL-LR-DWG 48620



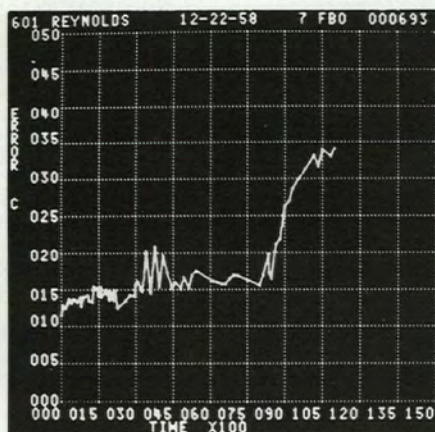
(a) CHROMEL-ALUMEL, 20 GAGE; SPECIAL HANDLING; CONAX BEADS; 1-FT INCONEL WELLS. 8B;  $DF = 0.132$ ,  $SE\bar{R} = 2.2219$ .



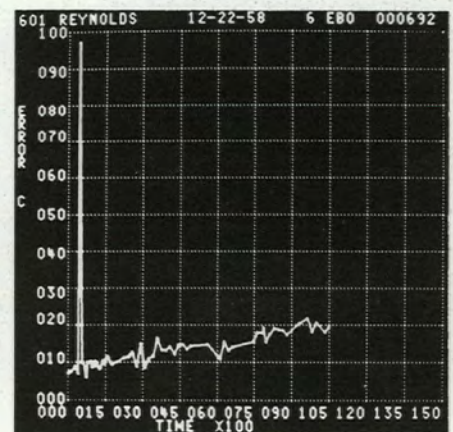
(b) CHROMEL-ALUMEL, 20 GAGE; SPECIAL HANDLING; CONAX BEADS; 3-FT INCONEL WELLS. DB;  $DF = 0.280$ ,  $SE\bar{R} = 14.0756$ .



(c) CHROMEL-ALUMEL, 20 GAGE; SPECIAL HANDLING; CONAX BEADS; 3-FT INCONEL WELLS; 1 TC REPLACED BY 2 Ti WIRES. 3T;  $DF = 0.135$ ,  $SE\bar{R} = 13.8981$ .

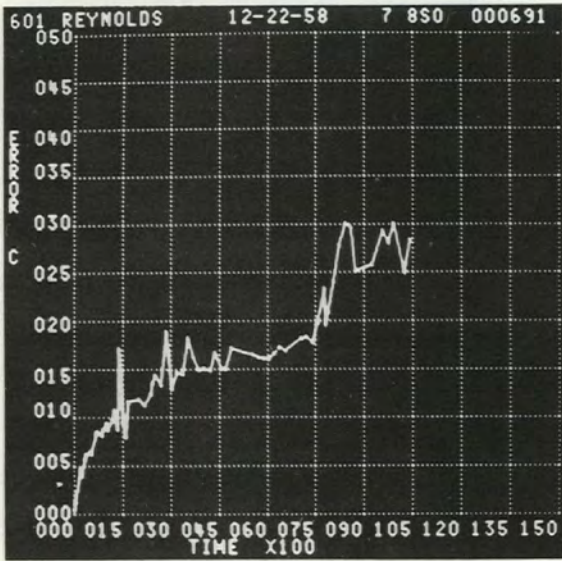


(d) KANTHAL, 22 GAGE; SPECIAL HANDLING; CONAX BEADS; 1-FT INCONEL WELLS. FB;  $DF = 0.364$ ,  $SE\bar{R} = 2.78$

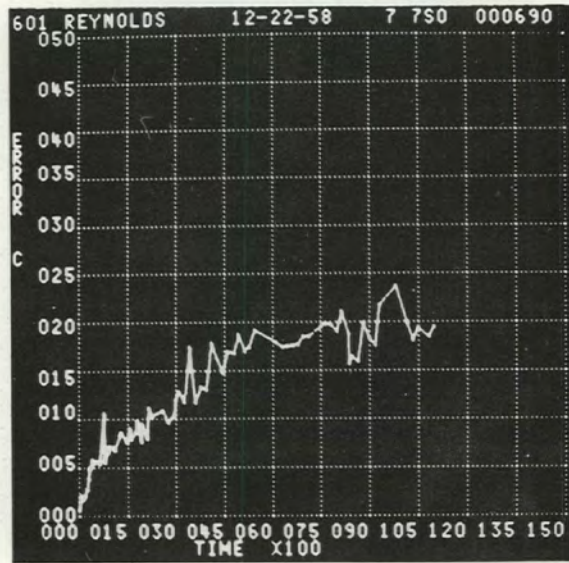


(e) GEMINOL-P/N, 20 GAGE; SPECIAL HANDLING; CONAX BEADS; 1-FT INCONEL WELLS. EB;  $DF = 0.314$ ,  $SE\bar{R} = 1.05$

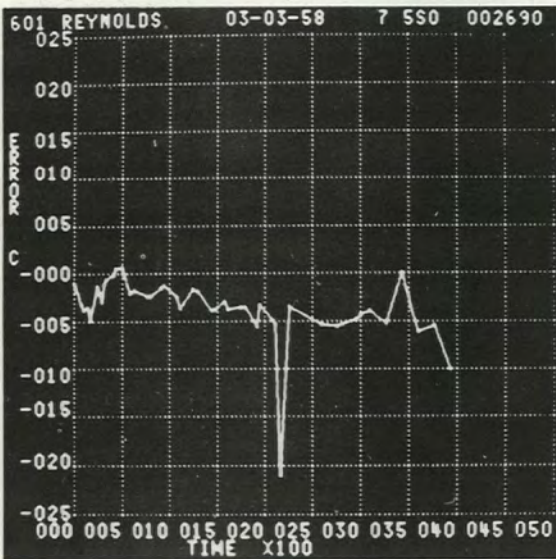
Fig. 6.13a-e.



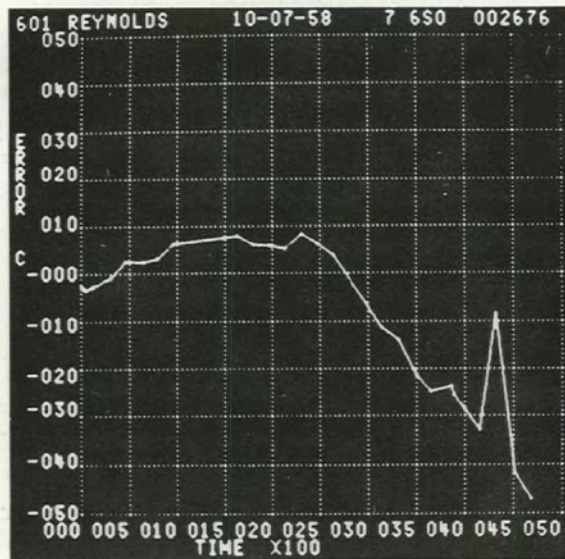
(f) CHROMEL-ALUMEL, 20 GAGE; 24 hr AGED; SWAGED 1/4-in.-OD INCONEL SHEATH; MgO INSULATED. 8S;  $DF=0196$ ,  $S\bar{E}R=3.6308$ .



(g) SAME CONDITIONS AS FOR (f), EXCEPT FOR 200 hr AGING. 7S;  $DF=0234$ ,  $S\bar{E}R=1.4994$ .

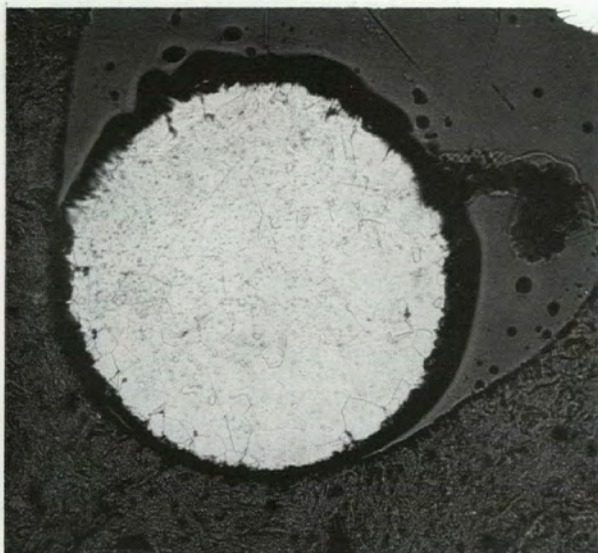


(h) CHROMEL-ALUMEL, 22 GAGE; SWAGED SHEATH; 1/8-in.-OD INCONEL; LOOSELY PACKED MgO. 5S;  $DF=0087$ ,  $S\bar{E}R=2.7428$ .

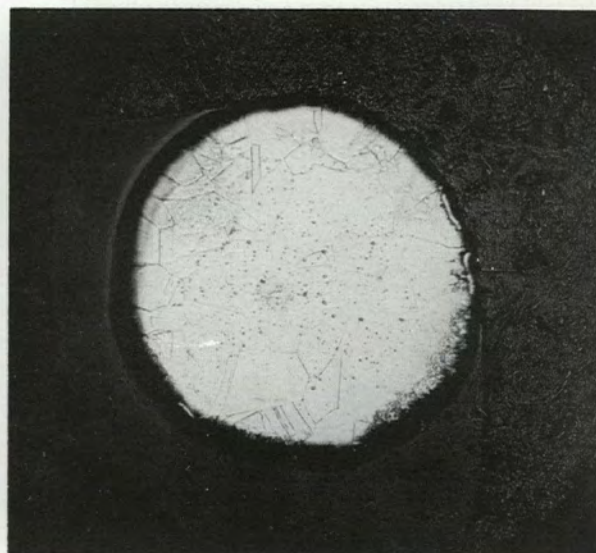


(i) SAME CONDITIONS AS FOR (h); REPEATED TEST. 6S;  $DF=0135$ ,  $S\bar{E}R=13.2061$ .

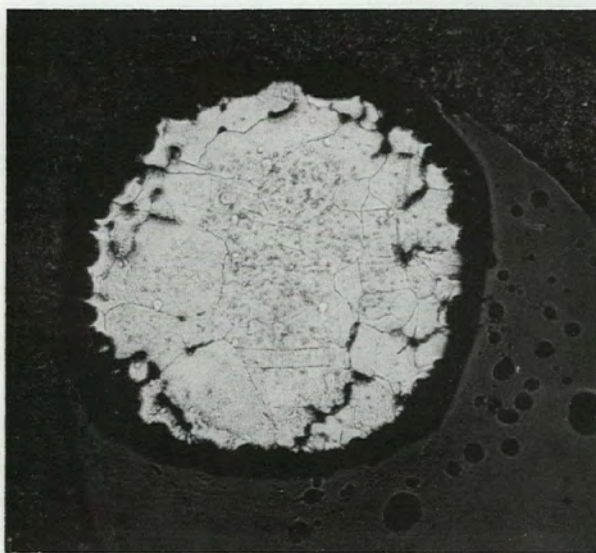
Fig. 6.13f-i.



(a) KANTHAL-P AFTER 10,000 hr AT 871°C  
TEST 7B



(b) KANTHAL-N TEST 7B

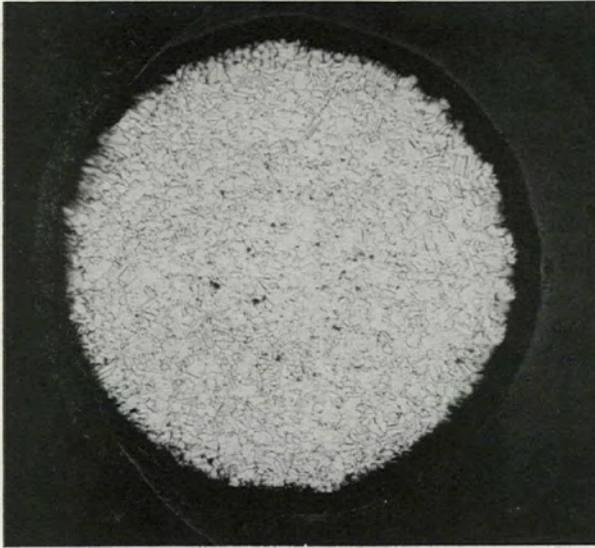


(c) KANTHAL-P AFTER 11,000 hr AT 982°C  
TEST BE

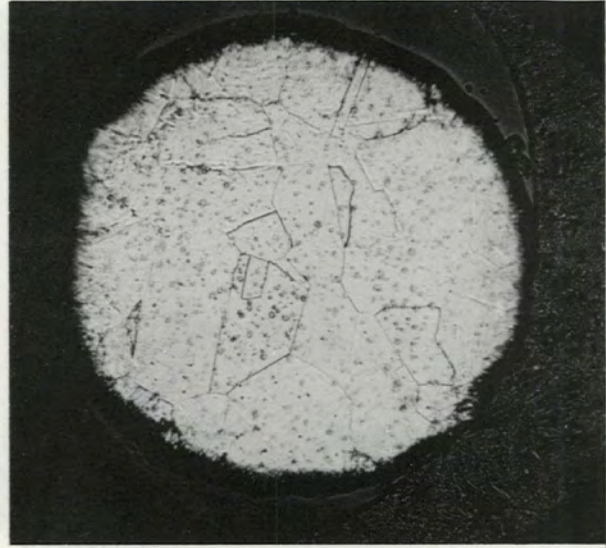


(d) KANTHAL-N TEST BE

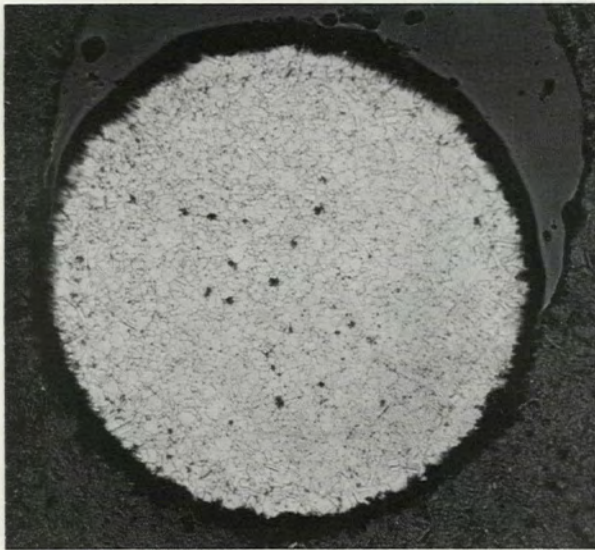
Fig. 6.14. Photomicrographs of Kanthal-P/N After Drift Tests at 871 and 982°C. Etched with glyceria regia. 75X.



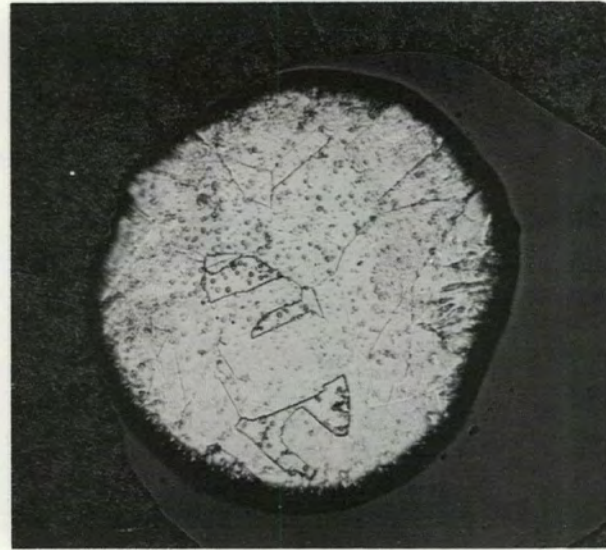
(a) GEMINOL-P AFTER 5500 hr AT 871 °C.  
TEST XB



(b) GEMINOL-N. TEST XB

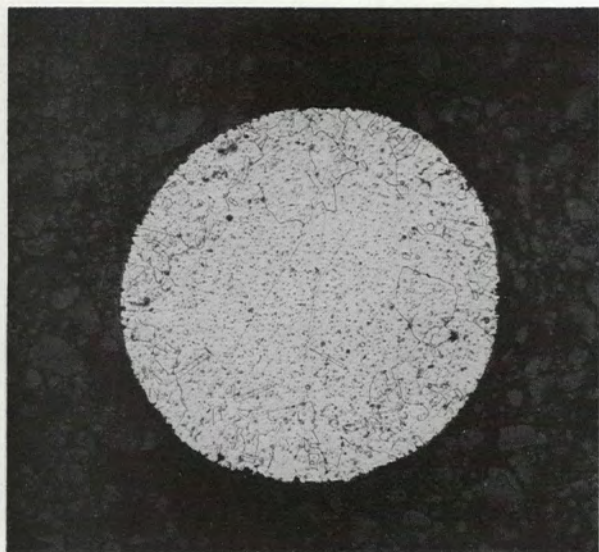


(c) GEMINOL-P AFTER 6000 hr AT 982 °C.  
TEST BC

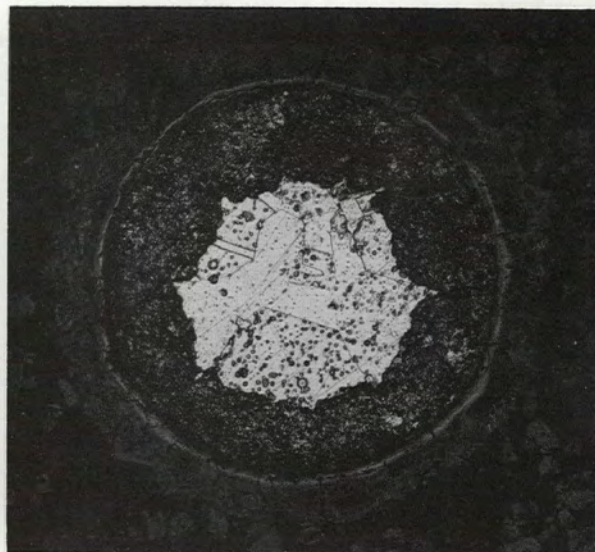


(d) GEMINOL-N TEST BC

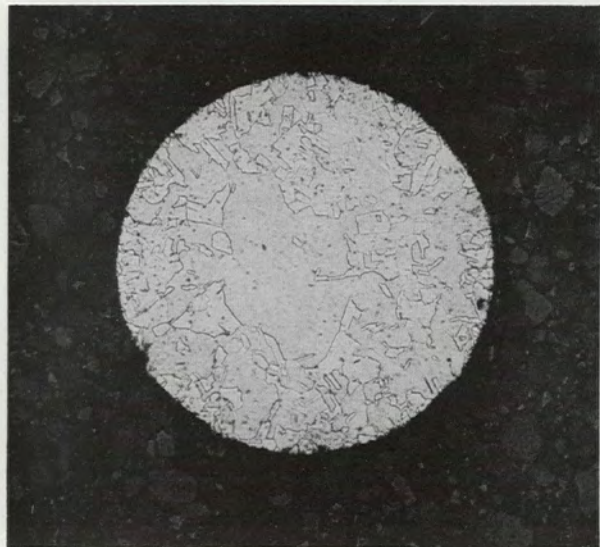
Fig. 6.15. Photomicrographs of Geminol-P/N After Drift Tests at 871 and 982°C. Etched with glyceria regia. 75X.



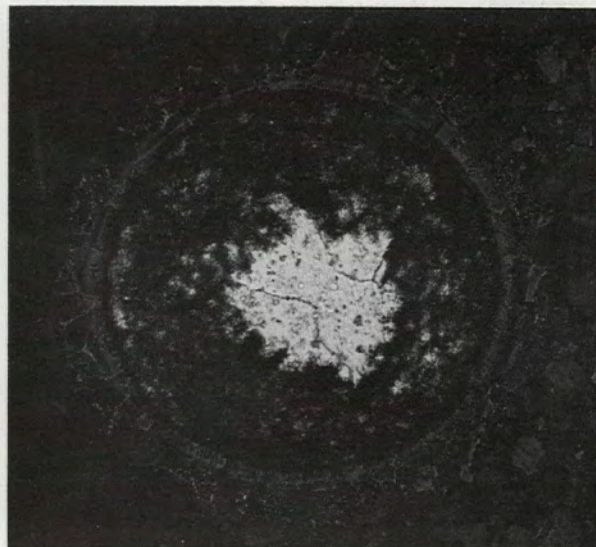
(a) CHROMEL-P AFTER 18,000 hr AT 871°C.  
TEST HS



(b) ALMEL TEST HS

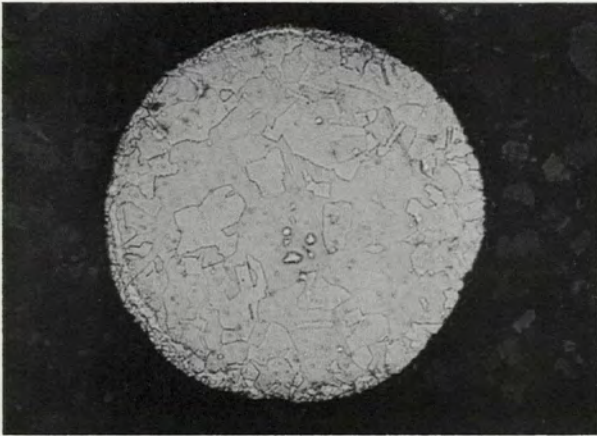


(c) CHROMEL-P AFTER 10,500 hr AT 871°C.  
TEST 3S

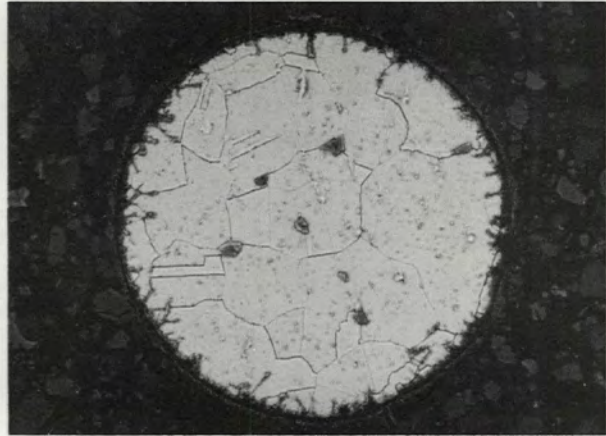


(d) ALMEL TEST 3S

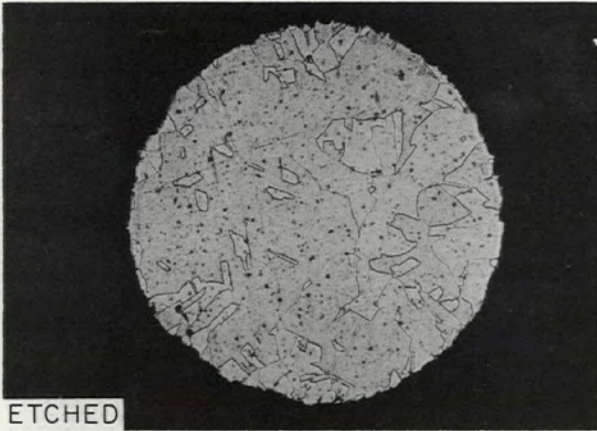
Fig. 6.16. Photomicrographs of  $\frac{1}{4}$ -in.-OD Swaged-Sheath Chromel-P, Almel After Drift Tests at 871°C. Etched with glyceria regia. 75X.



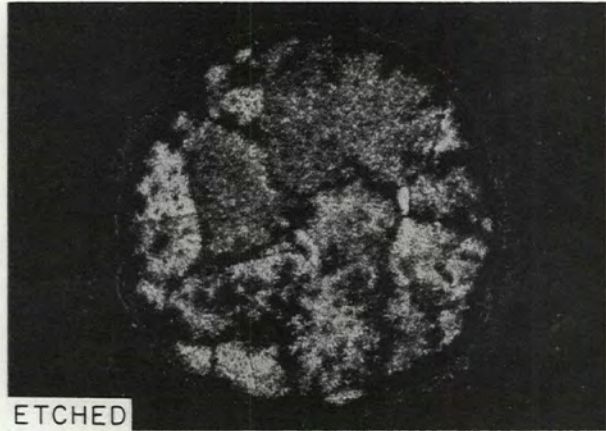
(a) CHROMEL-P AFTER 11,000 hr AT 982 °C,  
CONSTANT. TEST OS



(b) ALMEL TEST OS



(c) CHROMEL-P AFTER 10,500 hr AT 982 °C,  
CYCLIC. TEST 8S



(d) TEST 8S

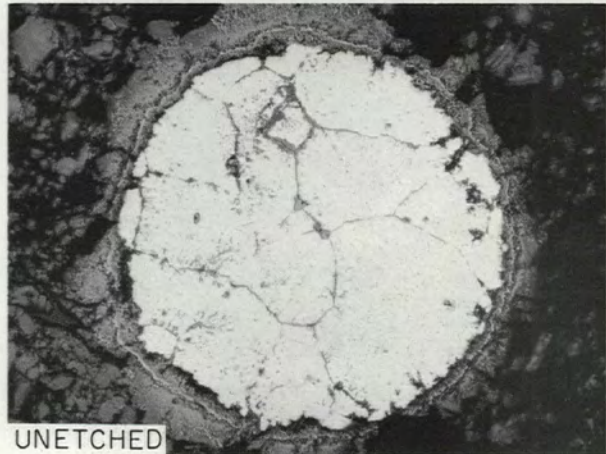
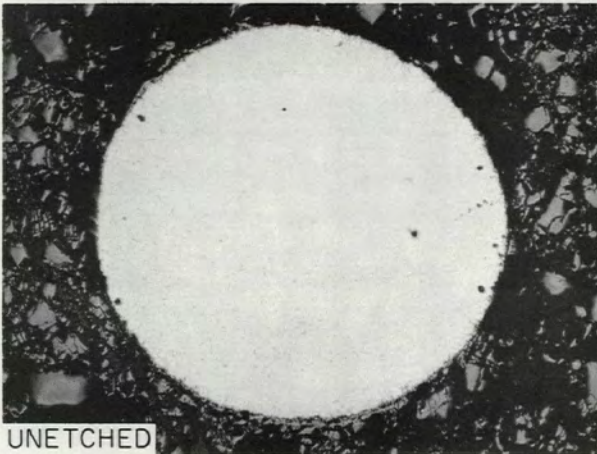
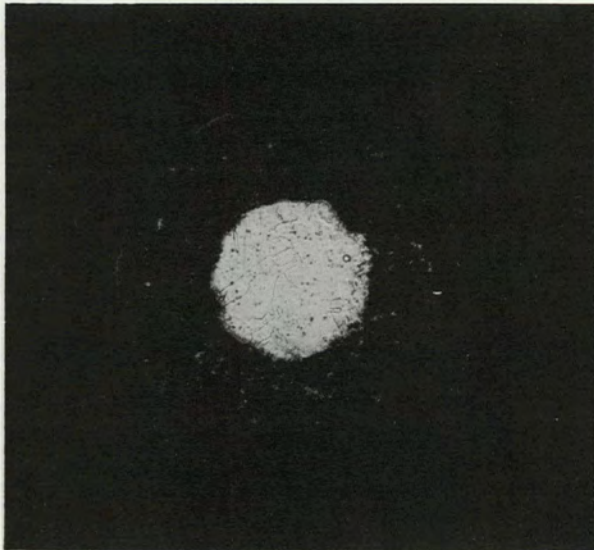
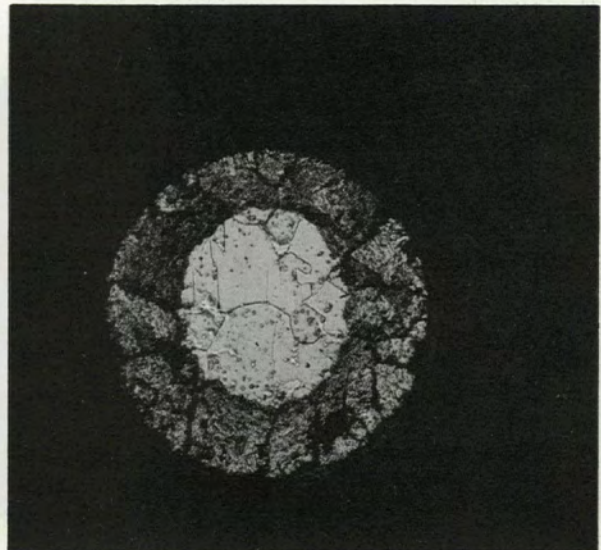


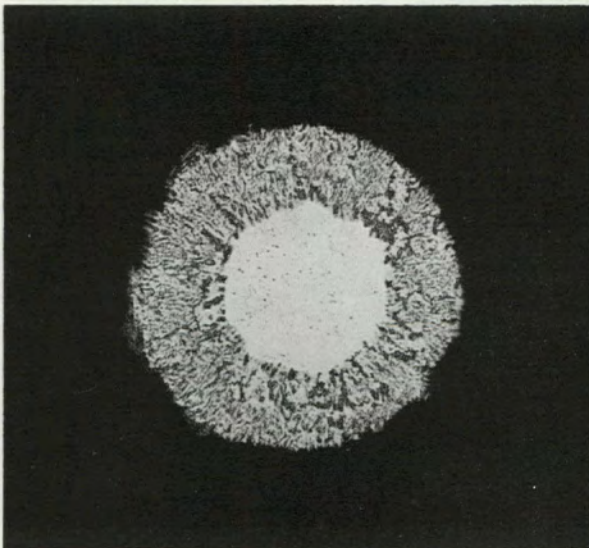
Fig. 6.17. Photomicrographs of  $\frac{1}{4}$ -in.-OD Swaged-Sheath Chromel-P, Almel After Drift Tests at 982°C. Etched with glyceria regia, except where otherwise indicated. 75X.



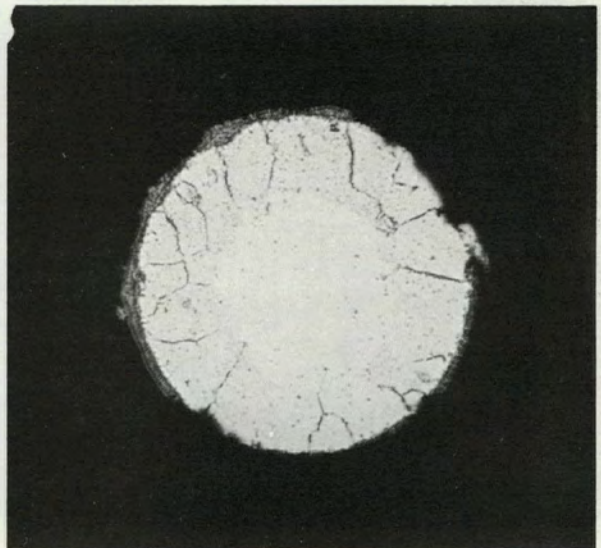
(a) CHROMEL-P AFTER 2500 hr. TEST JS



(b) ALUMEL TEST JS

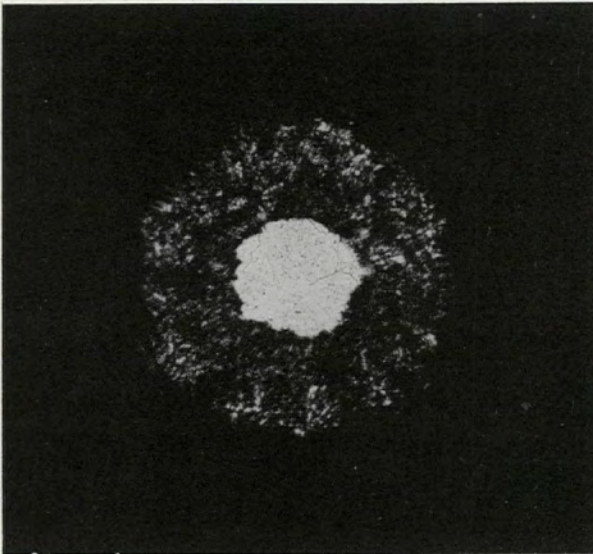


(c) CHROMEL-P AFTER 2500 hr. TEST JS  
UNETCHED

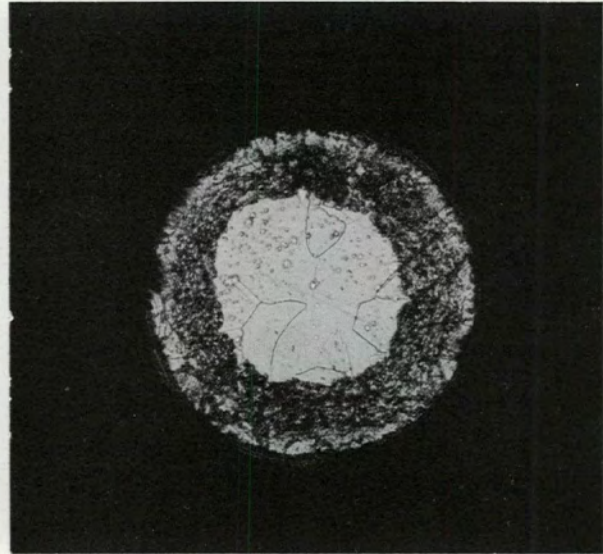


(d) ALUMEL TEST JS UNETCHED

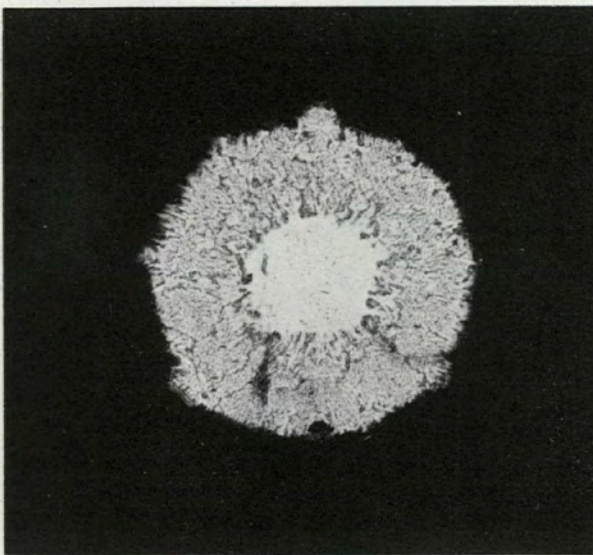
Fig. 6.18a-d. Photomicrographs of  $\frac{3}{16}$ -in.-OD Swaged-Sheath (Loosely Packed Magnesium Oxide) Chromel-P, Alumel After Drift Test at 871°C. Etched with glyceria regia, except where otherwise indicated. 75X.



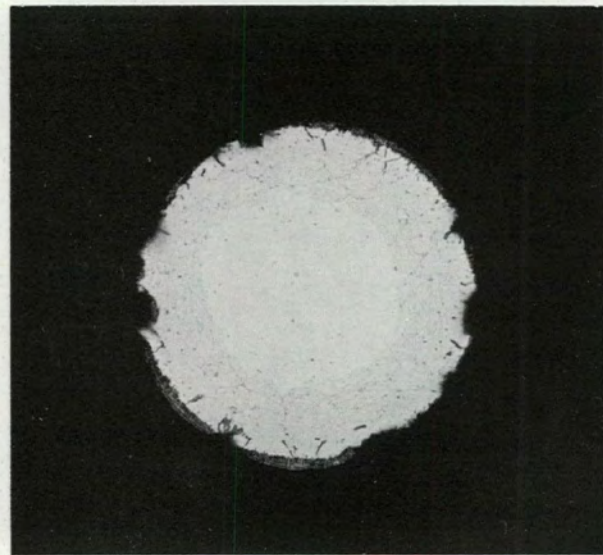
(e) CHROMEL-P AFTER 2500 hr. TEST 6T



(f) ALUMEL TEST 6T

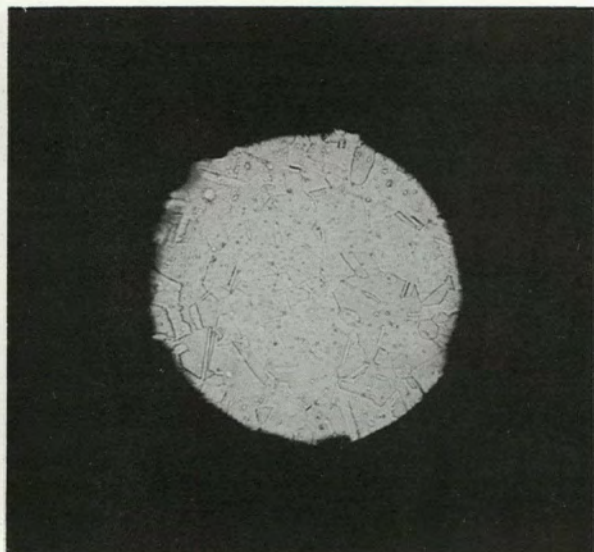


(g) CHROMEL-P AFTER 2500 hr. TEST 6T  
UNETCHED

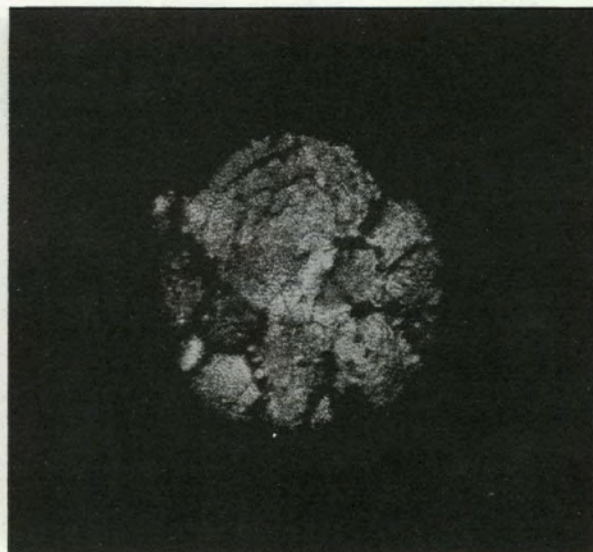


(h) ALUMEL TEST 6T UNETCHED

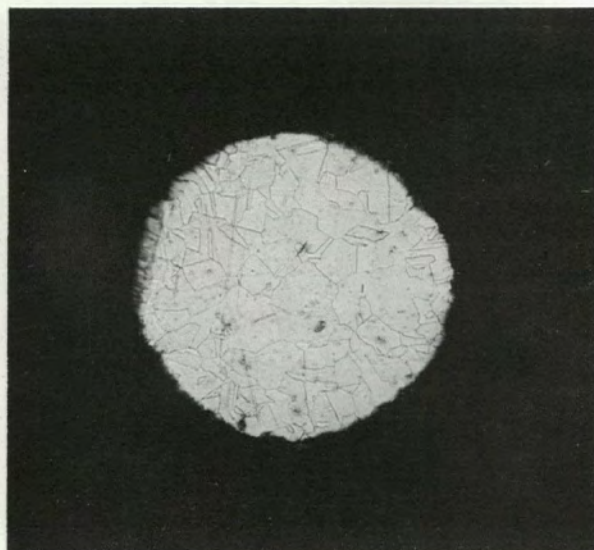
Fig. 6.18e-b. Photomicrographs of  $\frac{3}{16}$ -in.-OD Swaged-Sheath (Loosely Packed Magnesium Oxide) Chromel-P, Alumel with One of Duplex Thermocouples Replaced by Titanium Wire, After Drift Test at 871°C. Etched with glyceria regia, except where otherwise indicated. 75X.



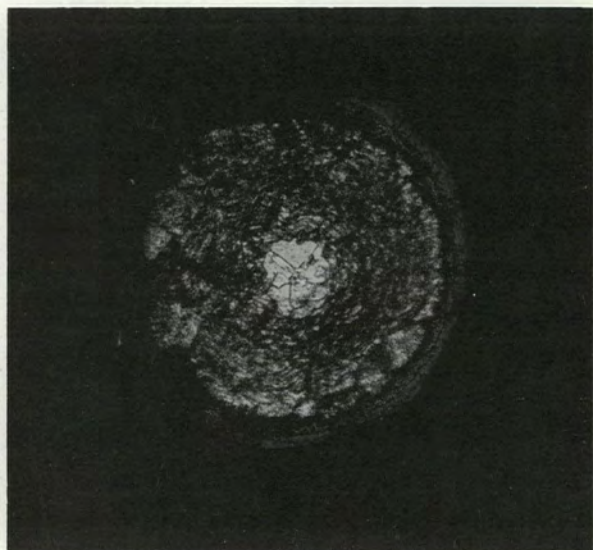
(a) CHROMEL-P AFTER 2500 hr. TEST MS



(b) ALUMEL TEST MS

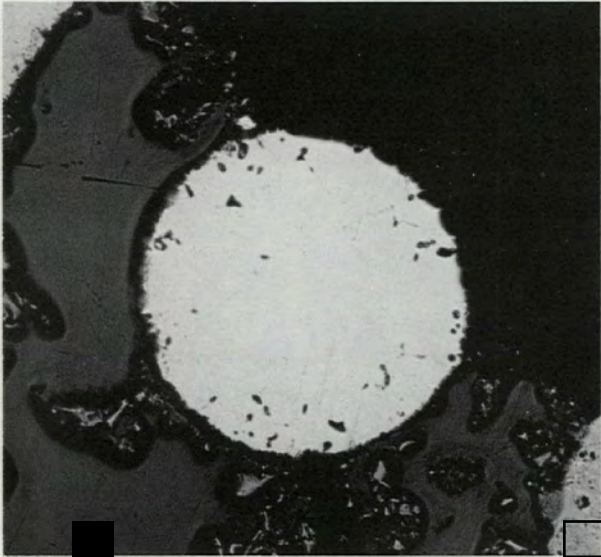


(c) CHROMEL-P AFTER 2500hr. TEST 7T  
ONE OF DUPLEX THERMOCOUPLES  
REPLACED BY TITANIUM

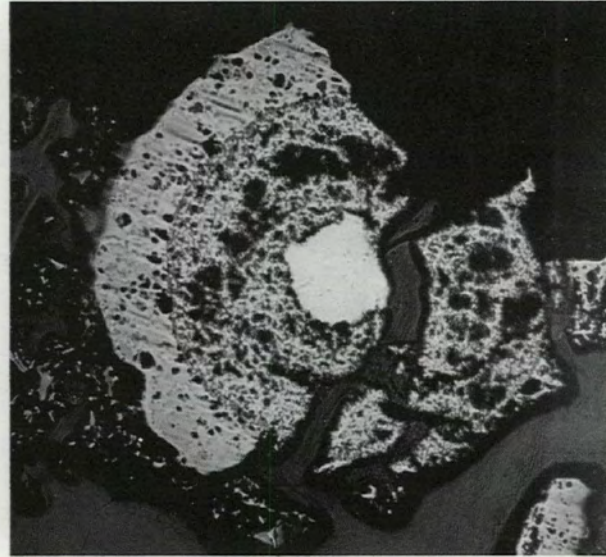


(d) ALUMEL TEST 7T

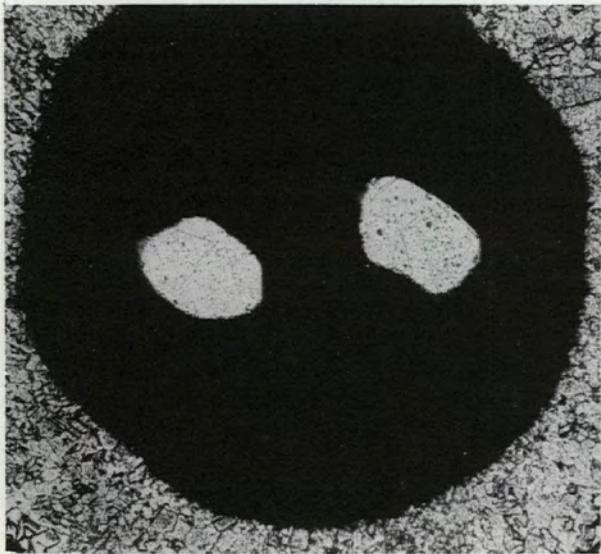
Fig. 6.19. Photomicrographs of  $\frac{3}{16}$ -in.-OD Swaged-Sheath (Loosely Packed Magnesium Oxide) Chromel-P, Alumel, After Drift Tests at 982°C. Etched with glyceria regia. 75X.



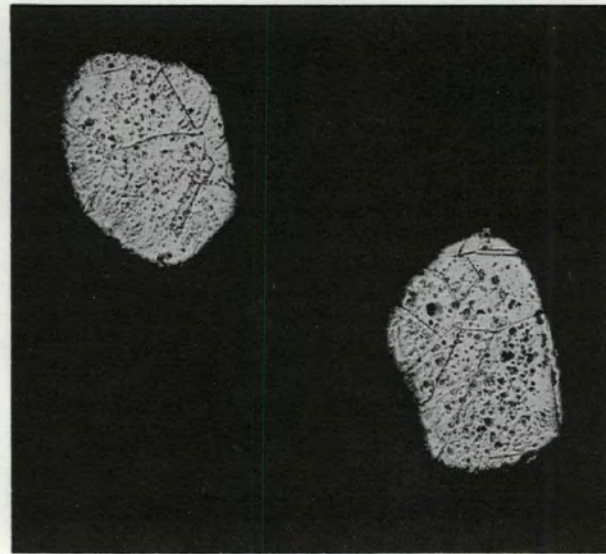
(a) CHROMEL-P,  $\frac{1}{8}$ -in.-OD SHEATH, AFTER 4000 hr. AT 982 °C, CYCLIC. TEST 5S ETCHED; 75 X



(b) ALUMEL TEST 5S



(c) CHROMEL-P,  $\frac{1}{16}$ -in.-OD SHEATH, AFTER 10,500 hr. AT 871 °C. TEST 4S. ETCHED WITH GLYCERIA REGIA. 75 X



(d) SAME AS FOR (c), EXCEPT FOR MAGNIFICATION. 150 X

Fig. 6.20. Photomicrographs of  $\frac{1}{8}$ - and  $\frac{1}{16}$ -in.-OD Swaged-Sheath Chromel-P, Alamel After Repeating Drift Tests at 982°C Cyclic and 871°C Constant Temperatures.

difference caused by length-to-diameter ratio of re-entry wells are: (1) A low partial pressure of oxygen causes chromium to be preferentially oxidized out of Chromel-P. (2) In a greatly restricted region, possibly enhanced by a suboxide of chromium with a high vapor pressure, chromium or iron is transported from the protection tube to Alumel. Either of these explanations is consistent with a negative drift. These phenomena are further tested in the special tube drift section and are the subject of continued work at ORNL by G. W. Keilholtz and W. Rainey. In the tests using titanium, one thermocouple of a duplex assembly was replaced by two titanium wires, 0.010 in. in diameter. The presence of the titanium did impede the negative drift rate but produced no lasting effect, probably because of the continuous source of oxygen from the open cold end of the thermocouple well. This point is borne out by the quite similar results with and without titanium (Figs. 6.13b and 6.13c) in the furnace subjected to cyclic temperature variation. An anomalous result is indicated by test 8T, Fig. 6.12f, wherein the drift of the average of the thermocouples was positive and two of the thermocouples drifted negative. This can only serve to confuse an otherwise consistent observation. No explanation was found for this. In these tests with beaded insulators one is cautioned against concluding that the asymptotic approach to a stable calibration suggests long preaging for stable performance. In all the above tests, the asymptotic approach is accompanied by complete oxidation of Alumel.

A comparison of both Kanthal-P/N<sup>6</sup> and Geminol-P/N<sup>6</sup> with Chromel-Alumel in this series of tests indicates their marked advantage from the point of view of both drift and fewer failures (indication of better mechanical strength). Figures 6.14a and 6.14b illustrate the lack of oxygen attack at 1600°F on Kanthal-P/N, and Fig. 6.11e bears this out by indicating only a +2°C drift in 10,000 hr. Some attack on Kanthal-P and fairly serious attack on Kanthal-N (Figs. 6.14c and 6.14d) are indicated at 1800°F after 11,000 hr. This is accompanied by a +18°C drift, as shown in Fig. 6.12g. Kanthal-P is virtually the same alloy as Chromel-P, and

behaves similarly. Kanthal-N is a decided improvement over Alumel. The only distinction between the tests on Kanthal-P/N and the above-discussed tests on Chromel-P, Alumel is that the former was 22-gage wire and the latter was 20-gage wire. The Kanthal-P/N did show serious drift and failure after 8000 hr in the 1800°F cyclic test (Fig. 6.13d), whereas Chromel-Alumel indicated complete failure after 3500 hr. The Geminol-P/N thermocouples were in 3-ft-long wells for the tests shown in Figs. 6.11f and 6.12b, with the respective photomicrographs shown in Fig. 6.15 for 1600 and 1800°F tests. These tests indicate a superior performance of the high-chromium positive leg and the nickel-silicon negative leg in the much more adverse (long-tube) environment. The essential difference between Geminol-N and Kanthal-N is that the former contains 2.75 wt % silicon, the latter 2.4 wt % silicon.

The 1/4-in.-OD swaged Inconel sheath, densely packed MgO insulated thermocouple materials exhibited a marked improvement over the same materials with loose insulating beads. This is evidenced by reduced drift, less spread between samples of a particular test, and the photomicrographs taken after the tests. The 90% Pt-10% Rh, Pt thermocouples showed excellent performance at 1800°F, as may be seen in Fig. 6.12i. The change noted in the first 400 hr was caused by human errors in reference-junction connections. At the time of this work, on the strength of quite preliminary and inconclusive tests elsewhere, swaged-sheath Chromel-Alumel materials were obtained with two different aging treatments at 1350°F after fabrication and prior to use, for periods of 24 and 200 hr, respectively. These tests have shown no difference in the performance of thermocouples with these two aging treatments. Any differences suggested by results presented here are only reflections of the limited number of samples in particular tests, which was verified by duplicate tests, the results of which are not generally shown. Figures 6.11g and 6.11b show the drift results on 1/4-in.-OD, swaged, 24-hr aged Chromel-Alumel thermocouples (two identical tests) at 1600°F. The average drift is similar in both cases, but the  $\overline{SER}$  (data spread) is ten times higher in test 3S than in test HS. It is noted that the Alumel in the sample from test 3S has been much more attacked than that in test HS; likewise the comparative freedom from attack of the Alumel

<sup>6</sup>For a comparison of the chemical analyses of these alloys, see D. L. McElroy, *Progress Report 1, Thermocouple Research, Report for Period Nov. 1, 1956, to Oct. 31, 1957, ORNL-2467, p 33-34.*

in test OS, Fig. 6.17*b*, at 1800°F constant is apparent. This is recognized as a promise of performance attainable from this type of configuration but is not representative of the average performance obtained, as demonstrated by the data spread and drift shown in Fig. 6.12*j*. This again illustrated the danger of drawing conclusions from tests with few samples and from photomicrographic examination of only one sample from the test. Figure 6.17*d* suggests the acceleration of oxidation failure at 1800°F with cyclic temperature variations when compared to static tests.

To test the possible advantage of including a titanium getter in swaged-sheath, MgO-insulated Chromel-Alumel thermocouples, as suggested by the work of Spooner and Thomas,<sup>5</sup> the authors had specially fabricated assemblies made under identical conditions wherein half the material was made with duplex 22-gage bright-finish Chromel-Alumel and half was made with one of the thermocouples replaced by two 22-gage titanium wires. A low pack density of MgO was used in these samples. Drift tests were performed on these materials at 1600 and 1800°F. Again, the statistics are not good because of the limited number of samples in each test. The drift tests (Figs. 6.11*j*, 6.11*k*, 6.12*l*, and 6.12*m*), because of the poor statistics, did not establish anything conclusive. The photomicrographs indicated that at 1600°F the Chromel was attacked more, and the Alumel less, in the assemblies with titanium. At 1800°F there was virtually no oxidation of the Chromel in either situation, but a slight amount of Alumel remained unoxidized in the sample with titanium, whereas Alumel was completely oxidized in the sample containing no titanium. These tests at 1600°F are the first here discussed where Chromel underwent serious attack at 1600°F. The environment of low-density MgO suggests the point made by Spooner,<sup>5</sup> that in a low partial pressure of oxygen, Chromel-P has chromium preferentially oxidized out, with a high rate of complete oxidation of the alloy. This result also suggests that the effect is greater at intermediate temperatures than at high temperatures. We verified this by examining a sample of Chromel-P from the 1800°F test (tests MS and 7T) where the hot-junction region was not oxidized. We found that in the region of the wire which was in the temperature gradient, a short length was heavily attacked, as evidenced by a dense scale and the fact that the wire surrounded by the scale was quite ferromagnetic only in this

region. A sample from one of the  $\frac{1}{4}$ -in.-OD dense pack samples (test OS) was similarly examined. The Chromel was slightly attacked and very slightly magnetic within the region which had been in the temperature gradient.

Samples of  $\frac{1}{8}$ -in.-OD, swaged-sheath, loosely packed MgO were tested at 1600 and 1800°F constant and at 1800°F cyclic. These tests (Figs. 6.11*l*, 6.11*m*, 6.12*n*, 6.13*b*, and 6.13*i*) showed a negative drift, somewhat similar to that exhibited by thermocouples with insulator beads in long re-entry wells. The attack on the Chromel-P, as shown in Fig. 6.20*a*, suggests that the oxygen conditions were here also favorable for preferential oxidation of chromium.

The results of test 4S, Fig. 6.11*n* and photomicrographs of Figs. 6.20*c* and 6.20*d*, suggest that the  $\frac{1}{16}$ -in.-OD, swaged-sheath Chromel-P, Alumel performed quite well, with a +5°C (+9°F) drift at 1600°F for 10,000 hr. There is no evidence of serious oxidation at the hot-junction end, as evidenced by Fig. 6.20*d*. It is believed that the very dense pack of the MgO insulation, as evidenced by the deformation of the wires, accounts for this favorable performance.

#### THERMOCOUPLE DRIFT TEST AT 900°C IN PRESSURIZED OXYGEN

The change in thermal emf of 20- and 30-gage wires of Kanthal-P and -N, Geminol-P and -N, Chromel-P + Nb, and Alumel, all relative to platinum, was measured for 772 hr at 900°C. A common 16-wire hot junction in a  $\frac{3}{4}$ -in.-ID sealed Alundum tube containing oxygen at a pressure of 30 psi was inserted into a Globar furnace. Measurements of emf were made relative to platinum as a function of time at temperature. The 30-gage wires of Chromel-P + Nb, Alumel, and Kanthal-P and -N all failed in less than 700 hr. There were no failures of the 20-gage wires. Table 6.6 summarizes the thermocouple behavior of the individual wires and their respective combinations during the tests.

Chromel-P + Nb, Alumel, Kanthal-P, and Kanthal-N all showed positive drifts of between +4 and +30°C. The positive drifts of all the above individual elements led to net thermocouple drifts of +5 to 35°C in 772 hr at 900°C. The Geminol-P drifted positive about 20°C in the first 624 hr and then negative about 15°C in the final 148 hr. Geminol-N showed just the opposite behavior, that is, a drift of -15°C in the first

Table 6.6. Thermocouple Behavior in Pressurized Oxygen System

Material	Drift Behavior
Chromel-P + Nb vs Alumel (20 gage)	+9.4°C in 772 hr
Chromel-P + Nb vs Alumel (30 gage)	+6.5°C in 150 hr and then failure
Chromel-P + Nb (20 gage) vs platinum	+8.8°C in 772 hr
Chromel-P + Nb (30 gage) vs platinum	+5°C in 150 hr and then failure
Alumel (20 gage) vs platinum	+4.4°C in 288 hr, then started drifting at a greater rate; total drift of +25°C in 772 hr
Alumel (30 gage) vs platinum	+14°C in 288 hr with total drift of +26.7°C in 624 hr; failed at 772 hr
Kanthal-P/N (20 gage)	+5.6°C in 772 hr
Kanthal-P (30 gage) vs Kanthal-N (20 gage)	Failed at 50 hr
Kanthal-P (20 gage) vs platinum	+9°C in 972 hr
Kanthal-N (20 gage) vs platinum	+5.2°C in 772 hr
Kanthal-P (30 gage) vs platinum	Failed at 50 hr
Geminol-P/N (20 gage)	+2°C in 772 hr
Geminol-P/N (30 gage)	+6°C in 772 hr
Geminol-P (20 gage) vs platinum	+19.7°C in 624 hr and then a drift of -16.1°C between 624 and 772 hr
Geminol-N (20 gage) vs platinum	-19.3°C in 624 hr, then a drift of +21.1°C between 624 and 772 hr
Geminol-P (30 gage) vs platinum	+20.8°C in 624 hr, then -12°C between 624 and 772 hr
Geminol-N (30 gage) vs platinum	-20.4°C in 624 hr, then a drift of +22.3°C between 624 and 772 hr

624 hr and a drift of +22°C between 624 and 772 hr. The individual drifts compensated almost exactly and resulted in a small drift of the combination Geminol-P/N. This agreed with results previously reported in Fig. 4.16 for Geminol-P.

The above data indicated that (1) a pressurized oxygen atmosphere produced drift greater than that produced in air, and that (2) oxidation was a controlling factor in thermocouple failure, especially on small wire sizes.

**NICKEL-SILICON ALLOYS - THERMOELECTRIC STABILITY IN AIR AT 980°C**

The emf relative to platinum of one assembly of 18-gage and one of 20-gage wires of nickel and five nickel-silicon alloys was measured as a function of time at 980°C. The results are shown

in Fig. 6.21. All data were plotted with reference to the first thermal-emf data point and were corrected for furnace temperature fluctuations by use of the calibration data of Appendix E. This test involved only two samples of each alloy; therefore only limited conclusions can be made. Table 6.7 summarizes the drift data.

Pure nickel showed practically no drift. The 1% silicon alloy exhibited the most serious positive drift, and these data points had the most scatter. The 2 and 3% silicon alloys behaved quite similarly and had about the same drift as pure nickel. The 4 and 5% alloys drifted first slightly negative and then slowly positive. The calibration drift placed the various nickel-silicon alloys in the same relative position as the oxidation and calibration data did. The results for pure

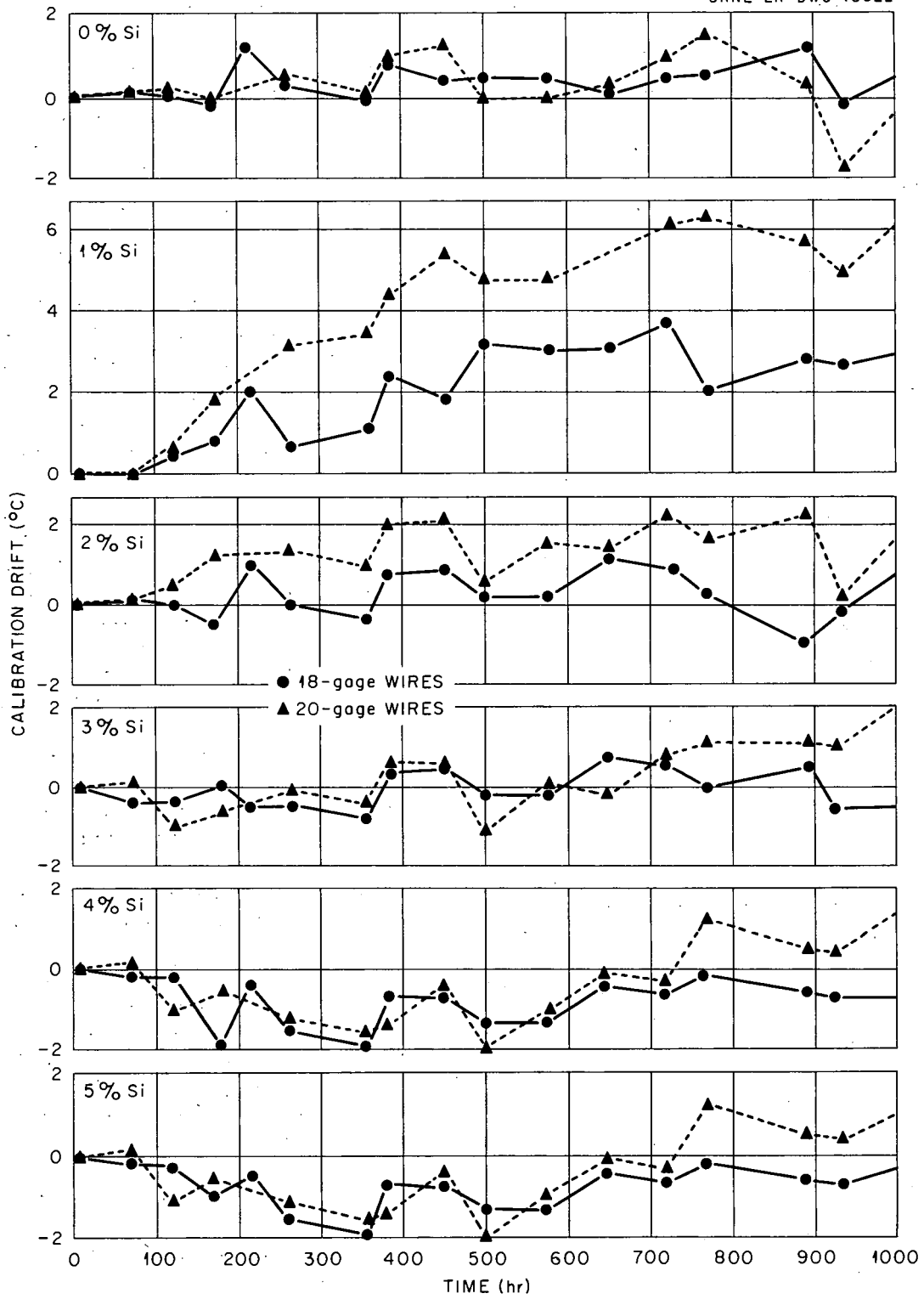


Fig. 6.21. Calibration Drift for Nickel and Five Ni-Si Alloys Relative to Platinum at 980°C.

Table 6.7. Summary of Drift Data for Nickel-Silicon Alloys

Material	Observed Error (°C) in Air at 980°C		
	500 hr	1000 hr	1500 hr
Nickel			
18 gage	+ $\frac{1}{2}$	+1	+1
20 gage	+ $\frac{1}{2}$	+1	+1
1% silicon alloy			
18 gage	+3	+3	+5
20 gage	+5	+6	+9
2% silicon alloy			
18 gage	+ $\frac{1}{2}$	+ $\frac{1}{2}$	+1
20 gage	+1	+2	+2
3% silicon alloy			
18 gage	0	0	+1
20 gage	0	+ $\frac{1}{2}$	+1
4% silicon alloy			
18 gage	- $\frac{1}{2}$	- $\frac{1}{2}$	- $\frac{1}{2}$
20 gage	- $\frac{1}{2}$	+1	+2
5% silicon alloy			
18 gage	- $\frac{1}{2}$	- $\frac{1}{2}$	+1
20 gage	- $\frac{1}{2}$	+1	+2

nickel indicated that it could be used satisfactorily as a thermoelement in an oxidizing atmosphere, except for mechanical considerations. According to Berry and Martin,<sup>7</sup> "Very pure nickel and silver were found to be quite stable at 780°C in air. Thermocouples made from these materials were reasonably stable, but some difficulty which results in eventual mechanical failure is not yet understood."

The positive drift of the 1% silicon alloy could be interpreted as due to oxidation and consequent loss of silicon, resulting in a larger negative thermal emf (a positive drift) as the composition

<sup>7</sup>J. M. Berry and D. L. Martin, *Thermoelectric Stability of Thermocouple Materials at Elevated Temperatures*, General Electric Co. Research Laboratory Report No. 55-RL-1234 (March 1955).

approached pure nickel. The minimum drifts observed in the 2 through 5% alloys were most probably due to their superior oxidation resistance and the low slope of the emf-composition curves (see Appendix E). The 3% silicon alloy appeared to be the optimum composition in this series of alloys because of good oxidation resistance, minimum change in calibration with composition, and calibration linearity. The drift observations are substantiated by microscopic examination of the materials, in essential agreement with the photomicrographs shown in Figs. 4.14a-4.14f.

#### DRIFT AT 1000°C OF NICKEL-BASE THERMOELEMENTS IN REFRACTORY PROTECTION TUBES CONTAINING SPECIAL ENVIRONMENTS

Spencer and Thomas<sup>8</sup> have investigated the effect of long, narrow metallic protection tubes on the errors generated in Chromel-Alumel thermocouples. Their tests at 1600°F and higher for 24 hr revealed that the length-to-diameter (L/D) ratio of the tube, the supply of oxygen to the thermocouple, and the presence of titanium near the thermocouple could influence the thermal emf of Chromel-P, Alumel thermocouples, with the general result that errors increased with increasing temperature. The above phenomena should be separated into two broad categories: (1) protection-tube test configuration and (2) environmental conditions caused by protection tube material, sealing methods, and metallic additions. In the present experiment, we have endeavored to investigate this separation of effects. Figure 6.22 is a schematic drawing of the various thermocouple positions and how environmental changes were introduced.

These drift tests were conducted in tube furnaces without the aid of a thermal inertia block and without sophisticated temperature control. As a result, rather large ( $\pm 30^\circ\text{C}$ ) temperature variations existed during the experiments. However, corrections were made for this variation in calculating the thermocouple error by using a standard 90% Pt-10% Rh, Pt thermocouple to monitor the furnace temperature. In any event, it was believed that observed drifts greater than  $\pm 5^\circ\text{C}$  were real. (This  $\pm 5^\circ\text{C}$  was the degree of randomness in some tests interpreted to have zero drift.)

<sup>8</sup>N. F. Spencer and J. M. Thomas, *Metal Progr.* 68, 81 (1955).

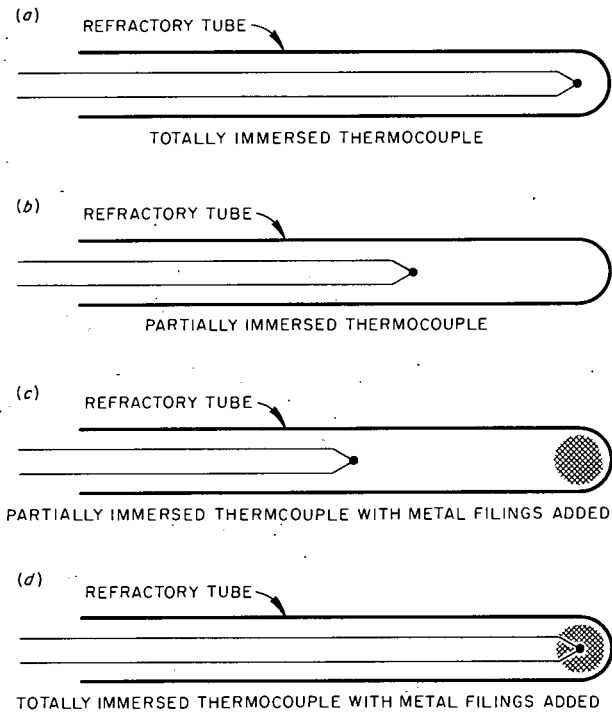


Fig. 6.22. Schematic Representation of the Drift Test Configurations Used To Study the Effects of Changes in Environment.

### Test Configuration

The effect of test configuration, or L/D ratio, in inert Alundum tubes on various types of thermocouples is shown in Fig. 6.23. The thermocouple materials were chosen for these tests as representing available alloy variations which might lead to an explanation of the mechanisms for drift rather than to vindicate any particular combination. This test indicated that the L/D ratio was not related to calibration shift if Alundum protection tubes were used. At 1000°C and for 600 hr these thermocouples drifted positive by 25°C at a fairly uniform rate. Generally, the drift appeared to be small for Geminol-P/N, larger for Kanthal-P/N, and largest for Chromel-P, Alumel.

Further verification of the configuration effect was determined by conducting the following tests, using Geminol-P/N, Kanthal-P/N, and Chromel-P/Alumel.

1. Alundum tube,  $\frac{1}{4}$  in. ID, 36 in. long, with a 24-in. thermocouple immersion (Fig. 6.22b).

2. Alundum tube,  $\frac{1}{4}$  in. ID, 36 in. long, with 36-in. thermocouple immersion (Fig. 6.22a).
3. Alundum tube,  $\frac{1}{4}$  in. ID, 36 in. long, with 24-in. thermocouple immersion, both ends of tube open.
4. Quartz tubes, 8 mm ID, 36 in. long, with 24-in. immersion (Fig. 6.22b).
5. Quartz tubes, 4 mm ID, 36 in. long, with 24-in. immersion (Fig. 6.22b).
6. Quartz tubes, 8 mm ID, 36 in. long, with 36-in. immersion (Fig. 6.22a).
7. Quartz tubes, 8 mm ID, 36 in. long, with 24-in. immersion, both ends of tube open.

All the tubes except 3 and 7 were closed on one end. In all the tests covered in this section, No. 20 B & S gage wires and  $\frac{7}{32}$ -in.-OD  $\times$  0.075-in.-hole  $\times$  30-in.-length refractory porcelain tubes were used.

The results of these tests are shown in Fig. 6.24 for Geminol-P/N. The results for Kanthal-P/N and Chromel-P, Alumel were not included, but were similar to those for Geminol-P/N. The curves of Fig. 6.24 indicate that, within  $\pm 5^\circ\text{C}$ , no difference in performance could be detected for the various changes of inert material and of test configuration. These results show less net drift with time at temperature than those shown in Fig. 6.23, but it is important to note that the drift was essentially zero or positive in all the above cases. There was no large negative drift, as would be associated with *preferential* oxidation.

### Environmental Changes

The environment of the hot junction was altered by using metal filings of Inconel, type 304 stainless steel, cast iron, titanium, and a mixture of Inconel and titanium. The effects of removing the thermocouple junction from the immediate vicinity of the filings (Fig. 6.22c) were observed. Comparative effects of Alundum and quartz tubes were also observed. The results of these observations follow.

**Inconel Filings.** - Since protection tubes are often constructed from Inconel, the effect of Inconel filings in the inert protection tubes was studied. The following tests were run on Geminol-P/N, Kanthal-P/N, and Chromel-P, Alumel:

1. 36 in. tube with 24 in. immersion containing Inconel filings at end (Fig. 6.22c),
2. 36 in. tube with 36 in. immersion containing Inconel filings at end (Fig. 6.22d),

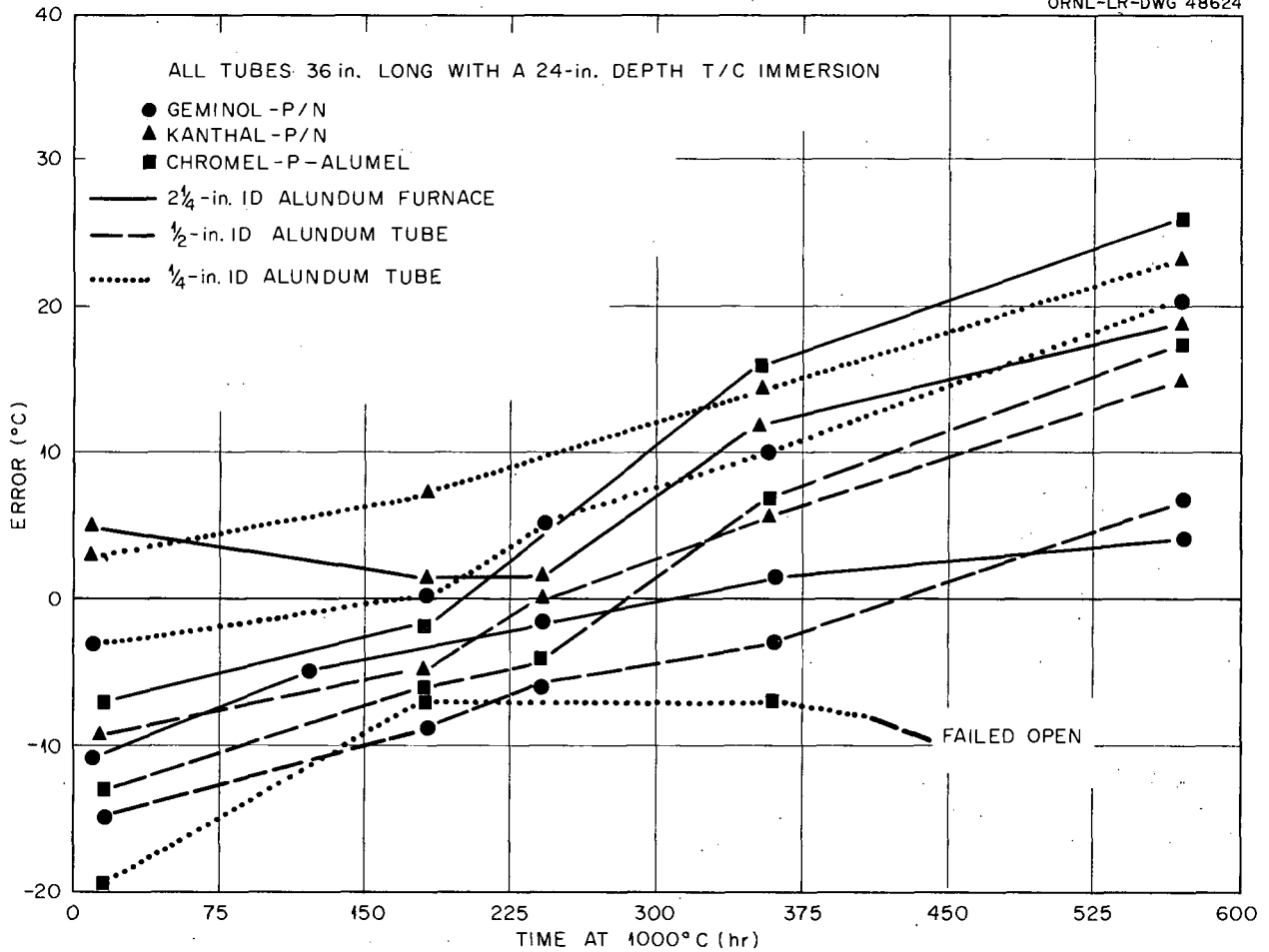


Fig. 6.23. Effect of Length-to-Diameter Ratio of Alundum Protection Tube on Drift of Various Thermocouple Materials in Air.

- 36 in. tube with 24 in. immersion containing Inconel filings at 30 in.,
- 36 in. tube with various immersion depths, with Inconel filings at end (Fig. 6.22c).

Figure 6.25 shows the results for Geminol-P/N for the first three conditions and shows that if the thermocouple was removed by as much as 6 in. from the filings there was no serious negative drift. However, if the thermocouple was in contact with or in the near vicinity of the filings, a large negative drift occurred. Within experimental error, the amount of drift for thermocouples that had the hot junction removed from the Inconel filings (test No. 1) did not vary with the tube material or test configuration.

Figures 6.26 and 6.27 show similar results for Kanthal-P/N and Chromel-P, Alumel. Repeat

tests on Kanthal-P/N further verified that a negative drift was occurring for the test No. 2 condition. For Kanthal-P/N, experiments with hot-junction distances of 0, 3, and 6 in. from the Inconel filings suggested that if there was a separation somewhat greater than 6 in. between thermocouple junction and filings, the drift would not be negative. The amount of drift at 3 in. separation was slightly less than that at contact, and that at 6 in. was less than at 3 in. This variation was associated with a changing environment as the separation between thermocouple junction and filings increased.

Results for the three thermocouples exposed to Inconel filings indicated that Kanthal-P/N and Chromel-P, Alumel had somewhat larger negative drifts than those for Geminol-P/N for conditions

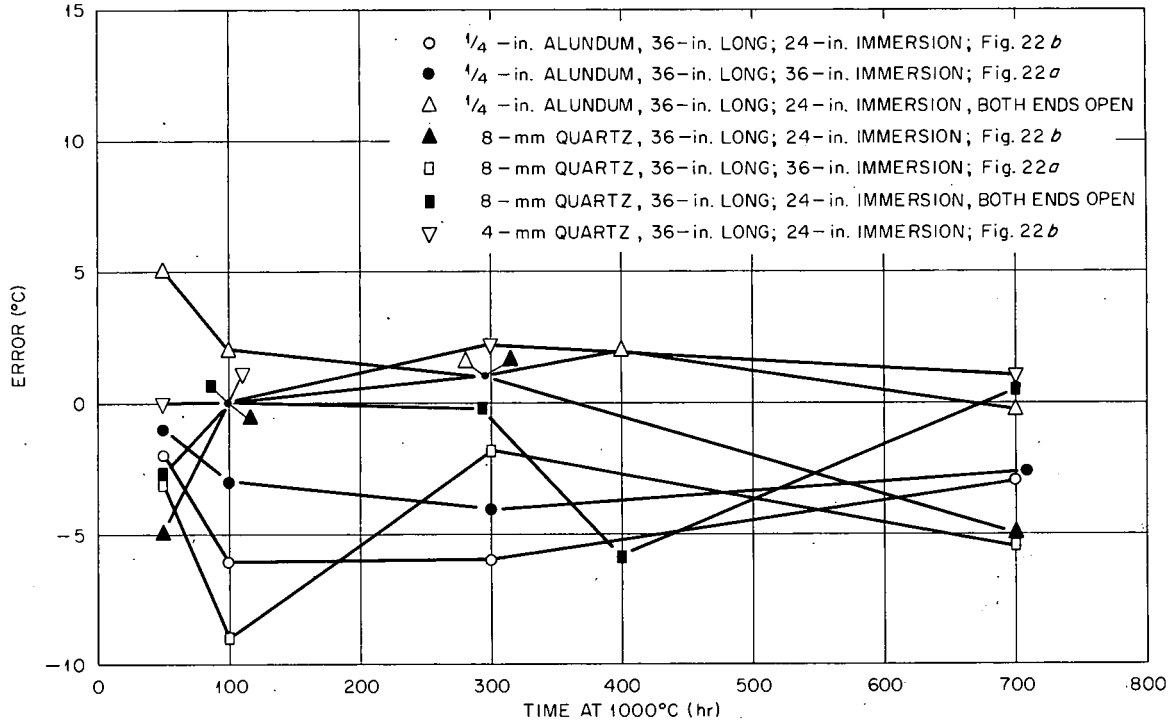


Fig. 6.24. Verification of the Independence of Thermocouple Drift on Length-to-Diameter Ratio of Alundum and Quartz Protection Tubes. All tests in air.

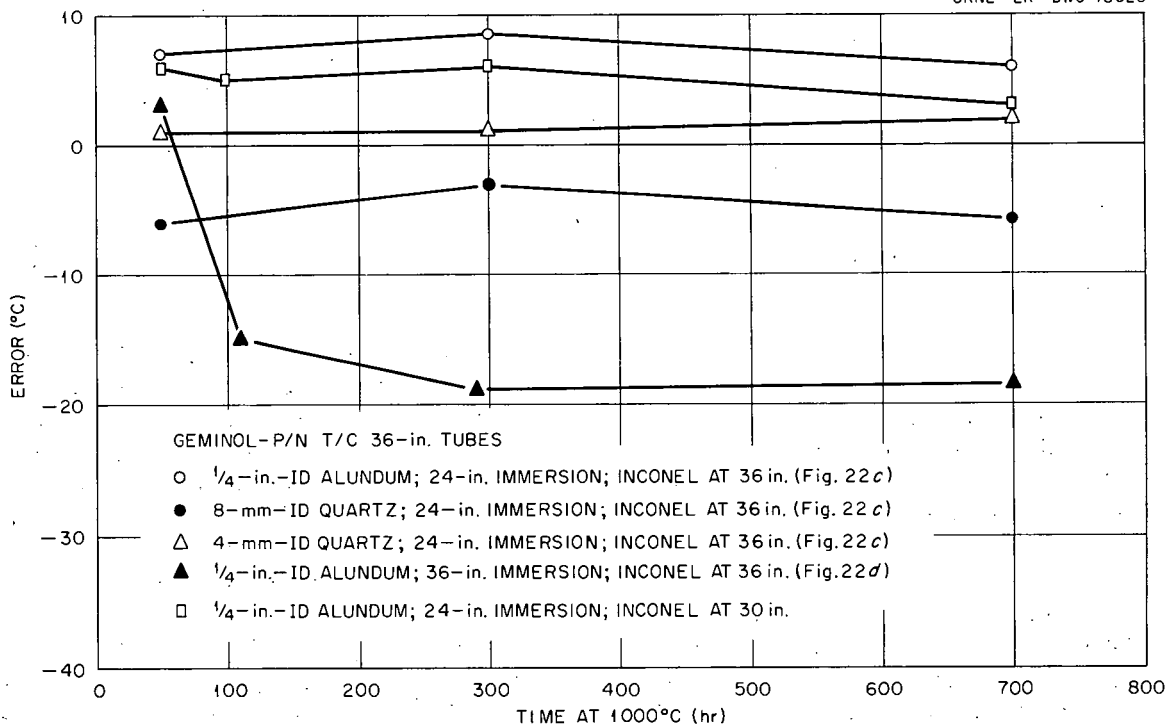


Fig. 6.25. Effect on Geminal-P/N of Separation Between Thermocouple Junction and Inconel Filings in Inert Protection Tubes.

- 1/4-in.-ID ALUNDUM; 24-in. IMMERSION; INCONEL AT 36 in. (Fig. 22 c)
- 8-mm-ID QUARTZ; 24-in. IMMERSION; INCONEL AT 36 in. (Fig. 22 c)
- △ 4-mm-ID QUARTZ; 24-in. IMMERSION; INCONEL AT 36 in. (Fig. 22 c)
- ▲ 1/4-in.-ID ALUNDUM; 36-in. IMMERSION; INCONEL AT 36 in. (Fig. 22 d)
- 1/4-in.-ID ALUNDUM; 24-in. IMMERSION; INCONEL AT 30 in.
- 1/4-in.-ID ALUNDUM; 36-in. IMMERSION; INCONEL AT 36 in.
- ▽ 1/4-in.-ID ALUNDUM; 33-in. IMMERSION; INCONEL AT 30 in.
- ▼ 1/4-in.-ID ALUNDUM; 30-in. IMMERSION; INCONEL AT 36 in.

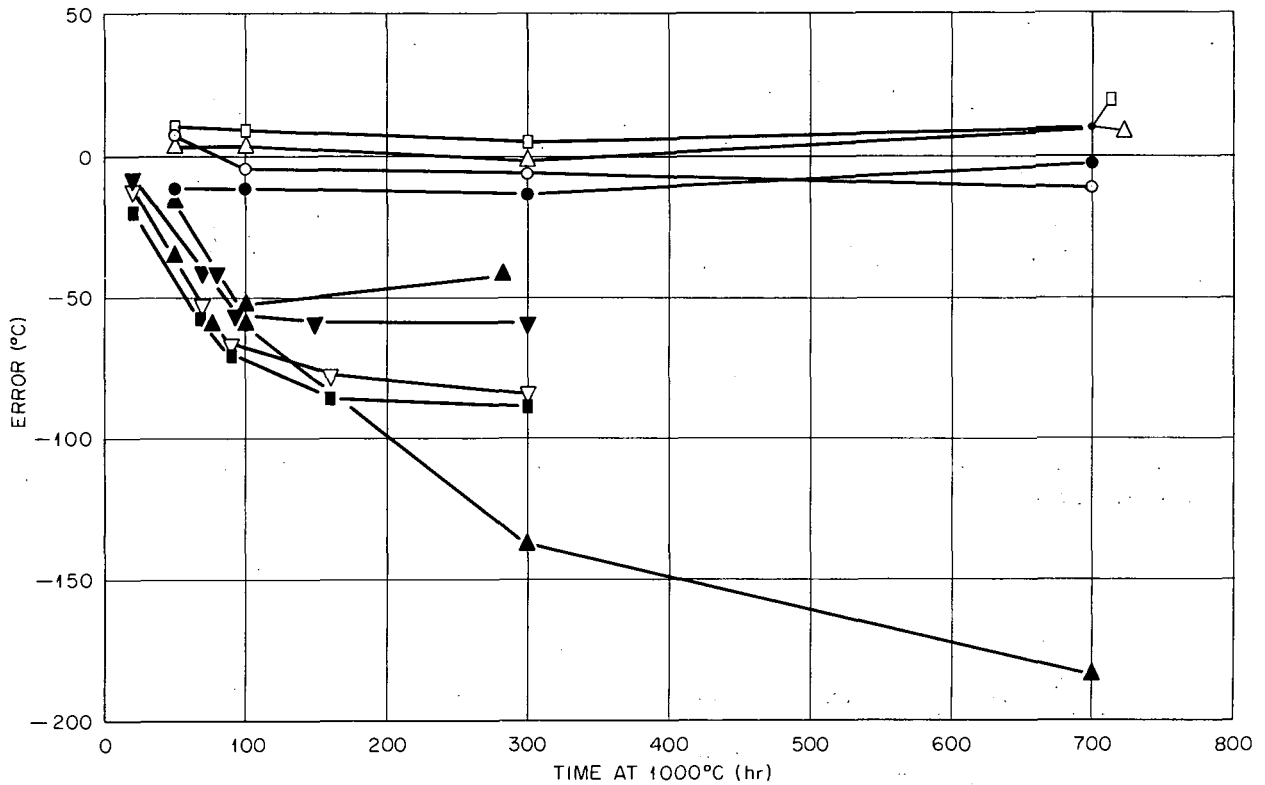


Fig. 6.26. Effect on Kanthal-P/N of Separation Between Thermocouple Junction and Inconel Filings in Inert Protection Tubes.

of test No. 2. A suggested explanation of these comparative results will be presented later.

**Stainless Steel Filings.** - Tests were run with stainless steel filings, similar to those in which Inconel filings were used. The results are shown in Fig. 6.28. Again, thermocouples with the 24-in. immersion in the different tubes showed no serious drifts in 700 hr at 1000°C. However, the thermocouples immersed 36 in. into stainless steel filings showed quite large negative deviations. In the test in which stainless steel filings were used, the shifts in Geminol-P/N, Chromel-P, Alumel, and Kanthal-P/N were approximately the same as when Inconel was used.

**Cast Iron Filing.** - Figure 6.29 shows the drifts observed for Geminol-P/N, Kanthal-P/N, and Chromel-P, Alumel thermocouples in 1/4-in.-ID Alundum tubes given a 36-in. immersion into cast iron filings. The Geminol-P/N showed very little drift, while Kanthal-P/N and Chromel-Alumel showed large negative drifts with cast iron, as was previously seen for Inconel and stainless steel filings.

**Titanium Filings.** - Figure 6.30 shows the results of using titanium filings, with immersions of 24 and 36 in. in Alundum and quartz tubes. The net drift was zero or slightly positive in most cases. No large negative drift was observed.

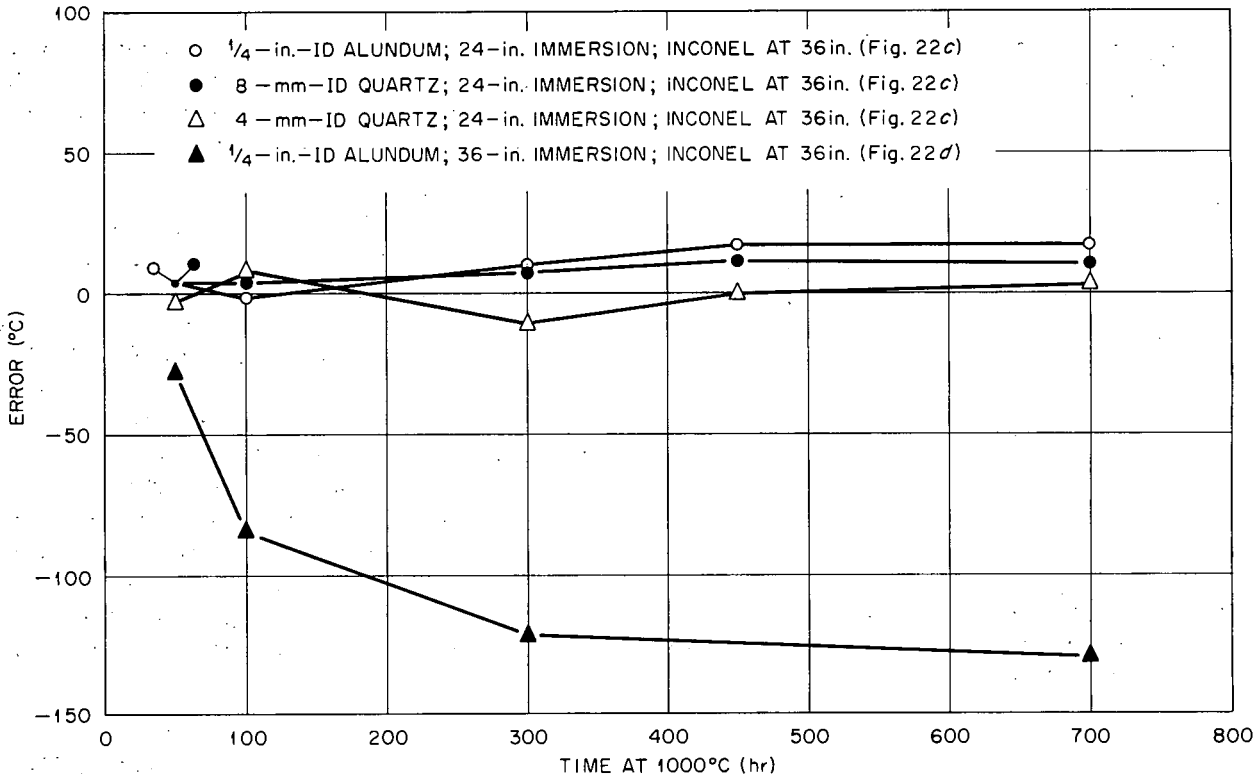


Fig. 6.27. Effect on Chromel-P, Alumel of Separation Between Thermocouple Junction and Inconel Filings in Inert Protection Tubes.

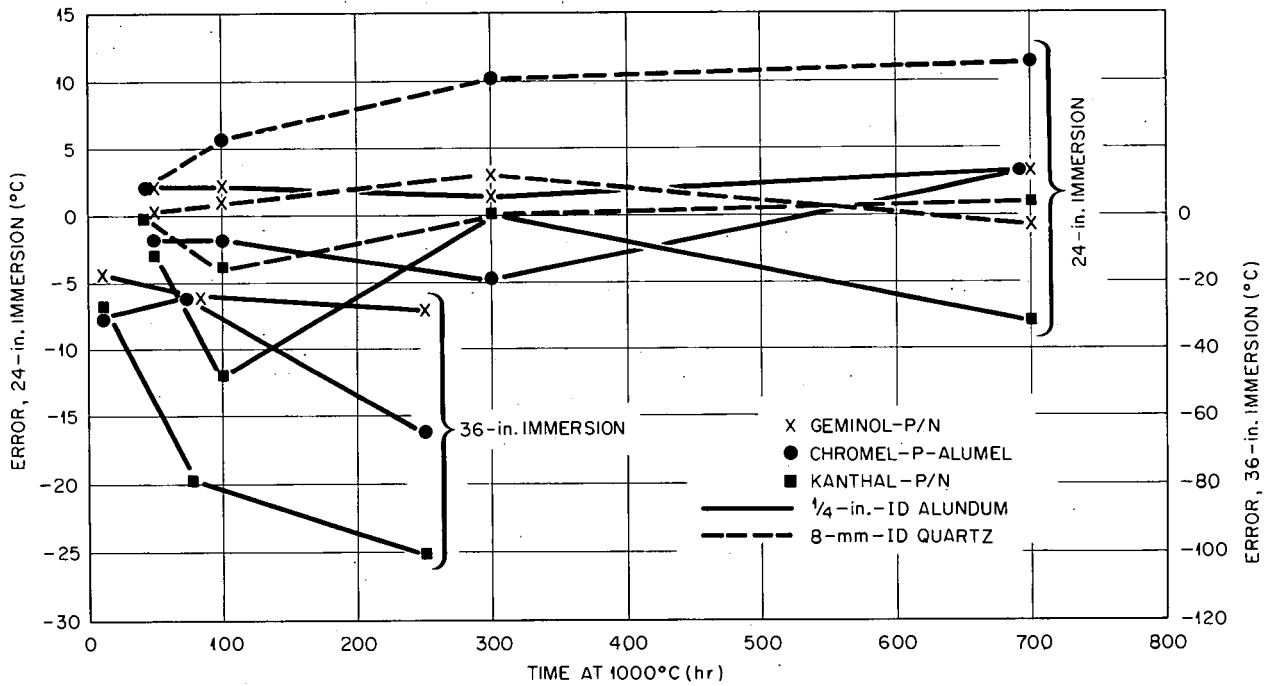


Fig. 6.28. Effect on Geminol-P/N, Kanthal-P/N, and Chromel-P, Alumel of Separation Between Thermocouple Junction and Stainless Steel Filings in Inert Protection Tubes.

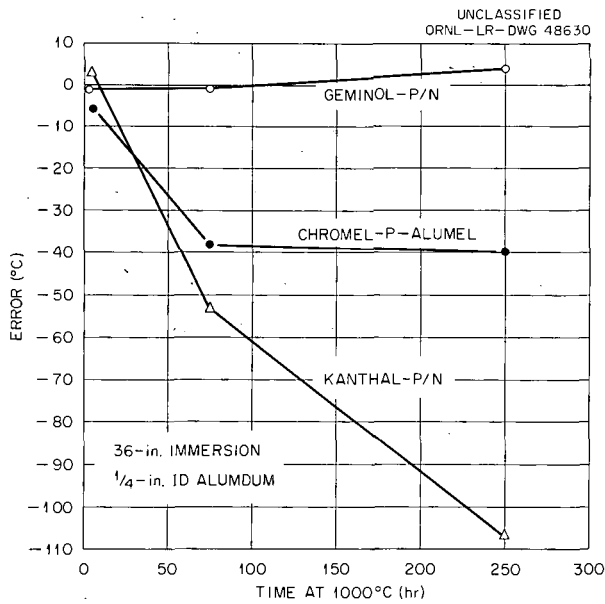


Fig. 6.29. Effect on Geminol-P/N, Kanthal-P/N, and Chromel-P, Alumel of Separation Between Thermocouple Junction and Cast-Iron Fillings in Inert Protection Tubes.

Thus, titanium seemed to exert some beneficial effect or had no effect on promoting negative drifts. By comparison with Fig. 6.24 it can be seen that the behavior was virtually the same with and without titanium filings.

**Titanium and Inconel.** - An experiment was run using a mixture of titanium and Inconel filings, with thermocouple immersed 36 in. in quartz and Alundum tubes. These results, shown in Fig. 6.31, revealed essentially no drift-(or slightly positive drifts), from which it was interpreted that titanium had a beneficial influence on the environment created by Inconel. These latter results are, as were most of the above, in essential agreement with those of Spooner and Thomas.<sup>8</sup> The important experimental difference was the elimination of a reactive protection tube, hence the removal of the L/D ratio effects caused by the tube material, rather than the configuration of the test. This left the effect of active additions only to be seen.

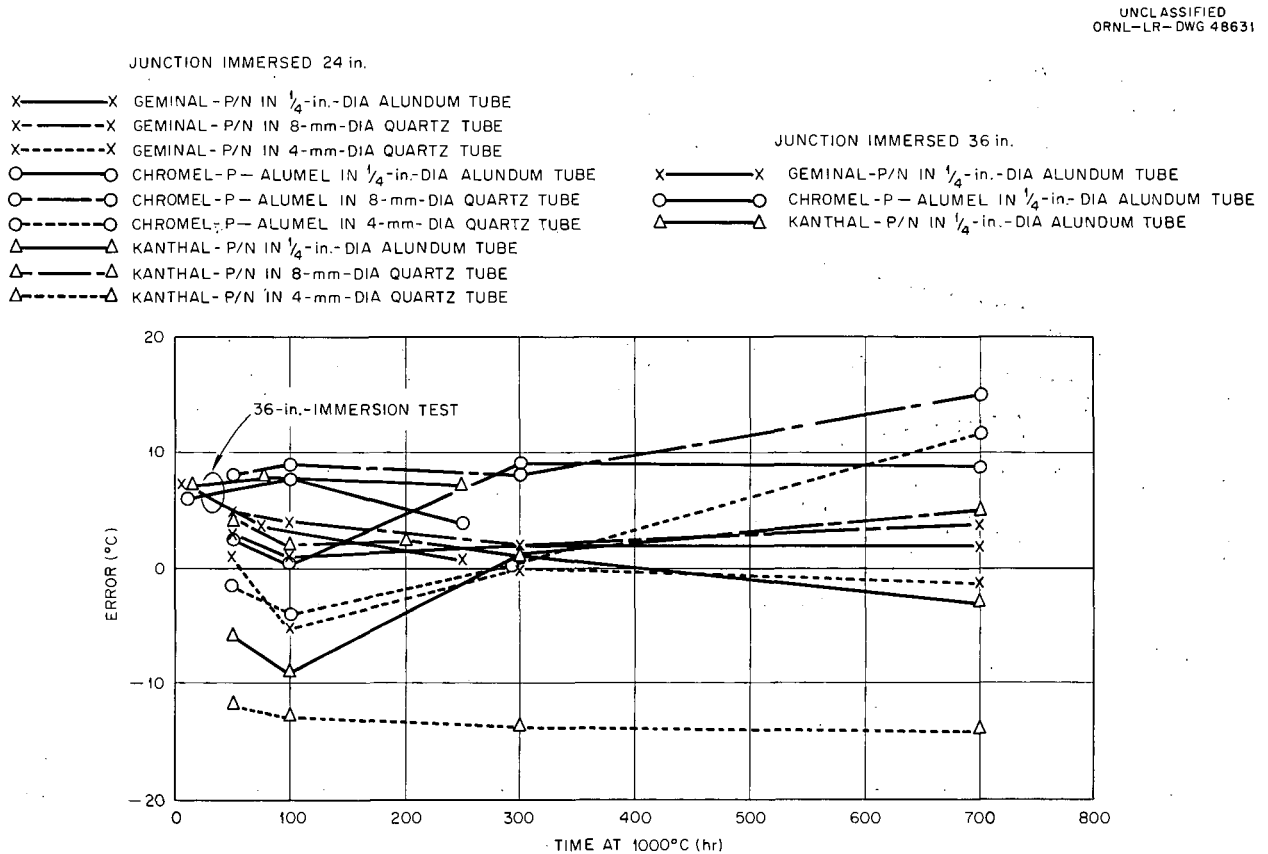


Fig. 6.30. Effect on Geminol-P/N, Kanthal-P/N, and Chromel-P, Alumel of Separation Between Thermocouple Junction and Titanium Filings in Inert Protection Tubes.

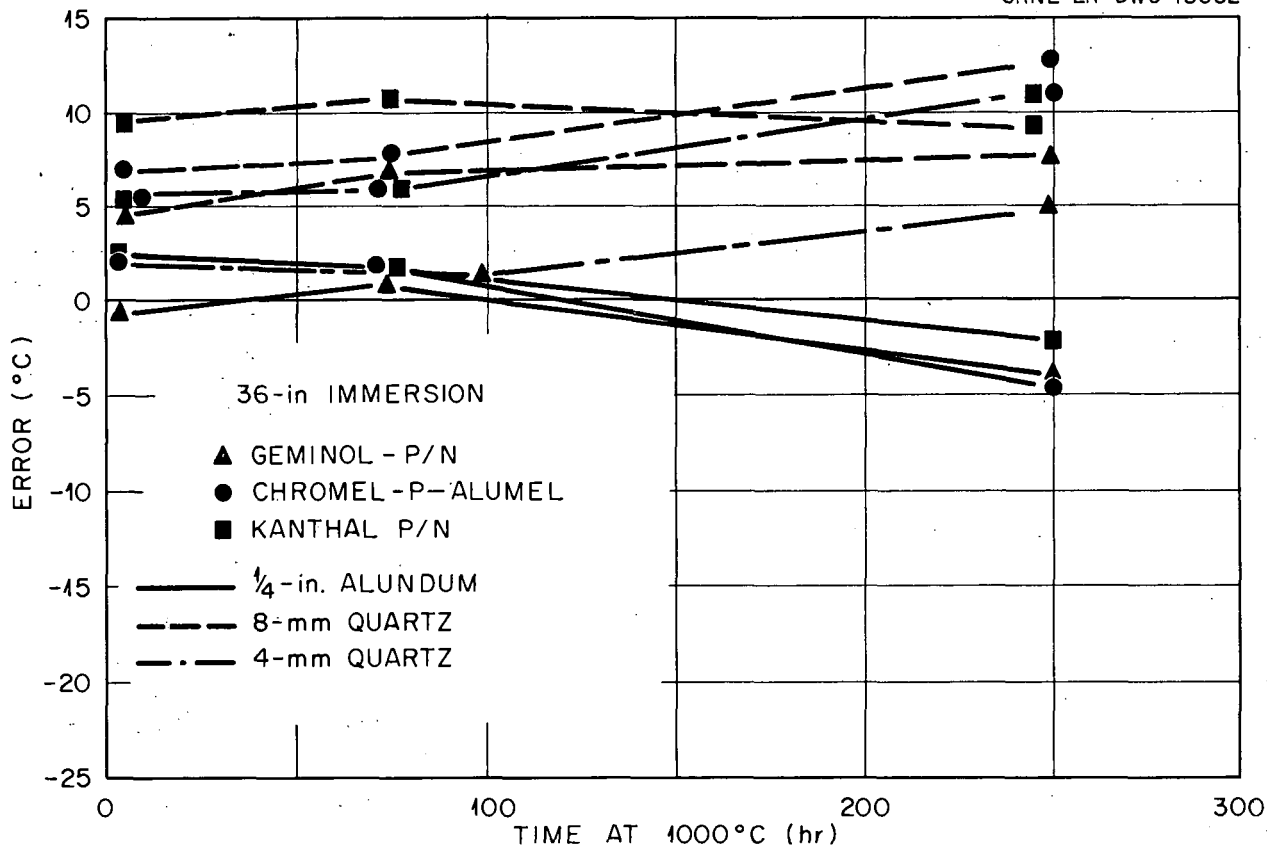


Fig. 6.31. Effect on Geminol-P/N, Kanthal-P/N, and Chromel-P, Alumel of Separation Between Thermocouple Junction and Mixture of Titanium and Inconel in Inert Protection Tubes.

#### Discussion of Results

Nickel-base alloy thermocouples in inert tubes of varying L/D ratios were seen to be essentially stable in calibration, or they drifted slightly positive. However, the cold end may have been sufficiently open to admit enough air to prevent the previously reported low partial pressure of oxygen. The phenomenon controlling drift in this case was possibly oxidation of the alloying constituents in the thermocouple materials. This hypothetical explanation is given in detail in a previous report.<sup>9</sup>

The effect of materials added into the refractory tubes was essentially one of producing isolated environmental changes. The measured thermocouple drift in this environment was related to the

proximity of the thermocouple to the active environment. If the thermocouple was removed from this environment, no drift was observed. If the thermocouple was in the immediate vicinity of the added material, then serious changes were observed. The causes for these changes are possibly related to (1) the difference in partial pressures between the constituents of the addition and the thermocouple becoming neutralized by exchange and to (2) the difference in affinities for oxygen or carbon between the thermocouple alloy and the added material. The first hypothesis seems more plausible from the viewpoint of element transfer and subsequent alloying with the thermocouple. An example should clarify this.

It is noted that Chromel-Alumel and Kanthal-P/N drift more than Geminol-P/N does. Geminol-P contains 18% chromium, whereas Kanthal-P and Chromel-P contains only 9.2 to 9.5%. If chromium is transferring from Inconel or stainless steel to

<sup>9</sup>D. L. McElroy, *Progress Report 1, Thermocouple Research, Report for Period Nov. 1, 1956, to Oct. 31, 1957*, ORNL-2467, p 67.

these thermocouple legs, then it seems logical to expect a larger effect in the low-chromium alloys than in the high-chromium alloys until equilibrium is established. A similar explanation can be made in the case of the cast iron addition, on the bases of both iron and carbon. Since chromium was adjusted to maximize the emf in Kanthal-P and Chromel but not in Geminol-P, then one would expect greater effects in the former materials. This indeed is the case. A similar argument can be made for chromium pickup by Alumel, which would lead to negative drifts of the combination. However, if the shift is due primarily to the changes in the negative leg, one would expect the changes in Geminol-P/N to be about the same as those in Kanthal-P/N. This is not the case; thus the argument for the positive leg. If the above arguments for drift hold, then one would expect similar results in a sealed system with an inert atmosphere. Small amounts of filings (4 to 5 g) were used in these experiments, and it was observed that reasonably complete oxidation of them had occurred at the completion of the test. This could account for the shape of the drift curves, since, once the active material was consumed, drift ceased. Or, the reaction rate was proportional to the amount of reactants present, leading to a logarithmic change of calibration.

#### SUPPLEMENTARY DRIFT EXPERIMENTS WITH REFRACTORY TUBES

After completion of the above-described drift tests, experimental evidence was reported by Hinkle<sup>10</sup> relating causes for Chromel-P, Alumel thermocouple drift in a helium-atmosphere furnace containing quartz fiber insulation as well as Inconel. In that work, their tests indicated shifts in calibration of the same magnitude as those we had observed due to Inconel. These shifts were attributed by Hinkle to the quartz fiber. Because of this, a final experiment was run using a helium atmosphere in 36-in.-long, 1/4-in.-ID prebaked Alundum tubes. The tube contents and the results of the tests after 25 hr at 1000°C are listed below.

Tube	Contents	Results at 1000°C for 25 hr
A	Thermocouple alone	Slight positive drift
B	Inconel, 5 g	Negative drift of 8°C
C	Fine quartz fibers	Slight negative drift
D	Cut quartz tape	Negative drift of 22°C

The results for A and B were as expected from previous tests. The results for C and D were somewhat baffling, and consequently two supplementary tests were run using:

1. Alundum tubes 36 in. long, 1/4 in. ID, prebaked at 1000°C with a nitrogen purge;
2. 20 gage Alumel, bright, and 22 gage Chromel-P, bright;
3. refractory insulator, 7/32 in. OD, 30 in. long, two-hole (0.075-in. holes), broken at 1-in. increments for 12 in. from the hot junction.

The two tests were as follows:

Tube No.	Additive
<b>Test 1. Static Air Atmosphere</b>	
1	Clean Inconel filings
2	Preoxidized Inconel filings
3	Pure chromium powder
4	Empty (except for thermocouple)
5	Clean Inconel filings + titanium (30 gage wire, wadded)
6	Pure chromium + titanium (30 gage wire, wadded)
<b>Test 2. Static Helium Atmosphere</b>	
7	Clean Inconel filings
8	Empty (except for thermocouple)
9	Pure chromium powder
10	Preoxidized Inconel filings
11	Quartz tape, chopped up, as received
12	Quartz tape, chopped up, pre-fired in air at 1000°C

The results of tests 1 and 2 are shown in Fig. 6.32, for an exposure of 25 hr at 1040°C. In static air and helium the tube without additive produced a positive drift, as expected. Pre-oxidized Inconel produced a positive drift in air and essentially zero drift in helium, which is understandable. Fresh Inconel filings produced a drift of nearly -8°C in air and about -5°C in helium. Fresh chromium powder produced a drift of -80°C in air in 25 hr (not shown was a drift of -120°C in 45 hr) and a drift of only -5°C in helium. The addition of titanium to fresh Inconel in air produced a drift of +1°C. The addition of titanium to chromium powder produced a drift of -40°C in 25 hr, which is about half that with

<sup>10</sup>N. E. Hinkle, ORNL, private communication, Mar. 20, 1959.

STAGNANT AIR-TEST 1

1. CLEAN INCONEL FILINGS
2. PREOXIDIZED INCONEL FILINGS
3. PURE CHROMEL POWDER
4. EMPTY (EXCEPT FOR T/C)
5. CLEAN INCONEL FILINGS AND TITANIUM GAUZE
6. PURE CHROMIUM AND TITANIUM GAUZE

HELIUM-TEST 2

7. CLEAN INCONEL FILINGS
8. EMPTY (EXCEPT FOR T/C)
9. PURE CHROMEL POWDER
10. PREOXIDIZED INCONEL FILINGS
11. QUARTZ TAPE, AS RECEIVED
12. QUARTZ TAPE, PREFIRED IN AIR AT 1000°C

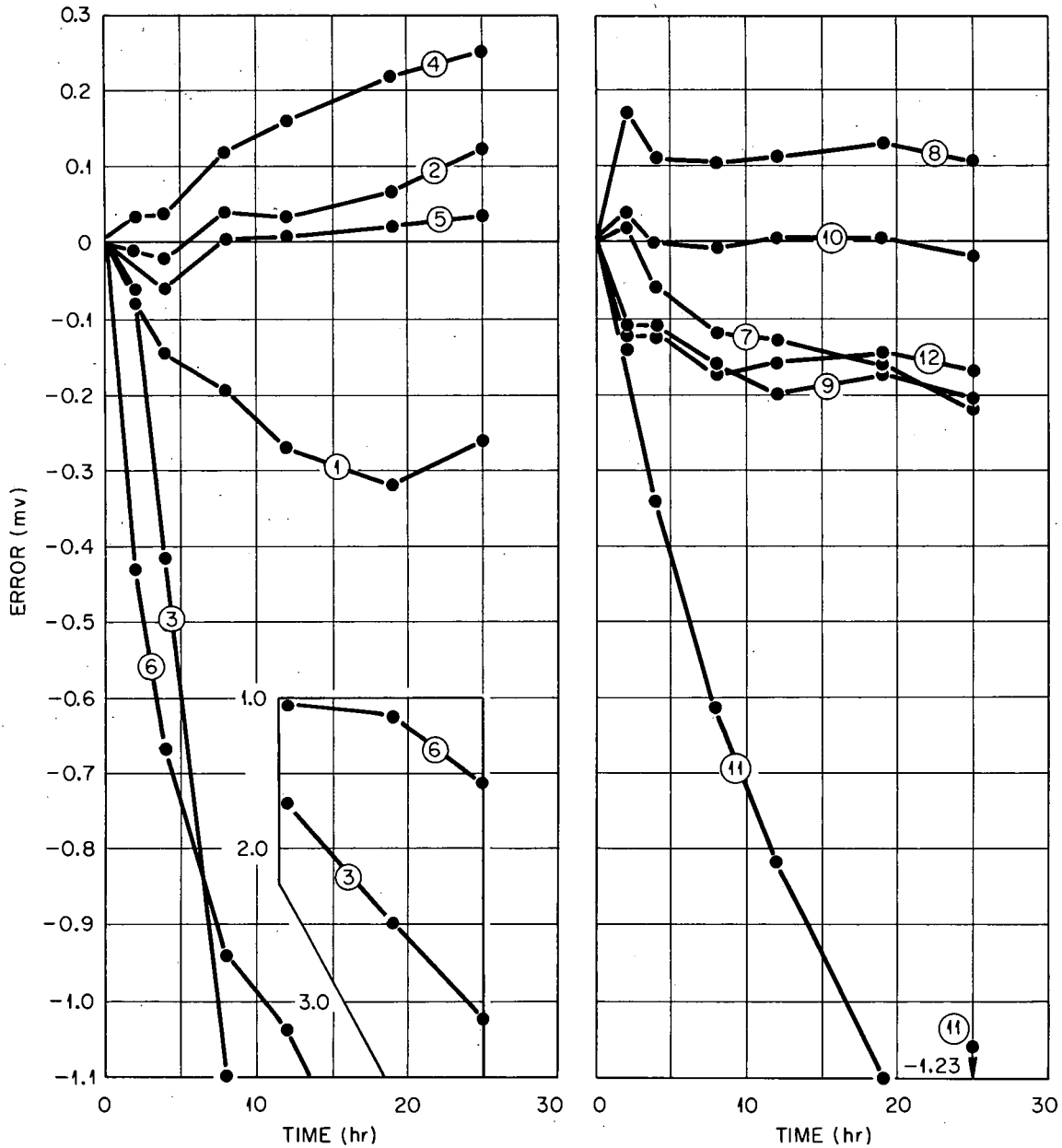


Fig. 6.32. Results of Supplementary Tests of the Effects of Various Additions to Inert Protection Tubes in Chromel-P, Alumel at 1040°C for 25 hr.

chromium but without titanium. These results may be interpreted in terms of the effects of available oxygen in the tubes in both air and helium, since the helium was not purified and contained some oxygen. It was observed that the drift with Inconel was more severe in air than in helium, so oxygen was certainly playing some role in the drift. Likewise air facilitated large drifts in the case of chromium but not so large a drift in the case of chromium in helium. This effectively rules out the transfer of chromium to the thermocouple from chromium or Inconel by the vapor transport of metallic chromium, since the vapor pressure of chromium would be the same in helium and in air. But if the transfer is by a vaporized suboxide of chromium, such as  $\text{CrO}$ ,  $\text{Cr}_2\text{O}$ , or  $\text{CrO}_2$ , then the presence of oxygen would be expected to promote chromium transfer to that portion of the thermocouple wires which was in a temperature gradient. This seemed to be the case. The action of titanium on reducing this transfer (and reducing the drift) was apparently related to the quantity of chromium present. For titanium plus Inconel of only about 15% Cr, the drift was zero, whereas with titanium plus chromium (100% Cr) the drift was reduced to only half that of pure chromium. So titanium can stop transfer for small quantities of chromium but cannot completely do this for larger quantities of chromium.

A negative drift of  $-35^\circ\text{C}$  was observed for unbaked quartz tape, whereas a drift of only  $-6^\circ\text{C}$  was found for baked quartz tape. Visual inspection of these systems after the test showed a large amount of clear liquid (looking like condensed water vapor) deposited on the cold end of the tube containing the unbaked quartz, but only a trace of this liquid for the baked quartz. This drift is apparently associated with a hygroscopic property of the unbaked quartz tape, which can produce a reducing atmosphere under the test conditions and lead to negative drifts. Complete drying was not achieved in the pre-fired sample of quartz since some negative drift and deposited liquid were observed.

None of the above results are contradictory to previously reported drift tests, even though the duration of these tests was significantly shorter. If the above-suggested mechanisms for mass transfer are correct, then they will have far-reaching consequences in the general field of oxidation protection in so-called purified atmospheres.

G. W. Keilholtz and W. T. Rainey of the ORNL Reactor Chemistry Division are continuing tests of the type described in this section. Some of their recent results suggest modifications of the above conclusions.

## Appendix A

### SMOOTHED CHROMEL-ALUMEL TABLES

At various times during this research the rounding-off of emf in NBS Circular 561, Table 6, for Chromel-Alumel thermocouples led to objectionable discontinuities in calculated temperature data involving interpolation. This NBS table is rounded off to within  $10 \mu\text{v}$  - good enough for most work with Chromel-Alumel - but we needed tables smooth to within  $0.5 \mu\text{v}$  for the combinations of Chromel-Alumel, Chromel-platinum, and Alumel-platinum.

Tables were accordingly obtained from the Hoskins Manufacturing Company wherein temperature was given in  $10^\circ\text{C}$  increments and emf to the nearest microvolt (Hoskins Tables E-271-BB, E-271-CC, and E-271-AA for Chromel-Alumel, Chromel-platinum, and Alumel-platinum, respectively). From these tables first differences of emf were calculated for each  $10^\circ\text{C}$  increment and plotted against temperature. For example, the increment  $E_{410^\circ\text{C}} - E_{400^\circ\text{C}}$  was plotted as  $\Delta E/\Delta T$  at  $405^\circ\text{C}$ , where  $E$  and  $\Delta E$  were in millivolts. This curve was smoothed visually to within  $\pm \frac{1}{4} \mu\text{v}$ . During the smoothing, some peculiar short-range irregularities in the original curves were removed and adjustments were made to fulfill the requirement that the sum of the first difference for Chromel-platinum and Alumel-platinum equal the first differences for Chromel-

Alumel. In addition, when the first-difference curve for Chromel-Alumel was integrated, the whole process was repeated until there was no difference greater than  $10 \mu\text{v}$  between the new curve of temperature vs millivolts and Table 6, NBS 561 - nor was a difference this large permitted to exist over an interval greater than  $50^\circ\text{C}$ .

It should not be construed that a revision of the NBS table is implicitly suggested by this work. Such a revision would require a considerable number of independent laboratory calibrations of thermocouples from a number of heats of metal, with wide agreement on the finished heat treatment (internal and surface conditions) of the alloys. Although this work has provided additional understanding of the thermoelectric properties of nickel-base alloys and established the improvement in thermocouple life of prefabricated swaged assemblies, there are still sufficient uncontrollable variables in the use of nickel-base alloys as thermocouple materials that their use as *standard* temperature measuring devices appears unlikely.

The smoothed data appear in Tables A.1, A.2, and A.3. Figure A.1 illustrates the extent of smoothing accomplished in these revised tables, by plotting the emf difference between the revised tables (Tables A.2 and A.3) and the respective Hoskins tables.

Table A.1. Calibrations for Chromel-P, Alumel Thermocouples\*

Electromotive force in absolute millivolts, temperature in degrees Celsius (Int. 1948), reference junction at 0°C  
(Numbers in italics are emf differences per 10°C increment)

°C	0	10	20	30	40	50	60	70	80	90	100
	Millivolts										
0	0	<i>(0.3950)</i> 0.3950	<i>(0.4000)</i> 0.7950	<i>(0.4040)</i> 1.1990	<i>(0.4080)</i> 1.6070	<i>(0.4110)</i> 2.0180	<i>(0.4140)</i> 2.4320	<i>(0.4160)</i> 2.8480	<i>(0.4170)</i> 3.2650	<i>(0.4175)</i> 3.6825	<i>(0.4170)</i> 4.0995
100	4.0995	<i>(0.4155)</i> 4.5150	<i>(0.4110)</i> 4.9260	<i>(0.4060)</i> 5.3320	<i>(0.4030)</i> 5.7350	<i>(0.4010)</i> 6.1360	<i>(0.3995)</i> 6.5355	<i>(0.3990)</i> 6.9345	<i>(0.3990)</i> 7.3335	<i>(0.3995)</i> 7.7330	<i>(0.4005)</i> 8.1335
200	8.1335	<i>(0.4015)</i> 8.5350	<i>(0.4030)</i> 8.9380	<i>(0.4045)</i> 9.3425	<i>(0.4060)</i> 9.7485	<i>(0.4075)</i> 10.1560	<i>(0.4090)</i> 10.5650	<i>(0.4100)</i> 10.9750	<i>(0.4110)</i> 11.3860	<i>(0.4125)</i> 11.7985	<i>(0.4135)</i> 12.2120
300	12.2120	<i>(0.4145)</i> 12.6265	<i>(0.4155)</i> 13.0420	<i>(0.4165)</i> 13.4585	<i>(0.4175)</i> 13.8760	<i>(0.4185)</i> 14.2945	<i>(0.4195)</i> 14.7140	<i>(0.4205)</i> 15.1345	<i>(0.4210)</i> 15.5555	<i>(0.4215)</i> 15.9770	<i>(0.4220)</i> 16.3990
400	16.3990	<i>(0.4225)</i> 16.8215	<i>(0.4230)</i> 17.2445	<i>(0.4235)</i> 17.6680	<i>(0.4240)</i> 18.0920	<i>(0.4245)</i> 18.5165	<i>(0.4250)</i> 18.9415	<i>(0.4255)</i> 19.3670	<i>(0.4260)</i> 19.7930	<i>(0.4265)</i> 20.2195	<i>(0.4265)</i> 20.6460
500	20.6460	<i>(0.4265)</i> 21.0725	<i>(0.4270)</i> 21.4995	<i>(0.4270)</i> 21.9265	<i>(0.4270)</i> 22.3535	<i>(0.4270)</i> 22.7805	<i>(0.4270)</i> 23.2075	<i>(0.4265)</i> 23.6340	<i>(0.4265)</i> 24.0605	<i>(0.4260)</i> 24.4865	<i>(0.4255)</i> 24.9120
600	24.9120	<i>(0.4255)</i> 25.3375	<i>(0.4250)</i> 25.7625	<i>(0.4245)</i> 26.1870	<i>(0.4240)</i> 26.6110	<i>(0.4235)</i> 27.0345	<i>(0.4230)</i> 27.4575	<i>(0.4225)</i> 27.8800	<i>(0.4220)</i> 28.3020	<i>(0.4215)</i> 28.7235	<i>(0.4210)</i> 29.1445
700	29.1445	<i>(0.4200)</i> 29.5645	<i>(0.4195)</i> 29.9840	<i>(0.4185)</i> 30.4025	<i>(0.4180)</i> 30.8205	<i>(0.4170)</i> 31.2375	<i>(0.4160)</i> 31.6535	<i>(0.4150)</i> 32.0685	<i>(0.4135)</i> 32.4820	<i>(0.4125)</i> 32.8945	<i>(0.4115)</i> 33.3060
800	33.3060	<i>(0.4105)</i> 33.7165	<i>(0.4095)</i> 34.1260	<i>(0.4085)</i> 34.5345	<i>(0.4075)</i> 34.9420	<i>(0.4065)</i> 35.3485	<i>(0.4055)</i> 35.7540	<i>(0.4045)</i> 36.1585	<i>(0.4030)</i> 36.5615	<i>(0.4020)</i> 36.9635	<i>(0.4010)</i> 37.3645
900	37.3645	<i>(0.4000)</i> 37.7645	<i>(0.3990)</i> 38.1635	<i>(0.3980)</i> 38.5615	<i>(0.3970)</i> 38.9585	<i>(0.3960)</i> 39.3545	<i>(0.3945)</i> 39.7490	<i>(0.3935)</i> 40.1425	<i>(0.3925)</i> 40.5350	<i>(0.3915)</i> 40.9265	<i>(0.3905)</i> 41.3170
1000	41.3170	<i>(0.3890)</i> 41.7060	<i>(0.3880)</i> 42.0940	<i>(0.3870)</i> 42.4810	<i>(0.3860)</i> 42.8670	<i>(0.3850)</i> 43.2520	<i>(0.3840)</i> 43.6360	<i>(0.3830)</i> 44.0190	<i>(0.3820)</i> 44.4010	<i>(0.3810)</i> 44.7820	<i>(0.3795)</i> 45.1615
1100	45.1615	<i>(0.3785)</i> 45.5400	<i>(0.3775)</i> 45.9175	<i>(0.3760)</i> 46.2935	<i>(0.3750)</i> 46.6685	<i>(0.3735)</i> 47.0420	<i>(0.3725)</i> 47.4145	<i>(0.3710)</i> 47.7855	<i>(0.3695)</i> 48.1550	<i>(0.3680)</i> 48.5230	<i>(0.3665)</i> 48.8895
1200	48.8895	<i>(0.3650)</i> 49.2545	<i>(0.3635)</i> 49.6180	<i>(0.3620)</i> 49.9800	<i>(0.3600)</i> 50.3400	<i>(0.3585)</i> 50.6985	<i>(0.3570)</i> 51.0555	<i>(0.3550)</i> 51.4105	<i>(0.3535)</i> 51.7640	<i>(0.3520)</i> 52.1160	<i>(0.3505)</i> 52.4665
1300	52.4665	<i>(0.3495)</i> 52.8160	<i>(0.3480)</i> 53.1640	<i>(0.3465)</i> 53.5105	<i>(0.3450)</i> 53.8555	<i>(0.3435)</i> 54.1990	<i>(0.3420)</i> 54.5410	<i>(0.3410)</i> 54.8820			

\*Based on NBS Circ. 561, Table 6 and Hoskins Mfg. Co. Table E-271-BB.

Table A.2. Calibrations for Chromel-P, Platinum Thermocouples\*

Electromotive force in absolute millivolts, temperature in degrees Celsius (Int. 1948), reference junction at 0°C  
(Numbers in italics are emf differences per 10°C increment)

°C	0	10	20	30	40	50	60	70	80	90	100
	Millivolts										
0	0	0.2590	0.5240	0.7940	1.0690	1.3490	1.6340	1.9230	2.2155	2.5115	2.8110
100	2.8110	3.1140	3.4200	3.7290	4.0410	4.3560	4.6740	4.9945	5.3175	5.6425	5.9695
200	5.9695	6.2985	6.6290	6.9615	7.2955	7.6310	7.9680	8.3060	8.6450	8.9850	9.3260
300	9.3260	9.6680	10.0105	10.3535	10.6970	11.0410	11.3855	11.7305	12.0755	12.4205	12.7655
400	12.7655	13.1105	13.4555	13.8005	14.1455	14.4905	14.8355	15.1805	15.5255	18.8705	16.2150
500	16.2150	16.5590	16.9025	17.2455	17.5875	17.9290	18.2695	18.6095	18.9485	19.2870	19.6245
600	19.6245	19.9615	20.2975	20.6330	20.9675	21.3015	21.6350	21.9675	22.2995	22.6305	22.9610
700	22.9610	23.2905	23.6195	23.9475	24.2750	24.6020	24.9280	25.2535	25.5780	25.9015	26.2240
800	26.2240	26.5455	26.8665	27.1870	27.5065	27.8255	28.1440	28.4620	28.7790	29.0955	29.4115
900	29.4115	29.7265	30.0410	30.3545	30.6675	30.9800	31.2915	31.6025	31.9130	32.2230	32.5320
1000	32.5320	32.8405	33.1485	33.4555	33.7620	34.0675	34.3720	34.6760	34.9790	35.2815	35.5830
1100	35.5830	35.8835	36.1835	36.4825	36.7805	37.0775	37.3735	37.6685	37.9625	38.2555	38.5475
1200	38.5475	38.8385	39.1285	39.4170	39.7045	39.9905	40.2755	40.5590	40.8410	41.1215	41.4005
1300	41.4005	41.6780	41.9540	42.2285	42.5015	42.7730	43.0430	43.3115			

\*Based on Hoskins Mfg. Co. Table E-271-CC.

**Table A.3. Calibrations for Alumel, Platinum Thermocouples\***

Electromotive force in absolute millivolts, temperature in degrees Celsius (Int. 1948), reference junction at 0°C  
(Numbers in italics are emf differences per 10°C increment)

°C	0	10	20	30	40	50	60	70	80	90	100
	Millivolts										
0	0	<i>(0.1360)</i> 0.1360	<i>(0.1350)</i> 0.2710	<i>(0.1340)</i> 0.4050	<i>(0.1330)</i> 0.5380	<i>(0.1310)</i> 0.6690	<i>(0.1290)</i> 0.7980	<i>(0.1270)</i> 0.9250	<i>(0.1245)</i> 1.0495	<i>(0.1215)</i> 1.1710	<i>(0.1175)</i> 1.2885
100	<i>(0.1125)</i> 1.2885	<i>(0.1050)</i> 1.4010	<i>(0.0970)</i> 1.5060	<i>(0.0910)</i> 1.6030	<i>(0.0860)</i> 1.6940	<i>(0.0815)</i> 1.7800	<i>(0.0785)</i> 1.8615	<i>(0.0760)</i> 1.9400	<i>(0.0745)</i> 2.0160	<i>(0.0735)</i> 2.0905	<i>(0.0735)</i> 2.1640
200	<i>(0.0725)</i> 2.1640	<i>(0.0725)</i> 2.2365	<i>(0.0720)</i> 2.3090	<i>(0.0720)</i> 2.3810	<i>(0.0720)</i> 2.4530	<i>(0.0720)</i> 2.5250	<i>(0.0720)</i> 2.5970	<i>(0.0720)</i> 2.6690	<i>(0.0720)</i> 2.7410	<i>(0.0725)</i> 2.8135	<i>(0.0725)</i> 2.8860
300	<i>(0.0725)</i> 2.8860	<i>(0.0730)</i> 2.9585	<i>(0.0735)</i> 3.0315	<i>(0.0740)</i> 3.1050	<i>(0.0745)</i> 3.1790	<i>(0.0750)</i> 3.2535	<i>(0.0755)</i> 3.3285	<i>(0.0760)</i> 3.4040	<i>(0.0765)</i> 3.4800	<i>(0.0770)</i> 3.5565	<i>(0.0770)</i> 3.6335
400	<i>(0.0775)</i> 3.6335	<i>(0.0780)</i> 3.7110	<i>(0.0785)</i> 3.7890	<i>(0.0790)</i> 3.8675	<i>(0.0795)</i> 3.9465	<i>(0.0800)</i> 4.0260	<i>(0.0805)</i> 4.1060	<i>(0.0810)</i> 4.1865	<i>(0.0815)</i> 4.2675	<i>(0.0820)</i> 4.3490	<i>(0.0820)</i> 4.4310
500	<i>(0.0825)</i> 4.4310	<i>(0.0835)</i> 4.5135	<i>(0.0840)</i> 4.5970	<i>(0.0850)</i> 4.6810	<i>(0.0855)</i> 4.7660	<i>(0.0865)</i> 4.8515	<i>(0.0865)</i> 4.9380	<i>(0.0875)</i> 5.0245	<i>(0.0875)</i> 5.1120	<i>(0.0880)</i> 5.1995	<i>(0.0880)</i> 5.2875
600	<i>(0.0885)</i> 5.2875	<i>(0.0890)</i> 5.3760	<i>(0.0890)</i> 5.4650	<i>(0.0895)</i> 5.5540	<i>(0.0895)</i> 5.6435	<i>(0.0895)</i> 5.7330	<i>(0.0900)</i> 5.8225	<i>(0.0900)</i> 5.9125	<i>(0.0905)</i> 6.0025	<i>(0.0905)</i> 6.0930	<i>(0.0905)</i> 6.1835
700	<i>(0.0905)</i> 6.1835	<i>(0.0905)</i> 6.2740	<i>(0.0905)</i> 6.3645	<i>(0.0905)</i> 6.4550	<i>(0.0900)</i> 6.5455	<i>(0.0900)</i> 6.6355	<i>(0.0895)</i> 6.7255	<i>(0.0890)</i> 6.8150	<i>(0.0890)</i> 6.9040	<i>(0.0890)</i> 6.9930	<i>(0.0890)</i> 7.0820
800	<i>(0.0890)</i> 7.0820	<i>(0.0885)</i> 7.1710	<i>(0.0880)</i> 7.2595	<i>(0.0880)</i> 7.3475	<i>(0.0875)</i> 7.4355	<i>(0.0870)</i> 7.5230	<i>(0.0865)</i> 7.6100	<i>(0.0860)</i> 7.6965	<i>(0.0855)</i> 7.7825	<i>(0.0850)</i> 7.8680	<i>(0.0850)</i> 7.9530
900	<i>(0.0850)</i> 7.9530	<i>(0.0845)</i> 8.0380	<i>(0.0845)</i> 8.1225	<i>(0.0840)</i> 8.2070	<i>(0.0835)</i> 8.2910	<i>(0.0830)</i> 8.3745	<i>(0.0825)</i> 8.4575	<i>(0.0820)</i> 8.5400	<i>(0.0815)</i> 8.6220	<i>(0.0815)</i> 8.7035	<i>(0.0815)</i> 8.7850
1000	<i>(0.0805)</i> 8.7850	<i>(0.0800)</i> 8.8655	<i>(0.0800)</i> 8.9455	<i>(0.0795)</i> 9.0255	<i>(0.0795)</i> 9.1050	<i>(0.0795)</i> 9.1845	<i>(0.0790)</i> 9.2640	<i>(0.0790)</i> 9.3430	<i>(0.0785)</i> 9.4220	<i>(0.0780)</i> 9.5005	<i>(0.0780)</i> 9.5785
1100	<i>(0.0780)</i> 9.5785	<i>(0.0775)</i> 9.6565	<i>(0.0770)</i> 9.7340	<i>(0.0770)</i> 9.8110	<i>(0.0765)</i> 9.8880	<i>(0.0765)</i> 9.9645	<i>(0.0760)</i> 10.0410	<i>(0.0755)</i> 10.1170	<i>(0.0750)</i> 10.1925	<i>(0.0745)</i> 10.2675	<i>(0.0745)</i> 10.3420
1200	<i>(0.0740)</i> 10.3420	<i>(0.0735)</i> 10.4160	<i>(0.0735)</i> 10.4895	<i>(0.0725)</i> 10.5630	<i>(0.0725)</i> 10.6355	<i>(0.0720)</i> 10.7080	<i>(0.0715)</i> 10.7800	<i>(0.0715)</i> 10.8515	<i>(0.0715)</i> 10.9230	<i>(0.0715)</i> 10.9945	<i>(0.0715)</i> 11.0660
1300	<i>(0.0720)</i> 11.0660	<i>(0.0720)</i> 11.1380	<i>(0.0720)</i> 11.2100	<i>(0.0720)</i> 11.2820	<i>(0.0720)</i> 11.3540	<i>(0.0720)</i> 11.4260	<i>(0.0720)</i> 11.4980	<i>(0.0725)</i> 11.5705			

\*Based on Hoskins Mfg. Co. Table E-271-AA.

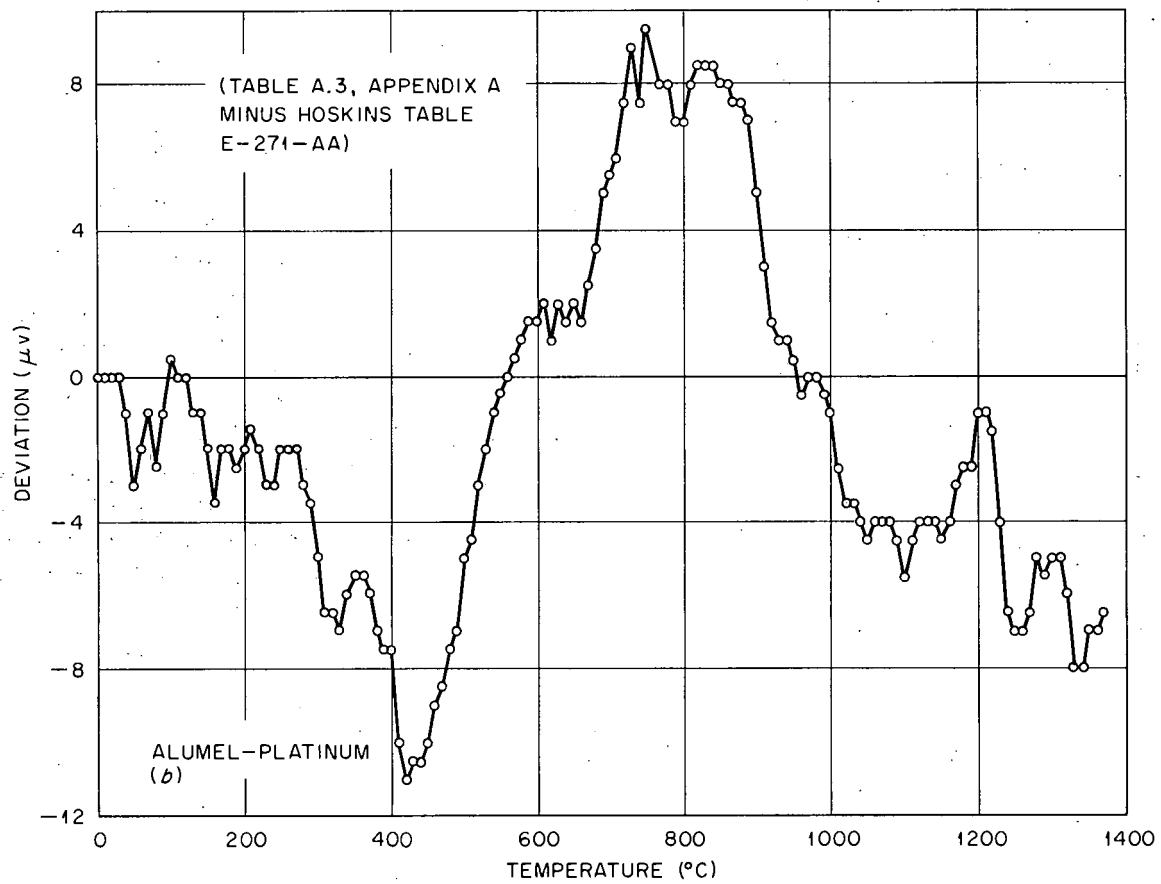
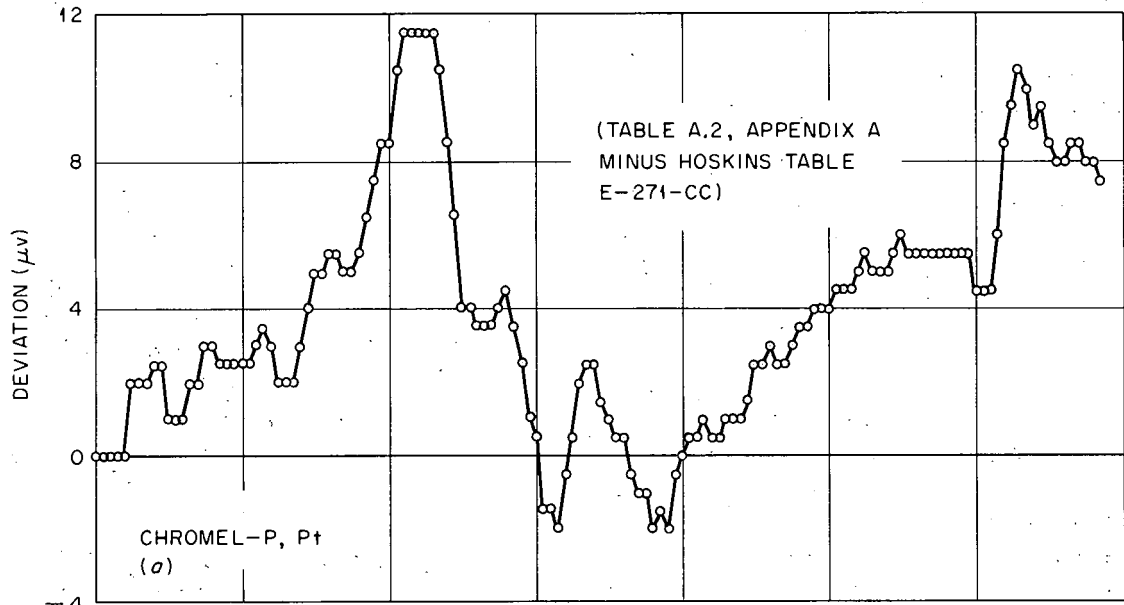


Fig. A.1. Deviation of Smoothed Chromel-P, Pt and Alumel, Pt Tables from the Respective Hoskins Tables.

## Appendix B

### COPPER-CONSTANTAN THERMOCOUPLE TABLE

A precision calibration of a duplex copper-constantan thermocouple was made from 0°C (32°F) to 60°C (140°F) using a standard platinum resistance thermometer and a copper block furnace. In order to present results as precisely as possible, a smoothed copper-constantan thermocouple table was constructed which matched NBS Circular 561, Table 10. The details of this table construction are as follows:

1. First differences of the NBS table were plotted against temperature ( $\Delta E/\Delta T$  vs  $T$ ).
2. A smooth curve was drawn through the values, and a second-difference plot was made vs temperature ( $\Delta^2 E/\Delta T^2$  vs  $T$ ).
3. A smooth curve was drawn through these values, and the tables were calculated at 1° increments by numerical integration from 0 to 60°C and from 32 to 140°F, respectively.

From the calculus of finite differences:

$$E_{T+\Delta T} = E_T + \left( \frac{\Delta E}{\Delta T} \right)_{T+\Delta T/2} \cdot \Delta T, \quad (1)$$

$$\left( \frac{\Delta E}{\Delta T} \right)_{T+\Delta T/2} = \left( \frac{\Delta E}{\Delta T} \right)_{T-\Delta T/2} + \left( \frac{\Delta^2 E}{\Delta T^2} \right)_T \cdot \Delta T. \quad (2)$$

From Eqs. (1) and (2) one obtains

$$E_{T+\Delta T} = E_T + \left( \frac{\Delta E}{\Delta T} \right)_{T-\Delta T/2} \cdot \Delta T + \left( \frac{\Delta^2 E}{\Delta T^2} \right)_T \cdot \Delta T \cdot \Delta T. \quad (3)$$

A sample calculation for  $\Delta T = 1^\circ\text{F}$  for  $E$  at 34°F follows:

$$E_T = E_{33^\circ\text{F}} = 21.340 \mu\text{v},$$

$$\left( \frac{\Delta E}{\Delta T} \right)_{T-\Delta T/2} = \left( \frac{\Delta E}{\Delta T} \right)_{32.5^\circ\text{F}} = 21.340 \mu\text{v}/^\circ\text{F},$$

$$\left( \frac{\Delta^2 E}{\Delta T^2} \right)_T = 0.030 \mu\text{v}/(^\circ\text{F})^2.$$

Therefore

$$\begin{aligned} E_{T+\Delta T} = E_{34^\circ\text{F}} &= 21.340 \mu\text{v} + \\ &+ 21.340 \mu\text{v}/^\circ\text{F} \cdot 1^\circ\text{F} + \\ &+ 0.030 \mu\text{v}/(^\circ\text{F})^2 \cdot (1)^2 (^\circ\text{F})^2, \\ E_{34^\circ\text{F}} &= 42.710 \mu\text{v}. \end{aligned}$$

Tables B.1 and B.2 show the calibrations for copper-constantan obtained in the above manner and include the thermal emf and the interpolation values. These tables were forced to agree with the NBS values to within  $\pm 0.5 \mu\text{v}$  but are smoother than the NBS table because they were rounded to the nearest  $0.001 \mu\text{v}$ . They are not better representations than the NBS table but are somewhat more useful in calculating temperatures and calibration errors.



Table B.2. Calibration for Copper-Constantan Thermocouples. Fahrenheit table.

°F	0	1	2	3	4	5	6	7	8	9	10
	Microvolts										
30			(21.340) -0-	(21.370) 21.340	(21.401) 42.710	(21.432) 64.111	(21.463) 85.543	(21.495) 107.006	(21.527) 128.501	(21.559) 150.028	171.587
40	(21.592) 171.587	(21.625) 193.179	(21.658) 214.804	(21.691) 236.462	(21.725) 258.153	(21.759) 279.878	(21.793) 301.637	(21.827) 323.430	(21.860) 345.257	(21.893) 367.117	389.010
50	(21.925) 389.010	(21.956) 410.935	(21.986) 432.891	(22.014) 454.877	(22.041) 476.891	(22.067) 498.932	(22.092) 520.999	(22.117) 543.091	(22.141) 565.208	(22.165) 587.349	609.514
60	(22.189) 609.514	(22.212) 631.703	(22.235) 653.915	(22.258) 676.150	(22.280) 698.408	(22.302) 720.688	(22.324) 742.990	(22.346) 765.314	(22.369) 787.660	(22.392) 810.029	832.421
70	(22.415) 832.421	(22.438) 854.836	(22.462) 877.274	(22.486) 899.736	(22.510) 922.222	(22.535) 944.732	(22.560) 967.267	(22.586) 989.827	(22.612) 1012.413	(22.639) 1035.025	1057.664
80	(22.666) 1057.664	(22.694) 1080.330	(22.722) 1103.024	(22.751) 1125.746	(22.780) 1148.497	(22.810) 1171.277	(22.840) 1194.087	(22.870) 1216.927	(22.901) 1239.797	(22.932) 1262.698	1285.630
90	(22.963) 1285.630	(22.994) 1308.593	(23.024) 1331.587	(23.054) 1354.611	(23.084) 1377.665	(23.114) 1400.749	(23.143) 1423.863	(23.172) 1447.006	(23.201) 1470.178	(23.230) 1493.449	1516.679
100	(23.259) 1516.679	(23.288) 1539.938	(23.311) 1563.226	(23.346) 1586.537	(23.374) 1609.883	(23.402) 1633.257	(23.430) 1656.659	(23.458) 1680.089	(23.486) 1703.547	(23.514) 1727.033	1750.547
110	(23.541) 1750.547	(23.568) 1774.088	(23.595) 1797.656	(23.622) 1821.251	(23.648) 1844.873	(23.674) 1868.521	(23.700) 1892.195	(23.725) 1915.895	(23.750) 1939.620	(23.774) 1963.370	1987.144
120	(23.798) 1987.144	(23.821) 2010.942	(23.844) 2034.763	(23.866) 2058.607	(23.887) 2082.473	(23.906) 2106.360	(23.924) 2130.266	(23.940) 2154.190	(23.954) 2178.130	(23.967) 2202.084	2226.051
130	(23.978) 2226.051	(23.987) 2250.029	(23.995) 2274.016	(24.001) 2298.011	(24.006) 2322.012	(24.009) 2346.018	(24.011) 2370.027	(24.012) 2394.038	(24.013) 2418.050	(24.014) 2442.063	2466.077
140	2466.077										

## Appendix C

### GEMINOL-P/N TEMPERATURE-EMF CALIBRATION TABLES

The emf-temperature relation for Geminol-P/N was somewhat in question in the summer of 1957 when work with these materials began. To establish this relation, we simultaneously calibrated at six temperatures, by comparison with a standard 90% Pt-10% Rh, Pt thermocouple, two thermocouples from wire supplied by the Driver-Harris Company. One thermocouple was B&S No. 20 gage, the other B&S No. 24 gage. The Geminol-P was from heat No. 5050 and the Geminol-N from heat No. 2799. The results of this calibration appear in Table C.1. The second-order polynomial

in temperature, derived by the least-squares method from the data of Table C.1, is

$$\text{millivolts} = 2.3074 \times 10^{-2} T + 9.3389 \times 10^{-6} T^2, \quad (1)$$

where  $T$  is in degrees C, and this was used in our research on these alloys. A table of values for temperature-emf of Geminol-P/N was computed from Eq. (1), a condensation of which appears in Table C.2.

**Table C.1. Original Geminol-P/N Calibration Data Used to Derive Least-Squares Equation**

Geminol-P: Driver-Harris Co. heat No. 5050

Geminol-N: Driver-Harris Co. heat No. 2799

Temperatures determined by standard 90% Pt-10% Rh, Pt thermocouple

Least-squares equation:  $\text{millivolts} = 2.3074 \times 10^{-2} T + 9.3389 \times 10^{-6} T^2$ ,  $T$  in  $^{\circ}\text{C}$

Thermocouple	Temperature ( $^{\circ}\text{C}$ )	EMF (mv)	Thermocouple	Temperature ( $^{\circ}\text{C}$ )	EMF (mv)
<b>20 Gage Wire</b>			<b>24 Gage Wire</b>		
Geminol-P/N	24.7	0.573	Geminol-P/N	24.7	0.574
	199.9	4.998		200.1	5.011
	398.2	10.622		400.0	10.742
	600.0	17.247		598.7	17.246
	800.0	24.510		800.0	24.568
	998.4	32.146		998.4	32.218
Geminol-P, Pt	24.7	0.270	Geminol-P, Pt	24.7	0.271
	200.2	2.860		199.9	2.863
	399.8	6.795		399.0	6.803
	599.3	11.389		599.7	11.437
	798.9	16.616		797.7	16.625
	998.7	22.397		999.5	22.465
Geminol-N, Pt	24.7	0.303	Geminol-N, Pt	24.7	0.303
	199.2	2.133		199.1	2.135
	397.8	3.864		397.7	3.865
	601.1	5.855		600.0	5.849
	799.6	7.861		798.9	7.869
	1000.6	9.768		1000.0	9.781

Table C.2. Temperature-EMF Relation of Geminal-P/N Thermocouples

Reference junction at 0°C

Calculated from relation

$$\text{millivolts} = 2.3074 \times 10^{-2} T + 9.3389 \times 10^{-6} T^2, \quad T \text{ in } ^\circ\text{C}$$

°C	0	10	20	30	40	50	60	70	80	90	100
	Millivolts										
0	0	0.232	0.465	0.701	0.938	1.177	1.418	1.661	1.906	2.152	2.401
100	2.401	2.651	2.903	3.157	3.413	3.671	3.931	4.192	4.456	4.721	4.988
200	4.988	5.257	5.528	5.801	6.076	6.352	6.631	6.911	7.193	7.477	7.763
300	7.763	8.050	8.340	8.631	8.925	9.220	9.517	9.816	10.117	10.419	10.724
400	10.724	11.030	11.338	11.649	11.961	12.274	12.590	12.908	13.227	13.548	13.872
500	13.872	14.197	14.524	14.852	15.183	15.516	15.850	16.186	16.525	16.865	17.206
600	17.206	17.550	17.896	18.243	18.593	18.944	19.297	19.652	20.009	20.367	20.728
700	20.728	21.090	21.455	21.821	22.189	22.559	22.930	23.304	23.680	24.057	24.436
800	24.436	24.817	25.200	25.585	25.972	26.360	26.751	27.143	27.537	27.933	28.331
900	28.331	28.731	29.133	29.536	29.941	30.349	30.758	31.169	31.582	31.996	32.413
1000	32.413	32.831	33.252	33.674	34.098	34.524	34.952	35.381	35.813	36.246	36.682
1100	36.682	37.119	37.558	37.999	38.441	38.886	39.332	39.781	40.231	40.683	41.137
1200	41.137										

Subsequent to the above work, materials were obtained from different heats, and a table of emf-temperature for Geminol-P/N was obtained from the Driver-Harris Company.<sup>1</sup> For a cursory evaluation of Table C.2 and the Driver-Harris table, three comparisons were made.

1. With the Driver-Harris table as a reference, a plot of the deviation of Table C.2 from the Driver-Harris table appears in Fig. C.1. The two tables agree to 400°C, but significant positive and negative deviations are found above 400°C. The differences observed in this plot are reflected in the other two comparisons.

<sup>1</sup>P. R. Marsh, Driver-Harris Co., private communication, June 5, 1958.

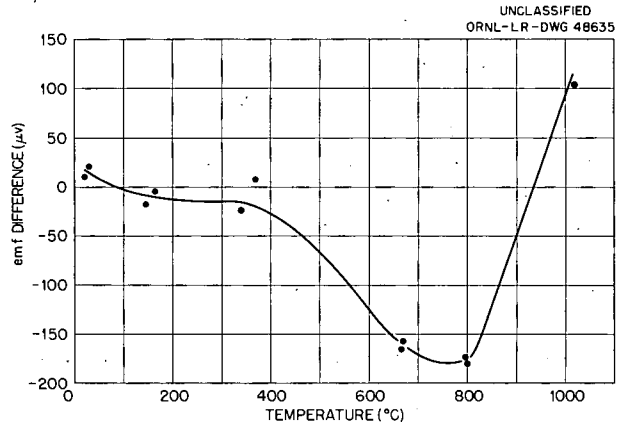


Fig. C.1. Deviation of ORNL-Calculated Values (Table C.2) from Driver-Harris Table Values for Geminol-P/N Thermocouples.

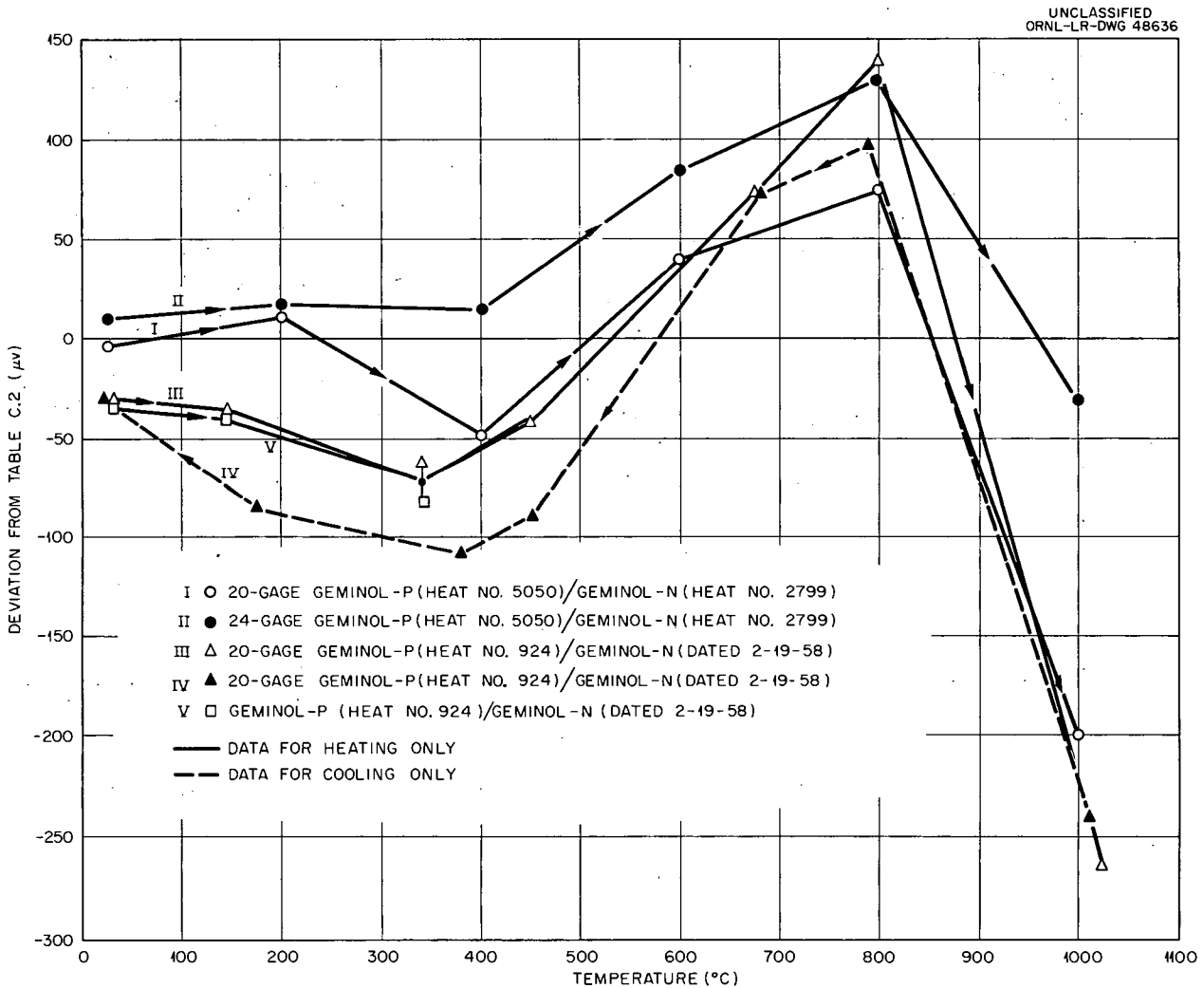


Fig. C.2. Comparison of Several Geminol-P/N Calibrations with Values in Table C.2.

2. Calibration data was obtained on Geminol-P/N from another heat. The deviation of this data from the original data in Table C.1 was plotted as a function of temperature, as shown in Fig. C.2. It may be seen that there is a systematic departure of data from all calibrations from the values in Table C.2. This indicates that a second-order polynomial is not an adequate representation of the temperature-emf relation for Geminol-P/N over the range 0 to 1000°C.

3. The deviation of the same data from the Driver-Harris table was plotted as a function of

temperature as shown in Fig. C.3. Although this plot does not show the systematic departure observed in Fig. C.1, it is definite indication that more information should be gathered on more heats, on conditions other than as-received, and for both heating and cooling before a "standard" curve can be established.

The above presentation illustrates the calibration problems and gives some superficial data which should aid further experimentation.

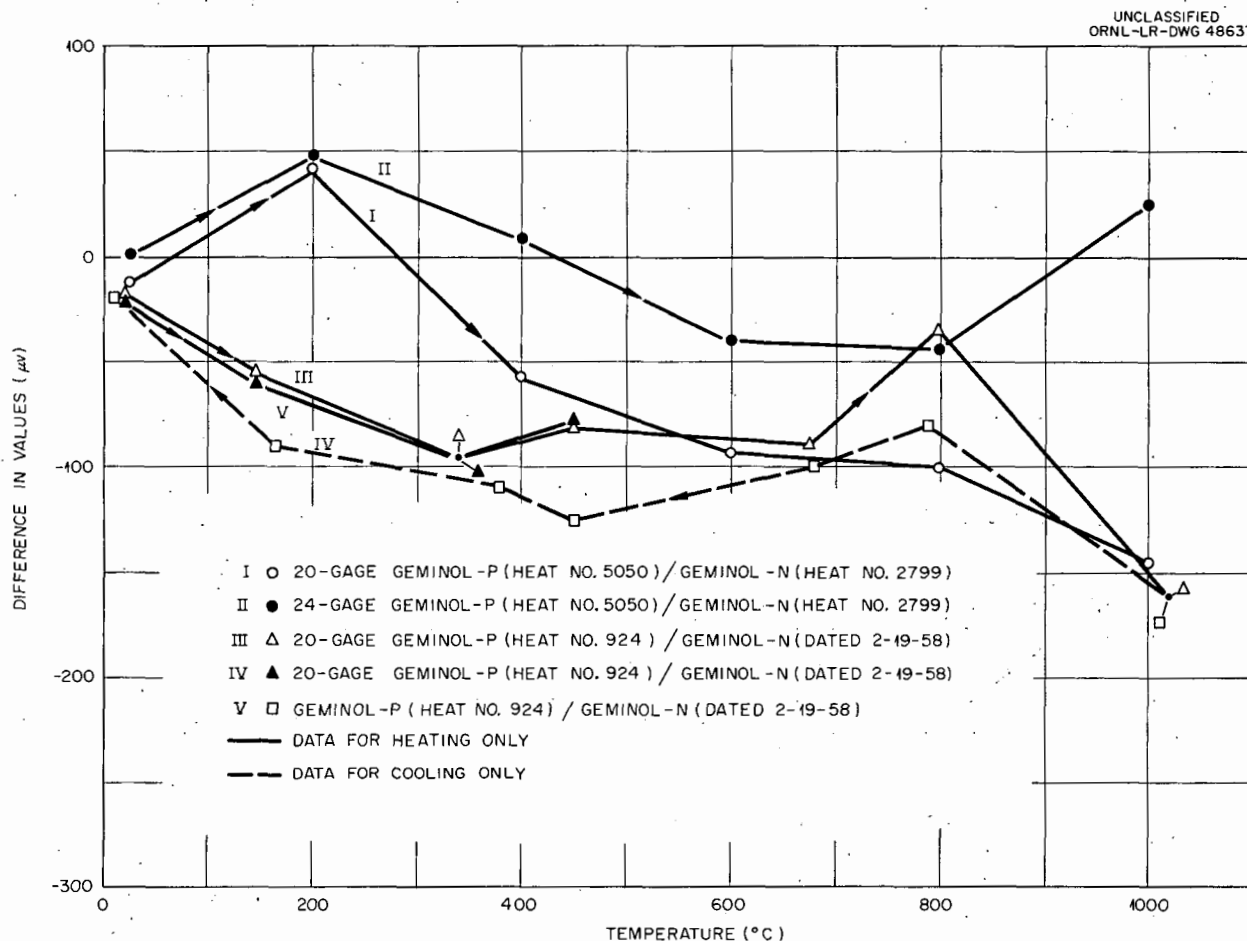


Fig. C.3. Comparison of Several Geminol-P/N Calibrations with Values in the Driver-Harris Table.

## Appendix D

### CHEMICAL ANALYSIS OF THERMOELEMENTS

Some chemical analyses were obtained on thermocouple materials since the first report,<sup>1</sup> including some special thermocouple wire which was not previously available. The wet-chemistry analyses in weight per cent are presented in Table D.1. The spaces without numbers indicate that less than 0.01 wt % was indicated by spectrographic techniques and hence wet chemistry was not attempted. Difficulty was encountered in obtaining consistent wet-chemistry analyses. It is not known whether all observed variations are

due to analytical limitations or are intentional manufacturer's differences introduced for "curve matching," as would be expected in the case of constantan. Constantan showed some variations in copper, nickel, iron, and manganese. Similar variations were observed for Alumel, and on duplicate samples of special Alumel and Chromel-P + Nb.

For nuclear reactor applications, the sixfold difference in cobalt in the Chromel-P + Nb analyses and the relatively large, but consistent, amount of cobalt found in Alumel could be significant.

Nominal manufacturers' analyses in weight per cent of other materials tested in this research are included in Table D.2.

<sup>1</sup>D. L. McElroy, *Progress Report I, Thermocouple Research, Report for Period Nov. 1, 1956 to Oct. 31, 1957*, ORNL-2467, p 33-34.

Table D.1. Wet Chemistry Analysis of Thermocouple Materials  
Analyses from the ORNL Analytical Chemistry Division  
Values in weight per cent

Material	Al	Co	Cr	Cu	Fe	Mn	Ni	Si	Nb	C
Constantan for ISA type J (vendor A)				55.10	0.20	0.96	45.01	0.05		
Constantan for ISA type J (vendor B)				51.22	0.22	0.069	47.46	0.05		
Constantan for ISA type T (vendor B)	0.089	0.026	0.04	54.07	0.37	0.81	44.69	0.02		0.011
Alumel (spool I) <sup>a</sup>	1.58	0.36			0.03	1.79	96.28	0.88		0.012
Alumel (spool II) <sup>a</sup>	1.60	0.33		0.04	0.02	3.35	95.20	0.74		0.016
Alumel (spool III) <sup>a</sup>	1.61	0.29			0.014	3.55	94.1	0.92		0.012
Special Alumel <sup>b</sup>	318 <sup>PPm</sup>	0.19			0.26	0.24	98.36	1.21		0.005
Special Alumel <sup>b</sup>		0.19			0.26		99.77	1.25		0.004
Vacomius	1.69	0.20			0.10	2.26	94.88	0.22		0.022
Vacoplus			9.04			2.06	88.11	0.24		0.008
Chromel-P (spool IV) <sup>a</sup>		652 <sup>PPm</sup>	9.43				89.55	0.37		0.010
Chromel-P (spool V) <sup>a</sup>		561 <sup>PPm</sup>	9.58				90.18	0.35		0.010
Chromel-P + Nb <sup>b</sup>		0.31	8.97	<0.10			89.57	0.35	0.2 <sup>c</sup>	0.012
Chromel-P + Nb <sup>b</sup>		498 <sup>PPm</sup>	9.41				89.80	0.35	0.2 <sup>c</sup>	0.016

<sup>a</sup>Not duplicates, but from different lots.

<sup>b</sup>Duplicate samples.

<sup>c</sup>By spectrographic analysis (below threshold for wet analysis).

**Table D.2. Manufacturer's Nominal Composition of  
Thermocouple Materials**

In weight per cent

Material	Al	Cr	Cu	Fe	Ni	Si
Hoskins alloy 875	6.0	22.5		Bal		0.5
Hoskins alloy 827		20		8.0	Bal	2.0
Hoskins alloy 717	Bal	20			Bal	0.25
Chromel-A	Bal	20			Bal	1.5
Chromnickel-B		20			80	
Nickel					100	
Nickel, 1% silicon					99	1
Nickel, 2% silicon					98	2
Nickel, 3% silicon					97	3
Nickel, 4% silicon					96	4
Nickel, 5% silicon					95	5
Copper				100		
Iron				Essentially SAE 1010		

## Appendix E

### CALIBRATION DATA FOR NICKEL-SILICON ALLOY

Six materials (pure nickel and alloys of 1, 2, 3, 4, and 5% silicon) were calibrated at the melting points of tin, zinc, aluminum, and silver. A comparison calibration was also made during heating at the beginning of the drift test discussed in Chap. 6, Table 6.2. Results of the fixed-point calibrations are presented in Table E.1 and Fig. E.1. The nickel-silicon alloys were homogenized in ingot form and were annealed after drawing to wire form and before calibration.

Nickel alloyed with silicon in the solid solution composition range produces a lower thermal emf to platinum than pure nickel. The shape of the emf-temperature curves changes with the amount of silicon in nickel, as illustrated by the curves of Fig. E.1. The effect of composition on thermal emf is shown in Fig. E.2.

An illustration of the relation between silicon concentration in nickel and the shapes of the emf-temperature curves appears in Fig. E.3, showing the difference between the temperature-emf curves and the arbitrarily chosen line  $E = -10T$ . Small additions of silicon to nickel produce a greater effect than large additions. A 3% silicon addition to nickel produces the most linear emf-temperature curve of the alloys tested. The curve for Alumel vs platinum is included for comparison in Figs. E.1 and E.3, and it may be seen that Alumel shows a greater nonlinearity at low temperatures than the 2 or 3% silicon in nickel alloys. Figure E.3 indicates a satisfactory agreement between melting point and comparison calibrations.

Table E.1. EMF of Nickel, Nickel-Silicon Alloys, and Alumel vs Platinum at Fixed Points

Values in millivolts  
All emf's negative with respect to platinum  
Reference junction at 0°C

Fixed Point	Temperature (°C)	Pure Nickel	Nickel-Silicon Alloys*					Alumel**
			1% Si	2% Si	3% Si	4% Si	5% Si	
Tin (freeze)	231.9	3.588	2.832	2.636	2.461	2.383	2.423	2.398
Zinc (freeze)	419.5	5.524	4.223	4.087	4.225	4.397	4.536	3.796
Aluminum (melt)	660.0	7.558	6.246	6.315	6.718	7.113	7.313	5.821
Silver								
(melt)	960.8	11.399	9.531	9.455	9.828	10.232	10.413	8.465
(freeze)	960.8	11.400	9.532	9.453	9.831	10.223	10.415	

\*Alloys fabricated at the University of Tennessee.

\*\*From Hoskins Manufacturing Co. Table E-271-AA.

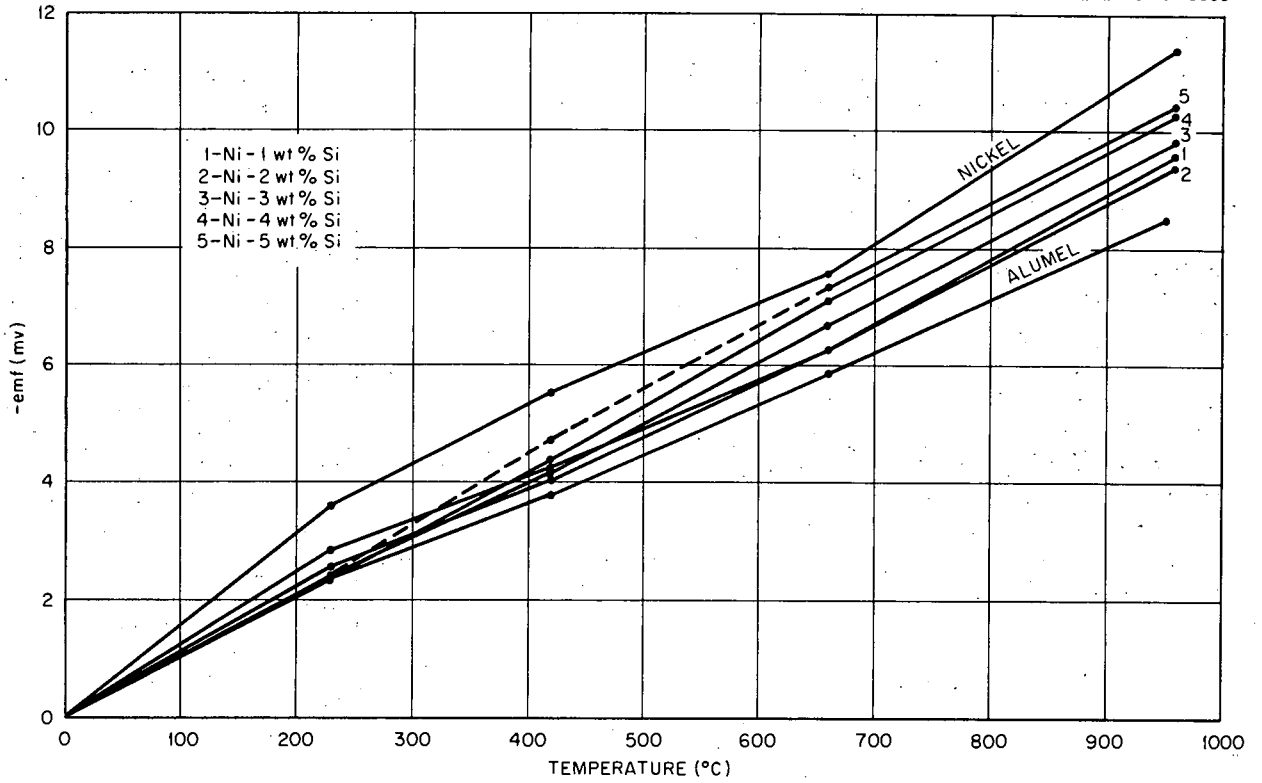


Fig. E.1. EMF of Pure Nickel, Nickel-Silicon Alloys, and Almel vs Platinum, at Fixed Points.

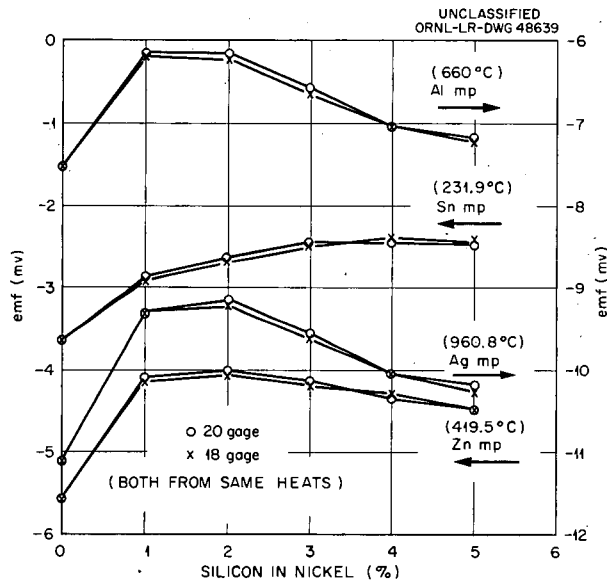


Fig. E.2. EMF of Pure Nickel and Nickel-Silicon Alloys vs Platinum, as a Function of Silicon Content at Four Fixed Points.

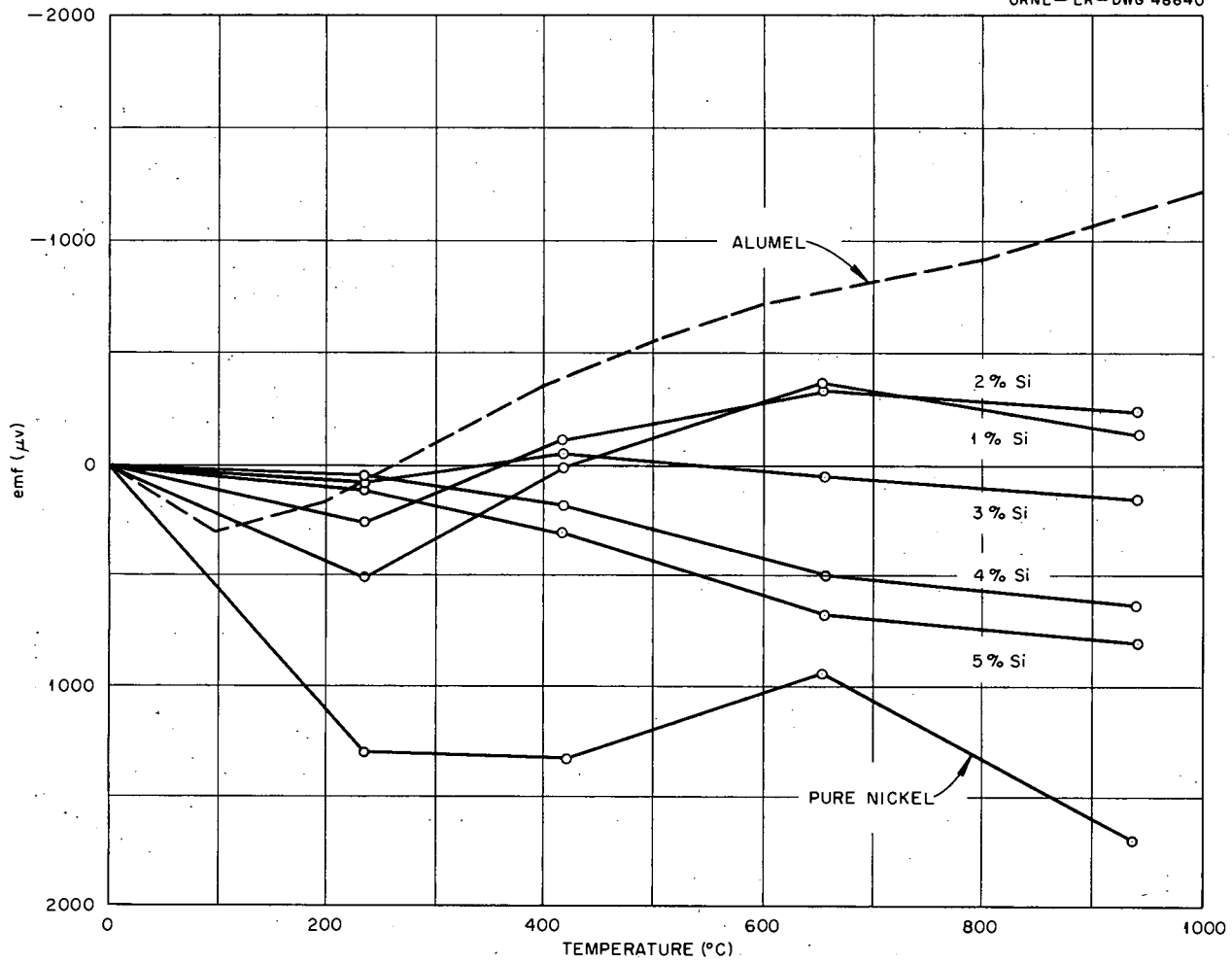


Fig. E.3. Divergence of Thermal EMF from the Arbitrary Line,  $E(\mu V) = -10T(^{\circ}C)$ , for Pure Nickel, Nickel-Silicon Alloys, and Alumel vs Platinum. Data from three independent calibrations.

**Appendix F**  
**MISCELLANEOUS CALIBRATIONS**

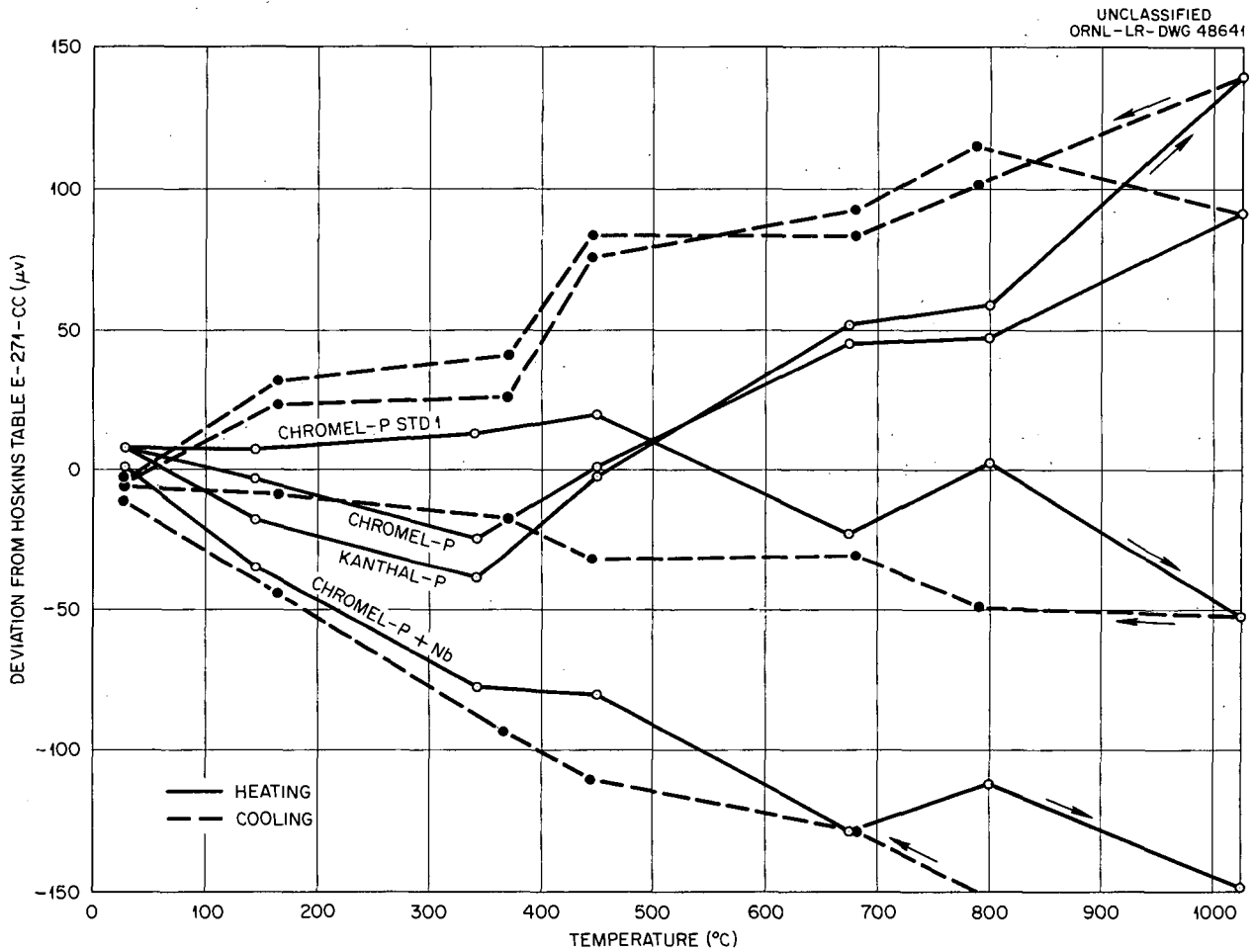
Comparison calibrations on the materials listed in Table F.1 were made using a 90% Pt-10% Rh, Pt standard thermocouple. The hot junction consisted of 14 wires, to which was attached the standard thermocouple. Conventional mercury U-tube connections were used for the reference junction (0°C).

Table F.1 lists the emf values determined on heating and cooling in the comparison calibration, as a function of temperature. Figures F.1 and F.2 show the deviations of certain of the positive and negative elements from Hoskins tables E-271-CC and E-271-AA, respectively, for Chromel-P vs platinum and Alumel vs platinum on heating and cooling. Calibrations on cooling were

different from the calibrations on heating. This hysteresis loop was first noted in an earlier report<sup>1</sup> and is due to annealing and oxidation during calibration. The direction of the dynamic shift in calibration appeared to be random. Except for Geminol-N (no standard curve yet established), all the calibrations plotted were within the standard ISA  $\pm \frac{3}{4}$ % tolerance.

Figure F.3 is a plot of thermal emf for the various materials tested vs platinum as a function of temperature. The more oxidation-resistant

<sup>1</sup>D. L. McElroy, *Progress Report 1, Thermocouple Research, Report for Period Nov. 1, 1956 to Oct. 31, 1957, ORNL-2467, p 72.*



**Fig. F.1. Calibration of Positive Thermoelements vs Platinum, Shown as Deviations from Hoskins Table E-271-CC (Chromel-Platinum).**

Table F.1. Observed Thermal EMF for Various Materials vs Platinum

Values in microvolts

Material	Heat No.	27°C	144°C	341°C	448°C	674°C	801°C	1023°C	791°C	681°C	446°C	371°C	165°C	21°C
Negative relative to platinum														
Alumel	8,575	360.4	1739.0	3,161.2	3,984.2	5,939.2	7,116.2	8,999.1	7,008.4	6,009.7	3,958.4	3,384.1	1915.0	279.1
Alumel std. 2*		356.6	1728.7	3,148.4	3,968.5	5,907.8	7,053.6	8,950.4	6,970.5	5,973.5	3,958.1	3,377.5	1909.3	273.8
Alumel std. 1*		356.7	1725.6	3,139.8	3,958.5	5,896.9	7,045.3	8,939.1	6,961.8	5,965.8	3,951.1	3,370.6	1904.9	276.5
Kanthal-N	69,227	313.1	1648.8	3,136.2	3,951.3	5,919.8	7,098.8	9,044.4	6,992.6	5,986.2	3,936.4	3,560.9	1865.3	240.1
Geminol-N	20	328.0	1548.3	3,279.7	4,305.3	6,607.7	7,915.9	9,959.1	7,792.9	6,680.6	4,273.5	3,360.5	1724.2	248.0
Special Alumel	4,559	319.7	1674.5	3,205.9	4,045.8	5,998.3	7,137.1	8,977.6	7,031.6	6,061.4	4,023.6	3,436.2	1883.7	243.7
Positive relative to platinum														
Chromel-P	221	712.8	4162.8	10,702.0	14,412.1	22,144	26,303	33,324	26,037	22,414	14,424.7	11,799.9	4864.3	547.2
Chromel-P std. 1*		713.5	4172.4	10,739.0	14,430.2	22,077	26,259	33,184	25,887	22,300	14,309.7	11,741.3	4824.0	546.6
Chromel-P + Nb**	982	706.8	4131.3	10,648.2	14,330.1	21,970	26,144	33,087	25,785	22,202	14,230.9	11,664.2	4788.8	540.4
Hoskins alloy No. 717	20 sample	333.7	2128.8	6,058.3	8,495.9	14,145	17,667	24,204	17,382	14,334	8,433.5	6,709.7	2490.8	253.6
Kanthal-P	69,228	712.9	4148.3	10,687.7	14,408.9	22,150	26,315	33,376	26,052	22,423	14,417.1	11,784.8	4856.4	547.6
Geminol-P	924	298.6	1932.3	5,572.7	7,864.0	13,260	16,699	23,154	16,401	13,436	7,786.1	6,167.8	2251.6	227.5
Hoskins alloy No. 827	733	212.0	1424.7	4,271.8	6,119.1	10,598	13,557	19,287	13,306	10,754	6,057.3	4,749.0	1676.2	160.5
Hoskins alloy No. 875	2,665	101.4	794.4	2,415.5	3,549.6	6,476	8,539	12,879	8,400	6,596	3,565.6	2,734.1	725.7	76.3

\*Rod supplied by Hoskins Manufacturing Co. as proposed Hoskins comparison standard.

\*\*Experimental alloy supplied by Hoskins Manufacturing Co.

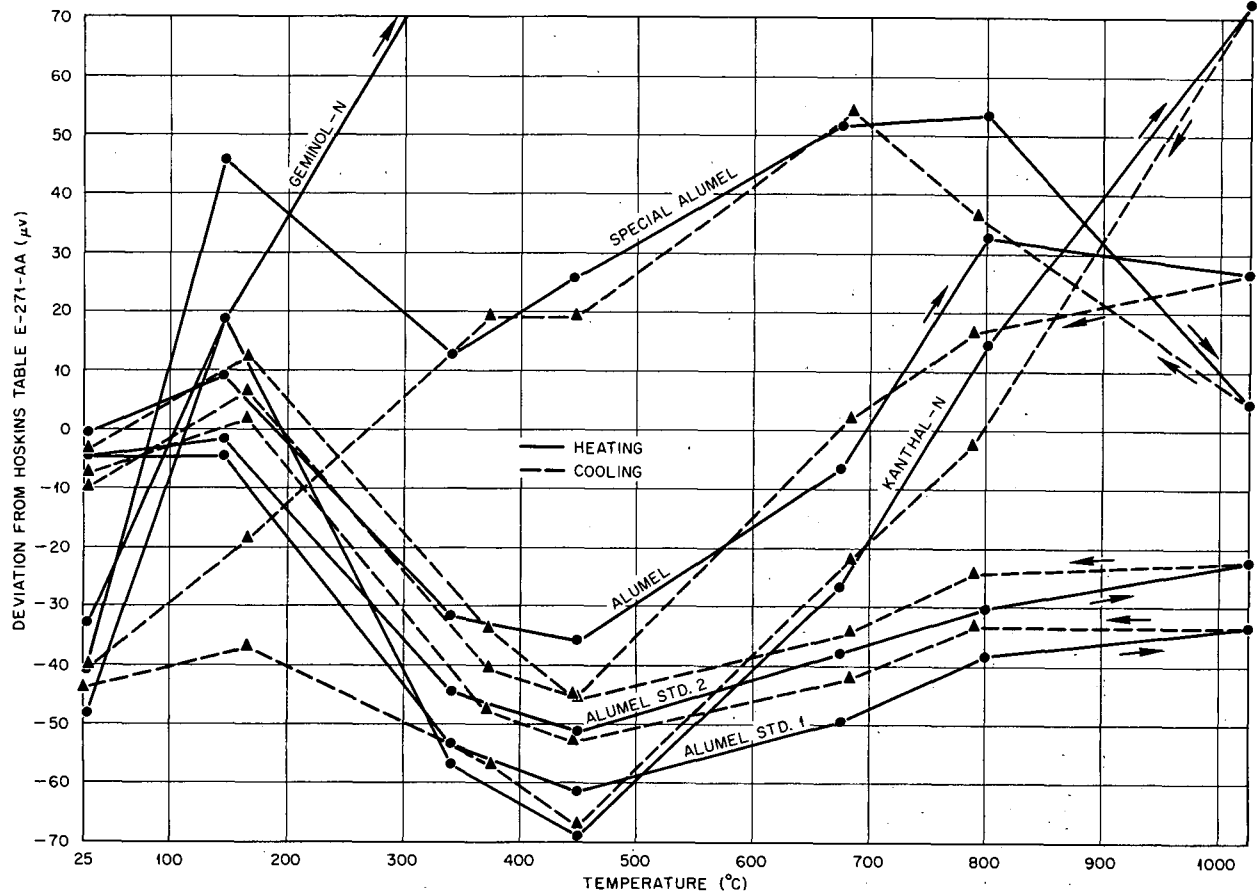


Fig. F.2. Calibration of Negative Thermoelements vs Platinum, Shown as Deviation from Hoskins Table E-271-AA (Alumel-Platinum).

positive thermoelements, Hoskins alloys 875, 827, 717, and Geminol-P, produced a lower thermal emf than did the 90% Ni-10% Cr class of alloys. The more oxidation-resistant negative thermoelements, Kanthal-N and Special Alumel, produced (not plotted in Fig. F.3) emf's which were close to Alumel vs platinum, but with small deviations at low temperatures. Geminol-N vs platinum exhibited considerable deviation from Alumel vs platinum at the higher temperatures. These plots may be of superficial value, but do indicate the sacrifice in emf necessary to obtain an oxidation-resistant alloy.

Low-temperature comparison calibrations made on alloys thermoelectrically negative to platinum are listed in Table F.2. These calibrations were made in a large copper inertia block contained in a furnace whose temperature could thus be changed

slowly. The values in Table F.2 were compared with the equation  $E (\mu v) = -10.5T (^\circ C)$  in Fig. F.4, in order to exaggerate their differences. A dominant feature of this plot was the positive deviation noted in the alloys near 100°C, after which the deviation was negative. Since these alloys would be considered as replacements for Alumel, the comparison of their calibration curves with Alumel is of interest. Above 200°C the agreement between Kanthal-N, special Alumel, and Alumel is good. There is a striking similarity between the calibration curves for Kanthal-N and special Alumel, although the chemical analysis showed that they differed significantly in silicon content. However, the equivalence of additions ( $Fe + Mn = Si$ ) may be an explanation. (Kanthal-N, which was higher in silicon, contained very little iron and manganese, whereas special Alumel contained

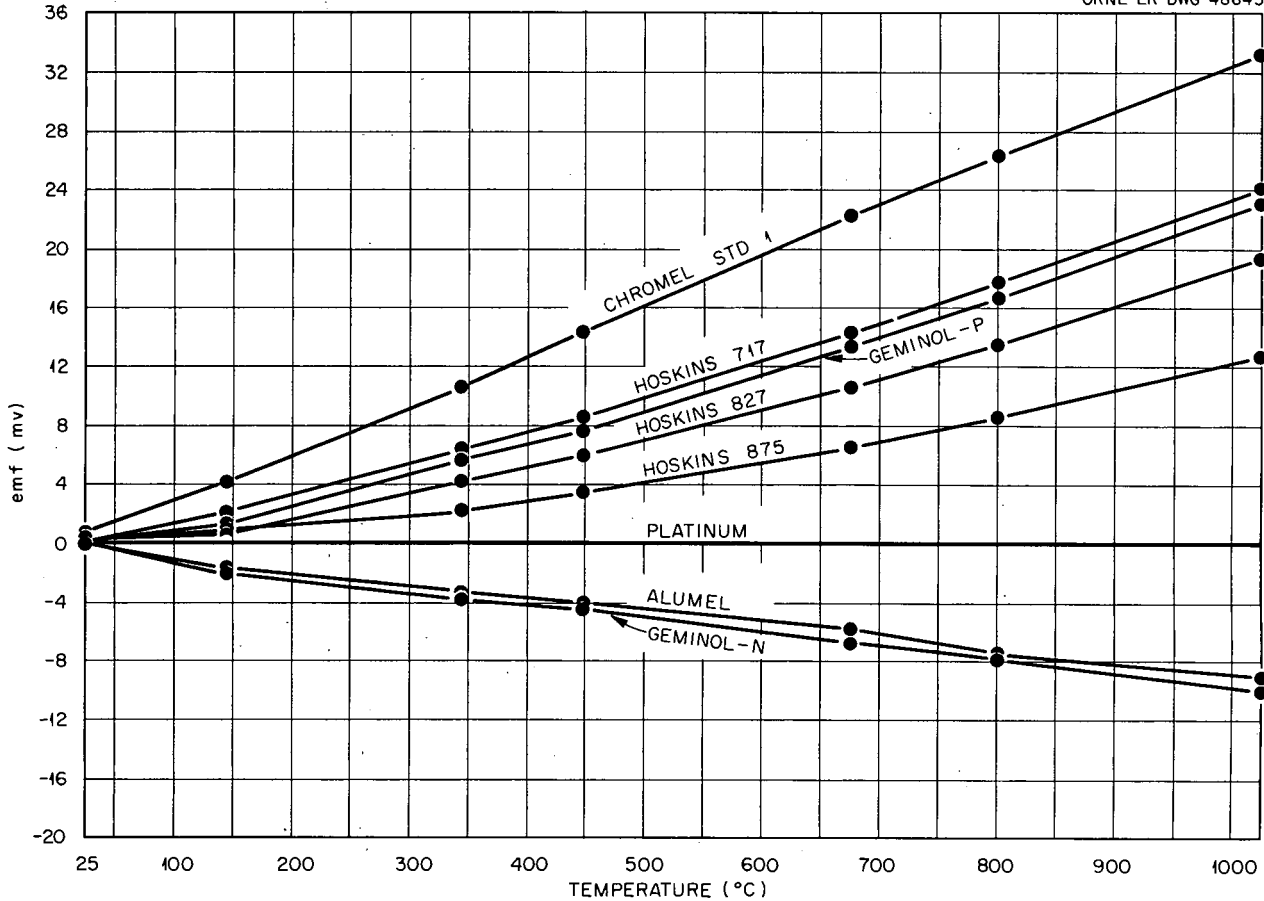


Fig. F.3. Thermal EMF of Various Nickel-Base Alloys Relative to Platinum.

0.25% iron and 0.35% manganese.) Below 200°C, significant differences in calibration appear, but this is of minor importance for high-temperature use. The dome-shaped deviation near the Curie temperature (350°C) for nickel is of interest. This behavior is also seen in the series of nickel-

silicon alloys and is suggestive of Curie-point shift associated with silicon content. This data also revealed the emf changes caused by changing only one alloying element. The Geminol-N calibration differed markedly from the AlumeL calibration through this temperature range.

**Table F.2. Low-Temperature Calibration of Various Materials vs Platinum**  
 All emf's in microvolts, negative to platinum

Material	21.3°C	36.0°C	95.3°C	149.8°C	168.1°C	181.2°C	200.2°C	211.5°C	225.0°C	292.5°C	323.3°C	400.5°C	470.2°C
Geminol-N	257.6	426.3	1089.4	1597.2	1754.6	1867.5	2030.3	2125.8	2240.9	2835.1	3198.3	3843.6	4527.0
Kanthal-N	247.4	414.1	1109.5	1703.7	1877.9	1995.3	2145.6	2227.1	2316.7	2788.7	3072.5	3583.1	4135.4
Special Alumel	254.0	428.8	1132.0	1731.4	1907.0	2022.4	2173.4	2257.8	2354.9	2846.9	3142.9	3670.8	4234.0
Alumel	287.1	482.0	1225.2	1792.2	1936.8	2037.1	2174.0	2253.1	2344.5	2819.2	3098.6	3604.6	4165.4
Nickel	294.8	496.1	1384.9	2258.1	2551.5	2769.2	3079.9	3259.4	3467.4	4451.2	4917.5	5403.2	5863.2
1% silicon, bal nickel	229.9	391.4	1108.4	1810.5	2044.1	2213.1	2450.4	2585.1	2735.5	3385.5	3642.0	4079.8	4575.1
2% silicon, bal nickel	247.1	419.6	1138.5	1787.2	1990.8	2128.6	2316.1	2416.0	2526.5	3022.8	3320.0	3856.0	4445.6
3% silicon, bal nickel	264.3	445.1	1147.4	1696.8	1858.6	1973.0	2139.1	2235.2	2354.0	2948.8	3315.5	3967.5	4663.8
4% silicon, bal nickel	250.8	413.7	1012.3	1545.8	1726.8	1856.8	2047.5	2160.0	2299.0	2995.7	3421.5	4168.3	4949.1
5% silicon, bal nickel	218.8	370.4	972.0	1537.0	1731.0	1869.5	2074.4	2193.6	2341.5	3071.0	3510.6	4280.3	5088.2
$E(\mu\text{v}) = -10.5T$ (°C)	223.6	378.0	1000.6	1572.9	1765.0	1902.6	2102.1	2220.7	2362.5	3071.2	3489.1	4205.2	4937.1

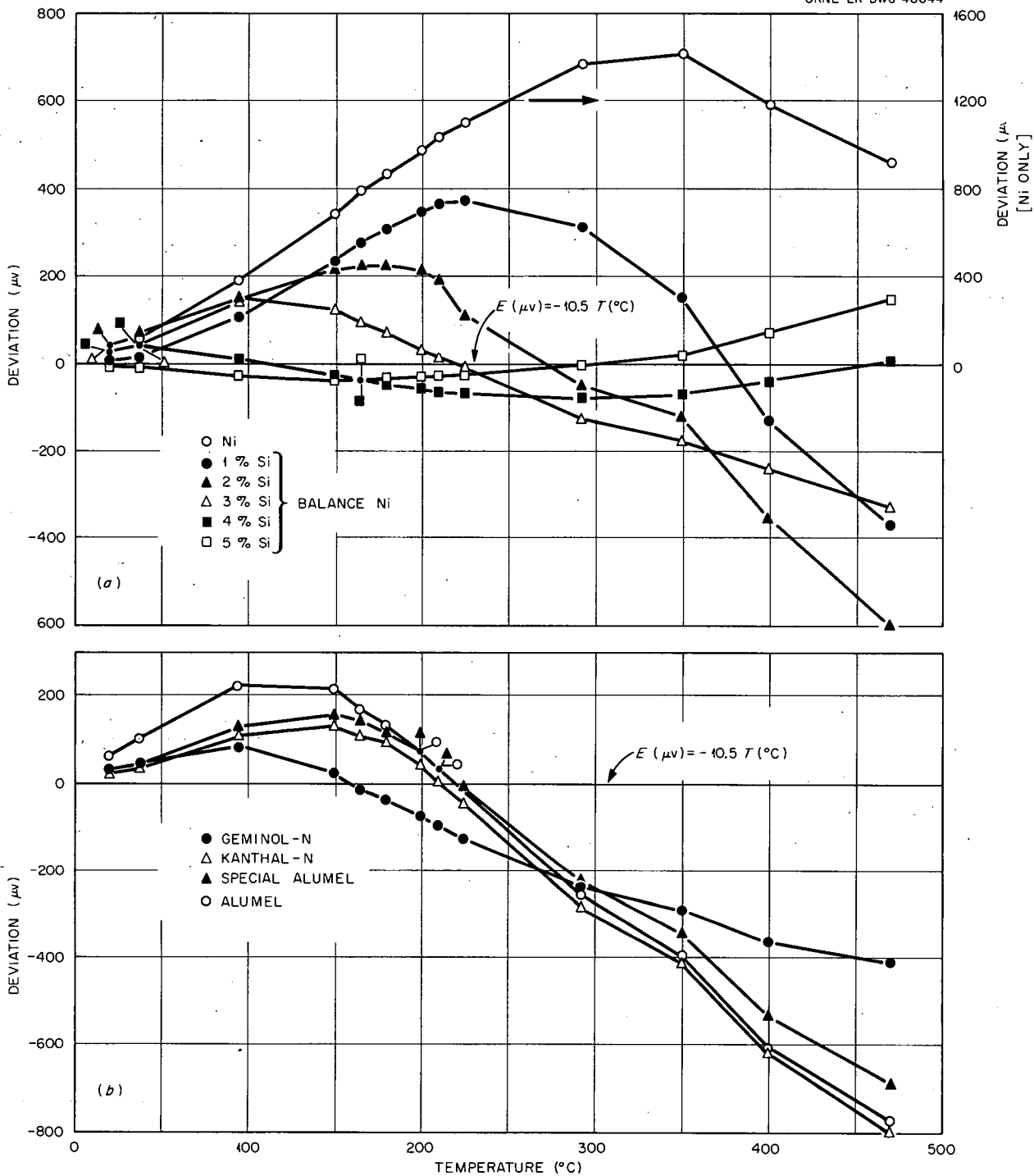


Fig. F.4. Deviation of Various Nickel-Base Alloys Thermoelectrically Negative to Platinum. From the equation  $E (\mu v) = -10.5T (^{\circ}C)$ .

## Appendix G

### EFFECTS OF ISOTHERMAL HEAT TREATMENTS ON CALIBRATION

Changes in calibration of Chromel-P, Alumel were measured for thermocouples which had been isothermally heat-treated for various times at 900°C in oxygen and helium. The results were supplemented with data from wires treated in oxygen and then pickled to remove the oxide. Figure G.1 shows the error in thermal emf for the individual thermoelements vs platinum at 580°C as a function of time at 900°C. For heat treatment in oxygen for more than 5 hr, the thermocouple calibration change was primarily caused by

Alumel. For heat-treatment times less than 5 hr in oxygen, Chromel-P controlled the calibration. The results with helium and oxygen, plus pickling, indicated that there was probably an oxide on the Chromel-P which contributed the large negative drift after 2 hr of heat-treating time.

In an effort to more definitely establish the above results as due to oxide formation and not to metallurgical changes, a series of helium-atmosphere heat treatments were imposed on positive thermoelements (Chromel-P; Chromel-P +

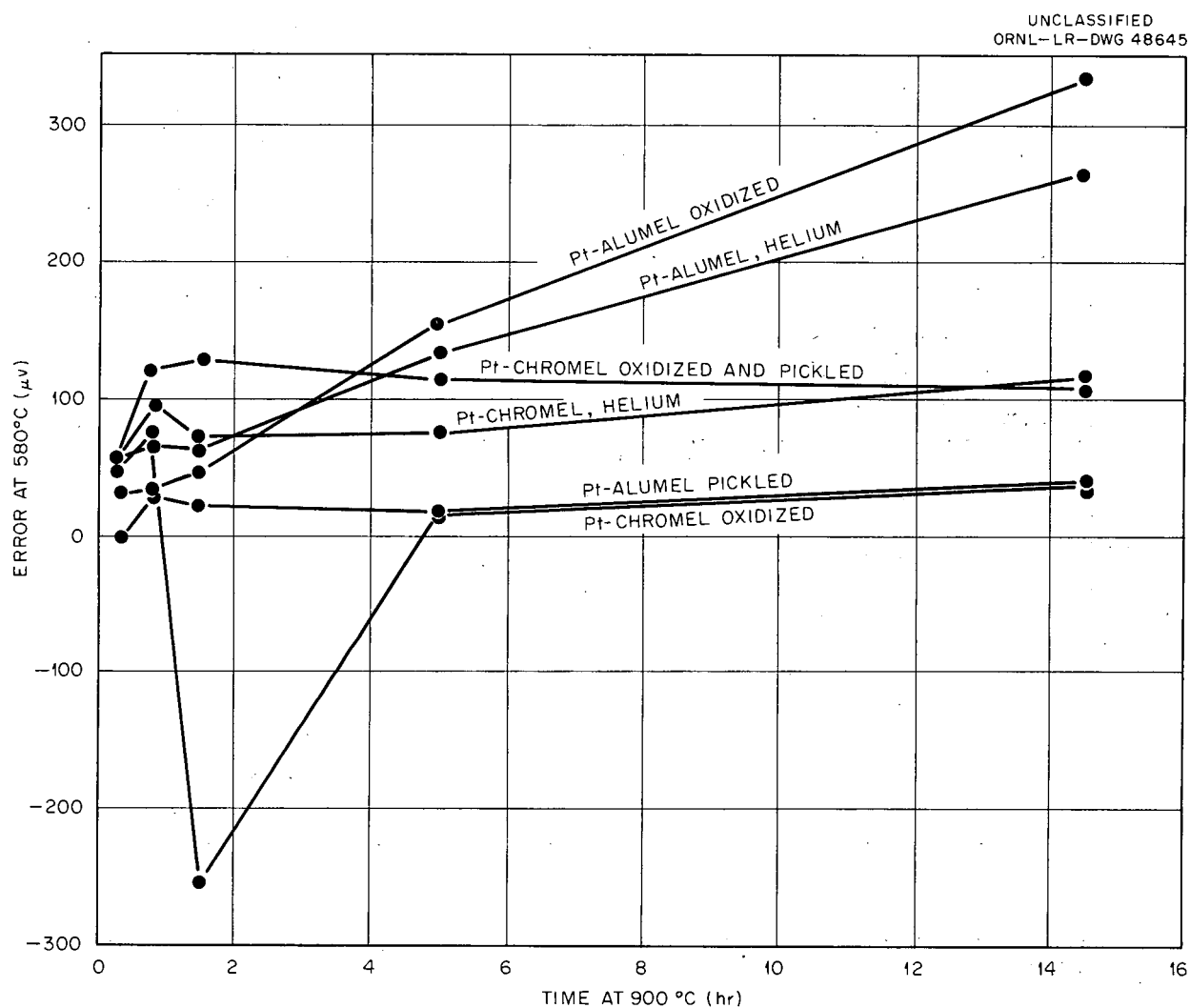


Fig. G.1. Error at 580°C of Chromel-P, Pt and Alumel, Pt Caused by Isothermal Heat Treatments at 900°C in Helium and in Oxygen.

Nb, Kanthal-P, and Geminol-P) at 500, 600, 700, and 800°C for 2, 4, 8, and 16 hr at each temperature. The resulting calibration data are shown in Figs. G.2–G.17 for the various heat-treating times and temperatures. Unfortunately, impurity of the helium used and the lack of tightness of the system prevented the complete isolation of metallurgical changes. Figure G.1 indicates that the oxide effect was more predominant at shorter times and hence for relatively thin oxide films. In every case in Figs. G.2–G.17 in which a large negative deviation was noted, the wire causing the deviation could be identified by the distinct appearance of an oxide film, despite the helium atmosphere. Almost without exception, it was for the higher temperatures and longer times of heat treatment that the data spread and the negativity were greatest. This would be expected if the heat-treating atmosphere were questionable.

Considering individual cases, the following details may be observed.

**Chromel-P.** – (See Figs. G.2–G.5, excluding the data for the 16-hr heat treatment at 800°C.)

On heating, the calibration asymptotically approached a +3 to +5°C error in the range 300 to 800°C as the heat-treating time and temperature increased, and the error on cooling approached +4 to +6°C. The difference in the calibration on heating and cooling was smallest for the 500°C treatments and largest for the 800°C treatments. All calibrations on heat-treated wire were above the calibration on as-received material, as might be expected because of the latter being somewhat cold-worked. At a given heat-treating temperature the maximum difference in calibration with time at that temperature was about 1°C. Thus after at least 2 hr at a given heat-treating temperature, the effect of metallurgical changes was quite small. There were differences of about 5°C between effects at different heat-treating temperatures, and this could well represent differences in the degree of recovery for the 500°C heat-treatment data and the differences in degree of recrystallization for the 800°C heat-treatment data. The direction of this shift was toward lower emf, which was in agreement with results shown

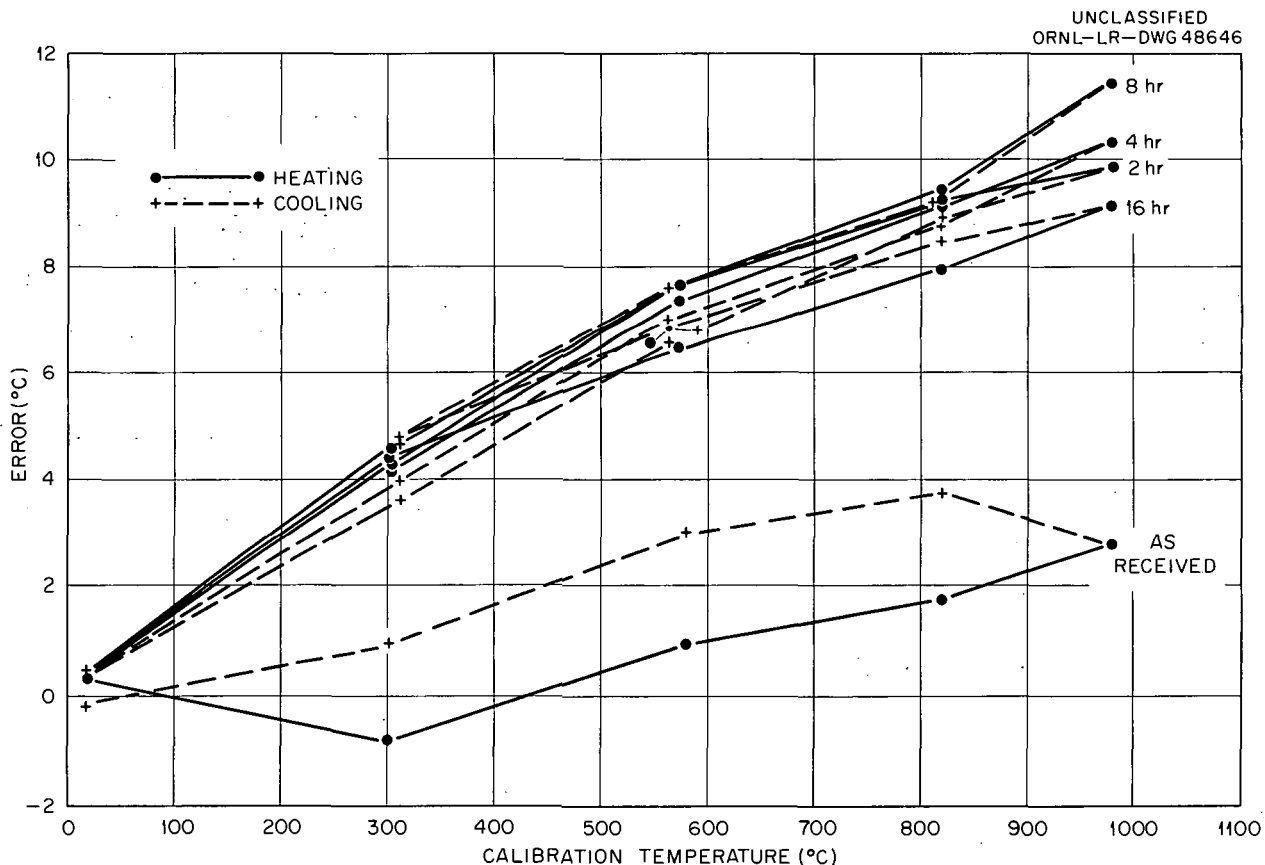


Fig. G.2. Calibration Deviation of Chromel-P vs Platinum for 2, 4, 8, and 16 hr at 500°C.

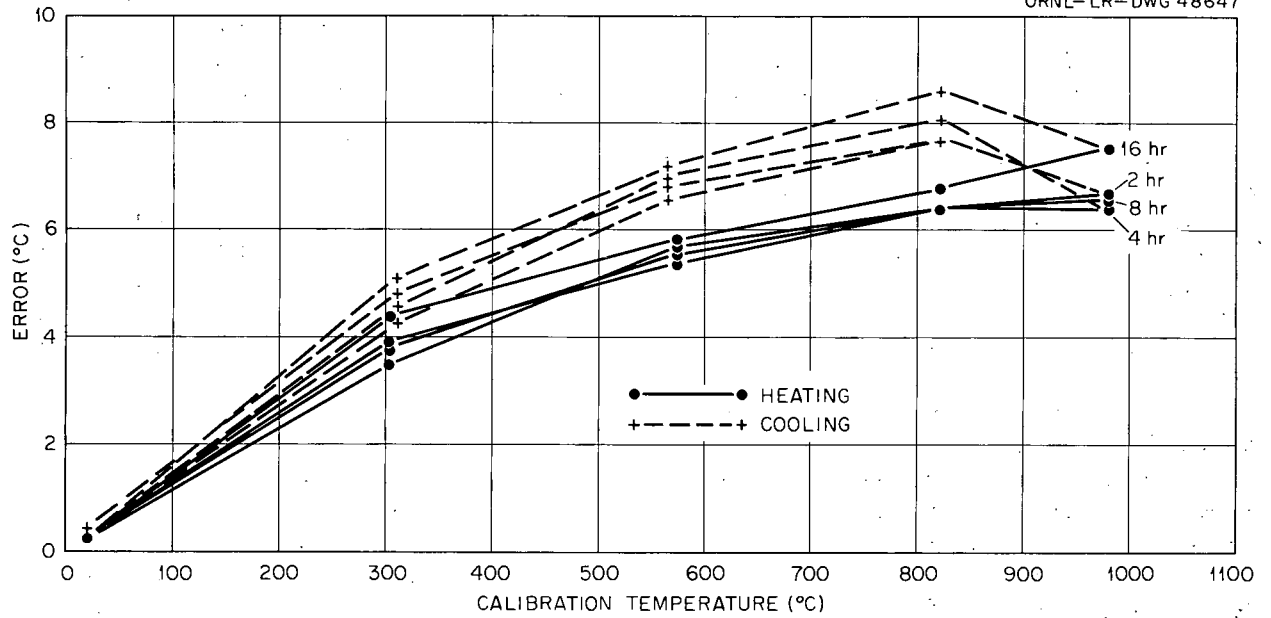


Fig. G.3. Calibration Deviation of Chromel-P vs Platinum for 2, 4, 8, and 16 hr at 600°C.

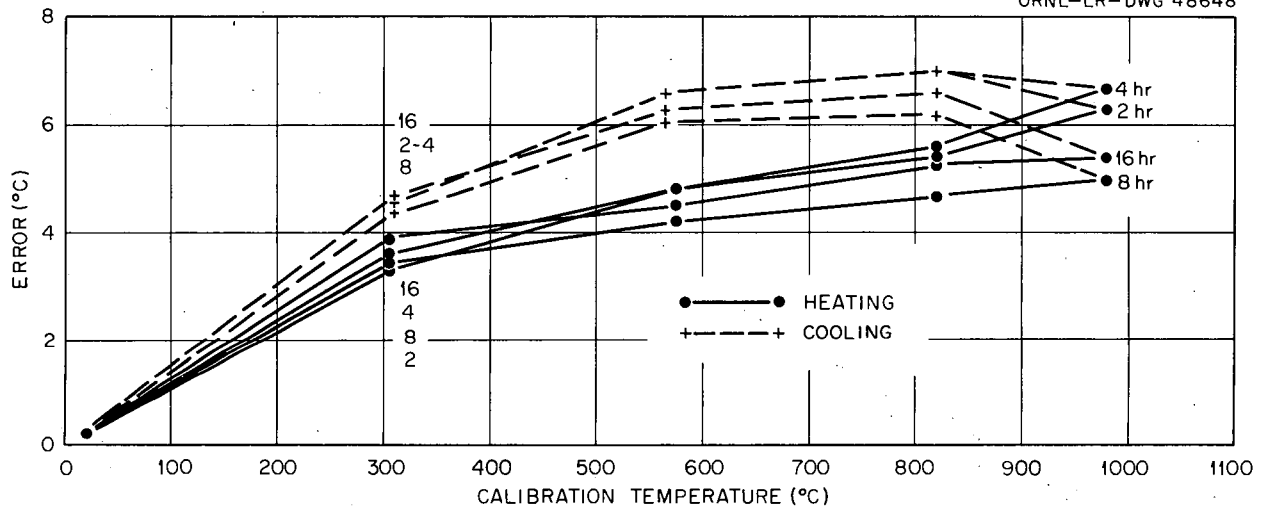


Fig. G.4. Calibration Deviation of Chromel-P vs Platinum for 2, 4, 8, and 16 hr at 700°C.

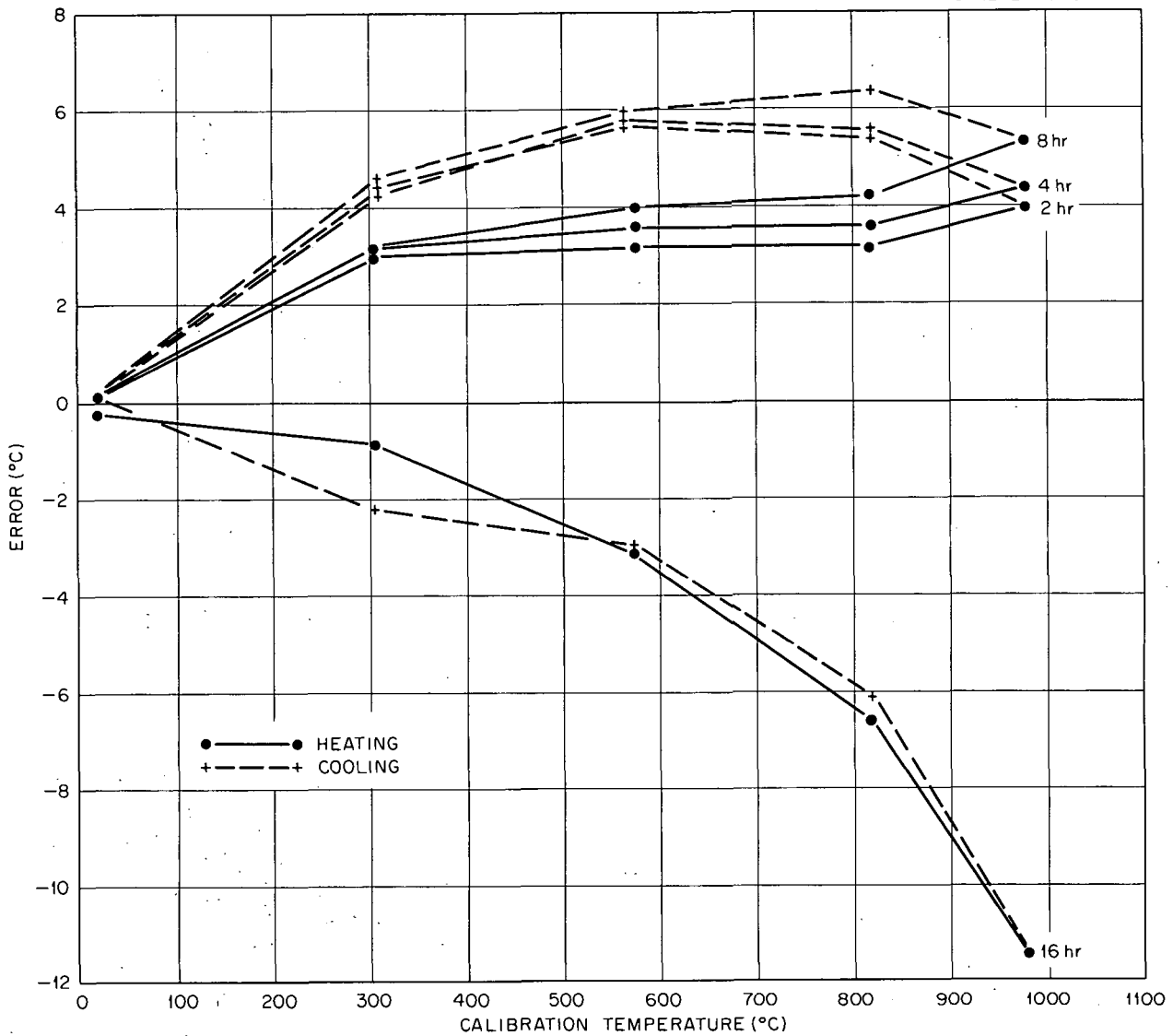


Fig. G.5. Calibration Deviation of Chromel-P vs Platinum for 2, 4, 8, and 16 hr at 800°C.

in Chap. 5. That is, recovery caused the emf to shift away from that of cold-worked wire, and recrystallization caused shifts in the opposite direction (i.e., away from the recovered state, back toward the cold-worked state).

**Chromel-P + Nb.** - (See Figs. G.6-G.9, excluding data for heat treatments of 2 hr at 600 and 700°C, 8 hr at 600°C, and 16 hr at 500 and 800°C.) The data at all temperatures showed that after at least 2 hr, the heat-treating time had little effect on the resulting calibration, although the calibrations on heating became progressively

lower as the testing temperature was increased. The calibrations on cooling were all close to being the same with increasing annealing temperatures. Reference to Fig. F.1 for the calibration on as-received Chromel-P + Nb shows that the change in calibration with heat treatment was about the same as for regular Chromel-P; that is, Chromel-P + Nb was below the curve in the as-received state, but on heat treatment it had moved closer to the established curve.

**Kanthal-P.** - (See Figs. G.10-G.13, excluding 2- and 16-hr data at 800°C.) These data were

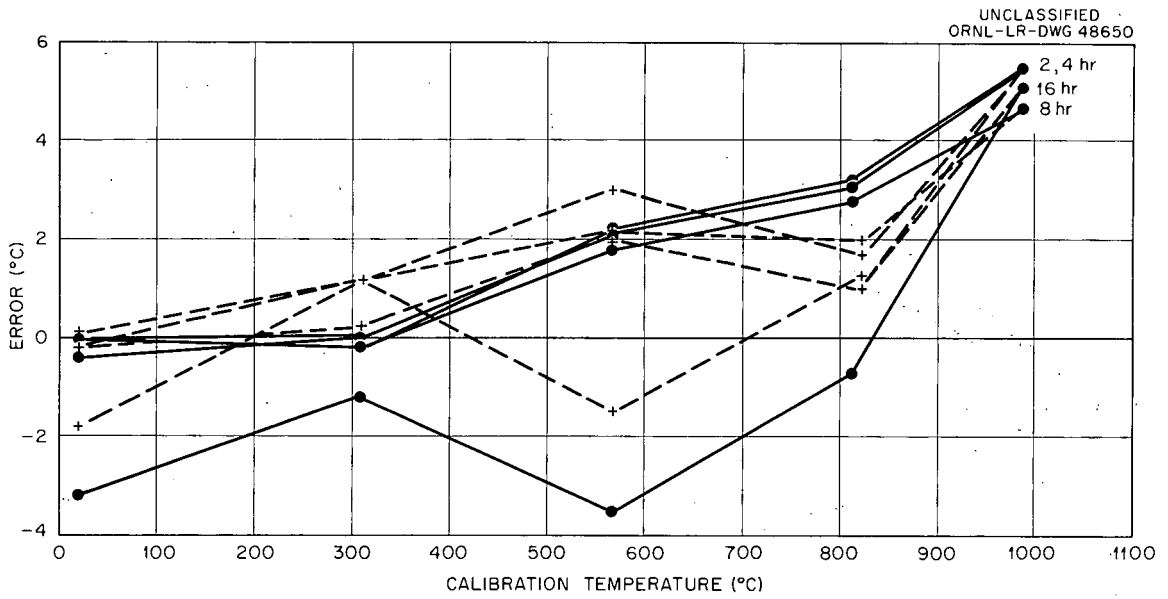


Fig. G.6. Calibration Deviation of Chromel-P + Nb vs Platinum for 2, 4, 8, and 16 hr at 500°C.

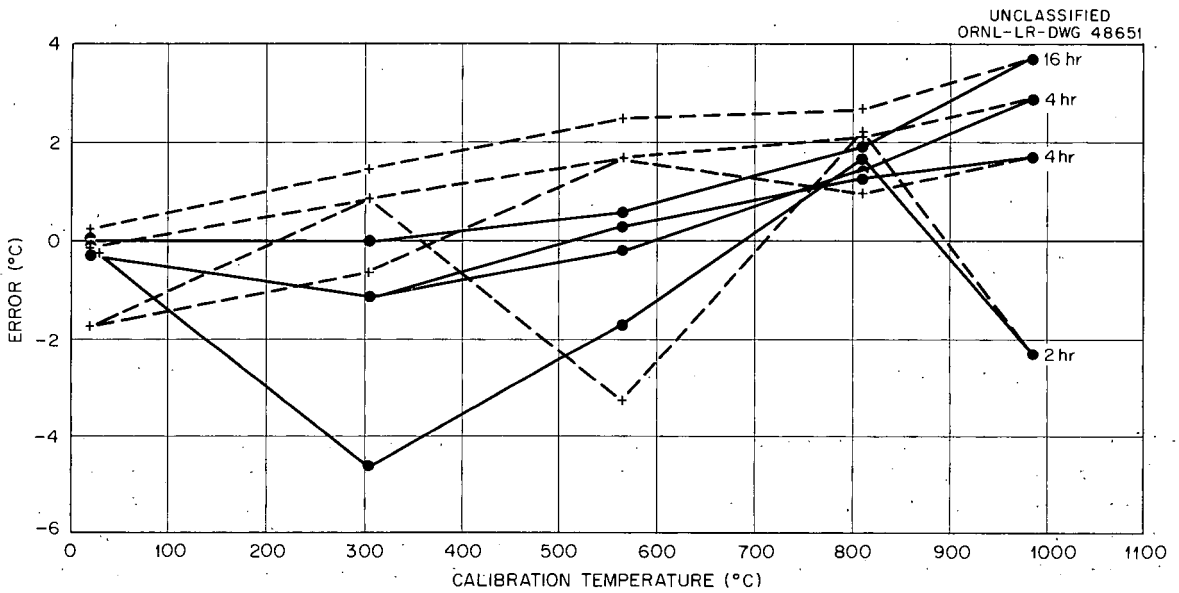


Fig. G.7. Calibration Deviation of Chromel-P + Nb vs Platinum for 2, 4, 8, and 16 hr at 600°C.

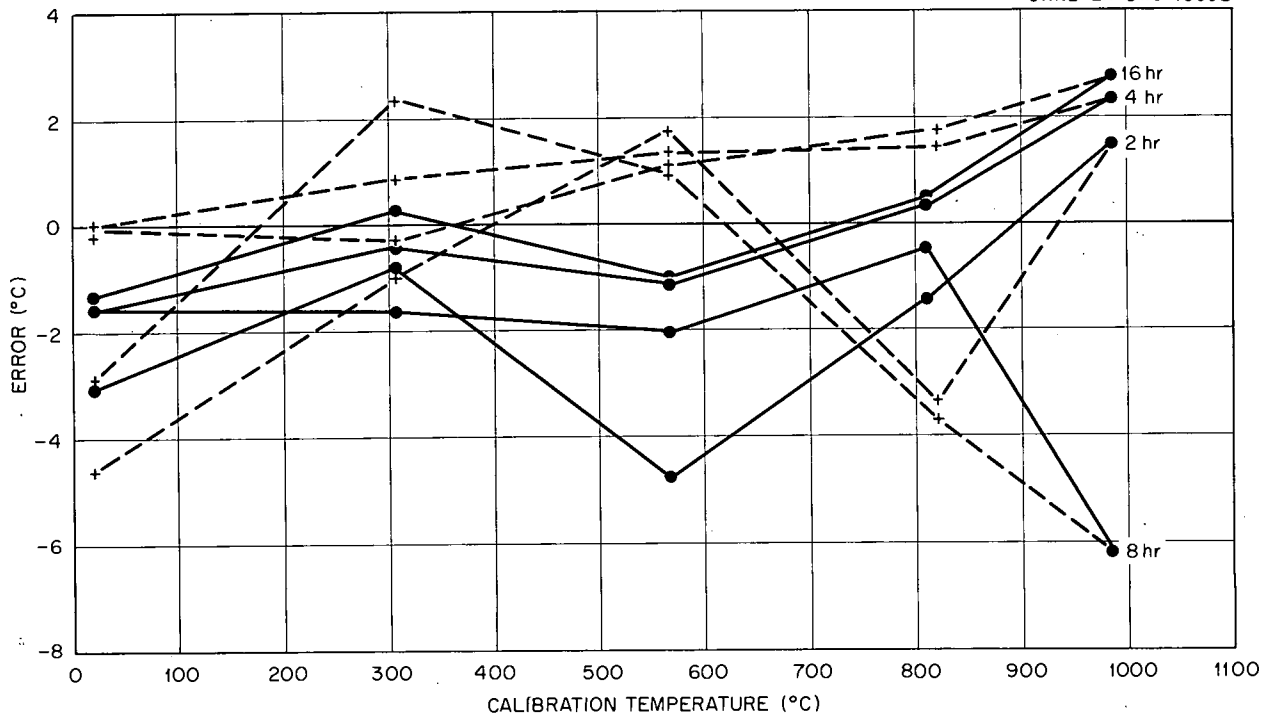


Fig. G.8. Calibration Deviation of Chromel-P + Nb vs Platinum for 2, 4, 8, and 16 hr at 700°C.

very similar to those described above and showed the same general trends: decreasing calibration error with increasing temperature, but only a small increasing calibration error with time at a particular temperature on heating. The calibration errors on cooling were nearly the same at all temperatures, but accentuated a negative deviation at room temperature, which was mildly apparent in the Chromel-P + Nb results. This error appeared to increase with increasing annealing temperature.

**Geminol-P.** — (See Figs. G.14–G.17, excluding the data for 16 hr at 500°C.) The calibration error on heating moved more positive with increasing heat-treating temperature, which is the reverse of the three previous cases. The effect of time at temperature showed a slightly different form on heating than in the former cases; that is, the error generally went through a maximum between 4 and 8 hr of heat-treating. The calibration on cooling was generally lower than the calibration on heating, also the reverse of the previous cases. Considerably more spread existed between the heating and cooling calibrations than in the previous cases. Generally the calibration errors

showed less change with temperature than the previous cases. These results add emphasis to the conclusions drawn in Appendix C regarding the difficulties encountered in establishing a standard emf-temperature table for Geminol-P/N.

These specific details about the individual calibrations indicated that internal changes associated with time at temperature were restricted to changes in thermal emf of less than 1°C after an initial 2 hr at temperature. Changes in heat-treating temperature caused changes of as much as 5°C. The latter was thought to be due to differences in the recovered and recrystallized states of these materials.

The differences in calibration on heating and on cooling apparently persisted in all these materials for all the temperatures studied, although the differences associated with the 500°C treatments were somewhat smaller than those of the higher treating temperatures. Calibration error appeared to be minimized by the helium treatment at the higher temperatures for Chromel-P, Kanthal-P, and Chromel-P + Nb, and times greater than 2 hr at temperature were only mildly influential.

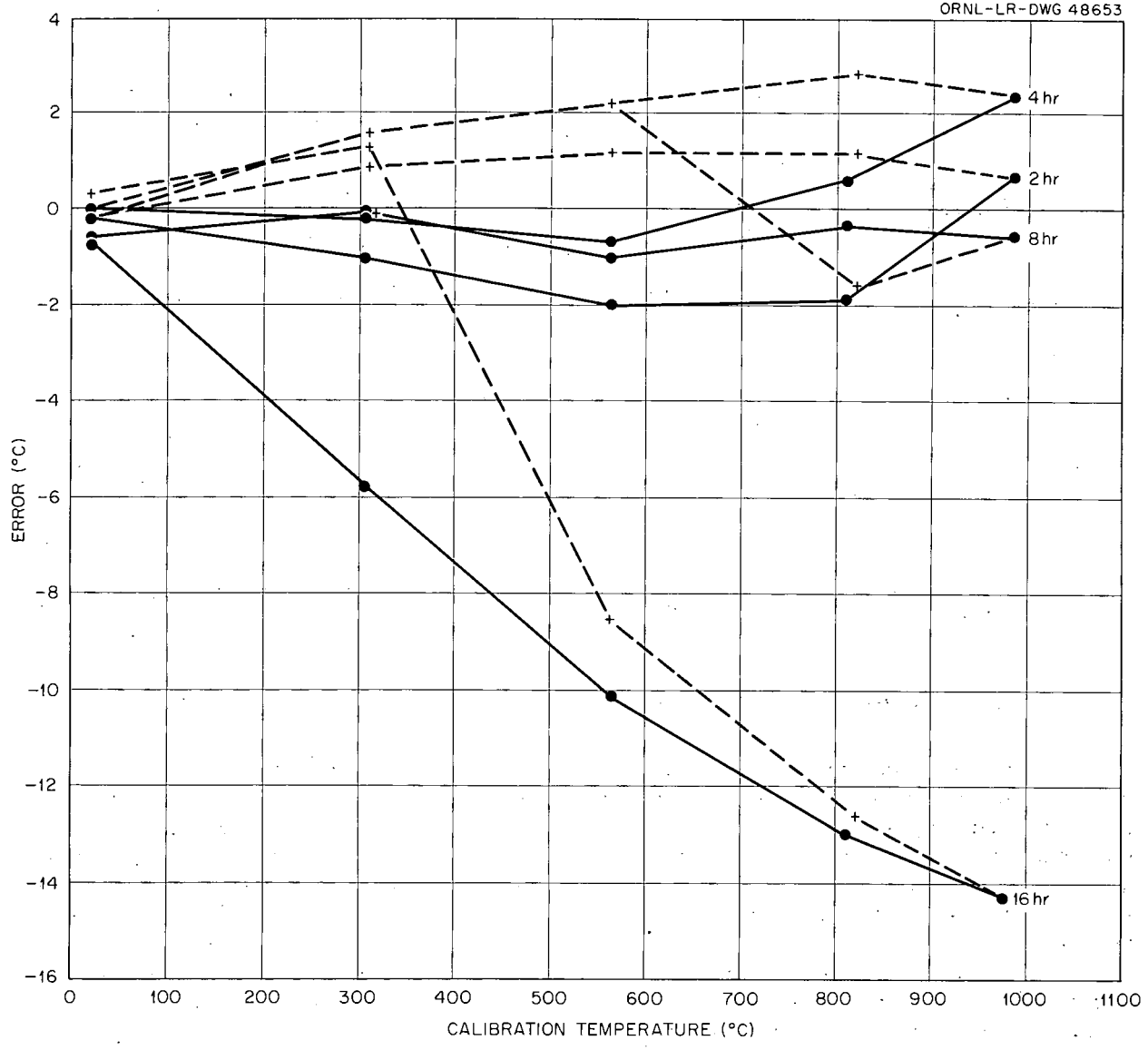


Fig. G.9. Calibration Deviation of Chromel-P + Nb vs Platinum for 2, 4, 8, and 16 hr at 800°C.

If the above excepted cases for these materials were considered (those in which oxide films were apparent) then it is apparent that very serious negative errors could be created. The 16 hr at 800°C treatments of Kanthal-P, Chromel-P + Nb, and Chromel-P were done in the same system and at the same time, and the resulting errors at 1000°C of -18, -14, and -12°C, respectively, illustrated the effects of oxide films. These were serious errors and emphasized that the utmost care should be exercised in inert-atmos-

phere heat treatment in order to study only internal changes.

One of the objectives of the above experiments was to look for the reflection of ordering effects in the Ni-Cr alloys in calibration. Any effects were probably masked by the oxidation effects or by the cooling rate after the heat treatment. In all cases the materials were quenched into water from the heat-treating temperatures, and this fast cooling rate could have influenced the results.

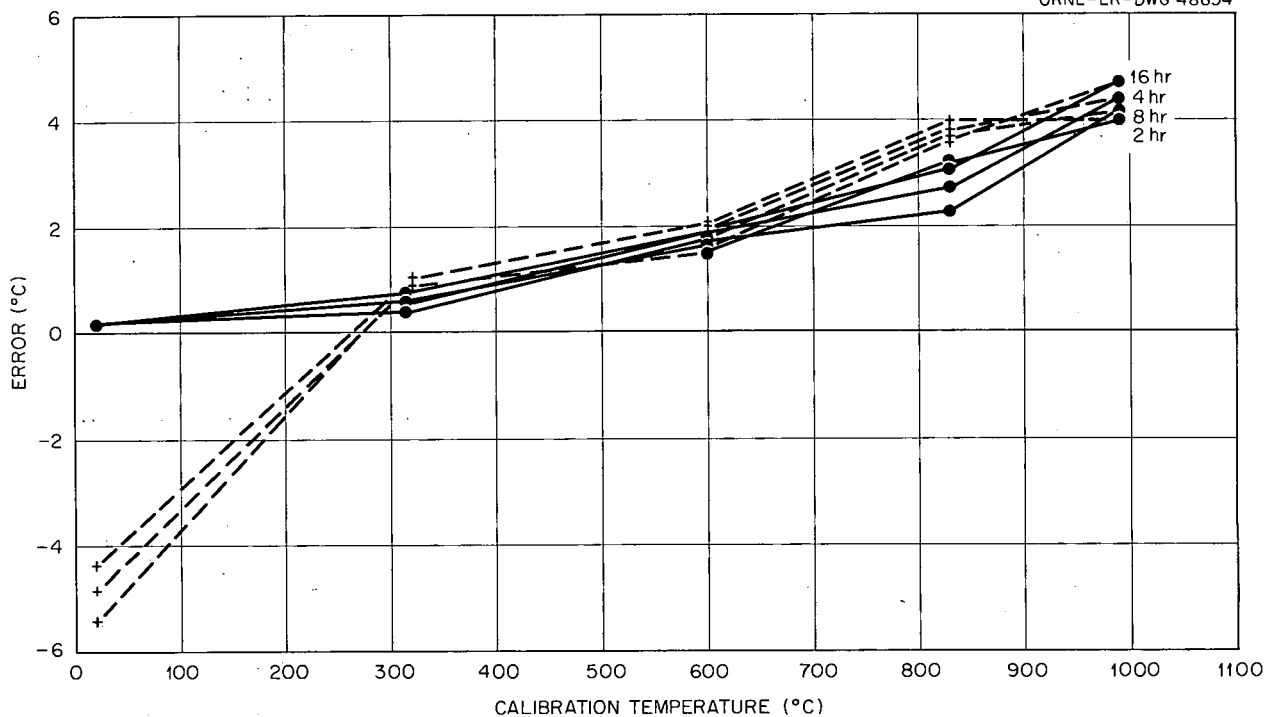


Fig. G.10. Calibration Deviation of Kanthal-P vs Platinum for 2, 4, 8, and 16 hr at 500°C.

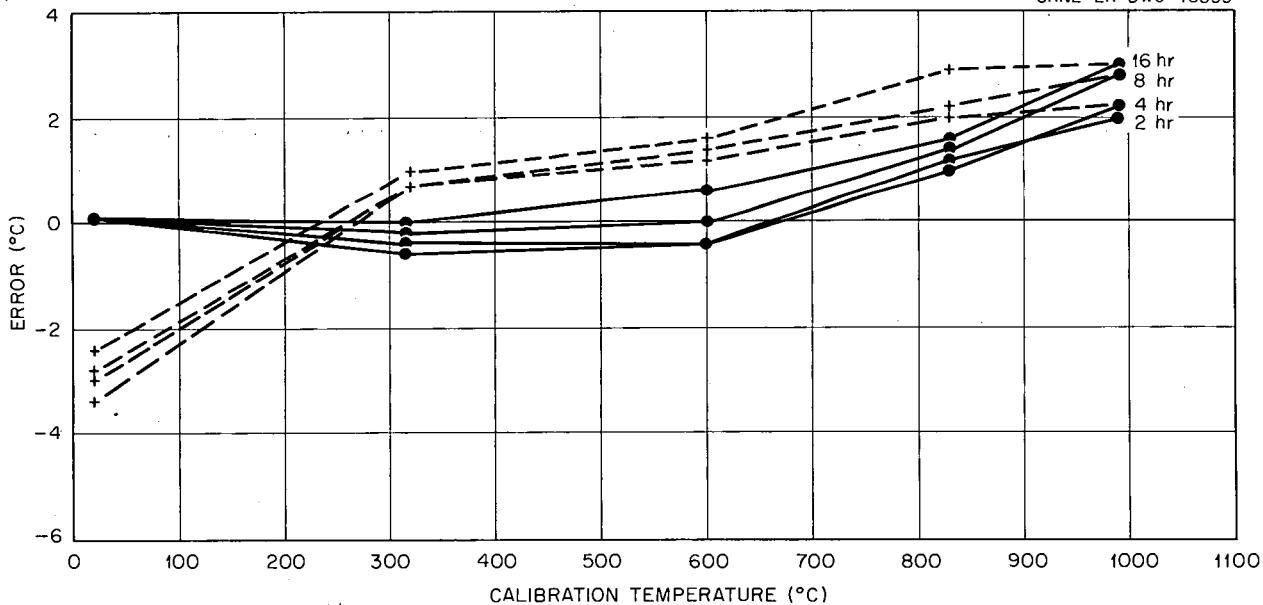


Fig. G.11. Calibration Deviation of Kanthal-P vs Platinum for 2, 4, 8, and 16 hr at 600°C.

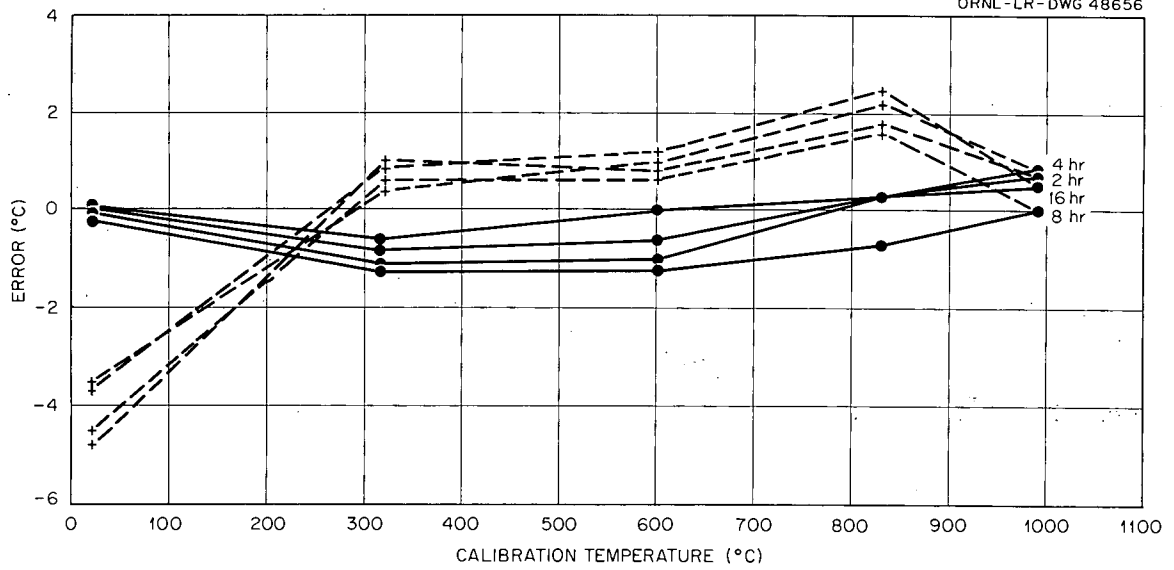


Fig. G.12. Calibration Deviation of Kanthal-P vs Platinum for 2, 4, 8, and 16 hr at 700°C.

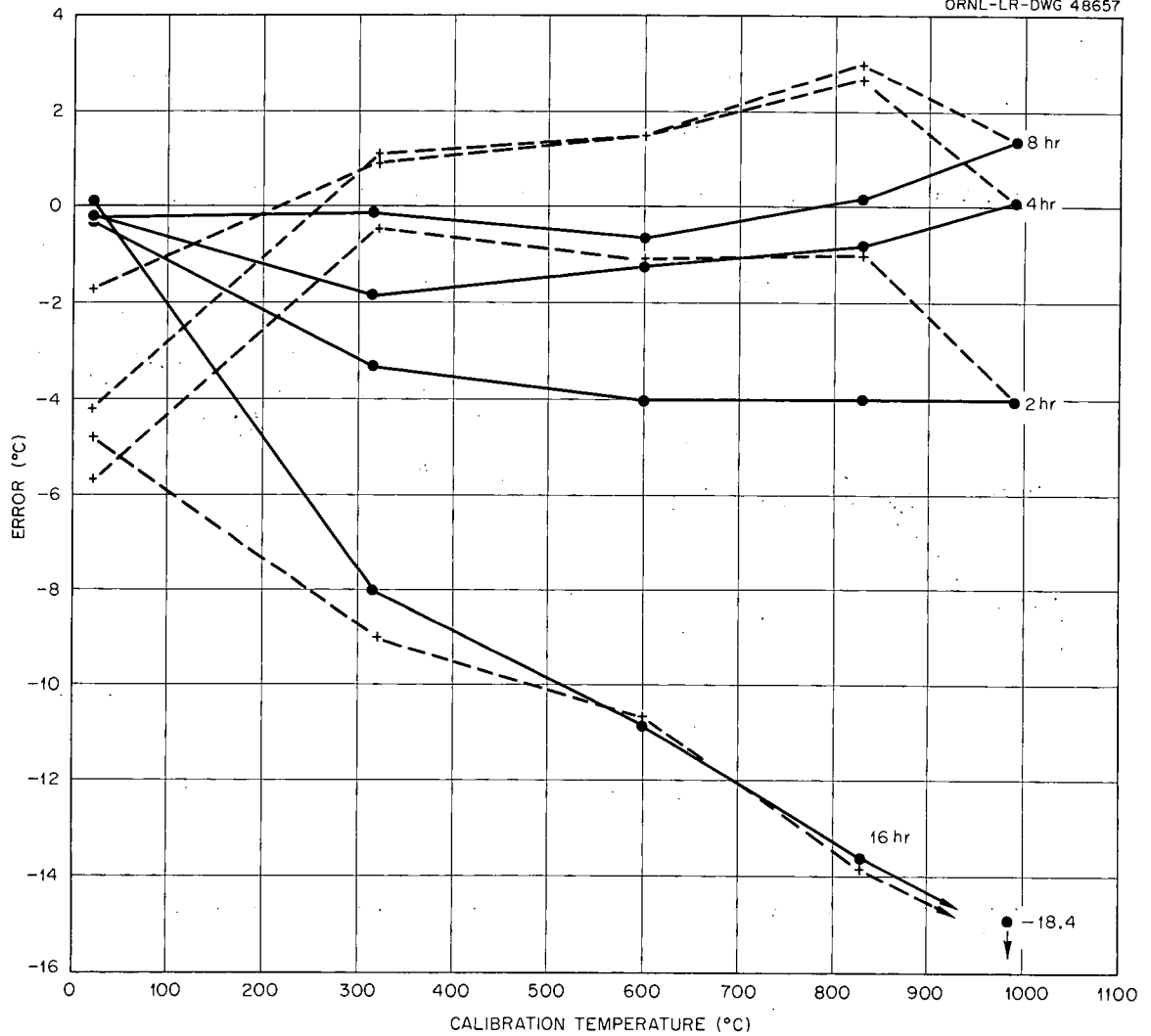


Fig. G.13. Calibration Deviation of Kanthal-P vs Platinum for 2, 4, 8, and 16 hr at 800°C.

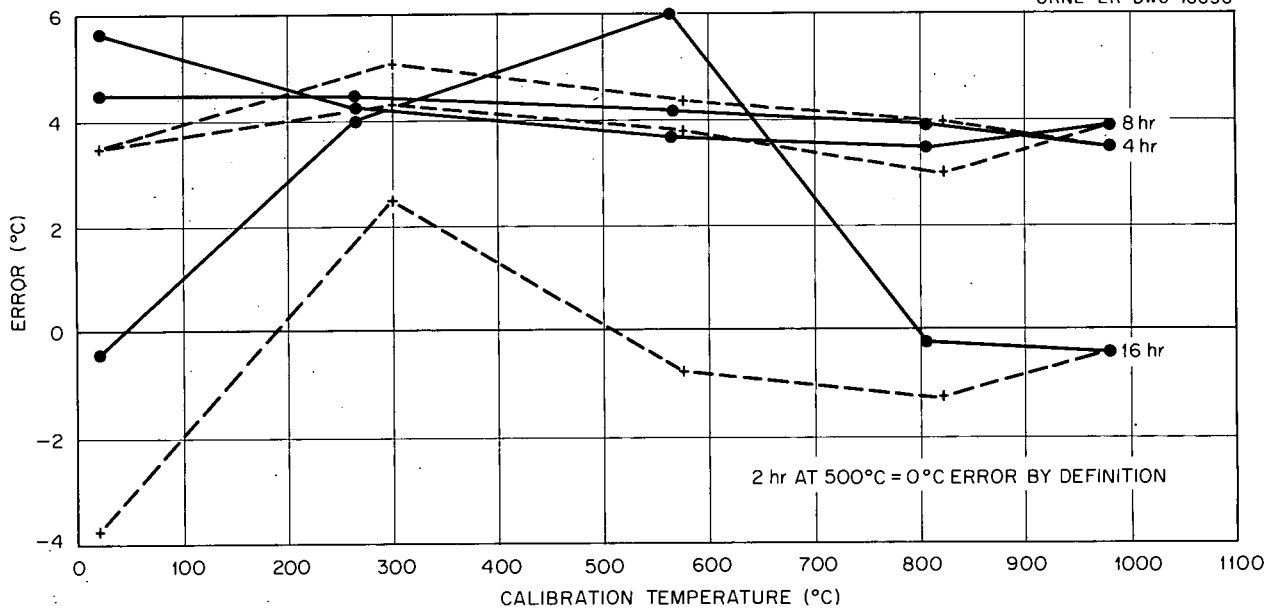


Fig. G.14. Calibration Deviation of Geminol-P vs Platinum for 2, 4, 8, and 16 hr at 500°C.

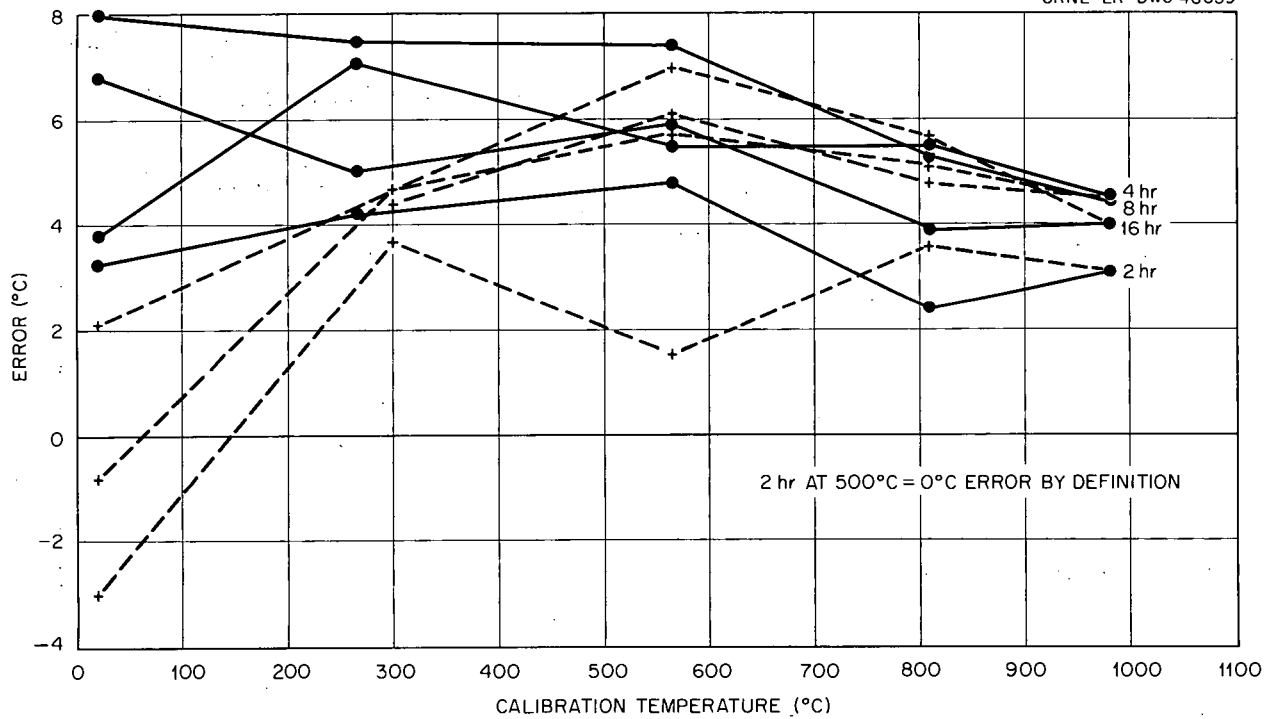


Fig. G.15. Calibration Deviation of Geminol-P vs Platinum for 2, 4, 8, and 16 hr at 600°C.

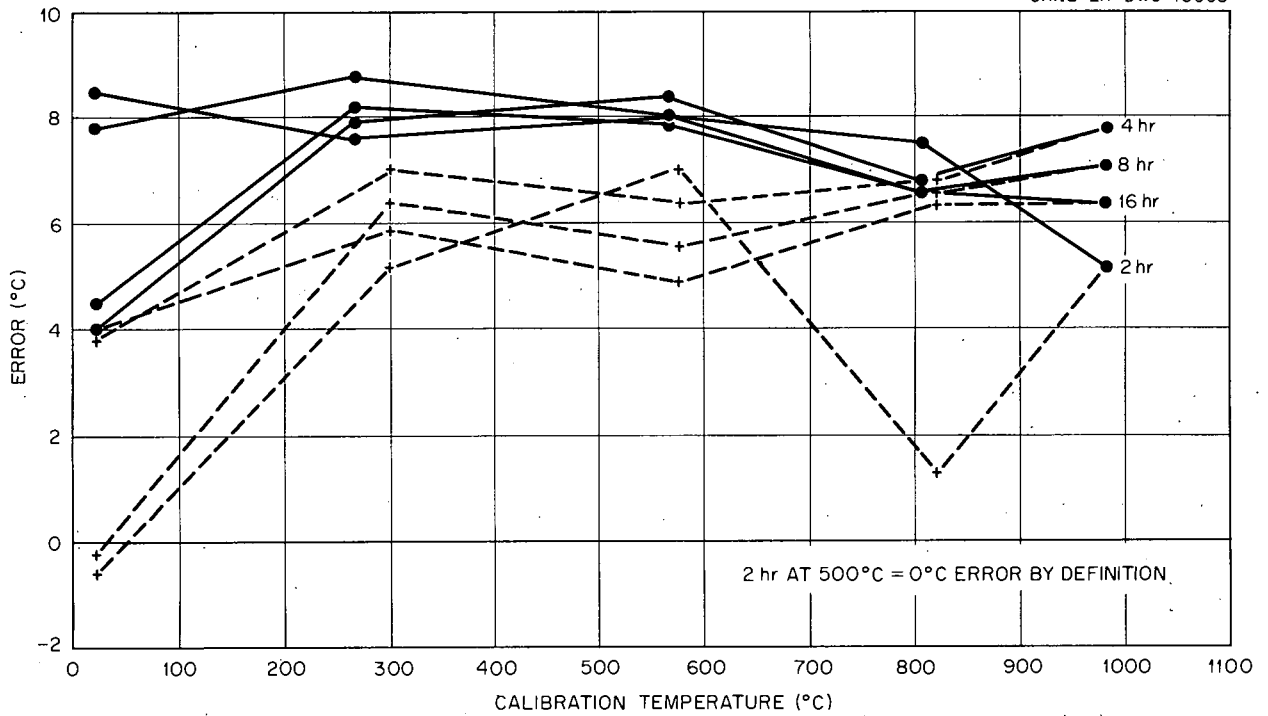


Fig. G.16. Calibration Deviation of Geminal-P vs Platinum for 2, 4, 8, and 16 hr at 700°C.

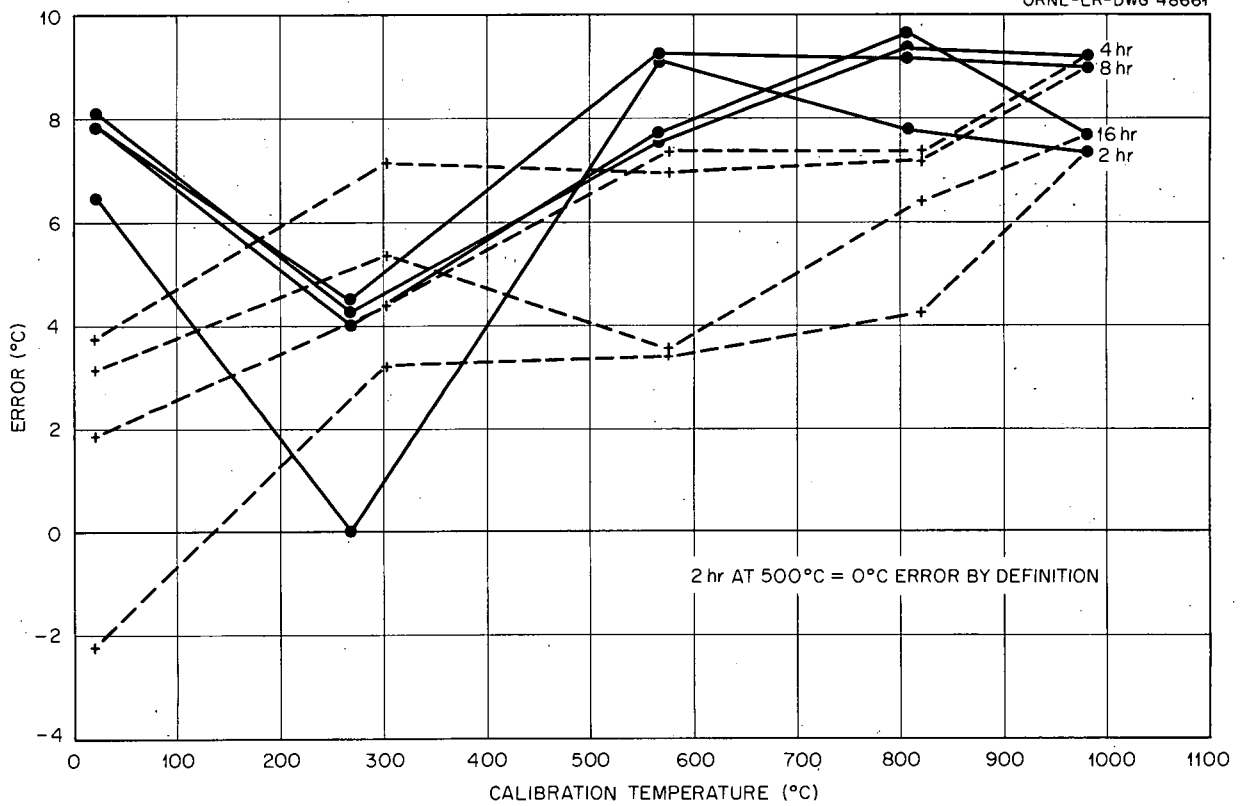


Fig. G.17. Calibration Deviation of Geminal-P vs Platinum for 2, 4, 8, and 16 hr at 800°C.

## Appendix H

### EVALUATION OF ACCURACY AND PRECISION OF CHROMEL-P, ALUMEL THERMOCOUPLES FOR A SPECIAL APPLICATION AT 400°C

We were consulted by H. W. Hoffman, Engineering Research Section, Reactor Projects Division, ORNL, concerning a problem in which he was committed to the use of Chromel-P, Alumel thermocouples for the measurement of differential temperatures of about 5°C at an operating temperature of about 400°C. Since experimental limitations precluded direct differential measurement, it was necessary to obtain the ultimate in measurement of absolute temperatures. Consideration of heat conduction losses by the thermocouple wires indicated the use of B&S 30 gage or smaller thermocouples.

Recommendations for attachment and insulating methods were supplied, and the problems of supplying homogeneous and stable thermocouple wire and of defining the precision obtainable from the wire were studied. The methods used and results obtained represent an application of some of the methods and understanding developed in the course of the present thermocouple research.

The unilateral gradient furnace (see Chap. 5) was employed along with comparison calibration against a standard 90% Pt-10% Rh, Pt thermocouple. Homogeneity checks on as-received B&S 30 gage Chromel-P and Alumel at 400°C indicated such nonuniformity that similar checks were made on B&S 24 gage wire. The latter material appeared to be sufficiently homogeneous that further tests were made, the results of which follow. The difference between the performance of 24 and 30 gage wire is probably the result of a factor of 2 decrease in the surface-to-volume ratio of 24 gage wire. This implies that irregularities in oxide coating thickness are more effective in promoting inhomogeneity of the smaller wire than of 24 gage wire. Wires of both sizes were oxidized in the as-received condition.

The results of the unilateral gradient tests and consequent heat treatment at 400°C for B&S 24 gage Chromel-P and B&S 24 gage Alumel are shown in Figs. H.1 and H.2, respectively. This temperature was chosen because (1) it represented the average temperature of the expected application, (2) it is in the temperature range of metallurgical recovery, and (3) the oxidation rate of Chromel-P and Alumel is low at this temperature.

As-received material was connected to the positive terminal of the microvolt recorder through the ice-bath reference junction. The wire was then strung into the side of the furnace (constituting a fixed temperature gradient) and onto the spool in the furnace. From the internal spool, the wire was strung out of the front of the furnace (constituting a moving temperature gradient with respect to the wire) and onto a second spool at ambient temperature. From the second spool, the wire was connected to the negative terminal of the microvolt recorder through a second ice-bath reference junction. Referring to Figs. H.1 and H.2, the following is an explanation of the significance of the unilateral gradient results.

Region A. - The initial offset is probably due to slight added cold-working during stringing of the wire onto the second spool.

Region B. - As-received wire was being run into the furnace, and the positive voltage represents a transient condition imposed by the feed speed being greater than recovery rate.

Region C. - The feed was stopped, and the drift to negative voltages represents a transient onset and a final steady-state metallurgical recovery which took approximately 20 min in both Chromel-P and Alumel.

Region D. - The recovered wire was run out of the furnace. The curve represents the degree of homogeneity of the wire in the recovered state and as delivered to the user. The cyclic variation in the residual thermal emf was probably due to a combination of slight variation in stress on the wire induced by the feed spools and a temperature gradient in the hot zone of the furnace. This places an uncertainty band around the results of about  $\pm 7 \mu\text{v}$  ( $\frac{1}{6}^\circ\text{C}$ ).

Region E. - The drive was stopped. This offset illustrates that the cyclic variations

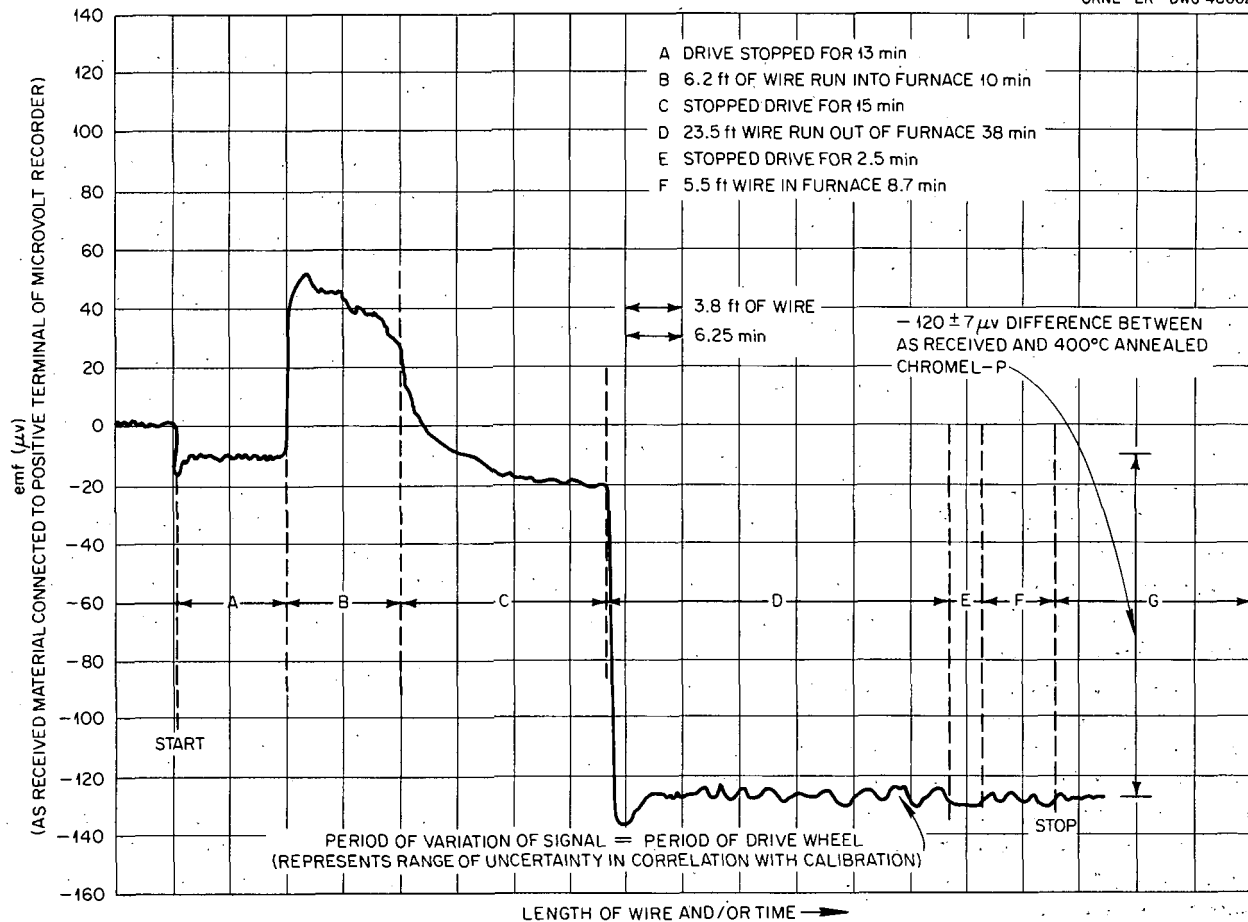


Fig. H.1. Unilateral-Gradient Test and Heat Treatment of B & S 24-Gage Chromel-P Thermocouple Wire at 400°C in Air.

described in region D are those of thermally induced potentials.

Region F. - The wire of region D was driven back into the furnace. The absence of further change illustrates that the heat-treated wire was stable at 400°C.

These results indicate that the heat-treated wire is stable at a maximum temperature not exceeding the heat-treating temperature, that the heat-treated Chromel-P shifts positive with respect to the as-received material by  $120 \pm 7 \mu\text{v}$ , and that the heat-treated Alumel shifts positive with respect to as-received Alumel by  $20 \pm 2 \mu\text{v}$ .

Subsequent to the unilateral gradient furnace heat treatment of the material, thermocouples were made from homogeneous regions of the heat-

treated Chromel-P and Alumel. Thermocouples were also constructed from as-received material. A common six-wire junction of these thermocouples and a 90% Pt-10% Rh, Pt thermocouple was made, and comparison calibrations were made at 25, 370, 400, and 420°C. In addition, the emf's of platinum vs the various base-metal legs were measured at these temperatures. The results of this calibration are presented in Table H.1. It may be seen that the comparative results of the calibration of the as-received and heat-treated thermocouples agree quite well with those predicted from the unilateral gradient tests. A preliminary check of data taken during the course of the heat transfer experiments using thermocouples heat-treated by a schedule based on the above work indicates that the variation of the temperature data is no worse than  $\pm \frac{1}{2}^\circ\text{C}$ .

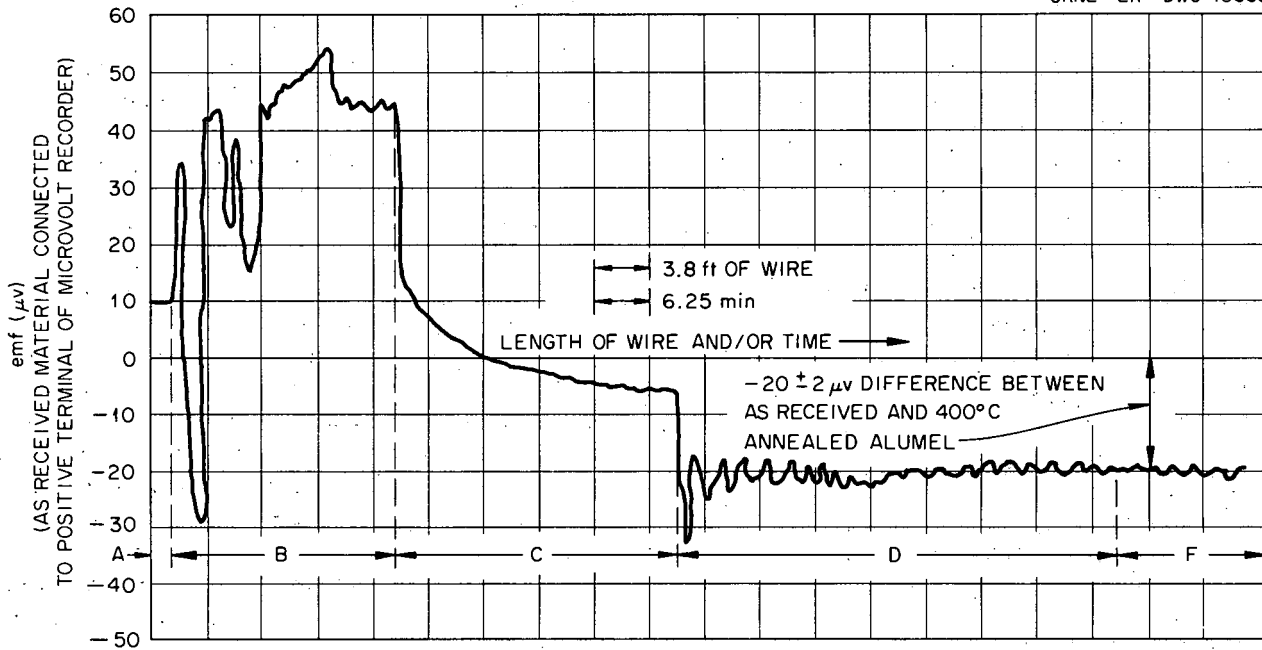


Fig. H.2. Unilateral-Gradient Test and Heat Treatment of B & S 24-Gage Alumel Thermocouple Wire at 400°C in Air.

Table H.1. Results of Calibration of As-Received and Heat-Treated 24 Gage Chromel-P and Alumel Thermocouples

Temperature (°C)	Wire Condition*	Deviation from Standard** (μv)		
		Chromel vs Platinum	Platinum vs Alumel	Chromel vs Alumel
25	As received	-8	-9	-17
	Heat-treated	0	-17	-17
370	As received	+2	-10	-8
	Heat-treated	+110	-40	+70
400	As received	-10	-10	-10
	Heat-treated	+110	-40	+70
420	As received	-25	+10	-15
	Heat-treated	+115	-40	+75

\*Heat-treated wire annealed in air longer than 30 min at 400°C, air quenched.

\*\*Compared with standard 90% Pt-10% Rh, Pt thermocouple.

## Appendix I

### CARBIDE STUDIES

Causes for the observed changes in thermal emf with time at temperature have been a primary concern of this research. The major changes observed have been related to oxidation and to cold-working and annealing. A third effect, the precipitation of chromium carbide and subsequent depletion of the solid solution of chromium, was stated as the reason for certain observed performances by persons in the thermocouple industry. The implication was that the carbide precipitated during exposures of 2 to 8 hr in the temperature range of 800 to 1200°F with 10 to 15°F positive drift of the thermocouple during this period. This change was believed to be serious enough to suggest alterations in aging cycles for sheathed thermocouple assemblies. Prior to the knowledge of the above data, experiments had shown (see Chapter 5) that cold-worked Chromel-P wires have negative deviations and that annealing causes the calibration to move in a positive direction, that is, toward the original annealed calibration. However, it was deemed feasible that other cooperative processes such as carbide precipitation might well be occurring in these alloys; so additional experiments were conducted.

Drift tests at 300, 390, 550, and 700°C for times in excess of 500 hr are reported in Chap. 6. None of these tests show the above-mentioned positive drift of +10 to +15°F in 2 to 8 hr, but the data was so taken that direct evidence of this effect could have been missed. Indirect, but conclusive, evidence that this does not occur is shown by the fact that all of the drift curves exhibit errors between +4 and -3°C for the long-time tests. If such a positive drift occurred early in the drift test, one would expect evidence of this to remain in the long-time tests with all of the errors maintaining a positive value of 6 to 9°C. Such is not the case. Positive drifts have been observed in short-time tests in the range 800 to 1200°F for wires which were intentionally cold-worked large amounts (see Chap. 5).

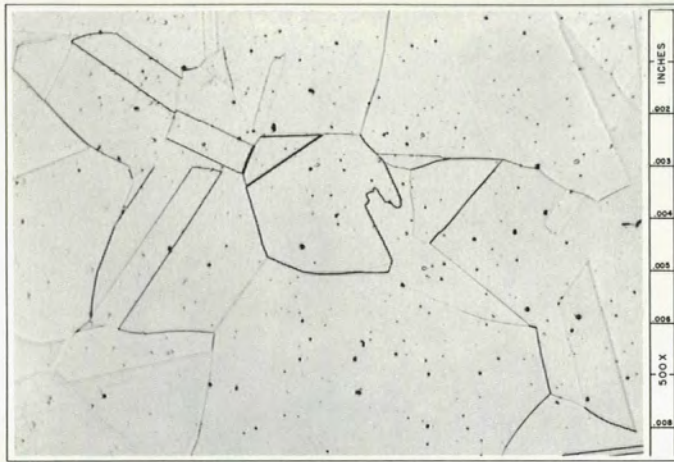
In an attempt to obtain direct evidence of this effect, two short-time drift tests were conducted at 1000 and 1200°F on a variety of Chromel-P-type materials both as received and annealed for 4 hr at 1800°F. The results show a positive drift in the as-received wire, but virtually no drift in the

heat-treated material, and this difference is apparently explainable only as a cold-working effect.

Calculations based on total consumption of carbon to  $\text{Cr}_3\text{C}$  reveal that for a 0.01 wt % carbon Chromel-P, the amount of chromium removed would be approximately 0.13 wt %. Analyses of Chromel-P show 0.02 wt % carbon as the maximum detected, and this would correspond to a 0.26 wt % chromium change. Detailed chemical analyses on the same spools of Chromel-P wire show variations as great as 1.2 wt % chromium. Furthermore, the flatness of the emf vs composition curve at a temperature of 700°C reveals that a composition change of 0.26 wt % chromium would result in a calibration shift of less than 40  $\mu\text{v}$ , or 1°C. This tends to refute a drift of 15°F, but shows the effects if carbide formed from the existing carbon in Chromel-P.

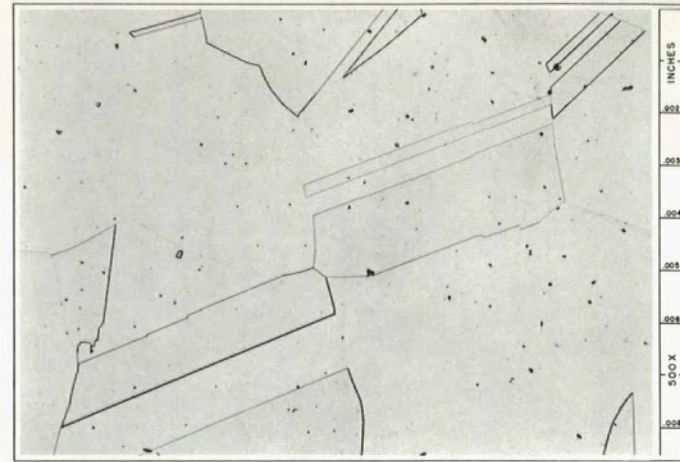
An attempt was made to determine whether chromium carbide was precipitating in heat-treated Chromel-P and what effect it has. Samples of Chromel-P and Alumel were solution heat-treated for 2 hr at 2100°F in argon and quenched to room temperature. Samples of the solution-heated Chromel-P and Alumel were aged 64 hr at 1500 and 1200°F in argon to facilitate precipitation of chromium carbide. As-received Chromel-P and Alumel were heated at 750°F for 4 hr to completely recover any cold-working effects. Samples of these were used to measure electrical resistivity at 0°C and to be calibrated at the tin and zinc points.

Figure 1.1a shows a transverse section of Chromel-P which was given an 1149°C solution heat treatment for 2 hr, then water-quenched. A grain growth over the original of about 20 was observed. No *definitive* carbide precipitates are present in this structure. Subsequent aging treatments (Figs. 1.1b and 1.1c) for 64 hr at 816 and 649°C, respectively, show no gross carbide precipitation. Since the microstructure of a longitudinal section of the 649°C aged sample (Fig. 1.1d) shows the observed precipitates were present as stringers in the direction of the wire axis, it was concluded that all of the precipitates observed in the other samples were present in the as-received wire.



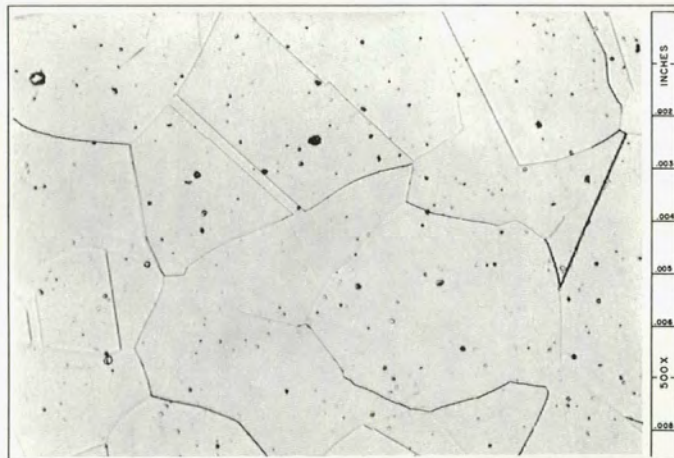
(a)

TREATMENT "A" ANNEALED AT 1149°C FOR 2 hr IN ARGON, FOLLOWED BY WATER QUENCH. CATHODIC ETCH. 500X. TRANSVERSE SECTION.



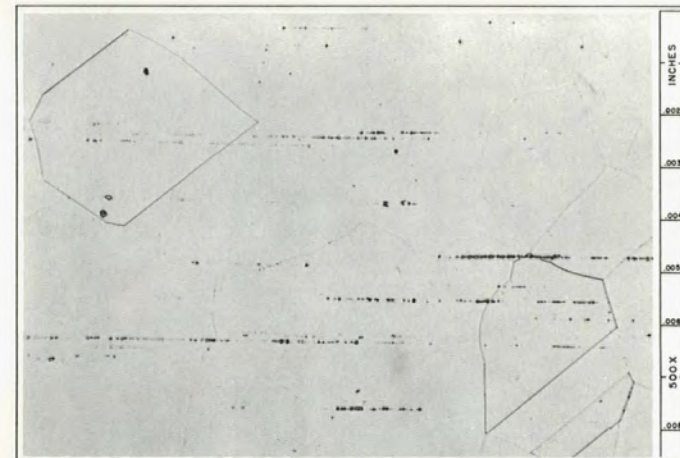
(b)

TREATMENT "A" FOLLOWED BY AGING AT 816°C FOR 64 hr IN ARGON, WATER QUENCH. CATHODIC ETCH. 500X. TRANSVERSE SECTION.



(c)

TREATMENT "A" FOLLOWED BY AGING AT 649°C FOR 64 hr IN ARGON, WATER QUENCH. CATHODIC ETCH. 500X. TRANSVERSE SECTION.



(d)

TREATMENT "A" FOLLOWED BY AGING AT 649°C FOR 64 hr IN ARGON, WATER QUENCH. CATHODIC ETCH. 500X. LONGITUDINAL SECTION.

Fig. 1.1. Photomicrographs of Chromel-P After Solution Heat Treatment and Aging Heat Treatments.

Calibration data obtained on these samples are shown in Table I.1. The 400°C recovery treatment caused a positive emf change which is associated with recovery of initially cold-worked material. Resistivity measurements before and after this treatment are shown in Table I.2 and verified that the as-received wire was cold-worked. The calibrations of the heat-treated wires showed no

changes greater than predicted in the preceding analysis of the effects of chromium carbide precipitation.

The above does not prevent carbide precipitation in Chromel-P or Alumel from occurring if a carbon source exists external to the wire. Indeed, as Fig. 1.2 shows, carbide precipitation can occur and is quite serious in its effect. Chromel-P,

Table I.1. Calibration Data of Heat-Treated Chromel-P and Alumel

Material and Condition	Deviation <sup>a</sup> ( $\mu\text{V}$ ) at Temperature Indicated		
	Tin Point <sup>b</sup>	Zinc Point	Tin Point <sup>c</sup>
Chromel-P			
As received	+18	+25	+62.6
Recovered 4 hr at 400°C	+126.9	+181	+140.3
Solution heat-treated 2 hr at 1149°C	+120.4	+198	+168.3
1149°C anneal and aged 64 hr at 816°C	+75.5	+138	+138.1
Alumel			
As received	+14.4	+13.5	-8.5
Recovered 4 hr at 400°C	-1.1	+6.3	-7.5
Solution heat-treated 2 hr at 1149°C	+51.8	+20.5	+34.1
1149°C anneal and aged 64 hr at 816°C	+162.5	+200.5	+157

<sup>a</sup>Deviation is positive if the Chromel-P, Pt (or Alumel, Pt) thermocouple gave more than the standard emf and negative if it gave less than the standard. The standard values (in millivolts) are:

Thermocouple	Tin Point	Zinc Point
Chromel-P, Pt	7.022	13.427
Alumel, Pt	2.397	3.796

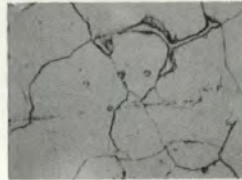
<sup>b</sup>Measured before heating to the zinc point.

<sup>c</sup>Measured after heating to the zinc point.

Table I.2. Electrical Resistivity at 0°C

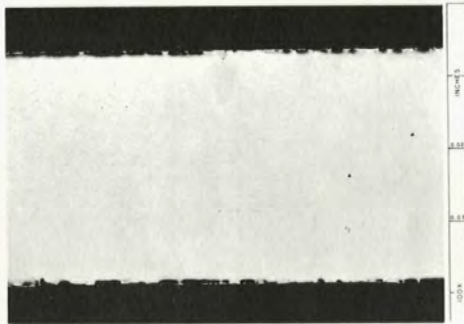
Values in ohm-centimeters

Condition	Alumel	Chromel-P
	$\times 10^{-6}$	$\times 10^{-6}$
As received	29.067	65.149
Recovered 4 hr at 400°C	29.052	67.368
Solution heat-treated 2 hr at 1149°C	28.252	64.7096
Aged 64 hr at 816°C	27.188 <sub>5</sub>	63.865



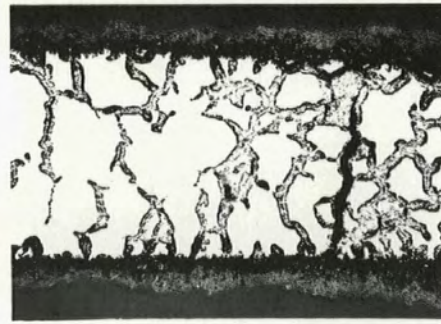
(a)

CHROMEL-P PACK-CARBURIZED AT 1000°C  
FOR 24 hr. GLYCEREGIA ETCH. 1000X.



(b)

AS-RECEIVED CHROMEL-P AND ALMEL PRIOR TO CO  
EXPOSURE UNETCHED.

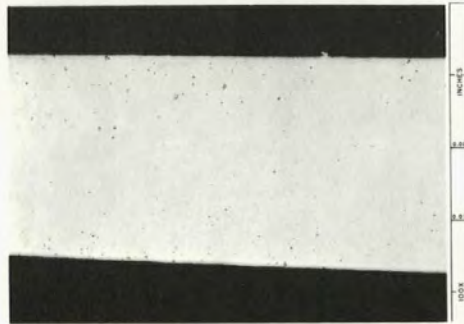


(c)

ALMEL AFTER 720 hr AT 816°C IN CO  
ATMOSPHERE (DEWPOINT, -46°C). UNETCHED

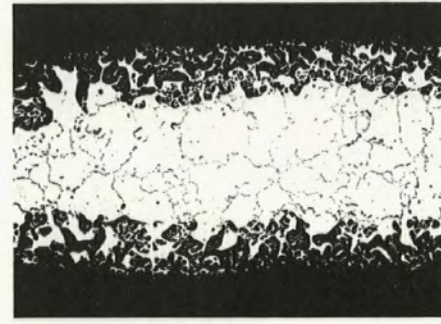


(d)



(e)

CHROMEL-P AFTER 720 hr AT 816°C IN CO  
ATMOSPHERE (DEWPOINT, -46°C). UNETCHED



(f)



(g)

Fig. 1.2. Photomicrographs Illustrating the Effect of Carburizing Atmosphere on Chromel-P and Almel.

pack-carburized at 1000°C for 24 hr (Fig. 1.2a), shows a gross precipitate in the grain boundaries, presumably chromium carbide. A Chromel-P, Alumel thermocouple drift test in a dry carbon monoxide atmosphere at 816°C for 720 hr (see Figs. 1.2b-1.2g) also shows a second phase present, which caused a 20% decrease in the thermal emf at 816°C. (A change of 7 mv in 34 was observed.) Chemical analysis of these Chromel and Alumel samples indicated more than 5 wt % carbon present, so some free carbon must

be present since this represents an excess of carbon for the available chromium to form chromium carbide.

From these tests it is concluded that carbide precipitation can occur and can cause large changes in thermal emf if some form of carbon is available to the thermocouple. However, if an inert or oxidizing atmosphere is maintained, there is not sufficient carbon in typical as-received Chromel-P to cause a detectable change in thermal emf attributable to carbide precipitation.



INTERNAL DISTRIBUTION

1. C. E. Center
2. Biology Library
3. Health Physics Library
- 4-5. Central Research Library
6. Reactor Division Library
- 7-26. Laboratory Records Department
27. Laboratory Records, ORNL R.C.
28. A. M. Weinberg
29. L. B. Emler (K-25)
30. J. P. Murray (Y-12)
31. J. A. Swartout
32. E. H. Taylor
33. E. D. Shipley
34. C. S. Harrill
35. C. P. Keim
36. J. H. Frye, Jr.
37. R. S. Livingston
38. W. H. Jordan
39. S. C. Lind
40. F. L. Culler
41. A. H. Snell
42. A. Hollaender
43. M. T. Kelley
44. K. Z. Morgan
45. T. A. Lincoln
46. A. S. Householder
47. C. E. Winters
48. H. E. Seagren
49. J. A. Lane
50. D. Phillips
51. M. J. Skinner
52. C. J. Borkowski
- 53-62. J. F. Potts, Jr.
63. G. C. Williams
- 64-73. D. L. McElroy
- 74-76. C. A. Mossman
- 77-78. H. J. Metz
- 79-80. R. L. Moore
81. W. W. Johnston
82. J. L. Horton
83. N. H. Briggs
84. R. G. Affel
85. K. W. West
86. J. A. Mahoney (K-25)
87. B. B. Bell (Y-12)
88. O. Sisman
89. G. W. Keilholtz
90. W. T. Rainey
91. J. C. Wilson
92. C. J. Whitmire
93. B. C. Thompson
94. D. A. Douglas
95. P. Patriarca
96. W. D. Manly
97. W. O. Harms
98. D. B. Trauger
99. M. J. Kelly
100. R. N. Lyon
101. J. H. Crawford
102. J. P. Nichols
103. P. M. Reyling
104. R. S. Cockreham
105. W. J. Kucera
106. ORNL - Y-12 Technical Library,  
Document Reference Section

EXTERNAL DISTRIBUTION

107. Division of Research and Development, AEC, ORO
- 108-109. U.S. Atomic Energy Commission, Washington (1 copy each to S. G. Nordlinger and F. C. Legler)
110. U.S. Atomic Energy Commission, Oak Ridge (D. C. Davis)
111. Battelle Memorial Institute (O. L. Linebrink)
- 112-114. National Bureau of Standards, Washington (1 copy each to F. R. Caldwell, W. A. Wildhack, and J. F. Swindells)
115. E. C. Smith Company, Conshohocken, Pennsylvania (E. C. Smith)
- 116-117. General Electric Company (ANPD) (1 copy each to M. Hebert and R. J. Freeman)
- 118-119. General Electric Company, Schenectady (1 copy to A. I. Dahl and D. L. Martin)

- 120-122. General Electric Company, Lynn, Massachusetts (1 copy each to R. C. Clark, W. C. Hagel, and R. C. Lever)
- 123-125. Hoskins Manufacturing Company, Detroit, Michigan (1 copy each to J. C. Lochman, N. F. Spooner, and F. Sibley)
  - 126. General Motors Research Laboratories, Warren, Michigan (R. J. Moffat)
  - 127. Los Alamos Scientific Laboratory (M. R. Nadler)
  - 128. Marquardt Corporation, Van Nuys, California (S. V. Castner)
  - 129. National Aeronautics and Space Administration, Cleveland (I. Warshawski)
  - 130. National Carbon Research Laboratories, Cleveland (R. L. Shepard)
  - 131. Thermo Electric Company, Saddle Brook, New Jersey (J. H. Collins)
- 132-133. Westinghouse Atomic Power Division, Pittsburgh (1 copy each to G. Johannesen and W. P. DiPietro)
  - 134. Minneapolis-Honeywell Regulator Company, Philadelphia (H. Schmitt)
  - 135. Kanthal Corporation, Stamford, Connecticut (R. Edwin)
  - 136. Rensselaer Polytechnic Institute, Harrison, New Jersey (M. A. Hunter)
  - 137. Driver-Harris Company, Harrison, New Jersey (P. R. Marsh)
  - 138. Pratt & Whitney Aircraft, East Hartford, Connecticut (V. E. Thornburg)
  - 139. Aero Research Instrument Company, Chicago (M. Scadron)
  - 140. Harco Laboratories, Inc., New Haven, Connecticut (M. B. Marshall)
  - 141. Leeds & Northrup Company, Philadelphia (D. I. Finch)
  - 142. U.S. Steel, Monroeville, Pennsylvania (J. W. Percy)
  - 143. Sidmund Cohn Company (B. C. Brenner)
  - 144. Wilbur B. Driver Company, Newark, New Jersey (T. P. Wang)
  - 145. AECD, ARO, Tullahoma (D. C. Holt)
  - 146. North American Aviation, Autometrics Division, Downey, California (L. A. Hendrix)
  - 147. Bayonne Research Laboratories, International Nickel Company, Bayonne, New Jersey (G. E. Zima)
  - 148. Combustion Engineering, Windsor, Connecticut (W. G. Cartier)
  - 149. University of Tennessee (E. E. Stansbury)
  - 150. Charles Englehard, Inc., E. Newark, New Jersey (H. J. Greenberg)
  - 151. Pratt & Whitney, Canel, Middletown, Connecticut (P. Bliss)
  - 152. Union Carbide Olefins Company, South Charleston (R. D. Webb)
  - 153. Union Carbide Chemicals Company, South Charleston (I. Thomas)
- 154-770. Given distribution as shown in TID-4500 (15th ed.) under Instruments category (100 copies - OTS)